PROGRAMA DE DOCTORADO EN INGENIERÍA INDUSTRIAL: TECNOLOGÍAS DE DISEÑO Y PRODUCCIÓN INDUSTRIAL

TESIS DOCTORAL

APROVECHAMIENTO DE RESIDUOS INDUSTRIALES COMO MATERIA PRIMA SECUNDARIA EN PRÁCTICAS DE PRODUCCION CIRCULAR

PhD THESIS

INDUSTRIAL WASTE UTILISATION AS SECONDARY RAW MATERIAL IN CIRCULAR PRODUCTION PRACTICES

AUTOR

JUAN DACUBA GARCÍA

DIRECTORA

ANA ANDRÉS PAYÁN

UNIVERSIDAD DE CANTABRIA

Escuela de Doctorado de la Universidad de Cantabria

Santander 2022

UNIVERSIDAD DE CANTABRIA

PROGRAMA DE DOCTORADO EN INGENIERÍA INDUSTRIAL: TECNOLOGÍAS DE DISEÑO Y PRODUCCIÓN INDUSTRIAL

TESIS DOCTORAL

Aprovechamiento de residuos industriales como materia prima secundaria en prácticas de producción circular

Ph.D. Thesis

Industrial waste utilisation as secondary raw material in circular production practices

Juan Dacuba García

Directora: Ana Andrés Payán

Escuela de Doctorado de la Universidad de Cantabria

Santander 2022

ACKNOWLEDGEMENTS

Esta Tesis Doctoral empezó hace años atrás, y después de muchas idas y venidas ha llegado a su fin, siendo muchas las personas a las que quiero agradecer el haber podido llegar al final de este largo camino.

En primer lugar, me gustaría agradecer a mi directora Ana Andrés Payan por confiar en mí para hacer este trabajo, por su flujo de ideas, apoyo y aliento, y también por ayudarme a mantener las cosas en perspectiva. El profesional que soy hoy en día te lo debo a ti por los años que he estado aprendiendo de ti para saber manejarme en las situaciones difíciles y en las fáciles. Nunca pensamos que un estudio de marketing daría para hacer una tesis como esta.

Gracias al Grupo de investigación "Green Engineering and Resources" (GER) del Departamento de Química e Ingeniería de Procesos y Recursos. A Jorge Santos, Eva Cifrian, María Coronado, Gema Ruiz, Javier Viguri y Alberto Coz y en especial a Elena Dosal y Tamara Llano por vuestro tiempo y compañía donde hemos pasado unos momentos fabulosos difíciles de olvidar compartiendo vivencias del doctorado. Siempre tendréis un recuerdo especial en esta tesis.

Gracias a mis amigos de toda la vida que nunca han entendido para qué sirve un doctorado, pero siempre me han apoyado y dado energías para que continuase con ello una vez llegaron a entender para qué podía valer.

Gracias a mis padres, Juan García y Mª Dolores Dacuba, que siempre me han dado y proporcionado su apoyo para que sacara adelante este trabajo. Si no llega a ser por el apoyo y la energía que me han transmitido a lo largo de estos años, nunca habría acabado este trabajo. ¿Quién os iba a decir a vosotros, cuando tenía 16 años, que iba a ser Doctor en Ingeniería Industrial? Nunca nadie lo hubiera imaginado, incluso yo sigo sin creérmelo. Vuestros valores y educación han permitido sacar esto adelante. Dar las gracias también a mi hermana, Sara Dacuba García, mi tío, Mario Dacuba, y mi abuela, Marisol Pascual, que me han apoyado a seguir formándome como persona y como profesional.

Por último y mis más sentidas gracias a mi nueva pequeña familia formada por Tamara Llano Astuy y nuestro pequeñín Nicolás Dacuba Llano. Para ti, Tamara, no hay suficientes palabras de agradecimiento. Todo lo que puedo escribir aquí se queda corto por todo tu apoyo, sacrificio, energía e involucración que has tenido en mi tesis hasta que ha llegado este momento. El momento de escribir unos agradecimientos que no hacen justicia por todo lo que has sufrido: mi mal humor,

mi desidia, mi despreocupación... Si no fuera por tu constancia y por tus ganas de verme como Doctor no estaría hoy aquí escribiendo estos agradecimientos. Esto que te he escrito igual no representa todo lo que has hecho por mí, pero para mí eres una de las mejores personas que han pasado por mi vida, mi mujer, madre de mi hijo y mi mejor amiga. A mi hijo, Nicolás, que durante estos últimos meses no te he podido hacer el caso que te mereces, pero eres lo más bonito que me ha pasado en la vida. Tamara, tú y yo estamos creando algo muy bonito.

Esta tesis se la quiero agradecer a personas que ya no están pero que sé que si estuviesen me hubieran apoyado hasta acabarla: Domitila García y Nicolás Dacuba (bisabuelo). Personas que han compartido mi vida y creo que se merecen estar en estos agradecimientos por lo que me han ayudado a formarme como persona.

TABLE OF CONTENTS

LIST OF ABBREVIATIONS

AABs	*Alkali-activated binders*
AAMs	*Alkali-activated materials*
AM	*Anode mud*
ANOVA	*Analysis of variance*
BA	*Bottom ash*
BAT	*Best available technologies*
BREFs	*Best available technologies reference documents*
C&DW	*Construction and demolition waste*
CE	*Circular economy*
CFA	*Coal fly ash*
CFA-FCBs	*Coal fly ash-fired clay bricks*
CFBC	*Circulating fluidized bed combustion*
CLSM	*Controlled low strength material*
CPR	*Construction products regulation*
CS	*Cadmium sponge*
EAFD	*Electric arc furnace dust*
EC	*European Commission*
EPA	*Environmental protection agency*
FA	*Fly ash*
FAA	*Fly ash type A*
FAB	*Fly ash type B*
FB	*Foundry by-product*
FB-FCBs	*Foundry by-products-fired clay bricks*
FBCB	*Fluidised bed coal boiler*
FCBs	*Fired clay bricks*
FESEM	*Field emission scanning electron microscopy*
GGBFS	*Ground granulated blast furnace slag*
GHG	*Greenhouse gas*
HW	*Hazardous waste*
ICP-AES	*Inductively coupled plasma-atomic emission spectroscopy*
ICP-MS	*Inductively coupled plasma-mass spectrometry*

IPPC	*Integrated Pollution Prevention and Control*
LCA	*Life cycle analysis*
LER	*List of European residues*
LOI	*Lost of ignition*
MCA	*Multi-criteria analysis*
MSWI	*Municipal solid waste incineration fly ash*
NHW	*Non-hazardous waste*
OPC	*Ordinary Portland cement*
PRTR	*Pollutant release and transfer register*
RLE	*Roasting-leaching-electrowinning process*
S/S	*Solidification/Stabilisation*
TCLP	*Toxicity characteristic leaching procedure*
TGA	*Thermogravimetric analysis*
TRL	*Technology readiness level*
XRD	*X-ray diffraction*
XRF	*X-ray fluorescence*
ZPR	*Zinc plant residues*

TABLES INDEX

FIGURES INDEX

Chapter .1

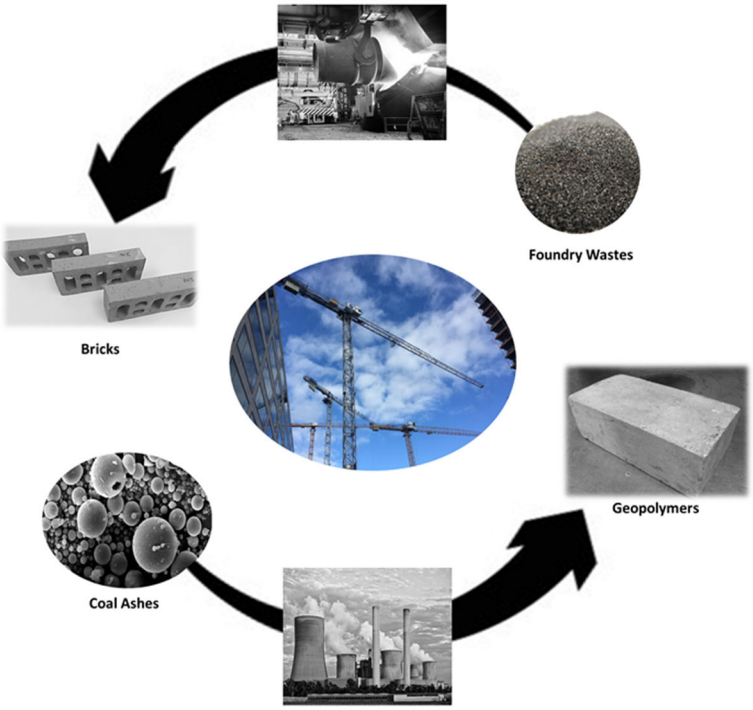

Thesis framework and research hypothesis

1 THESIS FRAMEWORK AND RESEARCH HYPOTHESIS

1.1. RESUMEN

El sistema económico actual está basado en una producción lineal y cerrado, donde cada uno de los procesos consume recursos naturales y genera residuos, que en su mayoría son depositados en vertederos. A lo largo de las últimas décadas, un nuevo pensamiento medioambiental está despertando y produciendo un cambio de mentalidad a todos los niveles. En esta línea, una de las iniciativas clave a nivel europeo es la estrategia 2020 que promueve el aprovechamiento de posibles sinergias en los procesos evitando el desperdicio de recursos, naturales y alternativos.

La ciencia ha dado lugar al planteamiento de un nuevo escenario tecnológico interconectado, donde los procesos industriales dejen de ser lineales y los residuos sean considerados como los nuevos recursos del siglo XXI. Las corrientes residuales procedentes de procesos industriales tienen potencial para su explotación en determinados ciclos productivos. El reto actual es delimitar qué procesos productivos son los más atractivos para absorber grandes cantidades de residuos, sin que esto conlleve un perjuicio en las propiedades de los productos finales, así como que causen daños al medioambiente.

El sector de la construcción lleva años introduciendo residuos industriales en sus productos. Desde el punto de vista productivo, el proceso cerámico presenta una gran variedad de materiales y composiciones para fabricar la amplia gama de productos cerámicos existentes. Esto último, sitúa a la industria cerámica como un sector que podría utilizar diferentes tipos de corrientes residuales. Por otro lado, el cemento Portland genera aproximadamente una tonelada de CO_2 por tonelada de cemento generado lo que representa que esta industria sea la responsable del 5-7 % de emisiones globales de CO_2 a la atmosfera. Por esta razón en la actualidad, la comunidad científica se está centrando en el desarrollo de nuevos cementos activados alcalinamente o geopolímeros. Los geopolímeros están basados en precursores de aluminosilicatos, por lo que, estos nuevos materiales representan una excelente vía para la utilización/valorización de residuos industriales.

De la necesidad de continuar rediseñando los procesos industriales tradicionales para lograr un sistema productivo interconectado, surge esta Tesis Doctoral que tiene por título "Aprovechamiento de residuos industriales como materia prima secundaria en prácticas de producción circular", desarrollada en el grupo de investigación "Green Engineering and Resources", del Departamento de Química e Ingeniería de Procesos y Recursos, de la Universidad de Cantabria. Partiendo del conocimiento adquirido tanto en los trabajos previos realizados en el grupo de

investigación como en la etapa de revisión bibliográfica, en este trabajo se ha establecido una premisa directamente ligada a tres hipótesis y tres preguntas de investigación.

Teniendo en cuenta las hipótesis y preguntas de investigación planteadas, el objetivo principal de esta tesis doctoral es incorporar y/o utilizar residuos industriales térmicos en procesos cerámicos y de baja energía (geopolímeros) para evaluar su viabilidad como materias primas secundarias en la producción de materiales de construcción y de este modo impulsando prácticas de economía circular. Para la consecución del objetivo general se han establecido una serie de objetivos específicos que se cumplirán con los resultados presentados en este trabajo.

Se obtuvieron resultados de la incorporación de residuos industriales de diferentes procesos térmicos en procesos cerámicos a escala laboratorio. Se analizaron las propiedades tecnológicas y medioambientales de los productos finales, así como la estimación de emisiones gaseosas del proceso de cocción. Además, se establecieron modelos matemáticos para predecir el comportamiento de incorporar estos residuos en las propiedades finales el producto y se realizó una optimización de las mezclas usando Análisis Multi-criterio como herramienta de toma de decisiones en base a unos criterios, técnicos, medioambientales, y económicos y escenarios propuestos. Se realizó una prueba industrial incorporando uno de estos residuos, arenas de fundición, en procesos cerámicos y se evaluaron las propiedades tecnológicas y medioambientales de los productos finales, así como la estimación de las emisiones gaseosas. Por último, se obtuvieron resultados del Análisis de Ciclo de Vida para determinar la evaluación ambiental de estos nuevos productos frente a los productos convencionales a escala industrial.

Se han realizado estudios para determinar la viabilidad de la incorporación de residuos térmicos como precursores y subproductos alcalinos como activadores en procesos de baja energía para obtener geopolímeros. Además de demostrar la viabilidad de los residuos y subproductos, se realizaron estudios de reactividad de los residuos, así como un análisis microestrutural de los geopolímeros finales para validar los productos obtenidos. Estos geopolímeros desarrollados con residuos y subproductos fueron utilizados para inmobilización residuos ácidos peligrosos procedentes de procesos hidrometalúrgicos. Los productos Solidification/Estabilización fueron evaluados tecnológica y medioambientalmente de acuerdo con la normativa europea de vertido. Para finalizar, se realizó un diseño factorial de experimentos para optimizar los parámetros de la geopolimerización usando como variables de respuesta la lixiviación de los contaminantes críticos.

Una vez demostrada la viabilidad de las cenizas volantes combustión de carbón en la obtención de geopolímeros en procesos de baja energía, se presenta el reto de

no usar ninguna materia prima virgen. Se realizaron geopolímeros con cenizas volantes y de fondo, procedentes de la combustión de lechos fluidizados, como precursores con bajos contenidos de Si y Al. La viabilidad técnica de estos residuos en aglutinantes activados alcalinamente se realizó mediante las propiedades tecnológicas de los productos finales. Además, un estudio mineralógico y microestructural fue realizado para determinar la validación de estos productos finales.

Con la realización de esta tesis, se ha demostrado y concluido la viabilidad de incorporar residuos industriales térmicos en procesos cerámicos y de baja energía. La incorporación de estos residuos permite una eficiencia de materiales en los procesos cerámicos, una eficiencia energética al poder ser utilizados en la obtención de geopolímeros y una eficiencia dual de materiales y energética al poder obtener geopolímeros exclusivamente con residuos sin emplear materias primas virgenes. Se ha concluido que estos residuos se pueden convertir en los principales recursos en procesos productivos permitiendo crear prácticas producciones circulares en lugar de las producciones lineares actuales.

- ABSTRACT

The current economic system is based on a lineal and close-cycle production where each one of the processes consumes natural resources and generates residues. Most of these residues are disposed of in landfills. Over the last decades, new environmental thinking is appearing producing a change of mentality at all levels. In this sense, one of the key European initiatives is the 2020 strategy that promotes possible synergies among the process avoiding waste of natural and alternative resources.

Science has given rise to the approach of a new interconnected technological scenario, where industrial processes are no longer closed and where waste were considered the new resources of the 21st century. Residual streams from industrial processes have the potential to be exploited in certain productive cycles. The current challenge is to delimit what processes are the most attractive to assimilate big amounts of residues without this harming the quality of the final products, as well as causing damage to the environment.

The construction and building sector has been introducing industrial residues in its processes for several years. From a productive viewpoint, the ceramic sector has a wide variety of materials and compositions to manufacture bricks, tiles, and so on. Thus, the ceramic industry can position itself as a sector that could use different types of waste streams. On the other hand, Portland cement generates around 1 tonne of CO_2 per tonne of cement which represents 5-7 % of global CO_2 emissions. For this

reason, the scientific community is being focused on the development o new alkali-activated cement, also known as geopolymers. Geopolymers are based on aluminosilicates precursors, so these new materials represent an excellent pathway for industrial waste use and valorisation.

From the need to redesign traditional industrial processes to achieve an interconnected production system, the line of this research entitled "Use of industrial waste as secondary raw material in circular production practices" appears. This line was developed by the research group "Green Engineering and Resources", in the Department of Chemistry, Process Engineering and Resources, of the University of Cantabria. Starting from the knowledge acquired both in the previous works carried out in the research group and the bibliographic review stage, in this work a premise directly linked to three hypotheses and three research questions has been established.

Taking into account the hypotheses and research questions raised, the main objective of this doctoral thesis is to incorporate and/or use thermal industrial waste in intensive energy processes (ceramics) and low-energy processes (geopolymers) to evaluate their viability as secondary raw materials in the production of construction materials promoting circular economy practices. To achieve the general objective, a series of specific objectives have been established that will be fulfilled with the results presented in this work.

From the incorporation of thermal industrial residues in ceramic processes, results at a laboratory scale were obtained. Then, the technological and environmental properties of the final products were analysed, as well as the estimation of gaseous emissions from the firing process. In addition, mathematical models were established to predict the behaviour of incorporating these residues in the final properties of the product, and optimisation of the mixtures was carried out using multi-criteria analysis as a decision-making tool based on proposed criteria and scenarios. An industrial test was carried out by incorporating these residues into ceramic processes and the technological and environmental properties of the final products were evaluated, as well as the estimation of gaseous emissions. Finally, the results of the Life Cycle Analysis were obtained to determine the environmental evaluation of these new products compared to conventional products.

Studies have been carried out to determine the feasibility of incorporating thermal residues as precursors and alkaline by-products as activators in low-energy processes to obtain geopolymers. In addition to demonstrating the viability of the residues and by-products, studies of the reactivity of the residues were carried out, as well as a microstructural analysis of the final geopolymers to validate the products obtained. These geopolymers developed with residues and by-products were used for S/S

hazardous acid residues from hydrometallurgical processes. The S/S products were technologically and environmentally evaluated by the European discharge regulations. Finally, a factorial design of experiments was carried out to optimize the geopolymerisation parameters using the leaching of critical contaminants as response variables.

Once the viability of fly ash in obtaining geopolymers in low-energy processes has been demonstrated, the challenge of not using any virgin raw material arises. Alkali-activated binders were made with fly and bottom ash, from the combustion of fluidized beds, as precursors with low contents of Si and Al. The technical feasibility of these residues in binders was made through the technological properties of the final products. In addition, a mineralogical and microstructural study was carried out to determine the validation of these final products.

With the completion of this thesis, the feasibility of incorporating thermal industrial waste in ceramic and low-energy processes has been demonstrated and concluded. The incorporation of these residues allows material efficiency in ceramic processes, energy efficiency as they can be used to obtain geopolymers, and dual material and energy efficiency as geopolymers can be obtained exclusively with waste without using natural raw materials. It has been concluded that these residues can be converted into the main resources in production processes, allowing the creation of circular productions instead of the current linear productions.

1.2. CONTEXTUALISATION AND CURRENT LANDSCAPE

1.2.1. Circular economy – intelligent reuse of waste

The recovery of the world's society from the impact of the COVID-19 pandemic may be an incentive to advance sustainable development strategies that respond to the challenges of climate change and environmental degradation. One of the most important tasks to achieve them is the mobilisation of the industry to promote a clean and circular economy, as proposed in the European Strategy of the Green Deal 2019 for a sustainable future and also contributes to achieving the long-term United Nations Sustainable Development Goals (Borchasdt, et al., 2020; Vinvevica-gaile et al., 2021). Circular Economy or also called Industrial Ecology has aroused a growing interest as a practical tool in the political-industrial field. Initially, the concept of Industrial Ecology was associated with the metaphor between natural and industrial ecosystems. In an industrial ecosystem, the waste generated by one company would be used as a resource by another, in this way the residual flows would not leave the industrial system nor would they have negative impacts on the systems as an emerging field that examines the flows of materials and energy at various scales within a strategic sustainable development (Grdic et al., 2020). It can be concluded that the Circular Economy model gives waste a fundamental role, based on its intelligent reuse, to convert it into raw material for new technological products, thus reducing energy expenditure and generating value as an asset for industry and companies (Sarc et al., 2019). Concretely, it is a fact that the materials industry is strategic for the European economy, moving towards a circular economy could generate a net increase of 700,000 jobs in the EU by 2030. It is therefore a first-rate technology sector, and any contribution to improving it is of great scientific and economic interest (Hertwich et al., 2020).

Construction is a sector that has very important economic dynamics worldwide since it is a natural engine for generating wealth. It is also fundamental in social terms due to its contribution to indirect employment, qualified workforce, professionals, and the generation of scientific and technological knowledge. But it cannot be ignored that it also has a great impact on the environment; since to its credit, there are effects of resource depletion, waste generation, greenhouse gas emissions, and hazardous substances, among others (Yifei Yu et al., 2022). Therefore, with the rise of Sustainable Construction, interest has arisen in environmentally optimizing the materials used in this important activity. On the other hand, the construction industry is a productive activity in which economic conditions play a very important role. To carry out any project it is necessary to consider that resources are limited, and energy saving is necessary, therefore the ecological criteria in the materialisation of the processes must

be applied. It is appropriate to frame it within the scope of the circular economy practice, based on producing goods and/or services, reducing the consumption and waste of resources used, by intersecting environmental and economic aspects. To promote this dynamic, the prices of raw materials should reflect the environmental impacts, in this way a rational use of resources could be achieved since it would reflect the real cost of the activity. In conclusion, raw materials extracted from nature should be taxed with a green tax, while if they replace technological nutrients or industrial residues, they should be credited. The main objective of green taxes is the conservation and protection of the environment. At the same time, they promote the use of technological nutrients that are usually abandoned, degrading the environment. These resources must be designed to be able to be assembled and reused many times, promoting the use of residual materials and energy savings, thus closing cycles, and therefore reducing their environmental impacts (Malabi Eberhardt et al., 2022).

The recovery of waste as secondary raw materials in the production of construction materials could solve the problems associated with both the depletion of natural resources and the disposal of industrial waste. The ceramic sector, as well as in the cement sector, can assimilate large flows of alternative materials of diverse origins without the need for significant modifications in the production process and negative effects on the properties of the final product. In addition, the availability of potentially toxic and/or dangerous substances in the environment is reduced, as is the depletion of natural resources and in some cases energy consumption, as well as the reduction of gaseous pollutant emissions (Cifrian et al., 2019; Grdic et al., 2020).

1.2.2. Fired clay products incorporating industrial waste

Clay minerals, mainly aluminosilicates, are a resource widely used in industry for their well-known properties such as plasticity, fire resistance, and their wide distribution, but from an environmental engineering point of view, the relevant properties are cation exchange capacity, structure, texture, and surface area. The use of clay minerals as potential sorbent material for organic and inorganic contaminants has increased in recent decades (Ozona et al., 2019). Also, the mineralogical composition of clay-based ceramic products includes silicate phases capable of dissolving considerable amounts of metals in their structure. Furthermore, high-temperature firing conditions required in the manufacture of clay-based ceramic products make them good potential agents to incorporate waste into their matrices (Magalhaes et al., 2004; Freyburg and Schwarz, 2007).

On the other hand, among the many industrial processes in which clay is used is the manufacture of fired clay bricks (FCBs), one of the most extended construction

materials (EC, 2020). FCBs are frequently produced from non-renewable materials or cementitious materials at high firing temperatures, which implies environmental damage due to the extraction of raw material, greenhouse gas (GHG) emissions, and air pollution globally. Recently, some authors are using a socio-technological lens to identify alternatives to mitigate the climatic effects of ceramic processes and products to make their life cycle more sustainable. In this line, transversal options for the decarbonisation of the ceramic industry as recycling, resource efficiency, and material substitution touch across all levels of the ceramic system are shown (Del Rio et al., 2022).

Research and application work carried out over the last decades have shown that the ceramic industry can incorporate different types of waste without degradation of properties. These residual materials can be classified according to their specific nature and origin, using the European waste list, as well as by the different roles they play in the ceramic matrix: (i) fluxing agents; (ii) filler materials; (iii) clay substitutes; (iv) fuels (oxidizers); (v) pore formers; (vi) agents affecting other properties (Coronado, et al., 2015) In this way, the incorporation of industrial waste in clay based-ceramics contributes toward cleaner production practices and has been addressed by many scientific works during the last two decades (Zhang et al., 2018). Four groups of waste can mainly be determined according to their nature (Muñoz-Velasco et al., 2014; Contreras et al. 2020): sludges from different industrial processes (Eliche-Quesada et al., 2016; Beshah et al., 2021; Amin et al., 2019); inorganic waste, mainly from mining and metallurgy waste processes (Belmonte et al., 2018; Sharif et al. 2017); organic waste from paper manufacturing plants and also biomass of different biological activities (Da Fonseca et al. 2014; Demir et al., 2005; Eliche-Quesada et al., 2012) and ashes, mainly from coal energy production, and municipal solid waste and biomass incineration (Eliche-Quesada et al., 2016; Sutcu et al., 2019; Brunner et al. 2015; Vassilev et al., 2013).

Recently, a comprehensive study presented by the research group of Dondi et al. (2021) shows that the main obstacle to waste recycling from a Circular Economy perspective is the lack of knowledge of the effect of waste in the manufacture of fired clay products. Waste recycling is analysed from the point of view of the industry, considering several aspects: technological behaviour, technical performance, environmental impact, and economic sustainability. The results are expressed in terms of Technology Readiness Level TRLs, at three levels: The higher TRLs, relative to industrial practice, residues with composition and technological behaviour similar to ceramic raw materials; An intermediate level is represented by residues suitable for recycling but not yet integrated into industrial production, such as sawing sludge, coal fly ash, spent foundry sand, sewage sludge, cathode tube glass. The issue preventing their recycling is due to the behaviour during the ceramic process and

the need for preventive treatments to avoid the release of hazardous components and potential pollutant emissions during firing. At the lowest TRLs, waste is evaluated at the laboratory scale. In this case, oil refining sludge, coal bottom ash, biomass ash, galvanic sludge, dredging soil, the criticism is due to waste pretreatment and environmental issues (bad odors, fermentation, acid release, or possible leaching of hazardous substances or gaseous emissions) than to ceramic manufacturing. It is concluded that several residues can play a role as filler or flux, if there is an adequate technological characterisation, therefore, more scientific and technological research is required to improve the tested residues to the lower TRLs (Dondi et al., 2021; Zanelli et al., 2021).

On the other hand, although the ceramic industry in the context of the European Union is showing innovative solutions to move toward the Circular Economy, technical and regulatory barriers do not allow scaling up current initiatives or starting new ones. Such as various interpretations of end-of-waste and by-products status among the Member States and the lack of a well-functioning European market for secondary raw materials through standards to improve their quality and traceability. For example, the limit values for eluates from leaching tests in recycled materials and industrial by-products should be harmonized in all European countries. While, concerning technical barriers, the need for a waste collection, sortion, and separation system, as well as the adaptation of technical requirements of installations are identified by the European Ceramic Industry Association (Cerame-Unie, 2020).

Construction Products Regulation (CPR) 305/2011 of the European Parliament and of the Council of March 9, 2011, establishes the harmonized conditions for the marketing of construction products. The CPR establishes that constructions must be designed and executed in such a way that they are not a threat to hygiene and the environment throughout their life cycle, both in use and in demolition. Sustainable use of natural resources is also established, in particular by promoting the use of secondary raw materials. The development of this regulation should establish technical compliance specifications that currently have not yet been established. The technological properties of the products and/or materials are defined by the requirements of the certificates of each product and/or material. However, there is no harmonisation to determine the environmental performance of materials derived from waste, when used in construction or civil works. Each member state must decide on the marketing of each construction product. For this reason, the European Commission (EC) is developing the regulations that will incorporate harmonized evaluation methods that will act as technical specifications that products must meet for a given use, together with a database where the dangerous substances that will be considered will be collected (Sebastian Wall, 2021).

Due to the different origins of the waste, its incorporation into ceramic processes must be evaluated from an integral point of view, considering the technological and environmental properties of the new materials, as well as the emissions generated during the process. The Construction Products Regulation (CPR), as well as the Life Cycle Analysis (LCA) and the Environmental Product Declaration (EPD) set the basic requirements on sustainability that define the relevant and specific information about the product and the associated environmental impacts throughout their life cycle (Allacker et al., 2014; Passer et al., 2015). Current trends in marketing policies and strategies for new products are aimed at providing product environmental information. This environmental information allows for evaluating the sustainability of new products before they are available on the market. On the other hand, decision-making tools such as Multi-Criteria Analysis (MCA) allow the final ceramic products to be evaluated from an optimal perspective, not only technological and environmental but also in economic and social aspects, making a truly innovative commitment in this sector and moving towards a Circular Economy (Dosal et al., 2013; Del Rosario, et al., 2021).

1.2.3. Alkali-activated materials from industrial waste

Currently, the International Energy Agency (IEA) proposes a global plan to reduce CO_2 emissions. This plan proposes a reduction of around 25 % in the cement industry between 2007 and 2050. In the same period, there is a forecast for the growth of cement production by 50 %. Both production and emission data seem incompatible (International Agency Energy, 2018). The use of alternative fuels, biomass, and supplementary materials in the concrete production industries does not seem sufficient to reduce CO_2 emissions (Damtoft et al., 2008, Barcelo et al., 2014). The study and investigation of new ecological and sustainable materials are crucial to reducing the Portland cement carbon footprint.

Alkali-activated materials (AAMs) or alkali-activated binders (AABs) encompass essentially any binder system that derives from the reaction between an alkali metal and a solid with some silicon content. This solid may be a silicate or aluminosilicate precursor, such as metallurgical slag, natural pozzolan, or thermal fly ash, while alkali sources may include any soluble substance that supplies alkali metal cations, raises the pH value of the mixed reaction, and accelerate the dissolution of the solid precursor, such as alkali hydroxides, silicates, carbonates, sulphates or aluminates. Among the AAMs, the so-called geopolymers stand out, considered in many cases as a subset of the AAMs, where the binder phase is a highly coordinated aluminosilicate, with an amorphous pseudo-zeolitic structure (Mellado et al., 2014; Pasuello et al. 2017). Although some researchers consider that the term

"geopolymer" and "alkali-activated binder" represent different chemical concepts, other authors consider that it is more appropriate to use them without distinction, despite their difference (Palomo et al., 2021).

Geopolymer materials have been applied in a wide variety of engineering sectors, including their use as a Portland cement substitute, for waste immobilisation, fire-resistant panels, and refractory cement. The use of these new inorganic materials, as a partial or total substitute for traditional cement, plastics, and ceramic-based products, contributes positively to the reduction of global pollution and growth in sustainable development, mainly because the production of traditional materials brings with it the emission of large volumes of polluting gases, high energy consumption and natural resources (Provis and Deventer, 2009; Pacheco-Torgal, 2015).

Geopolymers, of growing interest in the scientific-technological field, is an alternative to the extensive use of Ordinary Portland Cement (OPC), more sustainable and with a smaller environmental footprint; it requires less energy to manufacture and generate between 60 and 80 % less CO_2 emissions (Yang et al., 2013). In the 1960s, at a time of strong construction growth in Russia, Glukhovsky was one of the first researchers to study AAMs, looking for alternatives to OPC. He found that AAMs had similar hardening and compressive strength performance to OPCs. Years later, in 1972, in France, Davidovits first coined the term geopolymer to refer to a three-dimensional synthetic structure of alkali-activated aluminosilicates (Davidovits, 2011).

Obtaining geopolymers consists of the reaction of a powder precursor, with a high content of amorphous aluminosilicates, with a strongly alkaline activating solution. The result of the reaction, after a suitable curing time, is the obtaining of a compact solid with good mechanical properties and general formula: $Mn[\text{-Si-O}_2]z[\text{-Al-O}]_n{\cdot}wH_2O$. In general terms, the geopolymerisation reaction is a polycondensation, which begins when the aluminosilicates dissolve in the strongly alkaline medium to form free tetrahedrons of silica and aluminum cations coordinated with oxygen. The tetrahedrons are linked by oxygen atoms to form a three-dimensional structure similar to that of a zeolite, following the order (-Si-O-Al-O-). The cation in the alkaline activating solution provides the positive charge that maintains the electro neutrality of the solution. Under appropriate temperature conditions (between 20 and 90 ºC) and a certain curing time, a gel is formed that solidifies by ionic interaction, forming a three-dimensional solid structure, the base of the geopolymer. The reaction mechanisms can be summarized in the following stages: dissolution of the amorphous phases in the alkaline solution, condensation of the monomers, and gelation. The precursors become oriented, and the viscosity of the gel increases until the three-dimensional network is formed. Finally, the monomers polymerise, and

crystallisation takes place. Depending on the ratio of alumina to silica, different monomers and polymers can be formed (Xu and Deventer, 2000; Davidovits, 2011; Garcia-Lodeiro et al., 2015).

Numerous research works have emerged in recent years (Zhao et al., 2021; Zakka et al., 2021; Alnahhal et al., 2021; Ji and Pei, 2019; Samarakoon et al., 2019) to study the synthesis of geopolymers as a technique for incorporating waste or by-products into their formulation. It is an interesting solution for the revaluation of by-products that have completed their life cycle, being used as a secondary source in a second production cycle. In this sense, residues with alumina and silica content can be used as precursors for the formation of geopolymers, regardless of their alkali content. On the other hand, Palomo et al., (2021) consider that the industrial and commercial development of AABs is limited as an alternative to Portland clinker because it is not possible to guarantee a stable supply of precursors with the time. To avoid the raw material limitations for the manufacture of AABs worldwide, they propose the alkaline activation of natural (non-waste) materials mostly, manufacturing aluminosilicate precursors in industrial facilities (Palomo et al., 2021).

Despite the environmental benefits and the long history of academic and industrial development of AAM over the past half century, there has been until very recently no significant commercialisation of the technology. Which has been mainly due to a lack of drivers for uptake. Recently the image of OPC technology is being questioned due to energy costs in the form of carbon footprint. Which acts as an important motivating factor to consider using alternative materials. Therefore, it is necessary to quickly address the tangible barriers from technical to regulatory. Since, now the cost of carbon will have both a commercial and a social cost attached to it over the coming decades (Duxon and Deventer, 2009; Farooq et al., 2021). Therefore, based on the concept of sustainability, the industrialisation and commercialisation of any alkaline binder for the construction sector are advantageous compared to Portland cement. For this reason, there is an urgent need to explore standardisation formulas that allow the commercial development of sustainable binders (Palomo et al., 2021).

1.3. HYPOTHESIS & OBJECTIVES

The work presented in this doctoral dissertation was conducted at the Chemistry and Process & Resources Engineering Department of the University of Cantabria (Spain), within the Green Engineering & Resources (GER) research group, and specifically, on the topic of *Valorisation of industrial waste by incorporation to ceramic matrices*. This research topic arises from the need to redesign resource life cycles considering materials historically discarded as waste as high-value materials. The previous dissertation works carried out in this research group provided relevant results about the valorisation of sediments, foundry sand (Alonso-Santurde, 2010), Waelz slag (Quijorna, 2013), foundry waste (Coronado, 2014), and electric arc furnace dust (Díaz, 2016) in ceramic processes. In addition, previous dissertation work provided significant knowledge in the valorisation of coal fly ash to develop geopolymer matrices (Díaz, 2016). Considering this background, the present Ph.D. thesis aims to carry forward these works.

This Ph.D. study was supported by the project "*Valorisation of fly ash in ceramic products and fly ash-based products*" funded by Solvay Química S.L, and the project supported by the European Regional Development Fund "*Desarrollo experimental de productos cerámicos de arcilla cocida incorporando residuos de la industria de la fundición*".

Figure 1.1 shows the methodology applied in this thesis to establish the main hypotheses and the objectives, general and specifics, of this work. Firstly, one premise was formulated considering the knowledge of the state of art according to the literature review. Based on this premise, three hypotheses and three research questions were formulated, which are directly linked to the objectives established in this thesis.

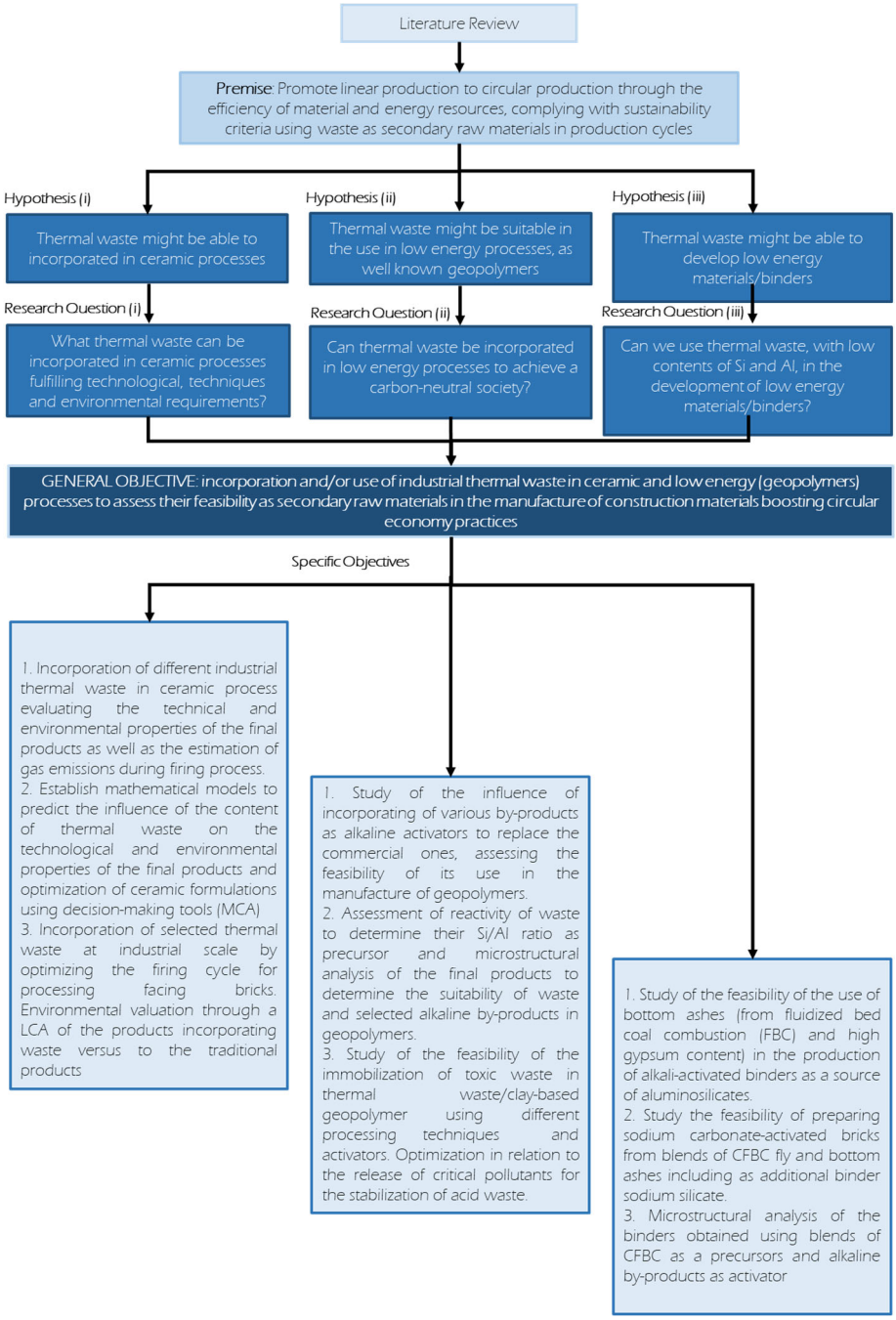

Figure 1.1. Methodology to establish the hypothesis and the main objective of this thesis.

1.4. STRUCTURE OF THE THESIS

The present thesis, as stated before, pursues the main objective of incorporating and/or using industrial thermal waste in ceramic and low energy (geopolymers) processes to assess their feasibility as secondary raw materials in the manufacture of construction materials, boosting circular economy practices. To achieve this goal, three results chapters were raised:

- CHAPTER 2 entitled "Thermal Process Waste in Fired Clay Ceramic Process"
- CHAPTER 3 entitled "Coal Combustion Ashes in Low Energy Clay Ceramic Process"
- CHAPTER 4 entitled "Coal Fluidized Bed Combustion Ashes in Low Energy Clay Ceramic Process"

Each one of the chapters requires a big set of experiments and results of waste characterisation, mixtures formulation to obtain ceramic bricks and geopolymers, analysis of technological, mineralogical, microstructural, environmental properties of the obtained products, and gas emission estimation of the ceramic process.

In chapter 2 results of incorporation of a combustion waste (coal fly ash) in ceramic processes were shown and coal fly ash-fired clay bricks (CFA-FCBs) at a laboratory scale were prepared. The second part of chapter 2 includes the incorporation of several foundry waste in ceramic processes and the preparation of foundry by-products-fired clay bricks (FB-FCBs) at a laboratory scale was performed. In the last part of chapter 2, foundry sands were selected to make foundry sand-fired clay bricks on an industrial scale.

Unlike the previous chapter where various residues were introduced into energy-intensive processes to obtain ceramics, chapter 3 relies on the incorporation of CFA in low energy-consuming processes to obtain geopolymers. In addition, alkaline by-products provided from a local industry were used as alkaline activators of the CFA-clay activated bricks. Finally, apart from the low energy-consuming bricks, CFA-clay binders were also made at a laboratory scale.

Once demonstrated the suitability of coal fly ashes to get alkali-activated binders into a low-energy consuming process, the challenge of avoiding any natural resource (clay) is proposed in chapter 4. Therefore waste-based alkali-activated binders were developed in this chapter by using circulating fluidized bed combustion (CFBC) bottom and fly ashes. The technical feasibility of CFBC was also checked in terms of compressive strength and water absorption. Besides mineralogical, microstructural, and thermogravimetric behaviour of the CFBC alkali-activated binders were also analysed.

The timeline containing the four chapters that formed this thesis is shown in Figure 1.2.

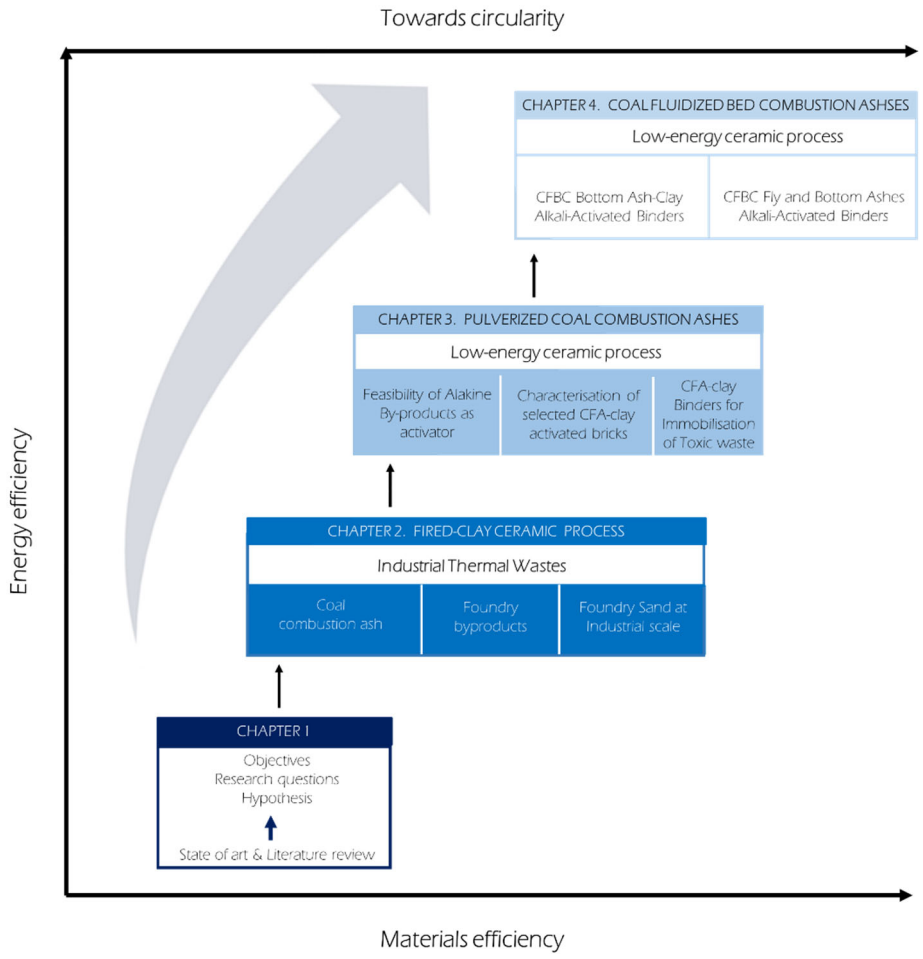

Figure 1.2. Evolution and summary of the thesis structure.

1.5. REFERENCES

- Allacker K, Mathieux F, Manfredi S, Pelletier N, de Camillis C, Ardente F, Pant R. Allocation solutions for secondary material production and end of life recovery: Proposals for product policy initiatives. Resour Conserv Recycl 2014; 88; 1-12. Doi: 10.1016/j.resconrec.2014.03.016.
- Alnahhal MF, Kim T, Hajimohammadi A. Waste-derived activators for alkali-activated materials: A review. Cem Con Comp 2021; 118; 103980. Doi: 10.1016/j.cemconcomp.2021.103980.
- Alonso-Santurde, R. (2010). Valorización de sedimentos marinos contaminados y arenas de fundición residuales en procesos cerámicos: evaluación técnica y medioambiental. Tesis Doctoral. Departamento de Química e Ingeniería de Procesos y Recursos. Universidad de Cantabria.
- Amin, S.H.K.; Elmahgary, M.G.; Abadir, M.F. Preparation and characterisation of dry pressed ceramic tiles incorporating ceramic sludge waste. Ceram. Silik. 2019, 63, 11–20.
- Belmonte, L.J.; Ottosen, L.M.; Kirkelund, G.M.; Jensen, P.E.; Vestbø, A.P. Screening of heavy metal containing waste types for use as raw material in Arctic clay-based bricks. Environ. Sci. Pollut. Res. 2018, 25, 32831–32843.
- Beshah, D.A.; Tiruye, G.A.; Mekonnen, Y.S. Characterisation and recycling of textile sludge for energy-efficient brick production in Ethiopia. Environ. Sci. Pollut. Res. 2021, 28, 16272–16281.
- Borchardt S, Buscaglia D, Barbero Vignola, G, Maroni M, Marelli, L. A text mining approach to map the EU recovery plan to the sustainable development goals. European Commission 2020.
- Brunner, P.H.; Rechberger, H. Waste to Energy—Key Element for Sustainable Waste Management. Waste Manag. 2015, 37, 3–12.
- Cifrian E, Coronado M, Quijorna N, Alonso-Santurde R, Andrés A. Waelz slag-based construction ceramics: effect of the trial scale on technological and environmental properties.J Mat Cyc Was Manag; 2019; 21; 1437-1448. Doi: 10.1007/s10163-019-00896-4.
- Contreras, M.; Gázquez, M.J.; Romero, M.; Bolívar, J.P. Recycling of industrial waste for value-added applications in clay-based ceramic products: A global review (2015–19). In New Materials in Civil Engineering; Samui, P., Kim, D., Iyer, N.R., Chaudhary, S., Eds.; Butterworth-Heinemann: Oxford, UK, 2020; pp. 155–219. ISBN 9780128189610.
- Coronado M., Blanco T., Quijorna N., Alonso-Santurde, R., Andrés, A. 2015. Chapter 3: Types of waste, properties and durability of waste-based fired masonry bricks. F. Pacheco-Torgal, P.B. Lourenco, J.A. Labrincha, V.M. John, N.P. Rajamane, (Eds) Eco-efficient Masonry Bricks and Blocks: Design, Properties and Durability. WP Wood head Publishing, Oxford, UK.
- Coronado, M. (2014). Foundry waste as new resources in ceramic processes – Analysis and modeling of technological & environmental properties. Doctoral Thesis. Department of Chemistry, Process & Resources Engineering. University of Cantabria.
- Davidovits J. Geopolymer: Chemistry & Applications; Institut Geopolymere: Saint Quentin, France, 2011.
- Del Rio, D.D.F.; Sovacool, B.K.; Foley, A.M.; Griffiths, S.; Bazilian, M.; Kim, J.; Rooney, D. Decarbonizing the ceramics industry: A systematic and critical review of policy options, developments and sociotechnical systems. Renew. Sustain. Energy Rev. 2022, 157, 112081.

- Demir, I.; Baspinar, M.S.; Orhan, M. Utilisation of kraft pulp production residues in clay brick production. Build. Environ. 2005, 40, 1533–1537.
- Díaz, M.C. (2016). Desarrollo de matrices cerámicas y geopoliméricas como vías de inmovilización de polvos de acería. Tesis Doctoral. Departamento de Química e Ingeniería de Procesos y Recursos. Universidad de Cantabria.
- Eliche-Quesada, D.; Corpas-Iglesias, F.A.; Pérez-Villarejo, L.; Iglesias-Godino, F.J. Recycling of sawdust, spent earth from oil filtration, compost and marble residues for brick manufacturing. Constr. Build. Mater. 2012, 34, 275–284.
- Eliche-Quesada, D.; Leite-Costa, J. Use of bottom ash from olive pomace combustion in the production of eco-friendly fired clay bricks. Waste Manag. 2016, 48, 323–333.
- Farooq F, Xin J, Javed MF, Akbar A, Shah MI, Aslam F, Alyousef R. Geopolymer concrete as sustainable material: A state of art review. Const Build Mat 2021; 306; 124762. Doi: 10.1016/j.conbuildmat.2021.124762.
- Freyburg S, Schwarz, A. 2007. Influence of the clay type on the pore structure of structural ceramics. J of the European Ceramic Society, 27: 1727-1733.
- Grdic ZS, Nizic MK, Rudan E. Circular economy concept in the context of economic development in EU countries. Sustainability 2020; 12; 3060. Doi: 10.3390/su12073060.
- Ji Z and Pei Y. Bibliographic and visualized analysis of geopolymer research and its application in heavy metal immobilisation: A review. J Envir Manag 2019; 231; 256-267. Doi: 10.1016/j.jenvman.2018.10.041.
- Magalhaes J.M., Silva J.E., Castro F.P., Labrincha J.A., 2004. Effect of experimental variables on the inertisation of galvanic sludges in Clay-based ceramics. J of Hazardous Materials, 106B: 136-147.
- Malabi Eberhardt LC, Birkved M, Birgisdottir H. Building design and construction strategies for a circular economy. Archit eng des manag 2022; 18; 93-113. Doi: 10.1080/17452007.2020.1781588.
- Mellado, A.; Catalán, C.; Bouzón, N.; Borrachero, M.V.; Monzó, J.M.; Payá, J. Carbon footprint of geopolymeric mortar: Study of the contribution of the alkaline activating solution and assessment of an alternative route. RSC Advances, 2014, 4(45), 23846-23852.
- Muñoz Velasco, P.; Morales Ortíz, M.P.; Mendívil Giró, M.A.; Muñoz Velasco, L. Fired clay bricks manufactured by adding waste as sustainable construction material—A review. Constr. Build. Mater. 2014, 63, 97–107.
- Pacheco-Torgal F, Labrincha J.A, Leonelli C, Palomo A, Chindaprasirt P. Handbook of alkali-activated cements, mortars and concretes. Woodhead publishing: Waltham, MA, USA, 2015.
- Palomo, A.; Maltseva, O.; García-Lodeiro, I.; Fernández-Jiménez, A. Portland Versus Alkaline Cement: Continuity or Clean Break: "A Key Decision for Global Sustainability". Frontiers Chem. 2021, 9, 705475.
- Passer A, Lasvaux S, Allacker K, de Lathauwer D, Spirinckx C, Wittstock B, Kellenberger D, Gschösser F, Wall J, Wallbaum H. Environmental product declarations entering the building sector:critical reflections based on 5 to 10 years experience in different European countries. Build Comp Builds 2015; 20; 1199-1212. Doi: 10.1007/s11367-015-0926-3.
- Passuello, A.; Rodríguez, E.D.; Hirt, E.; Longhi, M.; Bernal, S.A.; Provis, J.L.; Kirchheim, A.P. Evaluation of the potential improvement in the environmental footprint of geopolymers using waste-derived activators. J. Clean. Prod. 2017, 166, 680-689.
- Provis, J.L.; van Deventer, J.S.J. Geopolymers: Structures, Processing, Properties and Industrial Applications; Woodhead Publishing: Waltham, MA, USA, 2009.

- Quijorna, N. (2013). Incorporación de escoria Waelz al sector cerámico: ejemplo práctico de ecología industrial. Tesis Doctoral. Departamento de Química e Ingeniería de Procesos y Recursos. Universidad de Cantabria.
- Samarakoon MH, Ranjith PG, Rathnaweera TD, Perera MSA. Recent advances in alkaline cement binders: A review. J Clean Prod 2019; 227; 70-87. Doi: 10.1016/j.jclepro.2019.04.103.
- Sarc R, Curtis A, Kandlbauer L, Khodier K, Lorber K.E, Pomberger R. Digitalisation and intelligent robotics in value chain of circular economy oriented waste management – A review. Was Manag; 2019; 95; 476-492. Doi: 10.1016/j.wasman.2019.06.035.
- Sharif, N.M.; Lim, C.Y.; Teo, P.T.; Seman, A.A. Effects of body formulation and firing temperature to properties of ceramic tile incorporated with electric arc furnace (EAF) slag waste. AIP Conf. Proc. 2017, 1865, 1–7.
- Sutcu, M.; Erdogmus, E.; Gencel, O.; Gholampour, A.; Atan, E.; Ozbakkaloglu, T. Recycling of bottom ash and fly ash waste in eco-friendly clay brick production. J. Clean. Prod. 2019, 233, 753–764.
- Vassilev, S.V.; Baxter, D.; Andersen, L.K.; Vassileva, C.G. An Overview of the Composition and Application of Biomass Ash. Part 1. Phase–Mineral and Chemical Composition and Classification. Fuel 2013, 105, 40–76.
- Wall S. CE marking of construction products – evolution of the European approach to harmonisation of construction products in the light of environmental sustainability aspects. Sustainability 2021; 13; 6396. Doi: 10.3390/su13116396.
- Xu H and van Deventer J.S.J. Geopolymerisation of alumino-silicate minerals. Int J Miner Process; 2000; 59; 247-266. Doi: 10.1016/S0301-7516(99)00074-5.
- Yang, K.-H.; Song, J.-K.; Song, K.I.I. Assessment of CO_2 reduction of alkali-activated concrete. J. Clean. Prod. 2013, 39, 265-272.
- Yu Y, Junjan V, Yazan DM, Iacob M-E. A systematic literature review on circular economy implementation in the construction industry: a policy-making perspective. Resour Conserv Recycl 2022; 183; 106359. Doi: 10.1016/j.resconrec.2022.106359.
- Zakka WP, Lim NHAS, Khun MC. A scientometric review of geopolymer concrete. J Clean Prod 2021; 280; 124353. Doi: 10.1016/j.jclepro.2020.124353.
- Zanelli, C.; Conte, S.; Molinari, C.; Soldati, R.; Dondi, M. Waste recycling in ceramic tiles: A technological outlook. Resour. Conserv. Recycl. 2021, 168, 105289.
- Zhang, Z.; Wong, Y.C.; Arulrajah, A.; Horpibulsuk, S. A Review of Studies on Bricks Using Alternative Materials and Approaches. Constr. Build. Mater. 2018, 188, 1101–1118.
- Zhao J, Tong L, Li B, Chen T, Wang C, Yang G, Zheng Y. Eco-friendly geopolymer materials: A review of performance improvement, potential application and sustainability assessment. J Clean Prod 2021; 307; 127085. Doi: 10.1016/j.jclepro.2021.127085.

Chapter 2.

Thermal Process Wastes in Fired Clay Ceramic Process

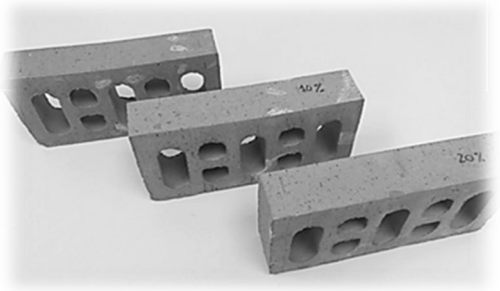

2. THERMAL PROCESS WASTE IN FIRED CLAY CERAMIC PROCESS

2.1. INTRODUCTION

Research works carried out in the last decade have demonstrated the ceramic industry can admit different kinds of residues without affecting end-quality properties. Such materials can be classified according to their specific nature and origin, according to the List of European Residues (LER), or the different roles they play within the ceramic matrix: fluxing agents, filler materials, clay substitutes, body fuels, pore formers and other agents (Coronado, 2014). Regarding the waste origin and the LER code, the most used for its valorisation in the ceramic industry are LER 01, 10, and 19. It is worth highlighting the residues that belong to the LER code number 10 that was used in this chapter. LER 10 are waste generated in the thermal process: power plants, other combustion plants, iron, steel, aluminium, lead industry, and zinc thermal metallurgy. Therefore, in this category coal fly ash, biomass fly ash, metal sludge, metal slags, and foundry sands are included (Baspinar et al., 2010; Jonker and Potgieter, 2005; Bhagat et al., 2011; Furnali et al., 2010).

The technological properties of the ceramic products resulting from the introduction of waste are defined by the requirements of the certificates of each product. The most commonly measured properties of fired clay bricks are compressive strength, water absorption, frost, efflorescence, shrinkage, and suction (Rehman et al., 2020). However, there is no harmonisation to determine the environmental behaviour of ceramic products derived from waste, neither in the tests nor in the components to be studied (Zhang et al., 2018). The Construction Products Regulation (Regulation EU 305/2011 CPR) establishes that construction materials must be designed and built in such a way that they do not cause damage to hygiene, health, or the environment during the life cycle of the material (use and demolition). The European Commission is developing the regulations that will incorporate harmonized evaluation methods that will act as technical specifications that products must meet for a given use, together with a database where the dangerous substances will be considered. The European Committee for Standardisation (CEN) is working on a draft in which release scenarios are proposed based on the characteristics and use of the construction product. Specifically, CEN/TC 351 'Construction Products - Assessment of release of dangerous substances' develops harmonized test methods to monitor the release of dangerous substances from construction products and (several

deliverables will publish in 2022, currently existing as Technical Specifications, EN 16637 on leaching tests and CEN/TS 17459 on ecotoxicity tests (CEN, 2022).

On the other hand, from the point of view of the environmental behaviour of the process, the cooking stage is a critical stage, due to emissions into the atmosphere (IPPC, 2007). In this stage, chemical and mineralogical transformations take place with absorption and release of heat, in which cooking gases are released, mainly carbon, nitrogen and sulphur oxides, fluorine, chlorinated compounds, heavy metals, and organic compounds due to the decomposition of the minerals present in the raw materials and the fuels used. It is due to these emissions that the ceramic industry is included in the scope of application of the European Directive on Integrated Pollution Prevention and Control (IPPC) and therefore in the European Pollutant Emission Register (EPER), establishing the Best Available Technologies (BATs), as well as the Emission Limit Values of the process (April 2021 Review of the CER BREF – Kick-off Meeting report).

In this chapter, several foundry by-products (FBs) were used as secondary materials for manufacturing fired-clay bricks. The Multi-Criteria Analysis (MCA) tool was applied to determine which one of the FBs is the most appropriate from technical, economic, and environmental criteria. Then, industrial tests will be conducted and Life Cycle Analysis (LCA) of the facing brick will be performed.

2.2. Coal Fly Ash-Clay Bricks

Coal Fly Ashes (CFA) are generated during the combustion of pulverised coal in coal-fired power stations; CFA is an industrial by-product. They are generated at 1200-1700 ºC from the various inorganic and organic constituents of the feed coal. Because of the scale of the variety of the components, CFA is one of the most complex anthropogenic materials that can be characterised. Approximately 316 individual minerals and 188 mineral groups have been identified in different CFA demonstrating their complexity (Blisset et al., 2012). This waste is an excellent illustration of the Circular Economy concept. Despite having a long history of utilisation, CFA is still being sent to landfills or stored in lagoons. 750 million tons of CFA are generated globally and of this only 20-50 % is utilised in applications other than land reclamation and restoration projects. CFA constitutes more than 75 % of carbon combustion products according to data from 2015, 300 million tons of CFA were landfilled per year in China, followed by Europe (100 million tons), India (100 million tons), and USA (70 million tons) (Vilakazi et al., 2022; Harris, 2016).

There are many varied applications where CFA can be valorised. These applications can be classified in different ways as shown in Figure 2.1. Classification is based on

the scale and the Technology Readiness Level (TRL) of the application: (i) Current: use of Fly Ash in applications at industrial scale; (ii) Future: use of Fly Ash in applications at laboratory scale or pilot plant. The second classification is based on whether the CFA need before or not for use treatments in this application. This classification can be distinguished: (i) Direct: Fly Ash does not require any pre-treatment for their use in these applications; (ii) Indirect: Fly Ash requires pre-treatment for their use in these applications. These two classifications are interrelated, as current applications use Fly Ash without needing any pre-treatment, while future applications that use Fly Ash need previous pre-treatments.

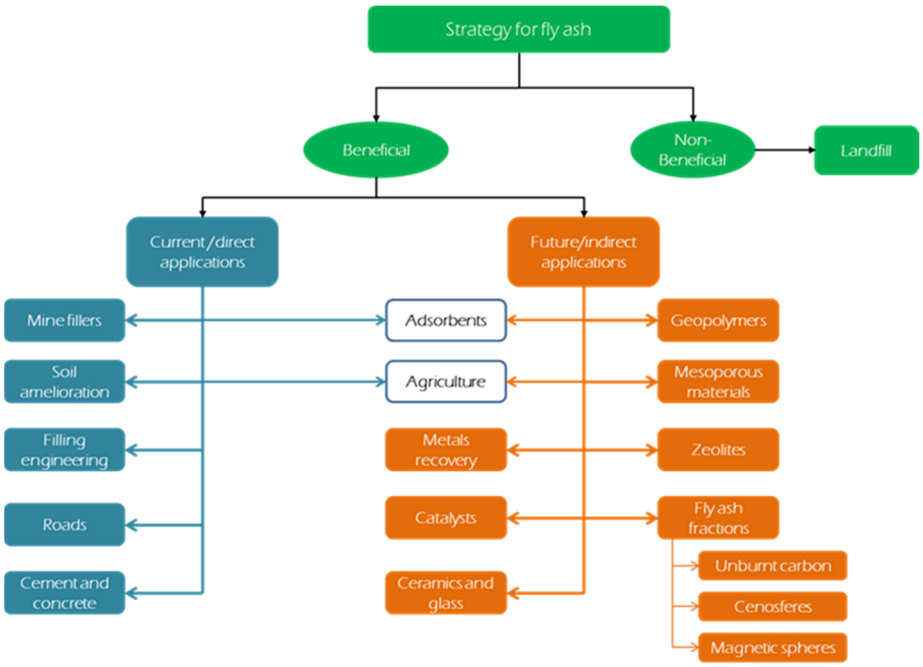

Figure 2.1. Scheme of the different applications of Coal Fly Ashes.

A comprehensive literature review was carried out checking more than 230 references. Based on the scheme presented in Figure 2.1, there is a wide variety of strategies for CFA valorisation. The strengths and weaknesses, and potential markets considerations of introducing CFA (class F) used in this thesis into four different sectors: (i) construction; (ii) civil engineering; (iii) cement, concrete, and ceramics; and (iv) agriculture are given in Tables A1.1 and A1.2 (Annex 1). These tables belong to the current and direct CFA applications. Regarding the future and indirect CFA applications, the strengths, weaknesses, and main remarks were again reviewed. In Table A1.3 two products, fired-clay bricks, and geopolymers were selected as the most promising CFA strategies in the ceramic, concrete, and cement industry. In

Table A1.4 the use of CFA as the catalyst and/or adsorbent for the treatment of effluent discharges. Finally, in Table A1.5, the recovery of CFA components is reviewed. Studies of metals, cenospheres, and unburnt carbon recovered from CFA were found in the literature.

CFA, which is generated in thermal power plants, typically constitutes around 80 % of the total ash, and approximately 30 % of the mass of coal consumed (CEDEX). It has been estimated that the world's 2300 coal-fired power station fleet creates approximately one billion tonnes of new fly ash each year. Therefore, the incorporation of CFA in the production of FCBs can be an important application, bearing in mind the large quantities of raw materials needed for FCB production (Xu et al. 2018). The valorisation of CFA contributes to the reduction in natural resources extracted as its composition is very similar to that of clay, SiO_2, Al_2O_3, and Fe_2O_3 with some minor constituents such as CaO and MgO and other inorganic elements. Amorphous material and crystalline phases as well as unburned or partially burned carbon residues represent its mineralogical composition (Hower et al. 2017). CFA is considered "non-hazardous" waste according to different regulations (EPA and EU) despite containing metals and metalloids such as, As, Pb, Zn, Ni, Cu, Mn, Cd, Cr, and Se at trace levels (Jayaranjan et al., 2014). However, due to serious environmental accidents, agencies such as the EPA have questioned the need to include them in a new classification such as special waste (Resource Conservation and Recovery Act, 2008) (EPA). Therefore, CFA disposal is an important issue worldwide due to its huge volume and its potential negative environmental impacts, which requires great disposal fees and the consequent negative Public Relations (PR) of the sector. On the other hand, unburned carbon in CFA is an indicator of defective combustion of the original fuel, mainly due to the ageing of the boilers (Elías, 2009). CFA can be valuable as a source of activated carbon or a source of coal to return to the boiler. However, an unburned carbon content greater than 10 % considerably reduces its pozzolanic capacity, preventing its recovery in cement and concrete industries (CEDEX). For this reason, in practice, only 30 % of the total ash produced in the world is re-used (ECOBA). These limitations in the recovery of ashes in the manufacture of concrete reinforce the need for a more rigorous study of its recovery in other industrial processes, specifically in the ceramic industry. Many studies have investigated the properties of clay-based bricks containing CFA to evaluate the technical performance of FCBs (Leiva et al., 2016; Wang et al. 2016; Kockal et al., 2012; Eliche-Quesada et al., 2018). Specifically, the study of the percentage of unburned in CFA on the final properties of FCBs, only Vasic et al. (Vasic et al., 2021) considered it as an input parameter in an artificial neural network model.

On the other hand, there is no harmonisation to determine the environmental behaviour of ceramic products incorporating waste; the most widely used leaching tests to evaluate them at the end of their useful life, as construction and demolition waste (C&DW), whether deposited in landfills or used as secondary raw material, are the compliance tests: TCLP (Toxicity Characteristic Leaching Procedure) (Eliche-Quesada et al., 2018; García-Ubaque et al., 2013; Singh et al., 2007) and the Equilibrium Leaching Test EN 12457 (Galán-Arboledas et al., 2017; Fernández-Pereira et al., 2011; Alonso-Santurde et al., 2010; Quijorna et al., 2011; Quijorna et al., 2012; Little et al., 2008). Specifically, in the case of ceramic products manufactured with coal ash, only very few authors (Leiva et al., 2016; Eliche-Quesada et al., 2018; Little et al., 2008) have reported equilibrium leaching test data of heavy metal mobility with different proportions CFA. Only Gupta et al. (2019) (Gupta et al., 2019) showed comparative results of batch and column leaching test of metal release, and the difference between bricks with/without CFA was minimal.

Furthermore, from the point of view of the environmental performance of the process, firing is a critical stage due to emissions into the atmosphere (EC, 2007). For this reason, the ceramic industry is included in the pollutant release and transfer register (PRTR), establishing the best available technologies (BAT) as well as the emission limit values of the process. Considering that the incorporation of waste can affect gaseous emissions, some authors have studied these effects on an industrial scale (Galán-Arboledas et al., 2017; Quijorna et al., 2011; Quijorna et al., 2012; Hamer et al., 2002; Anderson et al., 2002; García-Ubaque et al., 2007) and also on a laboratory scale (Dondi et al., 2002; Souza et al., 2008; Coronado et al., 2016). However, only extremely limited information has been obtained on the effects of the composition, mineral transformation, and firing parameters on these emissions.

As highlighted in the review of Zanelli et al. (Zanelli et al., 2021), it is essential for a technological transfer to the industrial practice of a correct evaluation of the technical performance of the FCBs incorporating waste as well as an assessment of the environmental behaviour through the leaching test of the final products and gas emissions during the firing process.

2.2.1. Raw Materials and Methodology

2.2.1.1. Raw Materials

Two illitic clays (Clay A and Clay B), currently used as traditional raw materials in two Spanish industrial ceramic processes (face bricks), and two combustion by-products, low calcium fly ashes (ASTM class F), with different contents of unburnt carbon, low (FAA) and high content (FAB), were used in this study to prepare the coal fly ash-fired clay bricks (CFA-FCBs).

Quarry clays were collected from two different industrial ceramic companies, and Fly ashes were supplied by coal combustion boilers. All of them are located in Cantabria region, Spain.

2.2.1.2. Processing Method

The methodology used in this work is represented in Figure 2.2. Both clays are subjected to a grinding process to achieve a particle size not exceeding 0.5 mm Clay A and 1 mm Clay B. The mixture of raw materials, Fly Ash, and Clay were realized with a laboratory mixer Raimondi, Iperbet model. The proportions of raw materials were calculated by weight and the necessary water was added to obtain a plastic mixture (between 5 and 10 % of moulding water). The mixture was processed by pressing in a hydraulic press Nanetti Mignon model SS/EA, which reaches 200 bar pressure, and prismatic moulds with dimensions of 80x40x20 mm. The samples were dried for 30 hours at 105 °C before the firing cycle, using a laboratory muffle furnace Hobersal, PR Model 12/300 capable of ramping temperature versus time of up to 16 points. The industrial firing cycle is provided by the ceramic companies reaching temperatures of 1021 °C for Clay A and 1058 °C for Clay B.

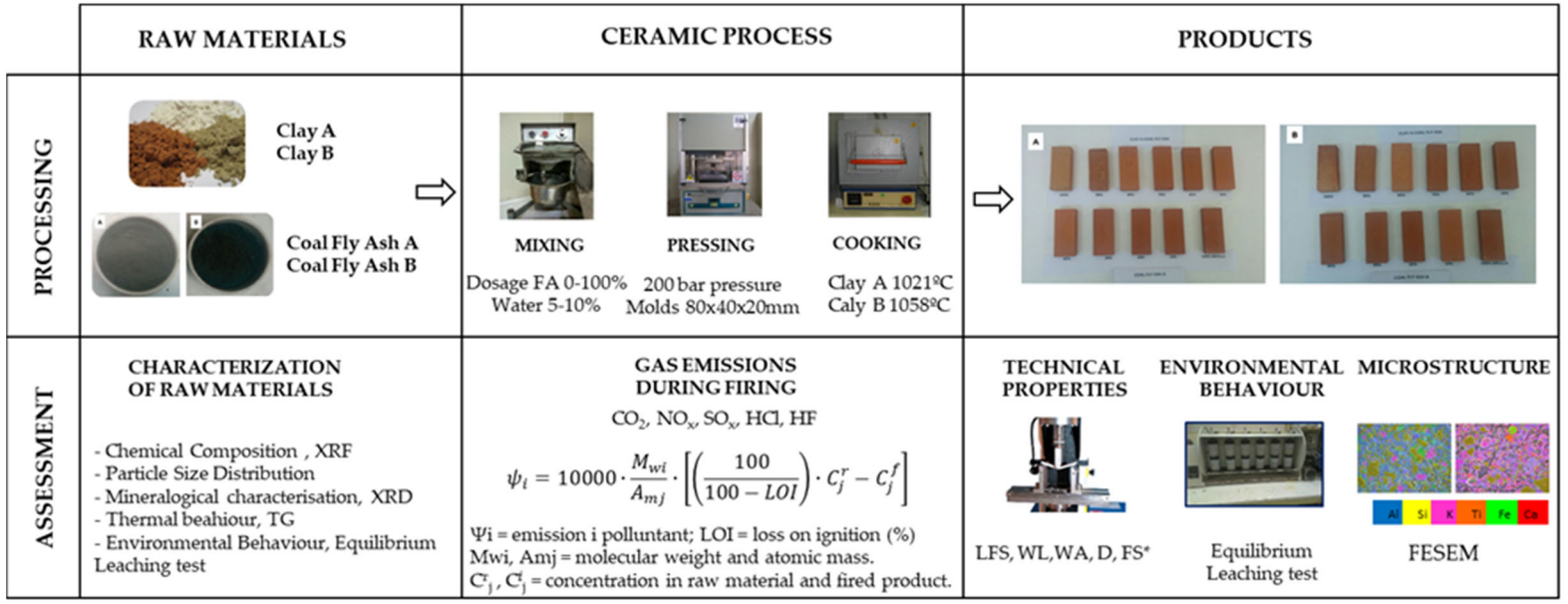

*LFS: Linear Firing Shrinkage, WL: Weight Loss during firing, WA: Water Absorption, D:Apparent Density and FS: 3-point Flexural Strength.

Figure 2.2. Methodology conducted in this study.

Table 2.1 shows the experimental formulations developed. Samples were prepared with additions of coal fly ashes, varying from 0 to 100 wt %. These formulations were studied for both types of coal fly ashes FAA and FAB, and clays.

Table 2.1. Coal Fly Ash-Clay Bricks Formulation.

Sample	Coal Fly Ash (A/B)	Clay (A/B)
P1	100	0
P2	90	10
P3	80	20
P4	70	30
P5	60	40
P6	50	50
P7	40	60
P8	30	70
P9	20	80
P10	10	90
P11	0	100

2.2.1.3. Characterisation of Raw Materials

Elemental analysis and major oxide composition were determined by inductively coupled plasma atomic emission spectroscopy (ICP-AES) with an ARL Fisons 3410 spectrometer and X-ray fluorescence, respectively, in Activations Laboratories (Ancaster, ON, Canada). The particle size distribution was determined by sieving (ISO series sieves) and weighing. The mineralogical characterisation of all materials was carried out by powder X-ray diffraction (XRD) using a D8 Advance Automatic Diffractometer in Bragg-Brentano geometry. Cu Kα1 radiation (λ = 1.5406 Å) was employed with 0.03° 2θ steps and a constant 8 s acquisition time in the 10–90° 2θ range. The effect of temperature was studied on the clays and coal fly ashes at 10 °C/min up to 1200 ºC using thermogravimetry (Setaram Setsys Evolution Thermogravimetric Analyser).

2.2.1.4. Characterisation of fired samples

Fired ceramic products of all replicates were characterised in terms of linear firing shrinkage (using a precision caliper), weight loss during firing (UNE 772–13), water absorption (UNE 67027), bulk density (UNE-EN 772–13:2001), and 3-point flexural strength (UNE-EN 843–1).

The compliance leaching behaviour of potentially hazardous pollutants was determined by applying the equilibrium leaching test EN12457-2 proposed by European regulation. This test was realized for raw materials and fired specimens (three replicates). Samples were milled to below 4 mm and contacted with deionized

water, used as leachant, at a liquid/solid ratio of 10 and 24 h stirring. At the end of the test, samples were filtered, and the leachates were analysed. The pH was measured and the concentrations of As, Ba, Cd, Cr, Cu, Mo, Ni, Pb, and Zn in the leachates were determined by Inductively coupled plasma mass spectrometry (ICP-MS). These concentrations were compared with the limits established for open landfill conditions (landfill Directive 2003/33/EC), to assess the environmental performance of the construction products at the end of life when they become demolition waste.

The mineralogical characterisation was obtained, as described earlier for the raw materials, by XRD. Microstructural analysis of the clays, coal fly ashes, and fired bricks was carried out by field emission scanning electron microscopy (FESEM) using an accelerating voltage of 20 kV. The microstructural porosity study was performed on polished fracture surfaces, while phase distribution observations were carried out on polished samples, which were subsequently etched for 10 seconds in a 5 % HF solution. Before observation, all samples were coated with a layer of C. The ion distribution between the different crystalline phases was determined by digital X-ray mapping. The mineralogical characterisation was obtained, as described earlier for the raw materials, by XRD.

Finally, the emission of potentially harmful species (HCl, HF, SOx, NOx, CO_2) into the atmosphere during the firing of ceramic bricks was determined according to the standard methodology described in BREF Document on Ceramic Manufacturing Industry. The method involves analysing the raw materials and the fired specimens for potentially polluting elements. The concentration of carbon, sulphur, and nitrogen was determined using a FISONS EA 1108 elemental analyzer, and the concentration of halogens (Cl and F) was determined by neutron activation (INAA) and an ion-selective electrode (ISE), respectively, in Activations Laboratories (Canada). Emission values (Ψ) for each element were determined by simple mass balance according to eq 1. This equation assumes that elemental Cl, F, S, N, and C are released into the atmosphere during the firing process in the form of HCl, HF, SO_2, NO_2, and CO_2, respectively:

$$\psi_i = 10000 \cdot \frac{M_{wi}}{A_{mj}} \cdot \left[\left(\frac{100}{100-LOI}\right) \cdot C_j^r - C_j^f\right] \quad (1)$$

Where i=polluting compounds (HCl, HF, SO_2, NO_2, CO_2) and j=constituting elements (Cl, F, S, N, and C) of the polluting compounds. Ψi = emission (in mg of compound i per kg of brick produced). LOI = loss on ignition (%). Mwi = molecular weight of the polluting compounds. Amj = atomic mass of the element. Crj = concentration of element (j) in the raw material and Cfj = concentration of element (j) in fired product.

2.2.2. Results of Incorporating CFA in Ceramic Processes

2.2.2.1. Characterisation of Raw Materials

Table 2.2 shows the results of the main oxides and elements in all the raw materials used to form bricks. Clays and FAA have three major oxides (silicon, aluminum, and iron) which represent over 75 % of raw materials whereas FAB represents 61%. The minor fraction consists of eight oxides: manganese, magnesium, calcium, sodium, potassium, titanium, and phosphorus. Loos on Ignition (LOI) values obtained for each type of clay are related to the content of unburned carbon. Furthermore, FAA and FAB have a higher content of alkaline, earth alkaline, and iron oxides, which make them suitable for their valorisation in fired clay ceramic bricks due to their melting character.

Table 2.2. Chemical composition of raw materials.

Major oxide, wt (%)	Clay A	Clay B	FAA	FAB
SiO_2	63.35	63.7	52.53	40.20
Al_2O_3	17.11	15.69	22.23	16.62
Fe_2O_3	5.89	6.26	8.38	5.26
MnO	0.054	0.079	0.103	0.057
MgO	0.85	0.86	2.25	1.71
CaO	0.47	0.58	4.70	3.37
Na_2O	0.61	0.69	1.11	0.88
K_2O	3.08	2.67	2.03	1.82
TiO_2	0.843	0.762	0.898	0.681
P_2O_5	0.10	0.10	0.61	0.56
LOI (Loss of ignition)[1]	6.15	7.40	5.43	27.03
Trace elements (ppm)				
As	23	25	31	39
Ba	634	1597	1965	1800
Cd	<0.5	<0.5	<0.5	<0.5
Cr	80	80	170	120
Cu	30	20	50	40
Mo	<2	<2	17	11
Ni	40	40	80	60
Pb	28	37	27	< 5
Sb	0.007	0.008	2.6	2.2
Zn	80	140	140	<30

[1] Determined at 650 °C.

The particle size distribution of fly ashes is given in Figure 2.3. FAA has a lower particle size than FAB.

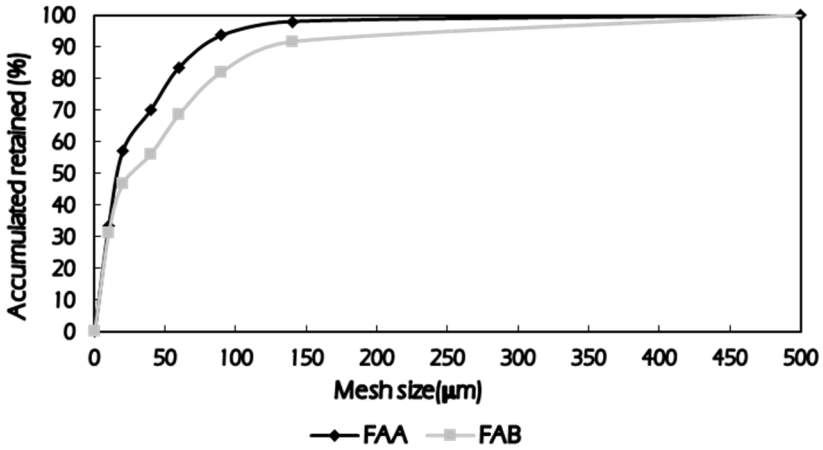

Figure 2.3. Particle size distribution of Coal Fly Ash A and B.

FAA shows 4 % of ash particles above 100 microns; 23 % of particles between 63 and 100 microns; and 73 % of FA with particle size below 63 microns. Instead, FAB has 25 % of particles with sizes greater than 100 microns; 23 % with sizes between 63 and 100 microns; and 52% of particles with sizes lower than 63 microns.

Mineralogical analysis of raw materials is shown in Figure 2.4. The mineralogical analysis of Clay A and B shows an amorphous fraction in the form of maximum width between 15 and 30 degrees. On the other hand, the crystal phases present are majority quartz (SiO_2), muscovite ($KAl_3Si_3O_{10}(OH)_{1.8}F_{0.2}$), dickite ($Al_2Si_2O_5(OH)_4$), and kaolinite ($Al_2Si_2O_5(OH)_4$). These phases can constitute approximately 90 % of the total clay, respectively. Furthermore, minority phases are iron oxides (Fe_3O_4). FAA and FAB show an amorphous fraction in the form of maximum width, much larger than clays, between 15 and 30 degrees. On the other hand, the crystal phases present are majority quartz (SiO_2), mullite ($Al_{4+2x}Si_{2-2x}O_{10-x}$ being x~0.4), and anhydrous aluminum silicate ($Al_2O_7Si_2$). These phases can constitute approximately 70 and 50 % of FAA and FAB, respectively. Furthermore, minority phases are dolomite $CaMg(CO_3)_2$, calcium aluminate ($xCaOyAl2O_3$ being x and y the number of molecules), calcium silicate ($2CaO.SiO_2$), and iron oxides (Fe_3O_4).

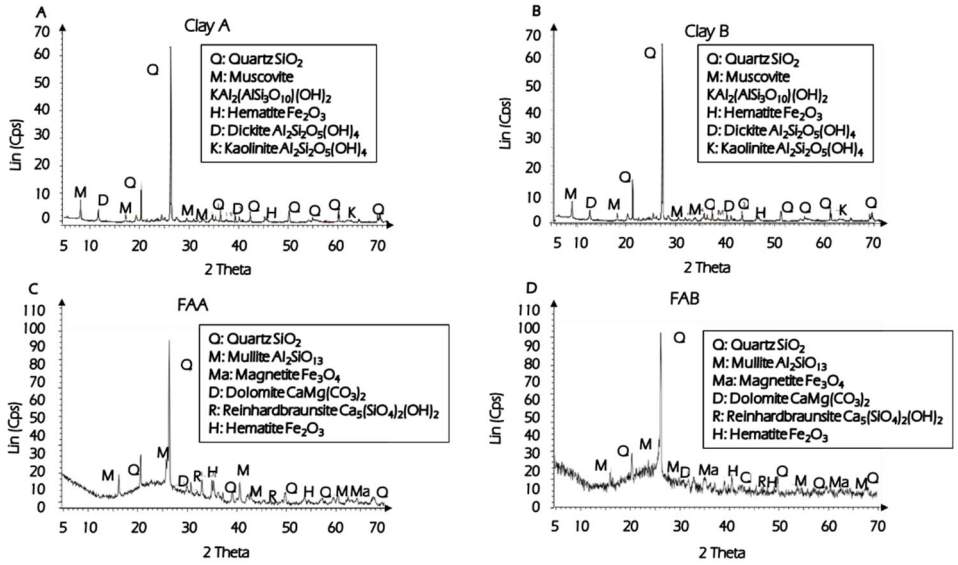

Figure 2.4. XRD pattern of Clay A (A), Clay B (B), FAA (C), and FAB (D).

Figure 2.5A shows the thermal behaviour during firing (10°C/min) of Clay A and B up to 1200 °C. Thermogravimetric analysis shows the typical clay dehydroxylation process (water of hydration) with a mass loss of 2.33 % and 3.57 % up to 100 °C, respectively. The second step is around 500-550 °C which corresponds with the dehydroxylation of clays (aluminosilicates decomposition) with a mass loss of 5.70 % and 5.84 %, respectively.

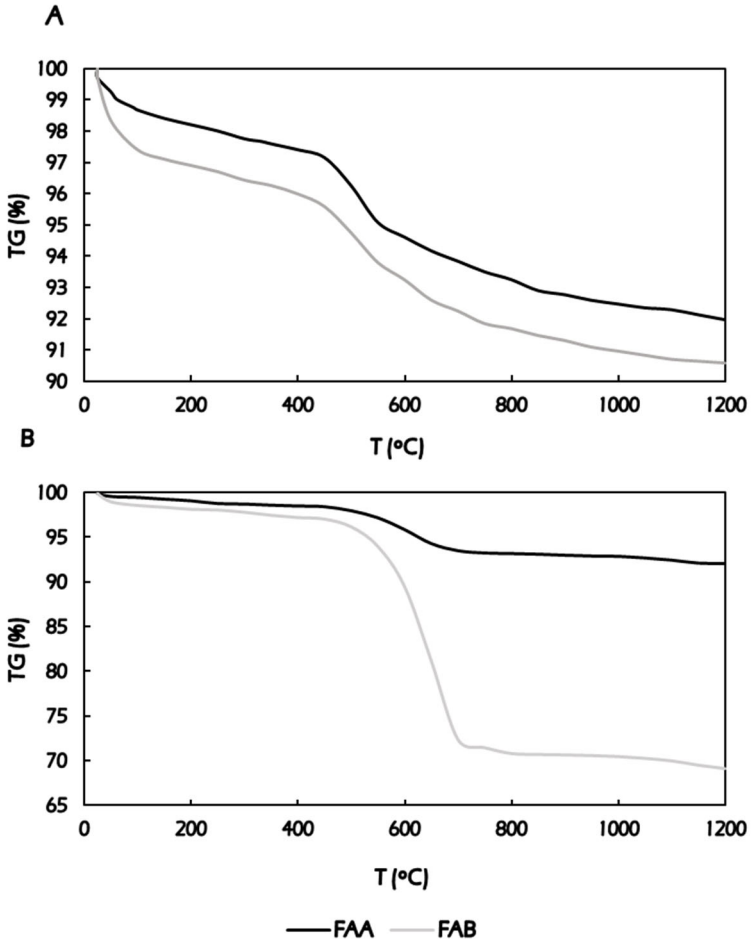

Figure 2.55B has represented the thermogravimetry of both FA. The mass loss of 1.55 % for FAA and 2.93 % for FAB between 100 and 400 °C corresponds to the thermal decomposition of water present in ashes. Between 500 and 700 °C, where the mass loss for FAA is 5.69 % and for FAB is 27.91 %, corresponds to the thermal decomposition of carbonates and unburned carbon. In this case, the decomposition of carbonates is due to the presence of dolomite $MgCa(CO_3)_2$, which is decomposed into calcium and magnesium oxides and carbon dioxide. The total mass loss due to thermal decomposition of water, carbonates, and unburned carbon for FAA is 7.95 % and for FAB is 30.84 %. In the case of FAB is much higher due to the high contents of unburned carbon of FAB.

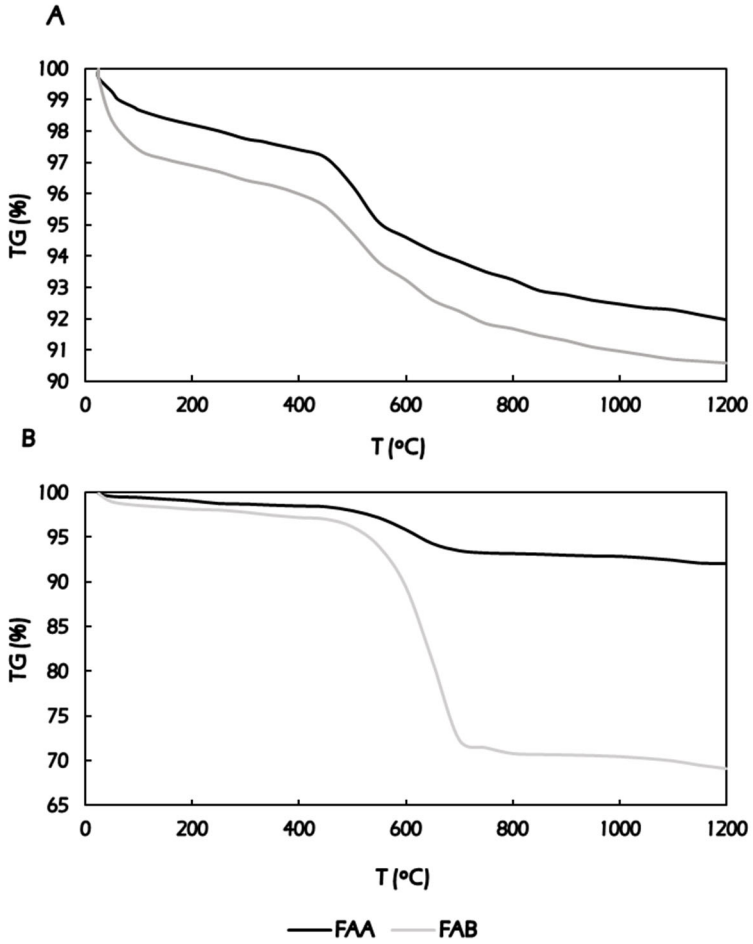

Figure 2.5. Thermogravimetric behaviour of A) Clay A and Clay B; B) FAA and FAB.

The Compliance Leaching test EN 12457-2 was performed in triplicate for raw materials and the results are presented as an average and standard deviation of concentrations in Table 2.3. For all the pollutants considered in the European landfill regulation, the concentrations on Clay A and B are below the inert threshold limit, but for Clay A, As is close to the inert limit. Most of the pollutants considered for the FAA and FAB are below the inert threshold limit, except Cr and Mo, which are below the non-hazardous limit for both ashes Only Se exceeds the non-hazardous limits, and it is well below the limit for landfilling hazardous waste landfills.

Table 2.3. pH values and leaching of major elements from raw materials according to compliance leaching test EN 12457-2.

	Leaching Concentrations (mg/kg)				Landfill Limits[1]	
	Clay A	Clay B	FAA	FAB	Inert	Non-Hazardous
pH	7.72	9.35	11.01	12.52	-	-
As	0.461±0.02	0.296±0.01	0.146±0.16	0.110±0.03	0.5	2
Ba	1.075±0.036	11.337±0.036	4.668±0.220	2.163±0.099	20	100
Cd	0.003±0.0001	0.013±0.0002	0.006±0.004	0.004±0.001	0.04	1
Cr	0.006±0.005	0.008±0.0002	1.375±0.13	1.998±0.128	0.5	10
Cu	0.106±0.003	0.095±0.001	0.046±0.004	0.059±0.005	2	50
Hg	0.002±0.0001	0.0013±0.0002	0.008±0.007	0.009±0.006	0.01	0.2
Mo	0.0183±0.0001	0.004±0.001	5.450±0.065	5.196±0.007	0.5	10
Ni	0.047±0.005	0.016±0.001	0.015±0.001	0.011±0.001	0.4	10
Pb	0.046±0.001	0.057±0.002	0.035±0.01	0.021±0.01	0.5	10
Sb	0.008±0.0002	0.008±0.0002	0.021±0.001	0.013±0.001	0.06	0.7
Se	0.021±0.007	0.087±0.0007	2.617±0.255	0.619±0.053	0.1	0.5
Zn	1.599±0.035	1.60±0.012	0.943±0.044	0.370±0.019	4	50

[1]Limits for inert and non-hazardous waste according to Landfill Decision 2003/33/EC

2.2.2.2. Technological properties of CFA-Clay Bricks

The effect of unburned carbon of Fly Ash on the linear shrinkage is shown in Figure 2.6. FAB/clay ceramics present a higher value of linear shrinkage for percentages of Fly Ash greater than 50 %. There is a difference of over 3 units between FAA and FAB for both clays. For concentrations between 10-50 % of Fly Ash, fired clay ceramics with FAB have a linear shrinkage close to the bricks with FAA. The difference between Ashes is lower than 0.5 units and presents a linear shrinkage close to the bricks with 100 % Clay. The same tendency of increasing the linear shrinkage, due to the addition of waste, was observed in other studies (Cultrone et al., 2009). Table A.2.1. of Annex 2 are shown the average values and standard deviation of the experimental values obtained for the linear shrinkage.

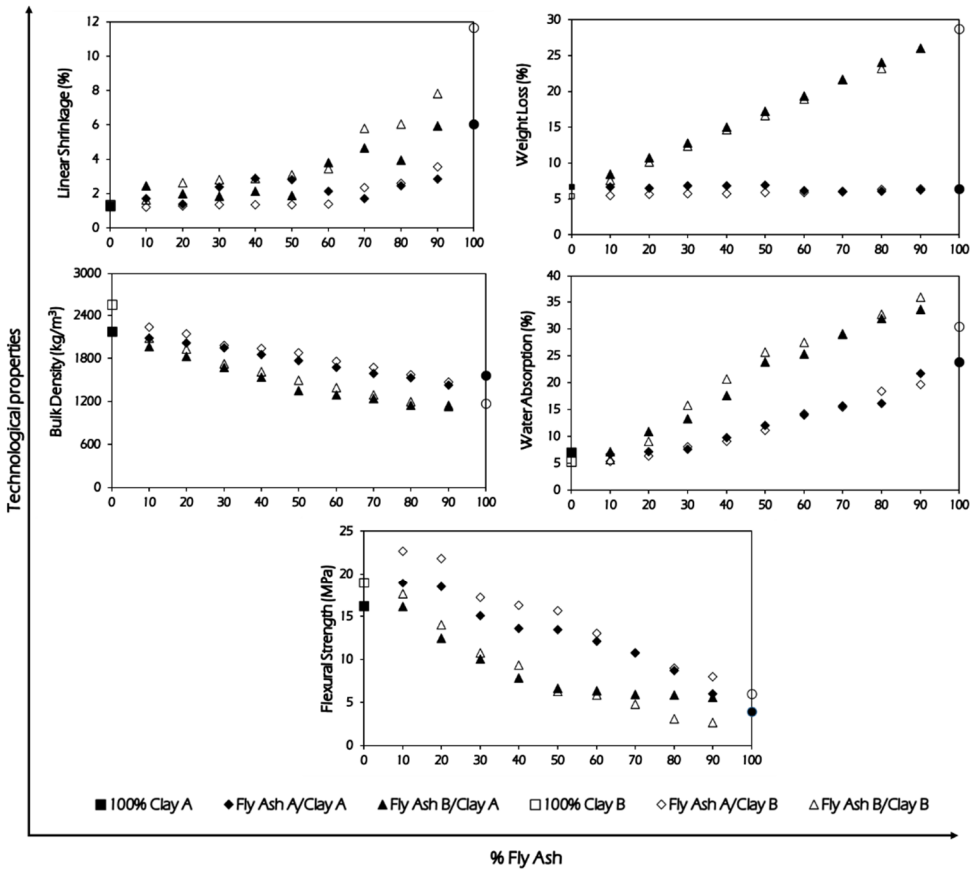

Figure 2.6. Main technological properties of fired clay bricks.

Weight loss increases as the percentage of FAB increases, due to the high carbon contents (Kockal, 2012). Samples are fired up to 1058ºC and at this range FAB experience a thermal decomposition of carbonates and unburned carbon (Naganathan et al., 2015). This decomposition supposes a loss of weight and is confirmed with the thermogravimetric analysis (Figure 2.5). Fired clay bricks with FAA present results of weight loss close to the bricks made with 100 % clay. Percentages of FAA upper 60% have slightly higher values due to the thermal decomposition of water and carbonates. The difference between fired bricks is 5 units for 10 % of Fly Ash, while 15 and 20 units for 60 % and 90 % of FAB respectively, so unburned carbon significantly influences the weight loss of fired clay bricks. The results of average weight loss and standard deviation are shown in Table A.2.2. of Annex 2.

FA is less dense than the clays used thereby lowering the density with increasing the ash content in the bricks. The percentage of FA used considerably affects the densification. The presence of unburned carbon in the FA provides less dense bricks.

Bricks with 10 % of FA present 100 units of difference between FAA and FAB and with 50 % have 400 units of difference. With percentages up to 20 % of FA, results of bulk density are very close between FAA and FAB, regardless of the Clay used. In Table A.2.3. of Annex 2 the results of bulk density are collected.

FAB/clay bricks present higher results of water absorption than FAA. The difference in results between bricks 100 % Clay and bricks incorporating FA is due to the porosity caused by the thermal decomposition of water and carbonates. In this case, FAB is greater due to the higher contents of unburned carbon which also experiences a thermal decomposition. This thermal decomposition releases gases that generate materials more porous. Bricks with 20 % FAB have the same results as bricks with FAA. Bricks up to 20 % FAA and 10 % FAB have water absorption close to 100 % clay bricks. Table A.2.4. of Annex 2 are shown the average values and standard deviation of the experimental values obtained.

Flexural strength is related to water absorption and density which are associated with the porosity of the ceramic brick. As FAB/clay bricks present the highest results of water absorption and the lowest density, in flexural strength these bricks have results related to these properties. Bricks with 10 % of FA present 2 units of difference between FAA and FAB and bricks with 50 % of FA have 7 units of difference. It can be concluded that a higher unburned carbon content, worse results of flexural strength, but at percentages of 10 the obtained values are close to fired clay bricks with FAA, and from 80 % ash, the values are close again. The results of average flexural strength and standard deviation are shown in Table A.2.5. of Annex 2.

2.2.2.3. Leaching Behaviour of Fired Bricks

Once a leaching test was applied, those elements than exceeded the limit of the inert waste landfill on raw materials were studied (Table 2.3). The contaminants associated with FA were Cr, Mo, and Se as shown in Figure 2.7a. Introducing FA into fired clay bricks in a dosage of 50 % reduces the mobility of Mo and immobilizes Cr and Se below the inert waste limit. The concentration of As for FA is below the limit of inert waste landfill but when it is incorporated into the ceramic bricks in 50 % of FAB, it is exceeded. 100 % Clay B is above the inert waste limit, so Clay B is the raw material, which favours that 50 % FAB/Clay B bricks exceeded this limit. The content of unburned carbon does not influence the mobility of contaminants.

It also studied the limits of non-hazardous waste landfills for these contaminants, as shown in Figure 2.7b. All the contaminants are below the limit of landfills for non-hazardous waste, and the unburned carbon content does not influence the mobility of elements. As mobility is due to its presence in Clay, concentrations of 100 % Clay

bricks are higher than 50 % FA/Clay bricks. In conclusion, the unburned carbon content does not affect the leaching of contaminants, so the obtained results are very interesting.

Oxyanions like Mo can be adsorbed on the surface of amorphous iron oxides that many alkaline waste contain. Furthermore, the complexation of these compounds has been studied and a relation between the specific surface area and the extension of the complexation process was found for MoO^{2-}_4. In his work, McKenzie concluded that the decrease in the specific surface leads to higher Mo leaching (McKenzie, 1983).

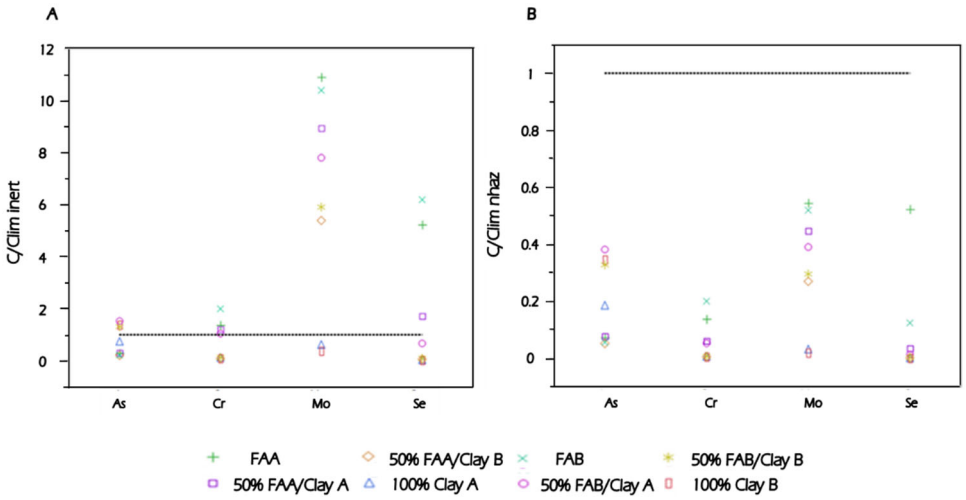

Figure 2.7. The concentration of contaminants of FA/Clay bricks regarding the inert waste landfill limits (A) and the non-hazardous waste landfill limits (B) according to Decision 2003/33/EC.

2.2.2.4. Microstructural Characterisation of Fired Clay Bricks

From the results obtained on the technological and environmental properties of the fired products, Clay B was chosen to carry out a microstructure study of the bricks obtained, and the gaseous emissions generated during the firing process.

XRD Characterisation

Figure 2.8 shows the XRD patterns of ceramic brick compositions with 10 – 50 % FAA, 10–50 % FAB, and without FA, only 100 % clay B that were fired at 1058 ºC. The mineral phases of the bricks were identified as quartz, sillimanite, microcline, kyanite, and iron oxide (hematite).

As can be seen, XRD patterns of FAA/clay and FAB/clay are close to the clay ones. The increase of peaks of quartz and Fe-containing phases, such as hematite, with the FAs amount in the ceramic matrix, can be observed. Mullite and dolomite, a significant phase in both FA samples, are not detected in bricks incorporating both FAA and FAB, which are mainly composed of quartz and hematite and other characteristics aluminosilicates of clay bricks. The presence of high amounts of unburned carbon in FAB samples does not imply differences in the final mineral phases of bricks.

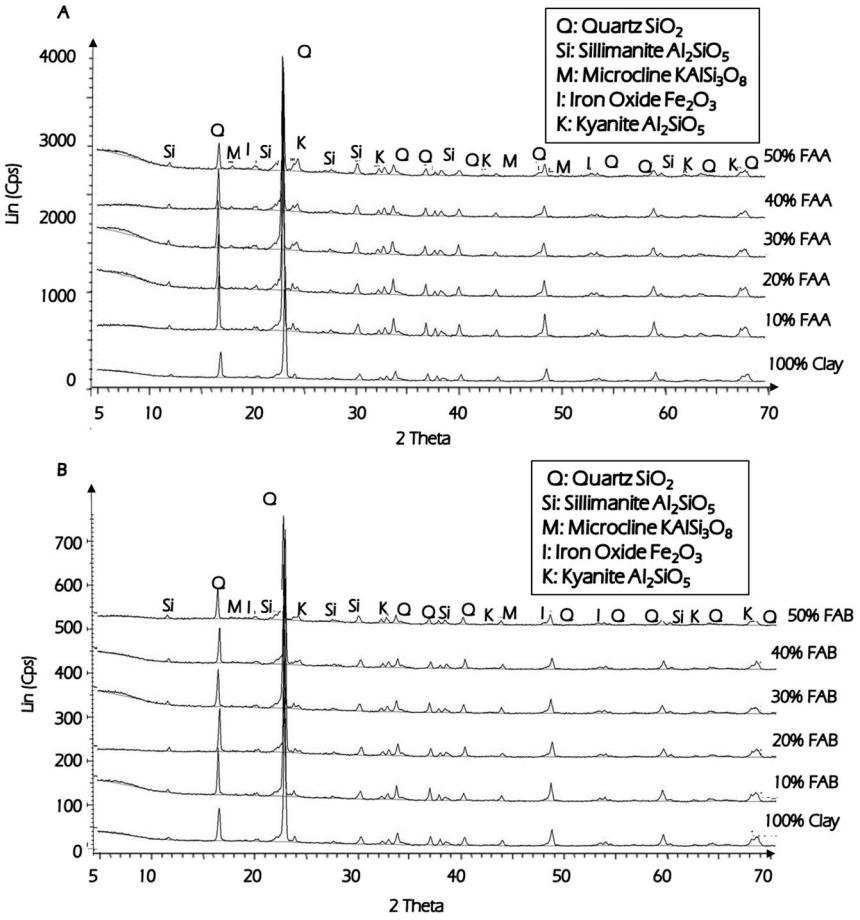

Figure 2.8. XRD patterns of: (A) FAA/Clay fired bricks; (B) FAB/Clay fired bricks.

FESEM analysis

Figure 2.9a, and Figure 2.9b show the microstructure observed by FESEM (field emission scanning electron microscopy) on the polished surfaces of FAA/clay and FAB/clay bricks, respectively. The main microstructural effect is the increase in porosity as the content of CFA in the brick body increases. The increase in porosity is mainly associated with the presence of dolomite and unburned carbon in the mineralogical composition of the FAs (Figure 2.4).

However, the incorporation of FAA and FAB leads to different impacts on the porosity. For further discussion, Figure 2.10 presents details of the polished surface microstructure of samples prepared from Clay B exclusively (100 % Clay B) and those prepared with 50 % FA incorporation (50 % FAA/Clay B and 50 % FAB/Clay B). The microstructure of the 100 % Clay B sample is characterised by the presence of open porosity consisting of interconnected and irregular cavities with a thickness of fewer than 5 μm. This porosity is the result of the dehydroxylation of the clay during firing, which causes a volume reduction. The increase in porosity observed when FA is incorporated into the brick body is probably due to the combined action of two factors, namely the larger particle size of FA compared to clay and the dolomite and unburned carbon content in FA. Thus, due to its larger average size, the inclusion of FA in the brick paste will result in green-shaped specimens with different porosity. According to Amorós et al. (Amorós et al., 2007) at equal pressing variables, a higher content of larger particles results in compacted specimens of higher bulk density (lower porosity), which, however, contain larger pores. As the pore size in the fired bodies depends more on the pore size in the green body than on the pore volume, the inclusion of FA in the brick paste will result in less densified fired bodies, and to achieve maximum densification of the product, a higher firing temperature would be required. On the other hand, FA contains dolomite and unburned carbon, which during the firing process will decompose with the consequent release of gases, causing the size of the open porosity to increase. FAA presents low dolomite and unburned carbon content, as can be inferred from its LOI value (Table 2.2), which is even lower than that of Clay B. Therefore, the major effect induced by the incorporation of FAA in the body of the brick is a slight increase in porosity associated with its larger particle size (Figure 2.10). In contrast, FAB contains much higher dolomite and unburned carbon than the clays, so during firing it will generate a high increase in porosity due to the release of the gases generated during its decomposition. This increase in porosity, which is evident in Figure 2.10, is associated with a significant increase in the water absorption of the brick specimens manufactured with this FA (Figure 2.6).

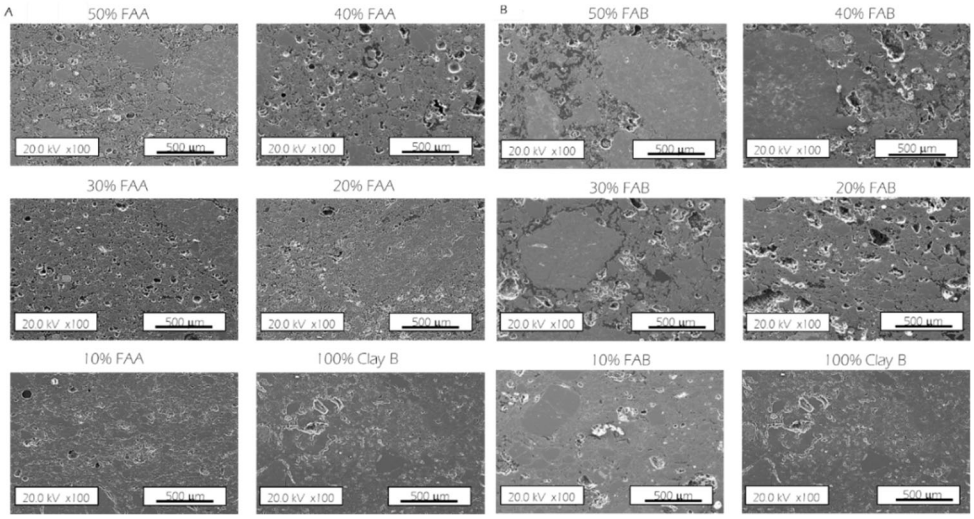

Figure 2.9. FESEM images of fired clay bricks: (A) FAA/Clay fired bricks; (B) FAB/Clay fired bricks.

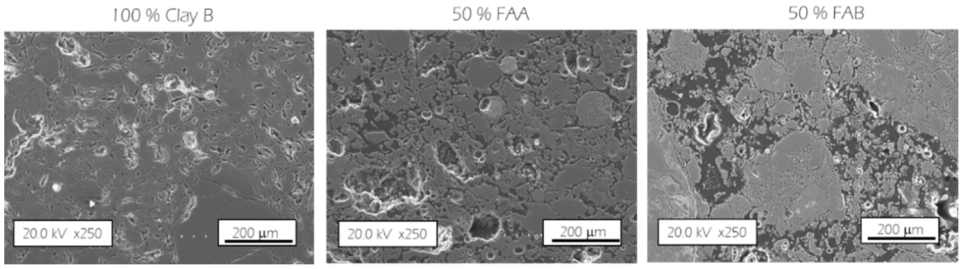

Figure 2.10. FESEM images of 100 % Clay B and 50 % FAA and FAB/Clay B fired clay bricks.

The incorporation of FA into the brick composition affects not only the porosity of the fired pieces but also their crystalline composition and the distribution of crystalline phases. Figure 2.11 presents FESEM images of polished and etched fracture surfaces of samples of 100 % Clay B and 50 % FAB/Clay B compositions, together with the mapping of the elements Al, Si, K, Ti, Fe and Ca. The different crystalline phases that comprise the mineralogical composition of the fired bricks are clearly distinguished by the colour differences caused by the varying concentrations of these ions in each of the crystalline phases. The 100 % Clay B sample shows the conventional phase distribution in traditional fired clay materials composed mainly of quartz grains embedded in a ceramic matrix enriched in aluminium oxide.

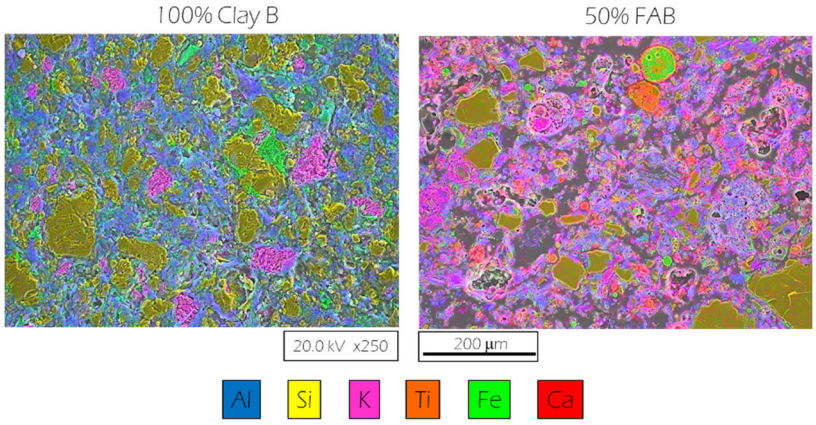

Figure 2.11. FESEM images and mapping of elements of samples 100 % Clay B and 50 % FAB/Clay B.

Figure 2.12A depicts FESEM images of different regions observed in the microstructure of 100 % clay B brick. Some of the quartz grains show micro cracks, which are likely formed as a result of the relaxation of micro stresses caused by the difference between the coefficients of thermal expansion of the quartz grains and the surrounding ceramic phase as stated in Romero et al. (Romero et al., 2015).

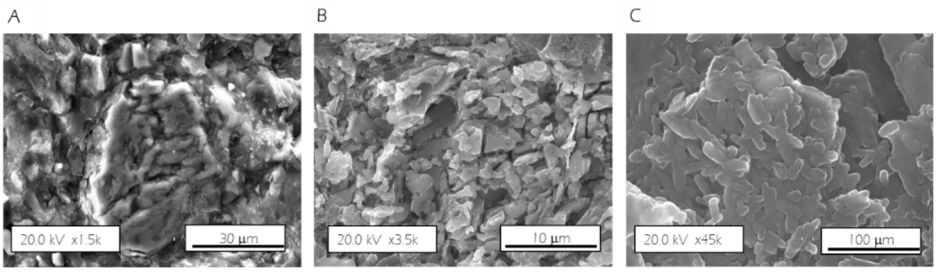

Figure 2.12. Microstructure FESEM images taken at different regions of 100% Clay B.

In addition to quartz particles, in the ceramic matrix, regions with high potassium oxide content with crystals of irregular morphology are identified in Figure 2.12B, which must correspond to the microcline phase as observed in the XRD of the fired bricks (Figure 2.8). Isolated iron oxide particles are also clearly distinguishable in the mapping image 100% clay B sample. Regarding the morphology of the ceramic matrix, FESEM observations at high magnification (Figure 2.12C) allow distinguishing regions with elongated crystals, which likely correspond to the sillimanite phase (as observed in Figure 2.8). As far as the microstructure of the 50% FAB/Clay B bricks, Figure 2.11 shows the presence of quartz grains to a smaller extent. The quartz grains show fewer micro-cracks, probably because they are surrounded by a much more

porous matrix that can absorb the stresses caused by the differences in expansion coefficients. The microcline crystals are not distinguishable and potassium oxide is dispersed throughout the matrix, which is more enriched in calcium oxide.

2.2.2.5. Estimation of Gas Emissions within the Firing Process

The content of Cl, F, S, C, and N for the Clay B and Fly Ash A (low LOI) and B (high LOI), as well as their corresponding acid gas emissions HCl, HF, SO_2, and CO_2 after the firing stage at the temperature of 1058 ºC simulating the industrial processes and estimated by mass balance (Eq. 1), are summarized in Table 2.4. The initial and final content of CFA and Clay of the elements mentioned before and after firing are collected in Table A.3.1. (Annex 3). The content of N is below the detection limit of the equipment used. Chlorine emissions will be related to its content in the samples. The chlorine in the clay comes from micas, halite, and organic matter, while in the ash it forms mainly chlorinated compounds associated with its organic matter. The significant increase in chlorine emissions in clay compared to fly ash, despite having the same initial content, may be due to the presence of chlorine as sodium chloride (halite), which is very unstable during the firing process. While the difference in emissions between the two types of ashes is directly related to the unburned content, the higher the LOI, the higher the decomposition of chlorinated compounds. Fluorine emissions also depend on the initial concentration of this element in the samples. The difference observed between the clay and the ashes may be due to the decomposition of phyllosilicates present in the clay. While the difference between both ashes may be due to the formation of thermally stable compounds (CaF_2) in samples with low carbonate content (González et al., 2011). Sulphur emissions depend on the mineralogy of the samples. Due to the oxidation and decomposition of pyrite and organic matter during the firing process, high values of sulphur emissions are obtained for ashes with a high content of unburned carbon (Uaciquete et al., 2021). Finally, in the case of CO_2 emissions, a direct relationship is observed between the initial carbon content in the raw materials and the level of emissions.

Table 2.4. Content and pollutants emissions of Clay B and Fly Ashes A and B.

Raw Materials	Initial Content (%)					Emissions (mg/kg)*				
	Cl	F	S	C	N	HCl	HF	SO_2	CO_2	N
Clay B	0.02	0.02	0.02	0.3	-	119.28	122.14	31.93	454.27	-
FAA (low LOI)	0.02	0.01	0.17	4.7	-	11.81	6.05	2992	17844	-
FAB (high LOI)	0.02	0.01	0.31	24.4	-	76.19	39.01	6090	122160	-

(-) < Detection Limit; (*) Gas emissions calculated according to the mass balance of eq. 1.

Gas emissions for the mixtures of FAA/Clay and FAB/Clay fired at the temperature of 1058 ºC simulating the industrial processes and estimated by mass balance (Eq. 1) are summarized in Figure 2.13. Emission limit values for HF, HCl, and SO_2 proposed by Gonzalez et al. (2011) aim to include them in the Andalusian-Spain legislation in response to the indications of the IPPC, have also been considered. From a study conducted with 40 ceramic factories in Andalusia, Spain through the median and the 90th percentile values of 180 samples, three ranges de emission values are established: "acceptable", "recommended intervention" and "compulsory intervention". The emission values are shown in Table A.3:2. (Annex 3) (González et al., 2011).

The introduction of Fly Ash in the mixtures reduces the emissions of HCl due to low chlorine emissions from fly ash. Incorporating up to 90 % of FAA and FAB, a reduction in emissions of HCl is achieved compared with the brick 100 % clay. The percentage of reduction obtained is 61 % for FAA and 25 % for FAB. The reduction of emissions by introducing FAA is higher due to the lower value of emission concerning FAB. As indicated above, it is probably due to a greater decomposition of chlorinated compounds associated with organic matter, that is, the content of unburned matter. The introduction of Fly Ash in the mixtures FAA/Clay and FAB/Clay reduces the emissions of HF due to the low contents of F that Fly Ash present. The reduction of HF emissions is higher for Fly Ash due to the lower contents of F before the firing process compared to Clay. This is because clay contains one of the most important sources of fluorine, such as phyllosilicates, therefore, the less clay in the mixture, the greater the reductions in fluorine emissions. Incorporating up to 90 % of FAA and FAB reduces the emissions of HF by 42 % and 60 % compared to 100 % clay brick.

The introduction of Fly Ash in the mixtures produces an increase in SO_2 emissions due to the high content of S present in the Fly Ash. FAB/Clay mixtures show extremely high levels due to the presence of the combination of different sulphur associated with inorganic, pyritic, and organic carbon.

The introduction of Fly Ash in the mixtures FAA/Clay and FAB/Clay increases the emissions of CO_2 due to the high contents of unburnt carbon that Fly Ash presents. The increase of CO_2 emissions is higher for FAB due to the high contents of unburnt carbon (27.03 %) before the firing process compared to FAA (5.43 %) and Clay. In this case, the CO_2 emissions from inorganic carbon are not important in an overall assessment.

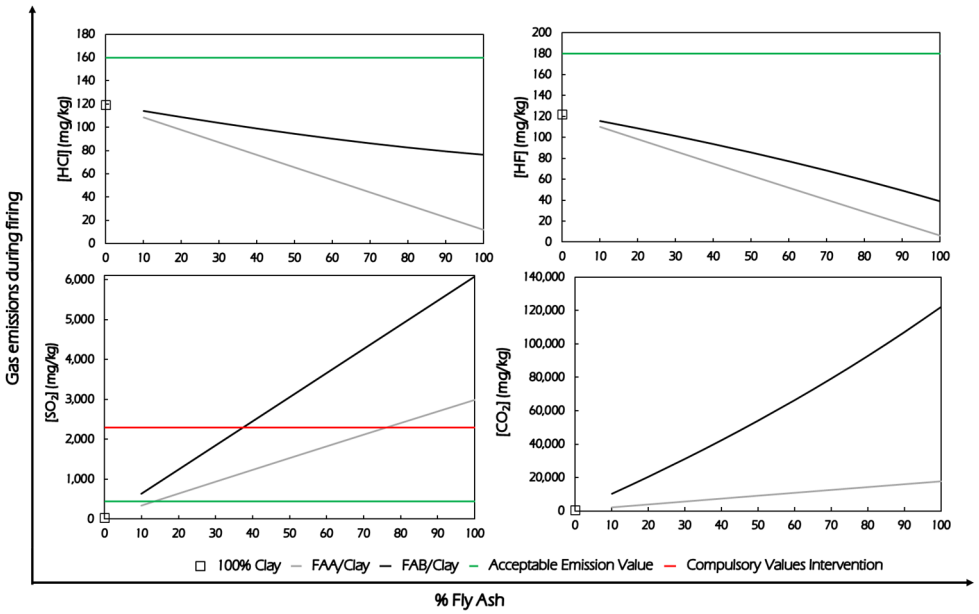

Figure 2.13. Estimation of HCl, HF, SO_2, and CO_2 emissions for mixtures performed with FAA/Clay B and FAB/Clay B during the firing process, including reference emission values proposed by I. Gonzalez et al. (González et al., 2011).

Considering the technological properties to the market of this type of brick according to AENOR Fired Clay Piece HD Clinker R-55 and the leaching behaviour, it could be possible to incorporate up to 20 % of FAA and 10 % of FAB. The reduction in emissions of HCl with these additions is 13 % and 5 %, respectively that according to reference emission values. As the HCl emission limit value is <160 ppm, the addition of 20 % FAA and 10 % FAB do not exceed the acceptable emission value proposed. In the case of HF, the introduction of FA supposes a reduction of 10-11 %, respectively. The HF emission limit value is < 180 ppm, therefore, the addition of 20 % FAA and 10 % FAB do not exceed the acceptable emission value. In the case of SO_2, the introduction of FA produces an increase in SO_2 emissions is 61 % and 65 %, respectively. The SO_2 emission limit value is < 450 ppm, therefore, exceeds the acceptable emission value, therefore, and an intervention to review the values would be advisable. For 20 % of FAA and 10 % of FAB in the mixtures, so the increase of CO_2 emissions is 62 % and 87 %, respectively. It is important to note that the level of CO_2 emissions must be estimated based on the total annual production of the ceramic factory.

2.2.3. Conclusions

The influence of the amount of unburned carbon present in coal fly ash on the proper- ties of fly ash-fired clay bricks was studied through the dosage of increased amounts of fly ashes with different unburned carbon content: FAA (low LOI) and FAB (high LOI).

The main microstructural effect was the increase in porosity as the content of coal fly ash (FAB) in the brick body increased. The porosity was associated with the release of the gases generated during the decomposition of dolomite and the content of unburned carbon of the fly ash. This increase in porosity corresponded with a significant increase in the water absorption and therefore, a bulk density and flexural strength reduction. Although unburned carbon plays an important role in the final properties, no detriment was observed in the properties of ceramic bricks containing up to 30 % FAA and percentages of 20 % FAB.

The leaching behaviour of critical contaminants associated with the presence of fly ash showed an immobilisation of Cr and Se in fired clay bricks while Mo reduced its mobility to values close to the inert landfill limit values. No influence of porosity on Mo leaching was observed, but higher retention, in samples with FAB, due to the adsorption of Mo on the surface of amorphous iron oxides. HF and HCl emissions were below the emissions of the 100 % clay bricks, so introducing fly ash would reduce the emissions of these pollutants in the firing process. The decomposition of chlorinated compounds associated with the unburned material was the main difference in the emission reduction values between both ashes. SO_2 emissions of FAB/clay mixtures showed high levels due to the presence of the combination of different sulphur associated with unburned carbon, mainly.

On the other hand, the level of CO_2 emissions should be estimated based on the total annual production of the company. Therefore, an unburned carbon separation option from fly ash would be advisable to obtain acceptable emission values in the CFB process.

2.3. FOUNDRY WASTE-CLAY BRICKS

The ceramic sector is affected by the implementation of the Integrated Pollution Prevention and Control (IPPC) Directive. Therefore, it is advisable to go to the source of the pollution by applying the best available technologies (BATs) to the production process. Currently, this sector is considered an improvement in the replacement of traditional raw materials with other alternative materials that minimize environmental impacts: saving natural resources, improving gaseous emissions, and reducing energy consumption, while eliminating management difficulties of such materials (IPPC, 2007).

The ceramic sector is an attractive alternative to valorise waste from a wide variety of industrial activities due to the heterogeneity of raw materials compositions used in this industry. Foundry processes produce different kinds of waste that could be incorporated into ceramic processes, as these waste could play a different role in ceramics. Foundry sands are used as inert or filler material. Foundry sands generated in moulding are characterised by a mixture of silica sand, bentonite (clay), and mineral black (coal) as an additive (Alonso-Santurde et al., 2012; Pytel, 2014; Heidemann et al., 2021). In addition, the use of sand is indicated in the conditioning of the plasticity characteristics of the mixture of raw materials, as well as a degreaser when too greasy clays are used, and as a pyrogenic material, replacing paper cuttings, in addition to providing carbon in the kiln (Lin et al., 2018; Mymrin et al., 2016).

The considered flux material, foundry sludge or steel dust, is a waste material that has properties very similar to ferritic clays since it contains important proportions of iron oxide or hydroxide (Mymrin et al., 2016. This sludge comes from the iron smelting process, it contains all the non-volatile components of the furnace, essentially iron oxides, lime, and silica. It has been observed that the content of alkali and alkaline earth oxides in this material act as network modifiers, reducing the stability of the network, which gives rise to liquid phases at lower temperatures and consequently improves the ceramic properties and reduces the firing temperature.

In this section 'FBs-fired clay bricks', waste from two companies allocated in the Cantabria region dedicated to iron cast has been selected. Due to the short distance to the fired brick company (Reciclados Cabezón), make its introduction into the production process viable, fulfilling the principle of proximity and as a circular economy paradigm. More specifically, one of the waste selected in this work comes from the cupola furnace where the metallic scrap is melting. During melting, two waste are generated, cupola flies ash and cupola bottom ash. The cupola fly ash is less dense and is trapped in the filters placed at the top of the furnace. On the other

hand, cupola bottom ash composes of metallic oxides non-reduced, scrap impurities, and coke and collected in the bottom of the furnace. Due to scrap melting in the cupola furnace, a purification system of gases locates in the furnace trapped the combustion gases by wet method generating the foundry sludge, and in the dry method which produced steel dust. In both cases, the resulting waste is classified as hazardous waste due to its high concentration of oxides of the most volatile metals. Then, the melting liquid is deposited in moulds made with silica sand and different types of additives, the most common being bentonite. Once the metal piece is obtained, the sand moulds are broken where the foundry sands are collected. Foundry sands, due to their large volume of production (around 2,500-3,000 tons/company year) and their carbon content, can be used as fuel for the furnace (CAEF, 2020). At this stage, there is an aspiration system with filters so that during the demoulding stage, the sand particles are not dispersed throughout the factory. This waste, from the aspiration system, is called fines (or Foundry sand dust). At last, a secondary vibration system is used for a more exhaustive demoulding process. During this stage, the wet sands are produced.

As part of the results, first, analysis and modelling of the technological and environmental properties of the FBs-fired clay bricks at a laboratory scale are carried out. Then, a statistical analysis of the results obtained was conducted. A selection of the optimal formulations based on technical, environmental, and economic requirements using MCA (Multi-Criteria Analysis) was developed to determine which ones of the tested FBs will be used at the industrial scale in the next section 'FS-fired clay bricks at industrial scale'.

2.3.1. Raw Materials and Methodology

2.3.1.1. Raw Materials Characterisation

Clay and seven different foundry by-products were the materials used in this work to prepare the foundry by-products-fired clay bricks (FB-FCBs).

On one hand, the illitic clay used in this work is currently being used as traditional raw materials in a Spanish industrial ceramic process for manufacturing face bricks. It is the Clay A used in CFA-FCBs. On the other hand, seven different thermal waste were used as by-products. Foundry by-products (FBs) used in this research were described in Table 2.5 according to List of European Residues (LER).

Table 2.5. Foundry by-products are used in this chapter in relation to List of European Residues (LER).

By-products	LER Code	Acronym	Line Process
Foundry Sand-cast iron	100907	FS	Moulding
Foundry Sludge	100213*	FSL	Wet Gas Cleaning
Steel Dust	100207*	SD	Dry gas Cleaning
Foundry Sand-ductile iron	100907	FS2	Moulding
Cupola Bottom Ash	100910	CA	Metal Melting
Wet Sand	100908	WS	Secondary vibration sakeout
Fines	100910	F	Aspiration

2.3.1.2. Processing Method

The methodology used in this work is represented in Figure 2.14.

The clay is subjected to a grinding process to achieve a particle size exceeding 1 mm, respectively. Then we proceed to the mixture of raw materials, Foundry by-products, and Clay, with a laboratory mixer Raimondi, Iperbet model. The proportions of raw materials are calculated by weight and the necessary water is added to obtain a plastic mixture. It has worked between 5 and 10 % water moulding.

Once the mixture of raw materials was done, we proceed to mould by pressing. To this end, a hydraulic press Nanetti Mignon model SS/EA, which reaches 200 bar pressure, was used. The mould used is prismatic 80x40x20 mm. The samples are dried for 30 hours at 105 °C before the cooking cycle. A laboratory muffle furnace Hobersal, PR Model 12/300 capable of ramps temperature versus time of up to 16 points was used. The industrial firing cycle is provided by the companies reaching temperatures of 1021 °C.

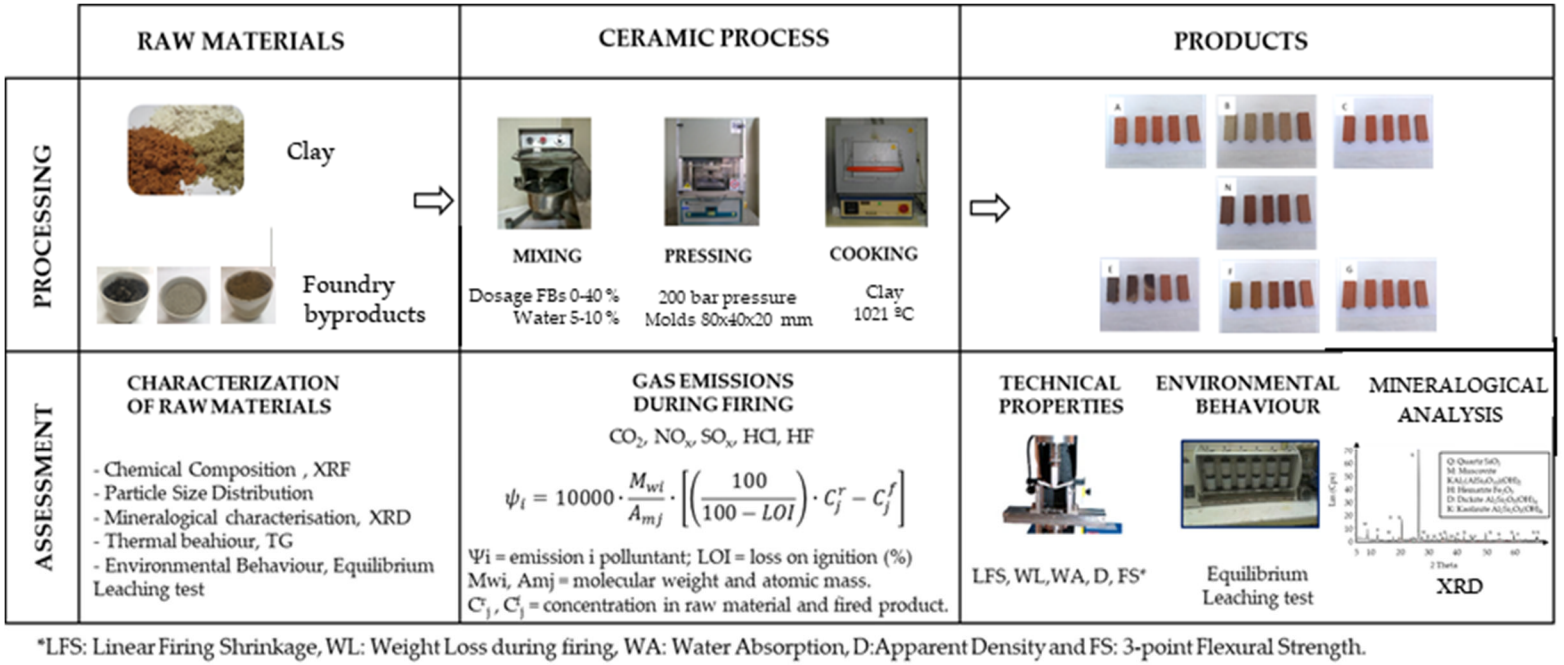

Figure 2.14. Methodology was carried out in the development of this study.

Table 2.6 shows the experimental formulations developed to study the viability of the introduction of foundry by-products (FBs) into lab-scale bricks.

Table 2.6. Design of formulations for foundry by-products.

Sample	Foundry by-product (%)	Clay (%)
X1	40	60
X2	30	70
X3	20	80
X4	10	90
X5	0	100

Samples were prepared with additions of FB, varying from 0 to 40 wt %. X is each of the FBs described in the materials section. In total, 15 bricks were prepared per sample, and 60 bricks per waste made a total of 420 bricks.

2.3.1.3. Characterisation of Raw Materials

Elemental analysis and major oxide composition were determined by inductively coupled plasma atomic emission spectroscopy (ICP-AES) with an ARL Fisons 3410 spectrometer and X-ray fluorescence, respectively, in Activations Laboratories (Ancaster, ON, Canada). The particle size distribution was determined by sieving (ISO series sieves) and weighing. The mineralogical characterisation of all materials was carried out by Dust X-ray diffraction (XRD) using a D8 Advance Automatic Diffractometer in Bragg-Brentano geometry. Cu Kα1 radiation (λ = 1.5406 Å) was employed with 0.03° 2θ steps and a constant 8 s acquisition time in the 10–90 ° 2θ range. The effect of temperature was studied on the clays and FBs at 10 °C/min up to 1200 ºC using thermogravimetry (Setaram Setsys Evolution Thermogravimetric Analyser).

2.3.1.4. Characterisation of Fired Bricks

Fired ceramic products of all replicates were characterised in terms of linear firing shrinkage (using a precision calliper), weight loss during firing (UNE 772-13), water absorption (UNE 67027), bulk density (UNE-EN 772–13), 3-point flexural strength (UNE-EN 843-1), and compression strength (UNE-EN 772-13).

The leaching behaviour of potentially hazardous pollutants was determined by applying the equilibrium leaching test EN12457-2 proposed by European regulation as described previously in section 2.1.1.4. The elements studied were As, Cr, Mo, Pb, Sb, and Se.

The potential emissions (ψ) of pollutants (HCl, HF, SO_2, CO_2, and NO_x) were calculated using equation 1 displayed in section 2.1.1.4.

2.3.1.5. Statistical Treatment of Results. Validation of Established Models

The statistical analysis entails an adjustment of the results of the three replications of the technological properties: physical and mechanical, as well as the mobility results of polynomial mathematical equations, usually of 1st and 2nd degree. The results obtained in its 3 replications have been used to iteratively calculate the regression coefficients of the statistically relevant equations (models), for each clay-residue mixture and each of the responses. In this way, the final properties of the fired pieces have been related to the proportions of clay and residues present in the non-fired formulations. The calculations have been carried out with Statistica 7.0.

2.3.1.6. Multi-Criteria Analysis: Selection of the Optimal Formulations

A multi-criteria analysis (MCA) has been carried out through the application of a decision-making tool. Based on environmental impacts and technological results, the products that allow reducing the associated environmental burden will be proposed, while considering economic aspects, always complying with technical requirements. For this, DEFINITIVE 3.0 software has been used. The standardisation method used was weighted summation.

To use this decision-making tool, it is first necessary to define the alternatives, criteria, and scenarios to determine the best industrial formulation from a technical, environmental, and economic point of view.

The alternatives that have been considered for conducting the MCA are the FBs that have shown good technological properties and environmental performance. These waste are FS, FSL, SD, FS2, WS, and F. These alternatives are considered for the incorporation of 10 %, 20 %, and 30 % of residue, therefore, 19 alternatives have been defined considering the 100 % clay brick as well.

Three types of criteria have been defined to determine the optimal formulation to be carried out at an industrial scale. These criteria are in turn broken down into sub-criteria. Each of the criteria and their associated sub-criteria are presented below:

- Technical criteria: to evaluate this criterion, the results of density, water absorption, and compression strength of the clay-foundry mixtures obtained on a laboratory scale have been considered, therefore, 3 sub-criteria have been considered.
- Environmental criteria: the results obtained at the laboratory scale of the concentrations of the pollutants As, Cr, Mo, Sb, Se, and Pb in the leachates of the

ceramic products, the estimated atmospheric emissions of SOx, HCl, HF, CO_2 were considered. In addition, NOx for each of the clay-foundry residue mixtures and the saving of land that would entail the non-deposition of these residues in a landfill. In total, 12 sub-criteria were evaluated.

- Economic criteria: the costs of clay extraction, the cost of transporting the waste to the company Reciclados de Cabezón and the economic benefit that the company could obtain as a waste manager were evaluated, therefore, in this criterion 3 sub-criteria were considered.

These criteria have been given different weights to determine which is the best alternative in the three different scenarios described below. Such scenarios were formulated by giving different weights to the previously described criteria as shown next.

1st Scenario: all criteria have the same weight.

2nd Scenario: 50 % weight is associated with the economic criteria, a weight of 25 % with the technical criteria, and another 25 % with the environmental criteria.

3rd Scenario: 75 % weight to economic criteria, 12.5 % weight to technical and environmental criteria, respectively.

2.3.2. Incorporating Foundry Waste in Ceramic Processes

2.3.2.1. Raw Materials Characterisation

The characterisation results obtained from the raw material (clay) and all the by-products that have been valued for use as ceramics will be presented. The visual appearance of all the materials used is shown below in Figure 2.15.

The clay, supplied by Reciclados Cabezón enterprise, is a reddish granular material with a moisture content of 0.305 %. The particle size used is less than 0.5 mm. FS is a black and grey granular material with a humidity of 0.77 %. FS has a bulk density of 0.96 g/mL and an apparent density of 1.85 g/mL. The visual aspect is presented in Figure 2.15A. The FSL has a greyish colour and a humidity of 27 %, as can be seen in Figure 2.15B. The FSL was dried at 40 ºC for 3 days to determine the bulk and apparent density, as well as the particle size distribution. The bulk density is 0.84 g/mL and the apparent one is 1.91 g/mL. SD is a mustard-coloured powder with a humidity of 0.29 %. The bulk and apparent density of said residue are 0.82 g/mL and 2.65 g/mL, respectively. In Figure 2.15C, the visual appearance of SD is shown. FS2 is a sand-coloured powder with a humidity of 0.036, as seen in Figure 2.15D. This residue has a bulk density of 1.57 g/mL and an apparent density of 2.40 g/mL. CA is

a granular material with small greenish-black stones with a humidity of 0.21%, as shown in Figure 2.15E. This residue has a bulk density of 0.65 g/mL and an apparent density of 1.76 g/mL. WS is a black powder with and humidity of 2.44. In addition, they have a bulk density of 0.69 g/mL and an apparent density of 1.33 g/mL. The visual appearance of WS is presented in Figure 2.15G. The F is a black powder, as seen in Figure 2.15H, and humidity of 0.36%. The F has a bulk and apparent density of 1.12 g/mL and 2.02 g/mL, respectively.

The particle size of all the by-products used in this work (FS, FSL, SD, FS2, CA, WS, and F) whose visual appearance has been previously discussed, is shown in Figure 2.16.

The particle size distribution of the FS is presented in Figure 2.16A. FS presents 3 % of particles below 0.1 mm. The greatest contribution is produced by particles between 0.4 and 1 mm with 50 %, and, in addition, they have 14 % greater than 2 mm, as can be seen in Figure 2.16A. The particle size distribution of the FSL is presented in Figure 2.16B. Given the results obtained, the FSL has 40 % of particles below 0.4 mm. There are 45 % of particles between 0.4 and 2 mm, and 12 % of particles above 2 mm, approximately. The FSL has a heterogeneous particle size distribution after the drying process. The particle size distribution of SD is presented in Figure 2.16C. All particles have a particle size of less than 1 mm. The largest contribution is produced by particles with a size less than 0.15 mm, representing 67 % of the size. Between particle sizes of 0.15 mm and 4 mm there are 30 % of the particles and 3 % have a particle size between 0.4 mm and 0.8 mm. The particle size distribution of the FS2 is presented in Figure 2.16D. In this case, all the particles have a size of less than 0.8 mm, as was the case with SD. 65 % of the particles have a particle size less than 0.1 mm and the remaining 35 % have a particle size between 0.1 and 0.4 mm. CA has a particle size of less than 2 mm, as shown in Figure 2.16E. The highest contribution is produced by the ashes with a particle size of less than 0.4 mm with 50 %, 40 % of particles have a size between 0.4 and 0.8 mm and 10 % have a particle size between 1 and 2 mm. The particle size distribution of WS is presented in Figure 2.16F. WS has a particle size of less than 1 mm. 75 % of the wet sand particles have a size less than 0.1 mm, 20 % have a size between 0.1 and 0.4 mm, and 5 % have a size between 0.4 and 1 mm. The particle size distribution of the F is presented in Figure 2.16G. The F has a particle size of less than 0.8 mm. The largest contribution is produced by fine particles with a size smaller than 1 mm with 85 % and the remaining 15 % has a particle size between 0.1 and 0.4 mm.

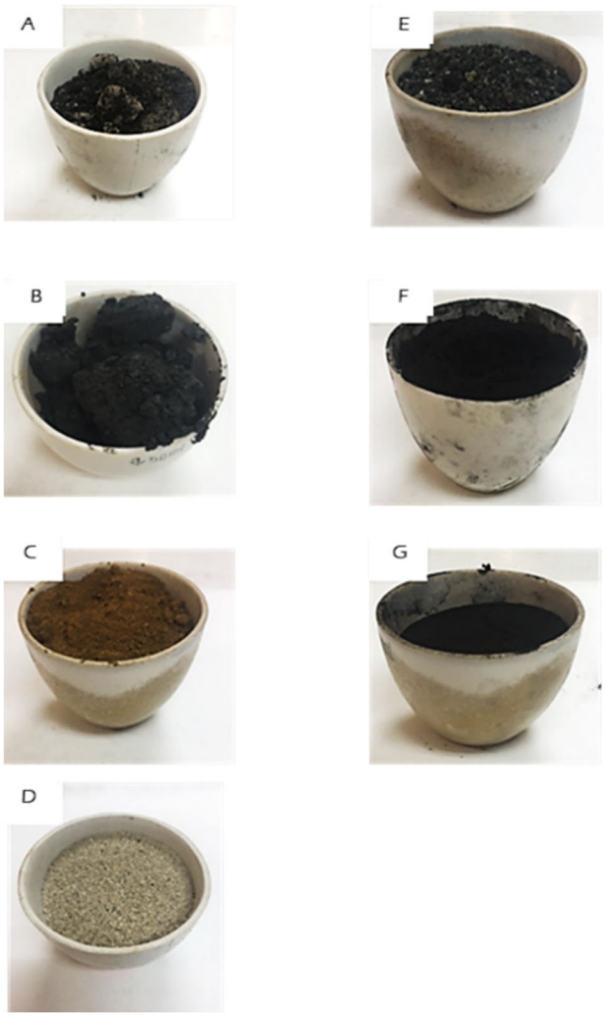

Figure 2.15. Visual appearance of the FBs used: (A) FS (Foundry Sand-cast iron); (B) FSL (Foundry Sludge); (C) SD (Steel Dust); (D) FS2 (Foundry Sand-ductile iron); (E) CA (Cupola Bottom Ash); (F) WS (Wet Sands); and (G) F (Fines).

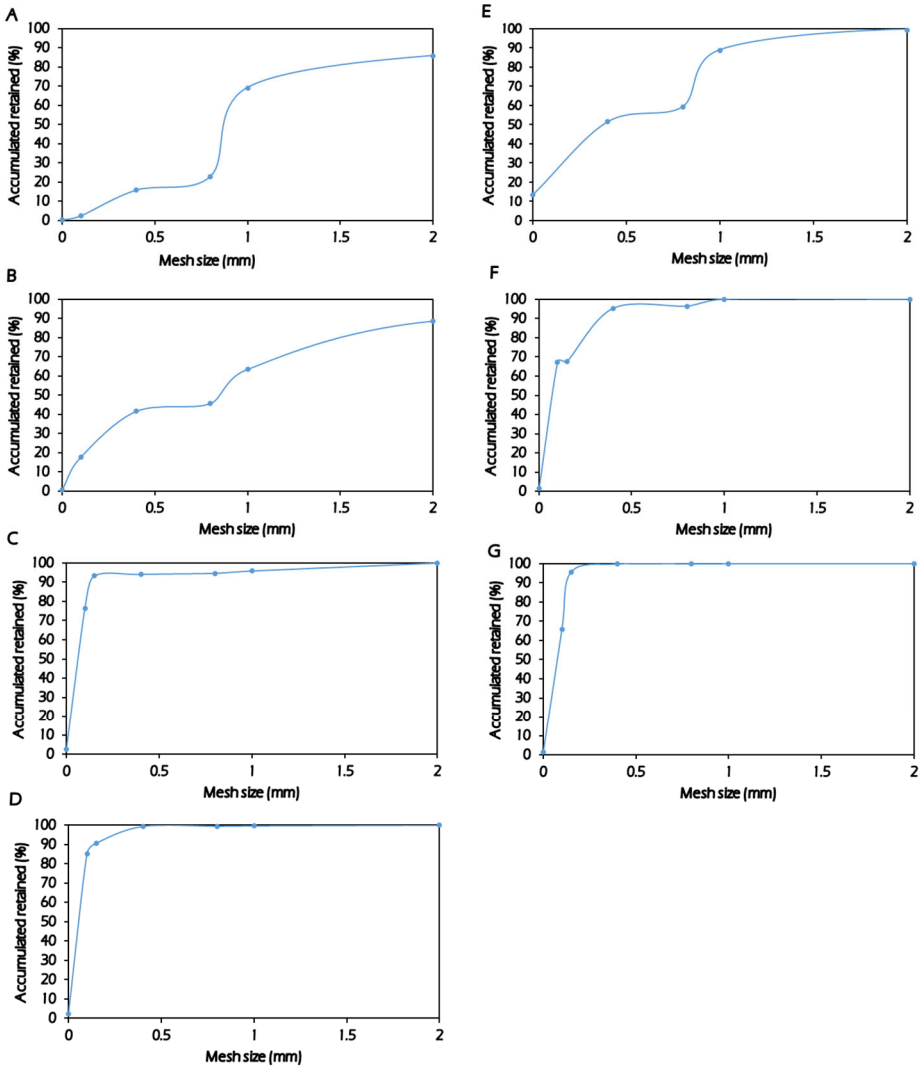

Figure 2.16. Particle size distribution of FBs: (A) FS (Foundry Sand-cast iron); (B) FSL (Foundry Sludge); (C) SD (Steel Dust); (D) FS2 (Foundry Sand-ductile iron); (E) CA (Cupola Bottom Ash); (F) WS (Wet Sands); and (G) F (Fines).

Table 2.7 shows the chemical composition (major and minor oxides and trace elements) of the clay from the company Reciclados Cabezón S.L. and the by-products used in this chapter.

The clay has three major oxides: silicon with 63.4 %, aluminium with 17.11%, and iron with 5.89 %, which together make up more than 75 % of the total clay. The minority fraction is made up of eight oxides: manganese (0.079 %), magnesium (0.86 %), calcium (0.58%), sodium (0.69 %), potassium (2.67 %), titanium (0.762 %) and

phosphorus (0.1 %). The contents of the major oxides and trace elements identified in raw materials are listed in Table 2.7.

The FS has silica (SiO_2) as the main oxide with 86.9 %. The other oxides that have a weight percentage greater than 1 % are Al_2O_3 (2.31 %) and Fe_2O_3 (4.31 %), the rest of the alkali, alkaline earth oxides, MnO, TiO_2, and SO_4 are below 0.5 % concentration. The trace elements with the highest content in FS are Ba, Cu, and Zn.

Loss of ignition (LOI) is associated with the presence of clay minerals, hydroxides, organic matter, and volatile components and is an important parameter in the ceramic process. The loss on ignition of the FS is 6.24 %. FSL has Zn as the main element in its composition since it has concentrations higher than 10,000 ppm. In addition to Zn, among the trace elements, Cu and Pb have the highest content in FSL.

Among the major oxides, those with the highest concentrations are SiO_2 (11.3 %) and Fe_2O_3 (9.25 %). Iron oxides act as fluidizing agents in the firing stage, favouring the development of the liquid phase. FSL has a loss on ignition of 18.07% due to the presence of organic matter. The main oxides of SD are SiO_2 (18.4 %), Fe_2O_3 (22.9 %), and CaO (9.97 %), it also presents concentrations higher than 1.00 % in alkali and alkaline earth oxides, as shown see in Table 2.7.

Alkali and alkaline earth oxides, together with iron oxides, act as fluidizing agents. Among the trace elements with the highest content are Cd, Cu, Cr, Pb, and Zn. SD has an LOI of 9.48 %. FS2 whose chemical composition is indicated in Table 2.7, present SiO_2 (99.1 %) as the main oxide in their composition, the rest of the oxides are found in concentrations lower than 0.50 %. The trace element with the highest content is Zn. The LOI is 0.04 % so it does not suffer losses in the ceramisation process. CA present as major oxides SiO_2 (8.73 %) and Fe_2O_3 (12.1 %).

The loss on ignition of CA is 58.0 %, as presented in Table 2.7. This may be due to the presence of organic matter. The trace elements with the highest content are Cu and Zn. WS present as major oxides SiO_2 (46.4 %) and Al_2O_3 (11.4 %), they also present important compositions in alkali, alkaline earth, and ferric oxides that could act as fluidizing agents in the ceramisation process. The LOI is 31.74, as presented in Table 2.7. The trace elements with the highest content are Ba and Zn. F present as two major oxides: silica with 43.5 % and iron with 41.3 %, which together represent more than 83.0 % of the total fines. The rest are made up of up to eight more oxides, the most important being: aluminium (6.41 %), manganese (1.32 %), magnesium (1.54 %), and calcium (1.22 %), and sodium (1.04 %). They have an LOI of 3.67 %, as observed in Table 2.7. Cr, Ni, and Zn are the trace elements with the highest content.

Table 2.7. Chemical composition of the raw material and foundry by-products used.

Oxides (%, weight)	Clay	FS	FSL	SD	FS2	CA	WS	F
SiO_2	63.35	86.94±0.95	11.26±0.12	18.43±0.01	99.06±0.21	8.73±0.21	46.37±0.25	43.51±0.05
Al_2O_3	17.11	2.31±0.04	0.56±0.02	4.54±0.01	0.31±0.00	2.13±0.03	11.42±0.19	6.41±0.06
Fe_2O_3	5.89	4.31±0.08	9.25±0.02	22.90±0.18	0.59±0.00	12.13±0.29	2.83±0.03	41.32±0.19
MnO	0.054	0.10±0.05	1.49±0.01	0.93±0.01	0.06±0.00	0.28±0.01	0.10±0.00	1.32±0.03
MgO	0.85	0.32±0.08	0.34±0.00	1.48±0.00	0.03±0.00	0.22±0.00	2.71±0.04	1.54±0.01
CaO	0.47	0.34±0.09	1.73±0.02	9.97±0.01	0.05±0.01	1.81±0.09	2.16±0.02	1.22±0.01
Na_2O	0.61	0.27±0.01	0.59±0.02	1.53±0.01	0.02±0.00	0.16±0.01	1.87±0.01	1.04±0.01
K_2O	3.08	0.52±0.04	0.68±0.03	1.29±0.01	0.04±0.00	0.33±0.01	0.50±0.01	0.35±0.01
TiO_2	0.843	0.20±0.05	0.02±0.00	0.19±0.00	0.07±0.00	0.13±0.00	0.30±0.00	0.24±0.00
P_2O_5	0.1	0.03±0.00	0.03±0.01	0.21±0.01	<0.01	0.03±0.01	0.05±0.01	0.04±0.01
LOI*	6.15	17.1±1.24	18.07±0.05	9.48±0.04	0.04±0.00	58.04±0.72	31.74±0.06	3.67±0.01
Trace elements (ppm)								
As	23	<5	<5	17.50±2.12	<5	7±0.00	<5	10.00±0.00
Ba	634	163.67±0.89	68.33±0.58	1095±4.24	40±0.00	163.67±0.89	337.33±1.53	230.00±1.53
Cd	<0.5	<0.5	1.93±0.15	1090±0.00	<0.5	<0.05	<0.5	0.55±0.07
Cr	80	76.61±0.91	80.00±0.00	440.00±0.00	50.00±0.00	133.33±0.77	23.33±0.77	743.33±5.77
Cu	30	164.33±0.89	405.67±7.37	1235±21.21	14±0.07	583.67±12.58	23.00±1.00	113.33±1.55
Hg (ppb)	-	14±0.72	60.67±0.58	871.50±10.61	<5	<5	10.00±0.00	6.33±0.58
Mo	<2	5.00±0.83	5.67±0.58	33.50±0.70	<2	9.00±0.00	<2	72±0.00
Ni	40	24.33±0.96	18.00±1.00	175.50±0.71	29.00±0.00	44.33±0.58	9.00±0.00	206.00±1.73
Pb	28	12.67±0.66	223.67±3.06	>5000	<5	14.67±1.15	13.67±1.15	11.67±1.15
Sb	<0.5	<0.5	6.30±1.51	>200	<0.5	2.17±0.06	<0.5	2.17±0.06
Sr	12	29.67±0.97	63.33±1.53	405.50±9.19	4.00±0.00	142±1.00	136.67±1.15	79.00±0.00
Zn	80	116.67±0.31	>10000	>10000	875.00±0.21	>10000	233.67±5.28	193.33±5.77

The mineralogical analyses of the clay (Figure 2.17A) show crystalline phases of quartz (SiO_2) and aluminosilicates such as muscovite (KAl_2 ($AlSi_3O_{10}$) $(OH)_2$), kaolinite ($Al_2Si_2O_5$ $(OH)_4$) and dickite ($Al_2Si_2O_5$ $(OH)_4$). These phases can constitute approximately 90.0 % of the total.

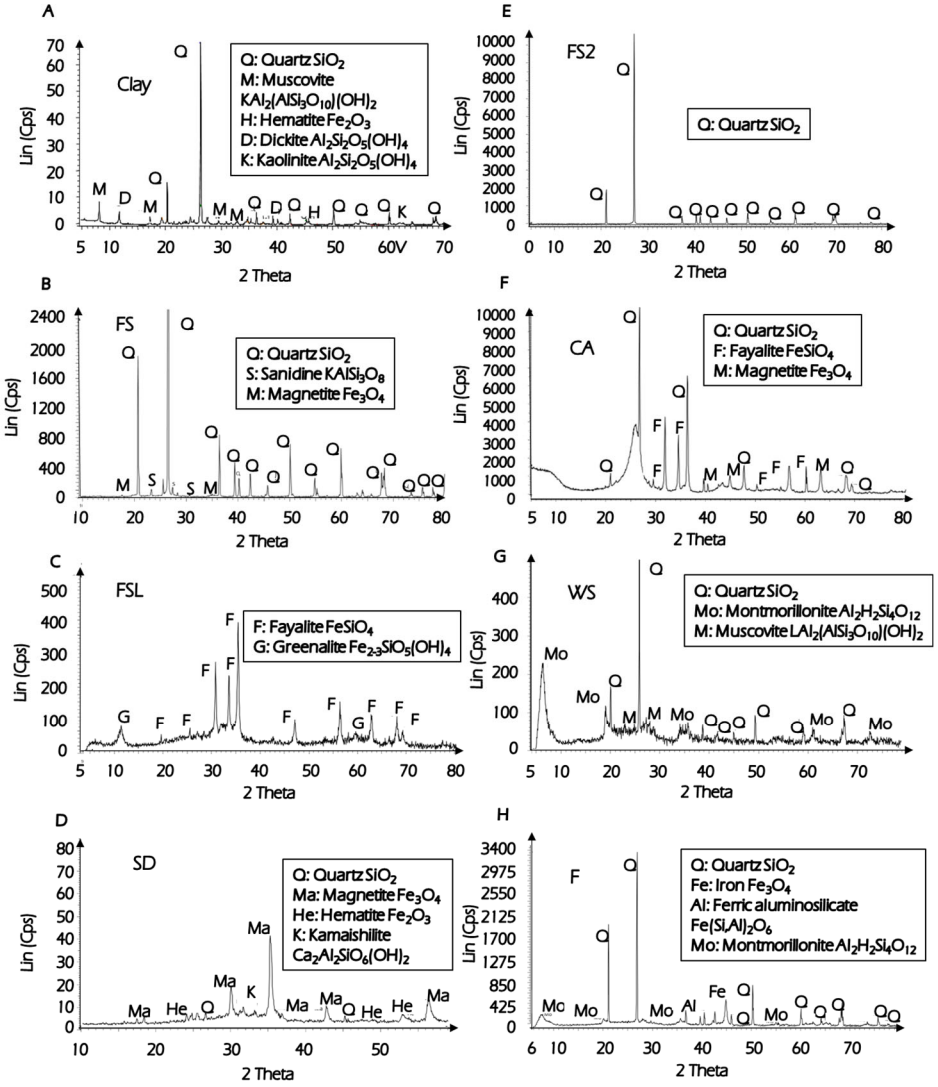

Figure 2.17. XRD of raw material and FBs: (A) Clay; (B) FS (Foundry Sand-cast iron); (C) FSL (Foundry Sludge); (D) SD (Steel Dust); (E) FS2 (Foundry Sand-ductile iron); (F) CA (Cupola Bottom Ash); (G) WS (Wet Sands); and (H) F (Fines).

The minority phase is iron oxide (Fe_2O_3), as observed in the X-ray diffractogram (XRD) in Figure 2.17A. FS has quartz (SiO_2) as the majority crystalline phase, which

represents approximately 85 % of this residue. The minority phases are sanidine (K($AlSi_3O_8$) and magnetite (Fe_3O_4), as shown in Figure 2.17B. Mineralogical analysis of the FSL shows crystalline major phases of fayalite (Fe_2SiO_4). This phase can constitute approximately 90 % of the total. The minority phase is greenalite ($Fe_3Si_2O_5OH_4$), as can be seen in Figure 2.17C. The majority phases of the SD are magnetite (Fe_3O_4) and hematite (Fe_2O_3) which represent approximately 80 % of this. SD has quartz (SiO_2) and kamaishilite ($Ca_2Al_2SiO_6$ $(OH)_2$) as minor phases, as shown in Figure 2.17D. FS2 has as crystalline phase the quartz (SiO_2) that constitutes approximately 100 % of this residue, as shown in Figure 2.17E. The mineralogical analysis of CA presents quartz (SiO_2) and fayalite (Fe_2SiO_4) as the main crystalline phases. In this sense, quartz and fayalite can constitute about 80 % of the residue, as presented in Figure 2.17F. As a minority phase, it presents magnetite (Fe_2O_3). The mineralogical analysis of the WS shows an amorphous fraction in the form of maximum width between 20 and 30 degrees. On the other hand, the main crystalline phases are quartz (SiO_2) and montmorillonite ($AlSi_2O_6$ $(OH)_2$), as shown in Figure 2.17G. These phases constitute approximately 80.0 % of WS. In addition, WS has minority phases of muscovite (KAl_2 $(AlSi_3O_{10})$ $(OH)_2$). The main crystalline phases of the F are quartz (SiO_2), iron (Fe), and ferric aluminosilicate ($Al_{0.5}Fe_3Si_{0.5}$). As a minority phase this montmorillonite ($AlSi_2O_6$ $(OH)_2$), as observed in Figure 2.17H.

The thermogravimetric analysis (TGA) of the clay, represented in Figure 2.18A, shows the typical dehydroxylation process with a loss of mass of 2 % up to 100 °C which is associated with the exothermic pick (Figure 2.18I). Furthermore, the clay presents two endothermic picks referred to as the dihydroxylation of the clays, and decomposition of aluminosilicates at 500-550 °C. The thermal behaviour of FS presents an endothermic peak at 127 °C accompanied by a weight loss of almost 2 %, indicating the evolution of physically adsorbed surface waters, as shown in Figure 2.18B and Figure 2.18J. Between 300 °C and 600 °C, two endothermic peaks (Figure 2.18J) are produced accompanied by a loss of mass of 4 %, which may be due to the decomposition of organic matter and combustion of volatile compounds, as observed in Figure 2.18B. FSL shows an endothermic peak 1 associated with a 10.0 % mass loss at 290 °C due to the decomposition of the phenols present in this residue, as shown in Figure 2.18C and Figure 2.18K. Between 300 °C and 700 °C, there is a 10 % loss of mass (Figure 2.18C) that is associated with three endothermic decompositions of organic matter and combustion of volatile compounds, as observed in Figure 2.18K. SD presents a loss of mass of 2 % at 120 °C (Figure 2.18D) associated with an exothermic peak 1 due to the elimination of absorbed surface waters, as observed in Figure 2.18L. The greatest mass loss of this residue occurs at 600 °C to 950 °C (Figure 2.18D), with 10 % associated with an endothermic peak 2

(Figure 2.18L) at 690 °C, due to the presence of clay minerals and hydroxides. FS2 presents a mass loss of 0.45 % up to 600 °C due to the elimination of surface water and organic matter, as observed in Figure 2.18E. The exothermic peak that appeared at 600 °C in Figure 2.18M, is associated with a weight gain in the TGA, which could be due to the oxidation of some compounds present in the atmosphere. The CA presents a 20 % mass loss between 600 °C and 850 °C (Figure 2.18F) that is associated with endothermic peaks 1 and 2 (Figure 2.18N) due to the combustion of volatile compounds and decomposition of organic material. At 900 °C there is an exothermic peak 3 that implies a mass gain in the residue up to 1050 °C of 10.0 %, as shown in Figure 2.18N. This mass gain may be due to the oxidation of Fe (II) to Fe (III) since it is the majority oxide in this residue. WS (Figure 2.18G and Figure 2.18O) present an endothermic peak at 120 °C accompanied by a 6 % loss of mass, indicating the evolution of physically absorbed surface waters. The greatest mass loss of WS occurs between 400 °C and 600 °C with a 24 % loss accompanied by an endothermic peak at 550 °C due to the decomposition of clay minerals, as shown in Figure 2.18G and Figure 2.18O. This loss of mass is in tune with the losses due to ignition presented by WS. F shows a loss of mass of 1.5 % at 130 °C (Figure 2.18H) accompanied by an endothermic peak due to the elimination of surface water. The greatest mass loss is 7 % between 500 °C and 600 °C (Figure 2.18H) due to the decomposition of clay minerals that are associated with an endothermic point at 540 °C, as shown in Figure 2.18P. At 800 °C, an exothermic peak occurs that is accompanied by a mass gain by the residue, due to the oxidation of iron, which is the main element of F.

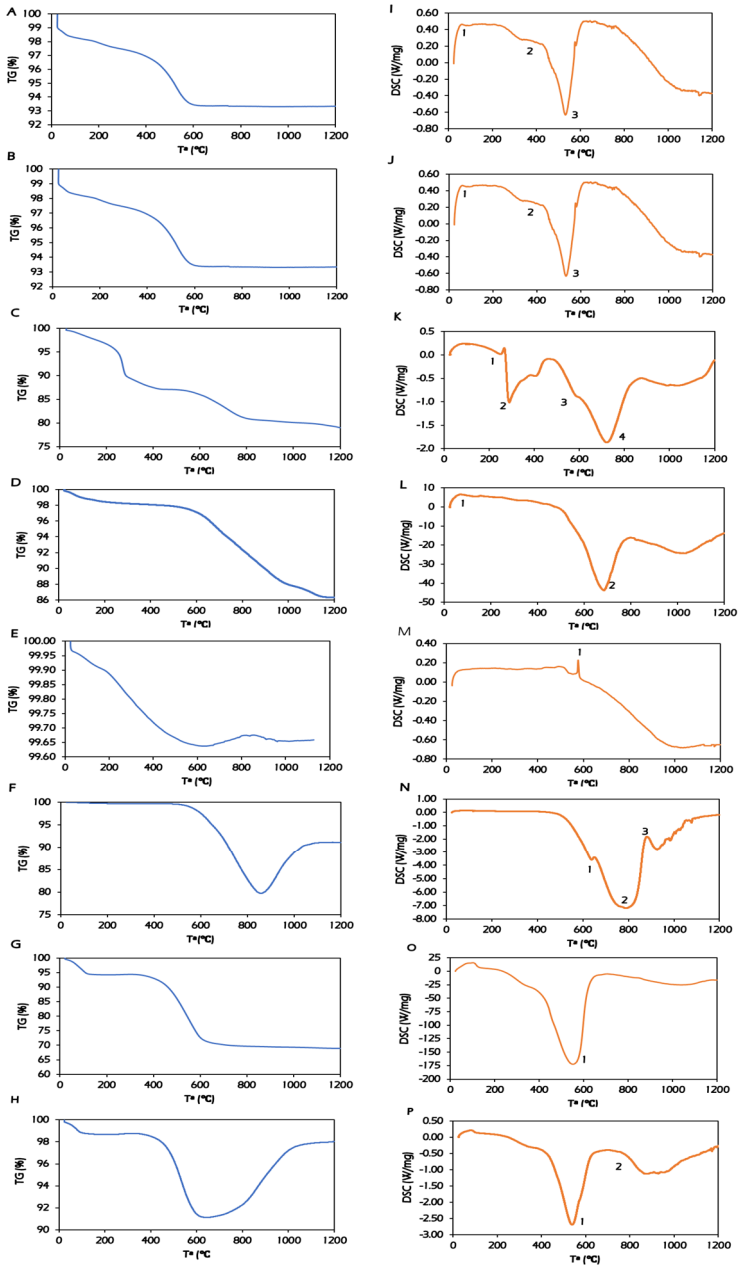

Figure 2.18. Thermal characterisation of raw materials and Foundry by-products. On the left: Thermogravimetric analysis (TGA); Right: Differential Scanning Calorimetry (DSC): (A) and (I) Clay; (B) and (J) FS (Foundry Sand-cast iron); (C) and (K) FSL (Foundry Sludge); (D) and (L) SD (Steel Dust); (E) and (M) FS2 (Foundry Sand-ductile iron); (F) and (N) CA (Cupola Bottom Ash); (G) and (O) WS (Wet Sands); and (H) and (P) F (Fines).

2.3.2.2. Technological Properties of Fired Bricks

Looking at the bricks of Figure 2.19, the pieces obtained with a percentage in FS, WS, F, and FS2 less than 40 %, show a visual appearance like the pieces made only with clay. FSL, CA, and SD with a percentage of 10 % show a visual appearance like that of 100 % clay-based bricks, undergoing changes in aspects at higher percentages as observed in Figure 2.19.

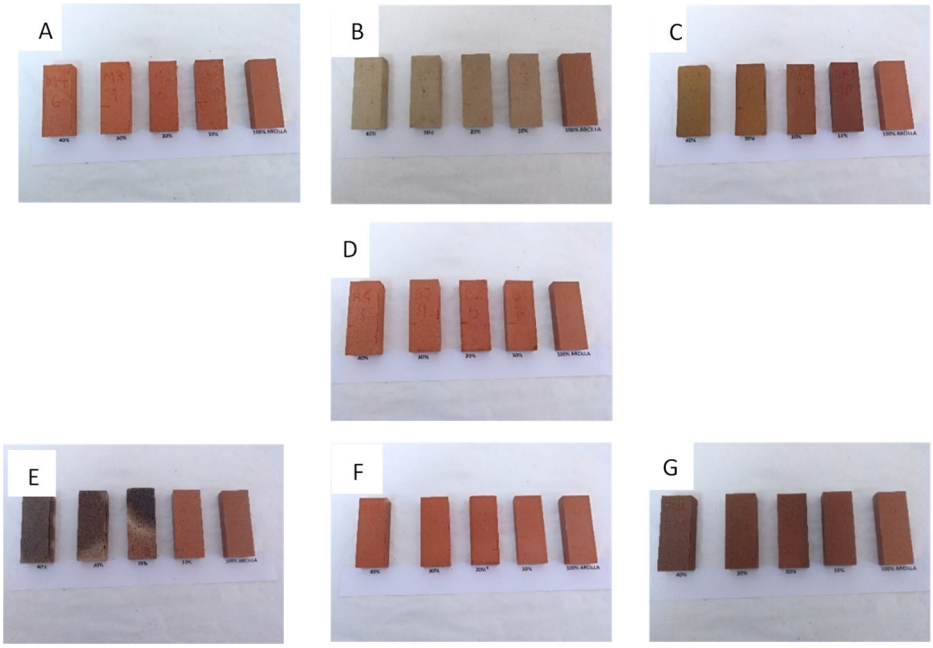

Figure 2.19. Ceramic pieces using clay-foundry by-products: (A) FS (Foundry Sand-cast iron); (B) FSL (Foundry Sludge); (C) SD (Steel Dust); (D) FS2 (Foundy Sand-ductile iron); (E) CA (Cupola Bottom Ash); (F) WS (Wet Sands); and (G) F (Fines).

The technological properties of the alternative ceramic products containing foundry by-products measured in this work were weight loss during firing, linear firing shrinkage, water absorption, bulk density, and flexural strength. Results are summarized in Figure 2.20.

The weight loss values can be mainly attributed to the elimination of both free water and water of crystallisation, the combustion and volatilisation of organic matter, and the decomposition of carbonates. The release of these species during the firing process leads to the development of a porous system in the ceramic product in general. Foundry sands FS and FS2 show weight loss results higher than 100 % clay-based bricks, however, higher percentages present better results. This may be due to

the low ignition loss content of these by-products (0.04 % and 6.24 %), which implies that it does not suffer losses due to the combustion of organic matter and volatile compounds. FSL and SD have LOI values of 18.0 % and 9.03 %, respectively, meaning a high loss of mass in the firing stage due to the decomposition of the organic matter. WS and CA have similar weight loss values to those of FSL and FS2. Their weight losses increase, as the percentage of FBs increases due to the high LOI values of these by-products (31 % and 57 %, respectively). On the other hand, F presents lower values of loss by firing than 100 % clay-based bricks even for the 40 % percentage, since it hardly undergoes decomposition at high temperatures. The results of average weight loss and standard deviation are shown in Table A.4.1. (Annex 4).

Linear shrinkage is the change in length measurements of specimens when firing and is a very important test in ceramic industries as it is related to the formation of the glass phase and the degree of densification during sintering. The linear shrinkage of FB-FCBs increases as more by-product is introduced into the brick. Introducing 10.0 % of FS2 the same results are obtained as for 100 % clay-based bricks. For FS and SD, up to 20 % can be introduced into FB-FCBs since shrinkage results are lower or like 100 % clay-based bricks. The only by-product that presents similar results to 100 % clay-based bricks for all dosages is FS. In the case of CA-based bricks and F-based bricks, there is an expansion caused by the high content of Fe_2O_3 present in both by-products. WS can be introduced up to 10 % obtaining lower results than 100 % clay-based bricks. In Table A.4.2. (Annex 4) the results of linear shrinkage are collected.

The results obtained for density are shown in Figure 2.20. As the dosage of by-products introduced into ceramics increases, the brick density decreases. Bricks made with 10 % of FS, 30 % of SD, and 30 % of FS2 present density results similar to or higher than 100 % clay-based bricks. The admissible amount of FS is lower in comparison with SD and FS2 because of the high LOI values, affecting the densification of the bricks. Regarding F, CA, and WS, these by-products also show lower density results as the FB dosage increases. For a percentage of 10 %, F-based bricks have similar densities to 100 % clay-based bricks. Bricks made of CA and WS, due to their LOI contents, present low values for 100 % clay-based bricks, and the density decreases more and more as the number of by-products increases. Table A.4.3. (Annex 4) are shown the average values and standard deviation of the experimental values obtained for the bulk density.

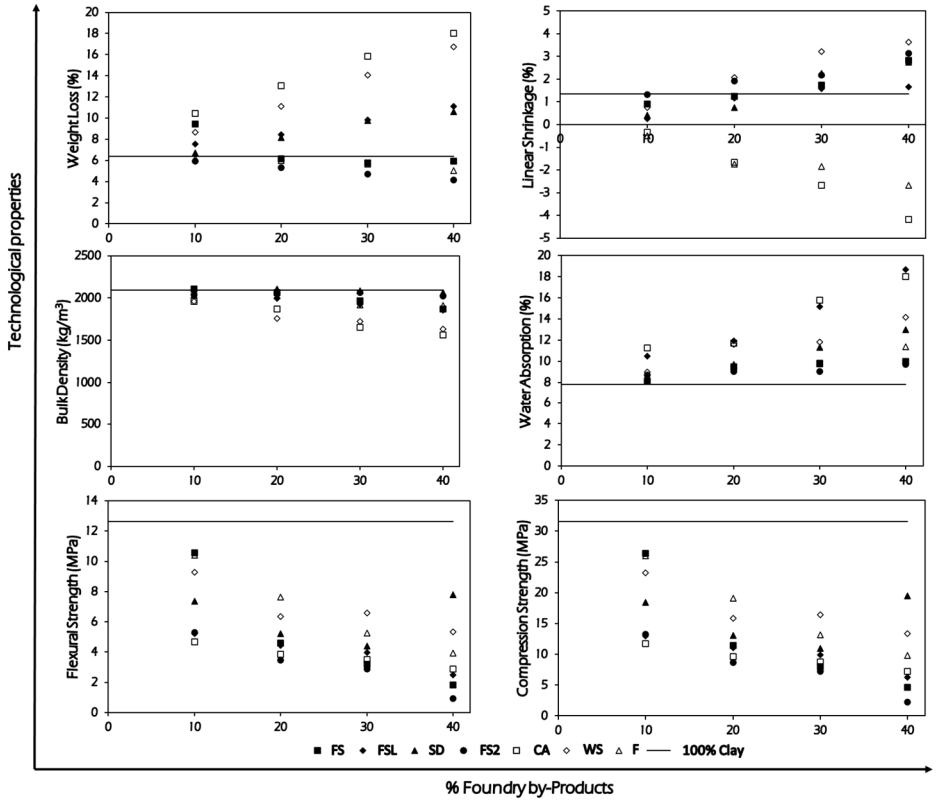

Figure 2.20. Technological properties of foundry by-products-fired clay bricks (FB-FCBs). FS (Foundry Sand-cast iron); FSL (Foundry Sludge); SD (Steel Dust); FS2 (Foundy Sand-ductile iron); CA (Cupola Bottom Ash); WS (Wet Sands); and F (Fines).

The specific absorption of the brick is the percentage of water absorbed with the mass of the dried brick. The water absorption for the seven tested FBs is also represented in Figure 2.20. As the content of FB increases, there is an increase in the absorption of water, because FB-FCBs are more porous than 100 % clay-based bricks. This is due to the decomposition of the organic matter present in the by-product. When the dosage of FB is below 10 %, the water absorption results of the FB-FCBs are quite similar to 100 % clay-based bricks, except for FSL. In terms of water absorption, FS2 could be introduced up to 40 % since similar results are obtained in the case of 100 % clay-based bricks. CA and WS, which have high LOI contents, present very high-water absorption values as the content of said residues increases. During the firing process of the bricks, the porosity of the bricks increases, due to the decomposition process of organic matter, increasing the final water absorption. CA dosage of 10 % can be introduced into the bricks to achieve similar absorption values

as the 100 % clay-based bricks. The results of average water absorption and standard deviation are shown in Table A.4.4. (Annex 4).

The results obtained for compression strength are shown in Figure 2.20. In general terms, the compression strength decreases as the dosage content of FBs increases. This property is related to the absorption of water which is equivalent to the porosity of the ceramic piece. The greater the water absorption, the less the compression force, due to the greater volume of pores in the brick that act as crack initiation points. Bricks with a 10 % content of FS present compression strength values close to 100 % clay-based bricks. Bricks with a 10 % content of F achieve a resistance like that of 100 % clay-based bricks. In Table A.4.5. and Table A.4.6. (Annex 4), the results of flexural and compression strength are collected.

Looking at the results of the technological properties previously discussed for each of the FBs tested, among all the by-products, the worst behaviour was shown in the bricks made with CA even at lower dosages. As can be seen in Figure 2.20, CA-based bricks presented the highest weight loss and water absorption, the lowest linear shrinkage, and one of the worst results of flexural strength and compression strength. Consequently, FB-FCBs containing CA, will not be studied in the subsequent sections.

2.3.2.3. Leaching Behaviour of Fired Bricks

For the study of environmental behaviour, mixtures of clay-foundry waste with good technological properties are considered, therefore, those obtained by incorporating Cupola Ash and mixtures with 40 % residue are discarded.

The FB-FCBS comply for Sb, Cr, Pb, and Se with the limits established by the ministerial order AAA / 661/2013 (Order AAA / 661, 2013) in landfills of inert waste at the end of its useful life at any FB dosage. As and Mo are below the non-hazardous waste landfill limit.

Looking at the results observed in Table 2.8, in all cases, concentrations of elements are below the limit for disposal in non-hazardous waste landfills. For all waste, Cr concentrations are below the limits for inert landfills. For all the percentages of WS, the values of concentrations obtained allow its dumping in the inert landfill. For SD and F, in all cases, the limit for Mo is exceeded for its discharge into an inert landfill. For FSL, in percentages equal to and greater than 20 %, the limit for its discharge into an inert landfill is exceeded for Mo. For FS, in percentages equal to and greater than 20 %, the limit for its dumping of inert is exceeded for As.

Table 2.8. Average values of the concentration (mg/kg) of the elements from compliance leaching test EN 12457-2 applied to FB-FCBs and the landfill limit established by Ministerial Order AAA / 661/2013.

Foundry By-products- Fired Clay Bricks (FB-FCBs)						
FB dosage (%)	As	Cr	Mo	Pb	Sb	Se
-	0.3±0.06	0.08±0.005	0.2±0.001	0.06	<0.06	<0.1
FS						
10	0.35±0.01	0.05±0.002	0.2±0.001	<0.05	<0.06	<0.1
20	0.7±0.08	0.055±0.001	0.1±0.008	<0.05	<0.06	<0.1
30	0.4±0.02	0.06±0.003	0.1±0.006	<0.05	<0.06	<0.1
FSL						
10	0.4±0.01	0.055±0.006	0.3±0.005	<0.05	<0.06	<0.1
20	0.4±0.01	0.05±0.001	0.6±0.003	<0.05	<0.06	<0.1
30	0.3±0.03	0.05±0.003	0.75±0.002	<0.05	<0.06	<0.1
SD						
10	0.3±0.04	0.09±0.002	1.2±0.009	<0.05	<0.06	<0.1
20	0.2±0.001	0.07±0.008	1.9±0.01	<0.05	<0.06	<0.1
30	0.2±0.009	0.055±0.001	2.1±0.03	<0.05	<0.06	<0.1
FS2						
10	0.4±0.03	0.065±0.004	0.2±0.005	<0.05	<0.06	<0.1
20	0.6±0.005	0.06±0.003	0.1±0.001	<0.05	<0.06	<0.1
30	0.85±0.06	0.065±0.002	0.1±0.007	<0.05	<0.06	<0.1
WS						
10	0.4±0.07	0.05±0.009	0.2±0.006	<0.05	<0.06	<0.1
20	0.25±0.009	0.09±0.001	0.2±0.003	<0.05	<0.06	<0.1
30	0.35±0.01	0.065±0.002	0.2±0.002	<0.05	<0.06	<0.1
F						
10	0.2±0.02	0.085±0.003	1.4±0.01	<0.05	<0.06	<0.1
20	0.4±0.003	0.085±0.004	3.5±0.09	<0.05	<0.06	<0.1
30	0.45±0.01	0.065±0.007	4.65±0.11	<0.05	<0.06	<0.1
Landfill Limit						
Inert	0.5	0.5	0.5	0.5	0.06	0.1
Non-hazardous	2	10	10	10	0.7	0.5

FS (Foundry Sand-cast iron); FSL (Foundry Sludge); SD (Steel Dust); FS2 (Foundy Sand-ductile iron); CA (Cupola Bottom Ash); WS (Wet Sands); and F (Fines).

2.3.2.4. Gas Emissions within the Firing Process

The content of Cl, F, S, C, and N for the Clay and FBs, as well as their corresponding acid gas emissions HCl, HF, SO_2, CO_2, and NOx after the firing stage at the temperature of 1050ºC simulating the industrial processes and estimated by mass balance (Eq. 1), are summarized in Table 2.9. The initial and final content of FBs and Clay of the elements mentioned before and after firing are collected in Table A.5.1. (Annex 3). FS2 presents lower emissions of pollutants than those of clay due to the high crystallinity of these FBs. FS2 is formed by quartz (SiO_2) which is very stable at a high temperature (Figure 2.17D). Chlorine emissions depend on the initial concentration of the samples (Galan et al., 2002). In Table 2.9, all the FBs present higher concentrations of Cl compared to clay, except FS and Fines. The significant increase in chlorine emissions in F compared to clay, despite having similar initial content, may be due to the presence of organic matter. Fluorine emissions also depend on the initial content of samples (Galan et al., 2002). All the FBs present higher concentrations of F than clay, except FS. In the case of CO_2 emissions, a direct relationship is observed between the initial carbon content in the raw materials and the level of emissions. As is observed in Table 2.9, all the FBs present C concentrations higher than clay. These C concentrations are related to the LOI content of FBs. Finally, in the case of NOx emissions, N is below the detention limit for Clay, FSL, SD, and FS2. FS, WS, and F present NOx emissions due to the foundry process where these FBs are generated. The NOx emissions in these FBs may be due to the presence of nitrogen as Phenolic-Isocyanate, which is very unstable during the firing process.

Table 2.9. Content and pollutants emissions of Clay and Foundy By-products.

Raw Materials	Initial Content (%)					Emissions (mg/kg)*				
	Cl	F	S	C	N	HCl	HF	SO_2	CO_2	NO_x
Clay	0.025	0.01	0.065	0.3	-	54.79	56.10	958.02	11323	-
FS	0.01	0	0.05	3.01	0.1	0	0	639.29	117242.9	334.82
FSL	0.21	0.08	0.72	10.7	-	1631.83	899.7	15558.7	476310	-
SD	3.3	0.3	0.89	4.35	-	36242.7	3373.7	5518.1	175277.6	-
FS2	0.01	0	0	0.01	-	0	0	0	0	-
WS	0.05	0.07	0.27	20.6	0.5	602.65	925.62	585.41	1105282	18413.6
F	0.02	0.05	0.27	8.95	0.2	106.76	437.27	4148.25	340062.7	3262

(-) < Detection Limit; (*) Gas emissions calculated according to the mass balance of eq. 1.

Gas emissions for the mixtures of FBs/Clay fired at the temperature of 1050 ºC simulating the industrial processes and estimated by mass balance (Eq. 1) are summarized in Figure 2.21. Emission limit values for HF, HCl, and SO_x proposed by

Gonzalez et al., 2011 (Gonzalez et al., 2011) aim to include in the Andalusian-Spain legislation in response to the indications of the IPPC, have also been considered. From a study conducted with 40 ceramic factories in Andalusia, Spain through the median and the 90th percentile values of 180 samples, three ranges de emission values are established: "acceptable", "recommended intervention" and "compulsory intervention". The emission values proposed by González et al. are shown in Table A.3:2. of Annex 3

The HCl emission for the FB-FCBs fired at a temperature of 1050 ºC is plotted in Figure 2.21. The introduction of FS, FS2, and F in the mixtures reduce HCl emissions due to the low content of Cl present in these waste (Quijorna et al.; 2012; Coronado et al., 2016). The reduction percentage obtained is 30 % for FS, 30 % for FS2 and 89 % for F. The estimated emission values for the clay mixtures with these residues are below the acceptable emission values proposed by Gonzalez et al., 2011 (González et al., 2011) up to 30 % dosages. On the other hand, FSL, SD, and WS increase HCl emissions. Although the atmospheric emissions of HCl increase, the addition of 30% WS presents emission values below the acceptable emission limit, the FSL presents acceptable emission values up to 10 %, and the SD is observed to exceed the emission values for mandatory intervention for dosages above 10 %, so it is recommended to introduce lower dosages.

The introduction of FS and FS2 in the FB-FCBs reduces HF emissions due to the low F content of these foundry sands, as shown in Figure 2.21B. Incorporating up to 30% FS and FS2 reduce HF emissions by 30 % compared to 100 % clay brick. The mixtures of clay with FSL, SD, WS, and F increase the estimated HF emission values calculated using equation 1, due to the higher F contents presented by these residues for clay (Coronado 2016). According to the values proposed in Gonzalez et al., 2011, the acceptable emission limit value of HF is <180 ppm, therefore, the addition of 30 % of FS, FS2, and F, 20 % of WS, and 10 % of FSL does not exceed the acceptable emission value proposed in the study. Additions of 10% of SD are below the recommended intervention values.

The SO_x emissions for the FB-FCBS fired at the temperature of 1050 ºC are shown in Figure 2.21C. The introduction of FS, FS2, and WS in the mixtures produce a decrease in SO_x emissions due to the low content of S for the FS and FS2 and little loss of S that the WS experience during the firing process. The introduction of these residues in the mixtures would reduce the emissions between 15-30 % for dosages of up to 30 %. FSL, SD, and F increase SO_x emissions in mixtures, being higher for SD (Ukwatta et al., 2018). Considering the emission values proposed in Gonzalez et al., 2011, FS, FS2, and WS would be below the acceptable value limit for dosages of 30 % of residue, and FSL and F would be between the recommended intervention values for

dosages of 30 % and SD would be between the recommended intervention values for 10 % of the introduction of this waste, for higher dosages it presents emission values of mandatory intervention.

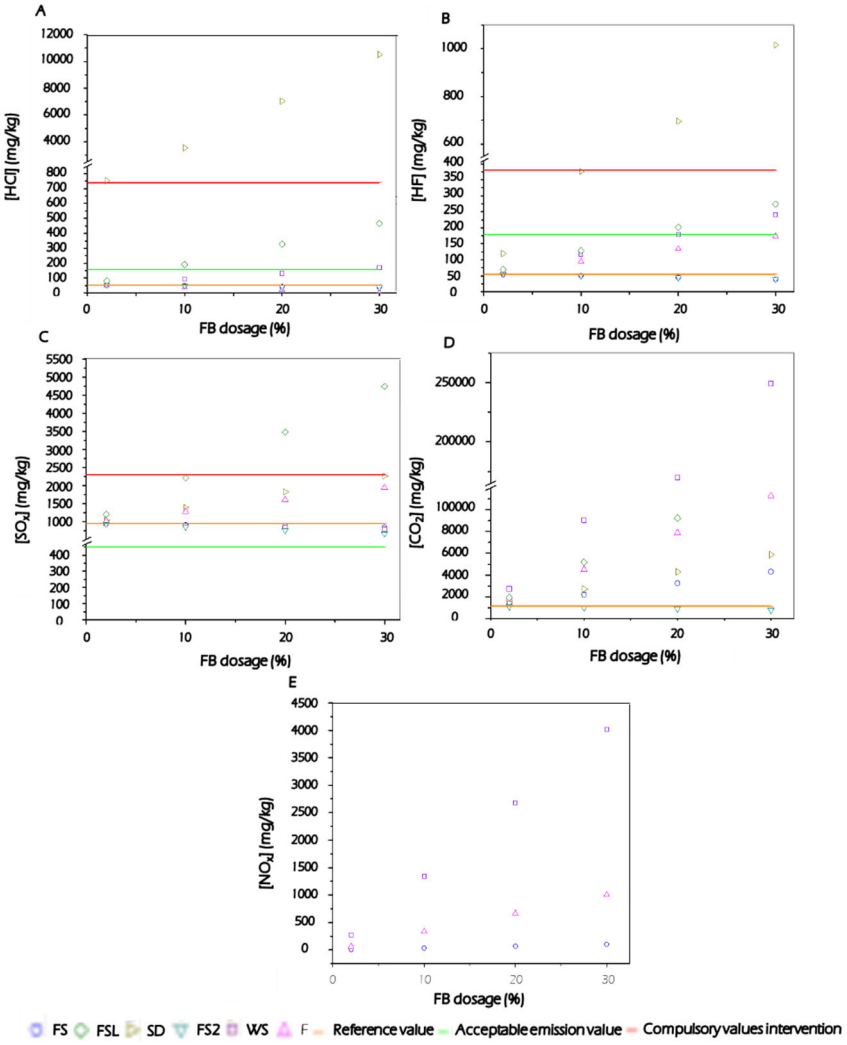

Figure 2.21. Estimated atmospheric emissions of FB-FCB mixtures: (A) HCl emissions; (B) HF emissions; (C); SOx emissions; (D) CO_2 emissions; and (E) NOx emissions.

The introduction of FBs in the FB-FCBs increases CO_2 emissions except for the FS2-clay mixture, as shown in Figure 2.21D. The introduction of FS2 reduces CO_2 emissions due to its low loss of ignition (LOI) content and its high crystallinity. The greater the loss of ignition of the waste used, the greater the estimated CO_2 emissions (Gonzalez et al., 2016; Ukwatta et. al., 2018; de la Casa and Castro, 2018). The

increase in CO_2 emissions is greater for WS with a loss on ignition of 31.74 % and FSL with 18.01 % LOI before the firing process compared to FS (17.1 %) and SD (9.48 %). According to González et al. (2011), depending on the carbonate content (calcite + dolomite), firing temperature, and percentage of CO_2 emitted (calcimetry and microanalysis), it is necessary to evaluate the company's production to establish the dangerousness of CO_2 emissions.

The introduction of FS, WS, and F in the FB-FCBs increase NOx emissions due to the higher N contents that they present for clay, as shown in Figure 2.21E. FS2, SD, and FSL present N contents below the equipment quantification limit, so there would be no problem in the introduction of these residues in the emissions NO_x (de la Casa and Castro, 2018).

2.3.2.5. Analysis and Modeling of the Technological and Environmental Properties. Selection of Optimal Formulations

Statistical treatment of technological properties

The technological properties that were studied on a laboratory scale and that have been the object of study for statistical treatment are weight loss, linear contraction, bulk density, water absorption, and flexural and compression strengths. These properties were studied incorporating 10 %, 20 %, 30 %, and 40 % of six FBs provided by two companies in the region. Three replicas of each of the technological properties were made. Tables of Annexe 4 show the experimental results obtained for each of the FBs used in the realisation of the FB-FCBs.

The representation of the values obtained for the 3 replications is shown in Figure 4.1 (Annex 4)Figure. The experimental results obtained on a laboratory scale are presented to fit them to first and second-order polynomials. In Table 2.10 the equations for each technological property as a function of % waste introduced, as well as the R^2 and DSR are presented. As can be observed, the technological properties of weight loss, water absorption, and density fit first-degree equations, while linear shrinkage and flexural and compression strengths better fit second-degree equations.

The technological properties present lower values as the residue is introduced into the FB-FCBs, as presented in Table 2.10. The fits to equations of 1st and 2nd degree are good since values of R^2 are obtained in all the technological properties and for all the residuals above 75 %, except the linear shrinkage. The experimental errors made, expressed with the DSR, present values below 10 % for all properties, except for linear shrinkage and the flexural and compression strengths in some waste such as FS2.

Table 2.10. Relationship between the percentage of waste and the technological properties of the waste studied.

Waste	Technological properties as a function of % waste	R^2	DSR (%)
FS	$\text{Weight Loss (\%)} = -1.31\ 10^{-2}\ (\%W) + 6.33$	0.581	2.98
	$\text{Linear Shrinkage (\%)} = 2.52\ 10^{-3}\ (\%W)^2 - 5.96\ 10^{-2}\ (\%W) + 1.33$	0.695	32.4
	$\text{Water Absorption (\%)} = 6.02\ 10^{-2}\ (\%W) + 7.86$	0.774	5.46
	$\text{Bulk Density (kg/m}^3) = -0.187\ (\%W)^2 + 1.58\ (\%W) + 2.10\ 10^3$	0.989	0.524
	$\text{Flexural Strength (MPa)} = 4.30\ 10^{-3}\ (\%W)^2 - 0.462\ (\%W) + 13.2$	0.952	15.9
	$\text{Compression Strength (MPa)} = 1.08\ 10^{-2}\ (\%W)^2 - 1.15\ (\%W) + 33.0$	0.952	15.8
FSL	$\text{Weight Loss (\%)} = 0.119\ (\%W) + 6.27$	0.973	3.50
	$\text{Linear Shrinkage (\%)} = 1.02\ 10^{-2}\ (\%W) + 1.19$	0.107	33.3
	$\text{Water Absorption (\%)} = 0.264\ (\%W) + 7.53$	0.965	6.00
	$\text{Bulk Density (kg/m}^3) = -6.05\ (\%W) + 2.10\ 10^3$	0.992	0.404
	$\text{Flexural Strength (MPa)} = 8.73\ 10^{-3}\ (\%W)^2 - 0.564\ (\%W) + 11.8$	0.894	22.6
	$\text{Compression Strength (MPa)} = 2.18\ 10^{-2}\ (\%W)^2 - 1.41\ (\%W) + 29.5$	0.894	22.6
SD	$\text{Weight Loss (\%)} = 0.116\ (\%W) + 6.00$	0.956	4.56
	$\text{Linear Shrinkage (\%)} = 1.80\ 10^{-2}\ (\%W)^2 - 3.24\ 10^{-2}\ (\%W) + 1.29$	0.716	25.3
	$\text{Water Absorption (\%)} = 0.132\ (\%W) + 7.44$	0.946	4.74
	$\text{Bulk Density (kg/m}^3) = -0.187\ (\%W)^2 + 1.58\ (\%W) + 2.10\ 10^3$	-	1.29
	$\text{Flexural Strength (MPa)} = 1.33\ 10^{-2}\ (\%W)^2 - 0.660\ (\%W) + 12.7$	0.974	7.03
	$\text{Compression Strength (MPa)} = 3.33\ 10^{-2}\ (\%W)^2 - 1.65\ (\%W) + 31.7$	0.974	7.03
FS2	$\text{Weight Loss (\%)} = 5.60\ 10^{-2}\ (\%W) + 6.41$	0.987	1.83
	$\text{Linear Shrinkage (\%)} = 1.21\ 10^{-3}\ (\%W)^2 - 3.90\ 10^{-3}\ (\%W) + 1.34$	0.567	32.6
	$\text{Water Absorption (\%)} = 4.08\ 10^{-2}\ (\%W) + 8.06$	0.746	4.07
	$\text{Bulk Density (kg/m}^3) = -1.27\ (\%W) + 2.08\ 10^3$	0.515	0.912
	$\text{Flexural Strength (MPa)} = 8.56\ 10^{-2}(\%W)^2 - 0.601\ (\%W) + 11.9$	0.935	23.0
	$\text{Compression Strength (MPa)} = 2.14\ 10^{-2}\ (\%W)^2 - 1.50\ (\%W) + 29.8$	0.935	22.8
WS	$\text{Weight Loss (\%)} = 0.263\ (\%W) + 6.15$	0.997	1.79
	$\text{Linear Shrinkage (\%)} = 8.60\ 10^{-4}\ (\%W)^2 + 3.03\ 10^{-2}\ (\%W) + 1.23$	0.868	17.1
	$\text{Water absorption (\%)} = 0.155\ (\%W) + 7.78$	0.920	6.37
	$\text{Bulk Density (kg/m}^3) = -11.6(\%W) + 2.07\ 10^3$	0.943	2.37
	$\text{Flexural Strength (MPa)} = 5.29\ 10^{-2}\ (\%W)^2 - 0.385\ (\%W) + 12.6$	0.945	8.68
	$\text{Compression Strength (MPa)} = 1.32\ 10^{-2}\ (\%W)^2 - 0.961\ (\%W) + 31.4$	0.945	8.70
F	$\text{Weight Loss (\%)} = -3.10\ 10^{-2}\ (\%W) + 6.45$	0.820	3.78
	$\text{Linear Shrinkage (\%)} = 2.29\ 10^{-3}\ (\%W)^2 - 0.185\ (\%W) + 1.25$	0.881	52.6
	$\text{Water Absorption (\%)} = 8.67\ 10^{-2}\ (\%W) + 7.60$	0.865	5.59
	$\text{Bulk Density (kg/m}^3) = -5.27\ (\%W) + 2.11\ 10^3$	0.908	1.27
	$\text{Flexural Strength (MPa)} = -0.261\ (\%W) + 12.5$	0.975	6.84
	$\text{Compression Strength (MPa)} = -0.564\ (\%W) + 31.2$	0.975	6.85

From the equations in Table 2.10, the values of the technological properties are estimated and are represented in Figure 2.22.

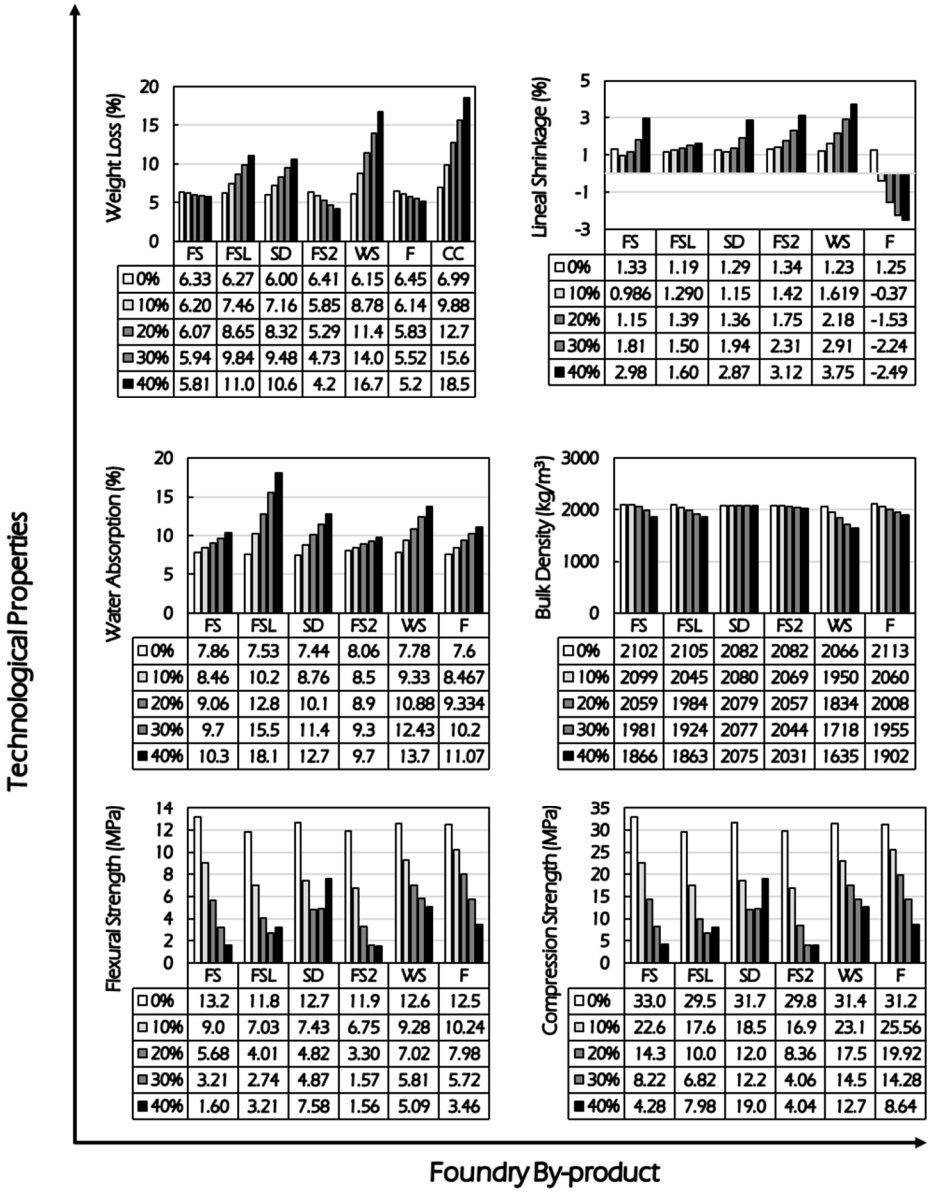

Weight Loss (%)	FS	FSL	SD	FS2	WS	F	CC
0%	6.33	6.27	6.00	6.41	6.15	6.45	6.99
10%	6.20	7.46	7.16	5.85	8.78	6.14	9.88
20%	6.07	8.65	8.32	5.29	11.4	5.83	12.7
30%	5.94	9.84	9.48	4.73	14.0	5.52	15.6
40%	5.81	11.0	10.6	4.2	16.7	5.2	18.5

Lineal Shrinkage (%)	FS	FSL	SD	FS2	WS	F
0%	1.33	1.19	1.29	1.34	1.23	1.25
10%	0.986	1.290	1.15	1.42	1.619	-0.37
20%	1.15	1.39	1.36	1.75	2.18	-1.53
30%	1.81	1.50	1.94	2.31	2.91	-2.24
40%	2.98	1.60	2.87	3.12	3.75	-2.49

Water Absorption (%)	FS	FSL	SD	FS2	WS	F
0%	7.86	7.53	7.44	8.06	7.78	7.6
10%	8.46	10.2	8.76	8.5	9.33	8.467
20%	9.06	12.8	10.1	8.9	10.88	9.334
30%	9.7	15.5	11.4	9.3	12.43	10.2
40%	10.3	18.1	12.7	9.7	13.7	11.07

Bulk Density (kg/m³)	FS	FSL	SD	FS2	WS	F
0%	2102	2105	2082	2082	2066	2113
10%	2099	2045	2080	2069	1950	2060
20%	2059	1984	2079	2057	1834	2008
30%	1981	1924	2077	2044	1718	1955
40%	1866	1863	2075	2031	1635	1902

Flexural Strength (MPa)	FS	FSL	SD	FS2	WS	F
0%	13.2	11.8	12.7	11.9	12.6	12.5
10%	9.0	7.03	7.43	6.75	9.28	10.24
20%	5.68	4.01	4.82	3.30	7.02	7.98
30%	3.21	2.74	4.87	1.57	5.81	5.72
40%	1.60	3.21	7.58	1.56	5.09	3.46

Compression Strength (MPa)	FS	FSL	SD	FS2	WS	F
0%	33.0	29.5	31.7	29.8	31.4	31.2
10%	22.6	17.6	18.5	16.9	23.1	25.56
20%	14.3	10.0	12.0	8.36	17.5	19.92
30%	8.22	6.82	12.2	4.06	14.5	14.28
40%	4.28	7.98	19.0	4.04	12.7	8.64

Figure 2.22. Estimated results of technological properties by type and percentage of waste. FS (Foundry Sand-cast iron); FSL (Foundry Sludge); SD (Steel Dust); FS2 (Foundy Sand-ductile iron); CA (Cupola Bottom Ash); WS (Wet Sands); and F (Fines).

Based on the results estimated with the equations in Table 2.10 and the results obtained at a laboratory scale, it can be concluded that up to 30 % of FS and FS2 could be introduced since these FBs present values close to the bricks 100 % clay. Regarding the rest of the waste, up to 20 % could be introduced without compromising the technological properties of the bricks.

Statistical Treatment of Environmental Behaviour

For the study of environmental behaviour, mixtures of clay-foundry waste with good technological properties are considered, therefore, those obtained by incorporating Cupola Ash and mixtures with 40 % residue are discarded. The equilibrium test has been carried out following the UNE-EN 12457-2 standard, with a liquid / solid 10 ratio. This leaching test involves the simulation of the management of this material at the end of its useful life. The test has been carried out in duplicate. Those pollutants (As, Cr, Mo, Sb, Se, and Pb) that have been seen in other works (Alonso-Santurde et al., 2011; Quijorna, 2013; Coronado, 2014) that present greater problems when introduced into ceramic matrices have been studied. Table 2.11 present the concentrations of the main contaminants of FBs.

As observed in Table 2.11, Sb, Se, and Pb are below the detection limit of the equipment that is below the discharge limit for inert waste landfills. Thus, Cr and Mo increase their concentration when the amount of waste introduced is greater. Due to Sb, Se, and Pb present concentrations below the detection limit is not possible to fit the experimental value to first and second-order polynomials. The mean values of As, Cr, and Mo concentrations are represented against % residue in Figure 2.23.

Table 2.11. Concentrations of contaminants in mg/kg from compliance leaching test EN 12457-2 applied to FB-FCBs (Foundry by-products-fired clay bricks).

Waste	% Waste	As	Cr	Mo	Pb	Sb	Se
Clay	0	0.3	<0.05	0.2	0.06	<0.2	<0.1
		0.3	0.08	0.2	<0.05	<0.2	<0.1
FS	10	0.4	0.05	0.2	<0.05	<0.2	<0.1
		0.3	0.05	0.2	<0.05	<0.2	<0.1
	20	0.7	0.06	0.1	<0.05	<0.2	<0.1
		0.7	0.05	0.1	<0.05	<0.2	<0.1
	30	0.4	0.06	0.1	<0.05	<0.2	<0.1
		0.4	0.06	0.1	<0.05	<0.2	<0.1
FSL	10	0.4	0.05	0.3	<0.05	<0.2	<0.1
		0.4	0.06	0.3	<0.05	<0.2	<0.1
	20	0.4	0.05	0.6	<0.05	<0.2	<0.1
		0.4	<0.05	0.6	<0.05	<0.2	<0.1
	30	0.3	0.05	0.8	<0.05	<0.2	<0.1
		0.3	<0.05	0.7	<0.05	<0.2	<0.1
SD	10	0.3	0.09	1.2	<0.05	<0.2	<0.1
		0.3	0.09	1.2	<0.05	<0.2	<0.1
	20	0.2	0.07	1.9	<0.05	<0.2	<0.1
		0.2	0.07	1.9	<0.05	<0.2	<0.1
	30	0.2	0.05	2.1	<0.05	<0.2	<0.1
		<0.2	0.06	2.1	<0.05	<0.2	<0.1
FS2	10	0.4	0.07	0.2	<0.05	<0.2	<0.1
		0.4	0.06	0.2	<0.05	<0.2	<0.1
	20	0.6	0.06	0.1	<0.05	<0.2	<0.1
		0.6	0.06	0.1	<0.05	<0.2	<0.1
	30	0.9	0.07	0.1	<0.05	<0.2	<0.1
		0.8	0.06	0.1	<0.05	<0.2	<0.1
WS	10	0.4	0.05	0.2	<0.05	<0.2	<0.1
		0.4	0.05	0.2	<0.05	<0.2	<0.1
	20	0.3	0.09	0.2	<0.05	<0.2	<0.1
		0.2	0.09	0.2	<0.05	<0.2	<0.1
	30	0.4	0.07	0.2	<0.05	<0.2	<0.1
		0.3	0.06	0.2	<0.05	<0.2	<0.1
F	10	0.2	0.09	1.4	<0.05	<0.2	<0.1
		0.2	0.08	1.4	<0.05	<0.2	<0.1
	20	0.4	0.08	3.5	<0.05	<0.2	<0.1
		0.4	0.09	3.5	<0.05	<0.2	<0.1
	30	0.5	0.06	4.7	<0.05	<0.2	<0.1
		0.4	0.07	4.6	<0.05	<0.2	<0.1

FS (Foundry Sand-cast iron); FSL (Foundry Sludge); SD (Steel Dust); FS2 (Foundy Sand-ductile iron); CA (Cupola Bottom Ash); WS (Wet Sands); and F (Fines).

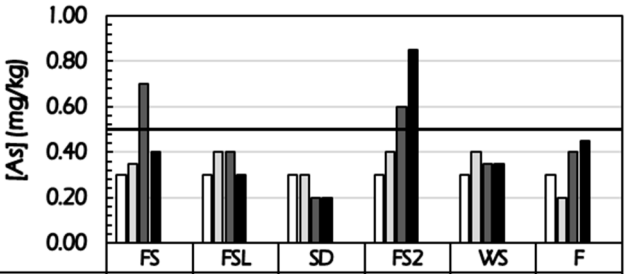

	FS	FSL	SD	FS2	WS	F
0%	0.30	0.30	0.30	0.30	0.30	0.30
10%	0.35	0.40	0.30	0.40	0.40	0.20
20%	0.70	0.40	0.20	0.60	0.35	0.40
30%	0.40	0.30	0.20	0.85	0.35	0.45
Inert Landfill Limit	0.5					
Non-hazardous Landfill Limit	2					

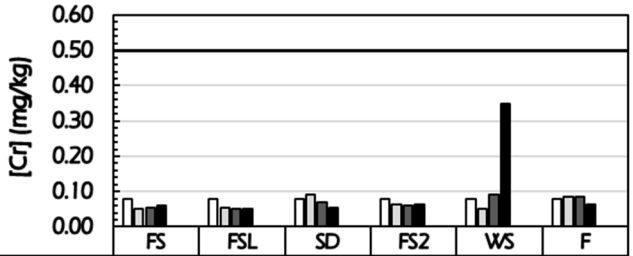

	FS	FSL	SD	FS2	WS	F
0%	0.080	0.080	0.080	0.080	0.080	0.080
10%	0.050	0.055	0.090	0.065	0.050	0.085
20%	0.055	0.050	0.070	0.060	0.090	0.085
30%	0.060	0.050	0.055	0.065	0.350	0.065
Inert Landfill Limit	0.5					
Non-hazardous Landfill Limit	10					

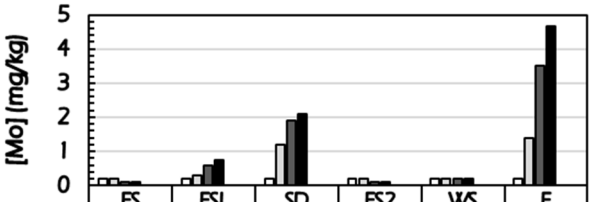

	FS	FSL	SD	FS2	WS	F
0%	0.2	0.2	0.2	0.2	0.2	0.2
10%	0.2	0.3	1.2	0.2	0.2	1.4
20%	0.1	0.6	1.9	0.1	0.2	3.5
30%	0.1	0.75	2.1	0.1	0.2	4.65
Inert Landfill Limit	0.5					
Non-hazardous Landfill Limit	10					

Figure 2.23. Average concentrations of As, Cr, and Mo in mg/kg in the FB-FCBs (Foundry by-products-fired clay bricks). FS (Foundry Sand-cast iron); FSL (Foundry Sludge); SD (Steel Dust); FS2 (Foundy Sand-ductile iron); CA (Cupola Bottom Ash); WS (Wet Sands); and F (Fines).

It is observed that for all cases the concentrations are below the limit for dumping in non-hazardous waste landfills. For all waste, Cr concentrations are below the limits for inert landfills. For all the percentages of WS, the values obtained from concentrations allow its dumping in the inert landfill. For F and SD, in all cases, the limit for Mo is exceeded for its discharge into an inert landfill. For FSL, in percentages equal to and greater than 20 %, the limit for its discharge into an inert landfill is exceeded for Mo. For FS, in percentages equal to and greater than 20 %, the limit for its dumping of inert is exceeded for As.

2.3.2.6. Multi-Criteria Analysis (MCA). Selection of the Optimal Formulations based on Technical, Environmental and Economic Requirements

In Figure 2.24 the alternatives for each of the different scenarios are presented. Table 2.12 shows the impact matrix of the multi-criteria analysis (MCA) for the different alternatives and criteria sets.

As can be seen in Figure 2.24, for scenario 1 where all the criteria have the same weight, 10 % of FS, FS2, and 10 % of F are the ones that are presented as the best alternatives for their development to industrial scale. As in scenario 1, in scenario 2 they repeat 10 % FS and F while FS2 are replaced in this case by 10 % of SD. The higher weights in the economic criteria the SD and FSL are presented as the best alternatives due to the economic benefit received by the company when managing this waste since it is hazardous waste. To maintain a balance between technical, environmental, and economic criteria, the second scenario was chosen as the best alternative for the development of mixtures at an industrial scale: FS incorporating 10 %. This residue is presented in each of the scenarios, as one of the three best possible alternatives for possible development at an industrial scale.

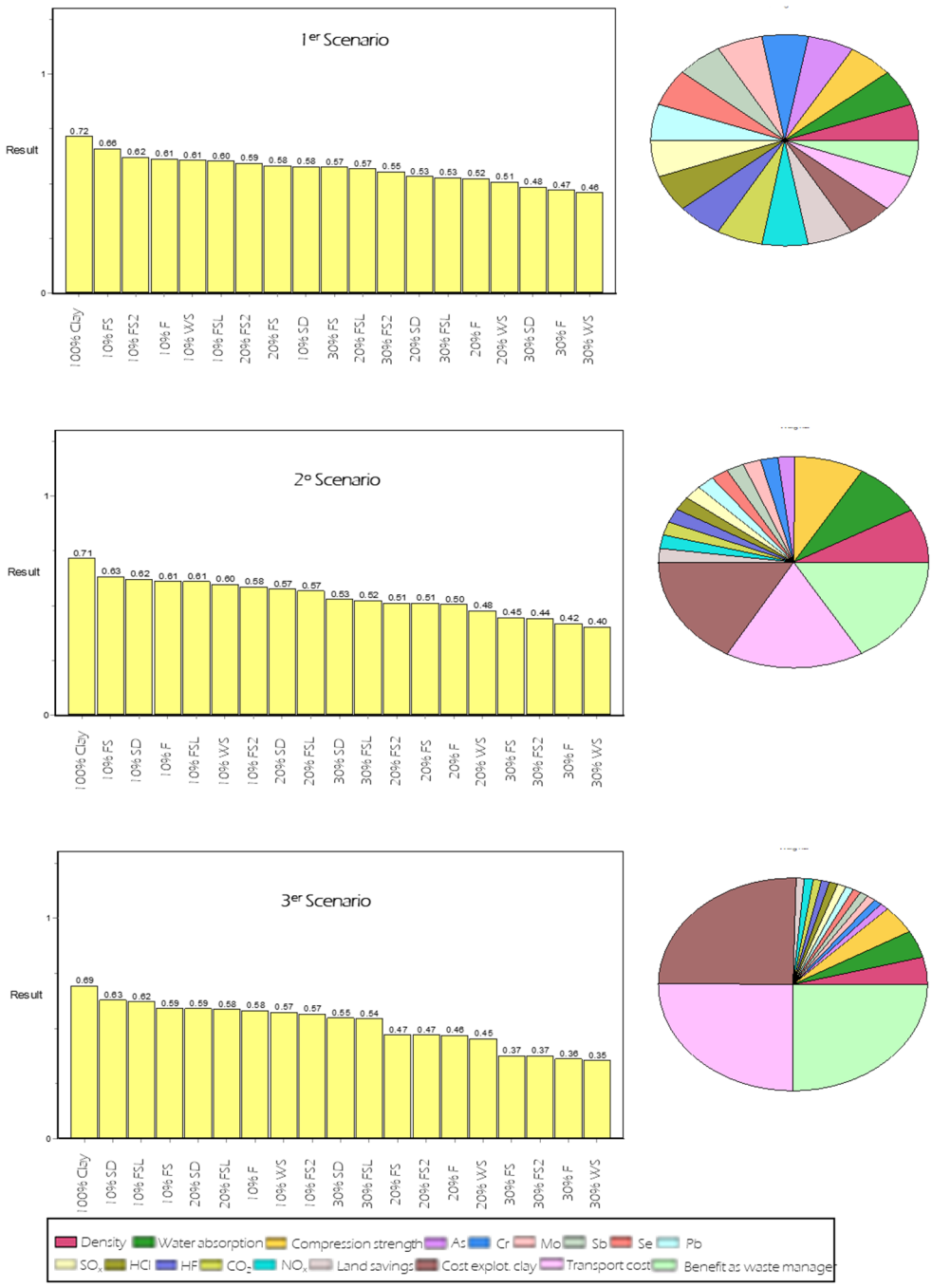

Figure 2.24. Results of the best alternatives based on the scenarios proposed.

Table 2.12. Impact matrix of the multi-criteria analysis of the different alternative clay-foundry by-products mixtures. FS (Foundry Sand-cast iron); FSL (Foundry Sludge); SD (Steel Dust); FS2 (Foundy Sand-ductile iron); CA (Cupola Bottom Ash); WS (Wet Sands); and F (Fines).

	Alternatives																		
Criteria	100% Clay	FS			FSL			FS2			SD			WS			F		
		10%	20%	30%	10%	20%	30%	10%	20%	30%	10%	20%	30%	10%	20%	30%	10%	20%	30%
C1. Density (kg/m$_3$)	2096	2107	2064	1964	2045	1995	1925	2041	2058	2063	2038	2107	2088	1959	1756	1724	2081	2029	1916
C2. Water absorption (%)	7,83	8,16	9,50	9,82	10,49	11,91	15,15	8,73	9,06	9,02	8,51	9,71	11,33	8,99	11,59	11,82	8,2	9,51	9,76
C3. Compression strength (MPa)	31,59	26,37	11,47	8,02	13,02	11,08	9,93	13,23	8,66	7,26	18,43	13,05	10,97	23,22	15,85	16,44	26,04	19,07	13,15
C4. [As] (mg/kg)	0,30	0,35	0,70	0,40	0,40	0,40	0,30	0,40	0,60	0,85	0,30	0,20	0,20	0,40	0,25	0,35	0,20	0,40	0,45
C5. [Cr] (mg/kg)	0,08	0,05	0,06	0,06	0,06	0,05	0,05	0,07	0,06	0,07	0,09	0,07	0,06	0,05	0,09	0,07	0,09	0,09	0,07
C6. [Mo] (mg/kg)	0,20	0,20	0,10	0,10	0,30	0,60	0,75	0,20	0,10	0,10	1,20	1,90	2,10	0,20	0,20	0,20	1,40	3,50	4,65
C7. [Sb] (mg/kg)	0,06	0,06	0,06	0,06	0,06	0,06	0,06	0,06	0,06	0,06	0,06	0,06	0,06	0,06	0,06	0,06	0,06	0,06	0,06
C8. [Se] (mg/kg)	0,10	0,10	0,10	0,10	0,10	0,10	0,10	0,10	0,10	0,10	0,10	0,10	0,10	0,10	0,10	0,10	0,10	0,10	0,10
C9. [Pb] (mg/kg)	0,06	0,05	0,05	0,05	0,05	0,05	0,05	0,05	0,05	0,05	0,05	0,05	0,05	0,05	0,05	0,05	0,05	0,05	0,05
C10. [SO_x] (mg/kg)	958,02	926	894	862	2220	3482	4745	862	766	670	1394	1830	2267	904	851	798	1288	1617	1947
C11. [HCl] (mg/kg)	54,79	49,31	43,83	38,35	191	328	465	49,31	43,83	38,3	3544	7035	10525	93	131	169	38,35	21,92	5,48
C12. [HF] (mg/kg)	56.1	50,49	44,88	39,27	129	201	274	50,90	44,88	39,27	375	695	1015	117	179	241	95.37	134	173
C13. [CO_2] (mg/kg)	11322	21903	32484	43064	51771	92220	132669	10190	9058	7925	27096	42869	58643	90580	169839	249047	45095	78867	112640
C14. [NOx] (mg/kg)	0	33,48	66,96	100	0	0	0	0	0	0	0	0	0	1339	2678	4017	334	669	1004
C15. Land Saving (%)	100	10	20	30	10	20	30	10	20	30	10	20	30	10	20	30	10	20	30
C16. Clay extraction cost (€)	45000	40500	36000	31500	40500	36000	31500	40500	36000	31500	40500	36000	31500	40500	36000	31500	40500	36000	31500
C17. Transport Cost (€)	0	600	1200	1800	600	1200	1800	600	1200	1800	600	1200	1800	600	1200	1800	600	1200	1800
C18. Benefit as waste manager (€)	0	7578	15156	22734	34629	69258	103887	7578	15156	22734	34629	69258	103887	7578	15156	22734	7578	15156	22734

2.3.3. Conclusions

The physical, chemical, mineralogical, and thermal characterisation of the clay and foundry residues has been carried out. SD, FS2, WS, and F present a 70 % distribution of particle size below 0.5 mm like clay, therefore it would not be necessary to carry out pre-treatments for its incorporation into the ceramic process. FS and CA would require grinding and FSL would require drying pre-treatment. Regarding the chemical characterisation, the FBs present significant amounts of compounds considered as network modifiers (FeO, CaO, and MgO) that increase the amount of liquid phase and decrease its viscosity, favouring both sintering and densification of the sample. The clay shows quartz and aluminosilicates such as muscovite, kaolinite, and dickite as the majority crystalline phases. The minor phase is iron oxide. All the FBs have the crystalline phases that the clay has present either as the majority or minority phases, except for the FS2, which only has quartz. The FBs present a thermal behaviour like that of clay since they show the typical dehydroxylation process up to 100 ºC, hydration waters, and the second around 500-550 ºC of dehydroxylation of clays, decomposition of aluminosilicates. CA and F show weight gains at temperatures above 800 ºC due to iron oxidation.

FB-FCBs present a similar behaviour, taking as a reference to the 100 % clay-fired pieces, against weight loss, linear contraction, density, water absorption, and compressive strength. It can be concluded that the viability of introducing FBs in ceramic clay matrices, under the processing conditions in which the study has been carried out, has been demonstrated for percentages of the order of 40 %. Taking into account the values required by AENOR UNE-EN 771-1: 2011 + A1: 2016 for the certification of facing brick and lightened ceramic block in the technological properties of water absorption and compressive force, it can be concluded that it is feasible to carry out ceramic pieces with the content of FBs in the order of 10-20 % in the case of facing brick and with contents in the order of 30 % in the case of the lightened ceramic block based on the moulding (pressing) and firing conditions applied on a laboratory scale.

The environmental behaviour of the FB-FCBs according to order AAA / 661/2013 relative to the disposal of waste shows that all pollutants are below the inert waste limit except As and Mo, which is below the limit. non-hazardous waste limit. For FB-FCBs, the emissions of HF and HCl by introducing FS and FS2 are below the emissions of 100 % of clay bricks, so the introduction of these sands would reduce the emissions of these pollutants in the combustion process and these emissions are lower than the acceptable emission values proposed to be incorporated in Andalusian legislation. The introduction of WS and F present estimated emission values below acceptable emission values. FSL and SD should be added to control due to the high concentrations of F and Cl that they present. On the other hand, SO_x emissions are

above 100 % emissions from clay bricks, except for FS, FS2, and WS, due to the high content of S present in the waste. CO_2 depends on the content of carbonates (calcite + dolomite) and unburned carbon, the firing temperature, and the percentage of CO_2 emitted (calcimetry and microanalysis), therefore, it is necessary to evaluate the company's production to establish the danger of CO_2 emissions. Finally, NOx emissions are negligible for FS2, SD, and FSL, and monitoring of these emissions is necessary for WS, F, and FS on an industrial scale.

The statistical analysis of the results obtained in the technological and environmental properties of the clay-foundry waste mixtures was adjusted to first and second-order mathematical equations. With these equations, the values of the technological and environmental properties were estimated and experimental errors below 10% were obtained, validating the established mathematical models that allow predicting the behaviour of future clay formulations with different foundry residues.

A multicriteria analysis was carried out defining different alternatives and criteria. 3 types of criteria were defined: technical, environmental, and economic. Considering these criteria, 3 scenarios were established. A first scenario where all the criteria have the same weight over the alternatives, a second scenario where the economic criteria have 50 % weight and the other two criteria 25 %, and the third scenario with 75 % weight for the economic criteria and 12.5 % for the other two criteria. In each of these scenarios, the ones that are presented as the best alternatives for its development at an industrial scale are 10 % FS, 10 % F, and 10 % SD. As FS was always among the best alternatives in the 3 scenarios proposed, it was decided to use this residue for its production at an industrial scale.

2.4. FOUNDRY SAND-CLAY BRICKS AT INDUSTRIAL SCALE

In the foundry industry, millions of tons of spent materials are generated worldwide, 70 % of which consists of sand, called foundry sand (FS). The sand is used as moulds in the casting of metal. It is reused until it becomes too fine due to heat degradation and loses the properties required for casting and must be replaced. This spent sand, produced in the sand-casting system, has been identified as the most important problem in foundries (Heidemann et al., 2021). According to the European Foundry Association (CAEF), the iron and steel foundries from 22 European countries produced 9.1 million tons of castings. On the order of approximately one ton of waste, sand is generated for each ton of cast metal. The six countries that dominate this industry in terms of weight, namely Germany, Turkey, France, Spain, and Italy, account for 79.8 % of the production of ferrous metal castings (CAEF, 2020).

Given its great availability, particle size, and its chemical composition, FS is regarded as a suitable raw material for brick production. In this chapter, FS was selected to replace clay content in brick ceramic materials on an industrial scale.

Depending on the casting process followed in the foundry industry, FS can be classified as green sand and core sand. Green sands are generated in the sand cast system whereas core sands are generated in the chemically bonded sand cast system. Green sand consists of high-quality silica sand (85-95 %), bentonite clay (4-10 %), sea coal (2-10 %), and water (2-5 %). Core sand is composed of silica (93-99 %) and chemical binder (1- 3%) that could be phenolic-urethanes, epoxy-resins, furfuryl alcohol, and sodium silicates (Alonso-Santurde et al., 2010). According to the European regulation, code 100907*, both sand are classified as hazardous materials due to their content of heavy metals and organic contaminants that can be released into the atmosphere or condensed in the foundry sand. Due to its composition core sand is difficult to reuse and needs to be solidified/stabilized to be disposed of in a landfill after each use, resulting in approximately 10 million tons of sand per year in the world (Pittenger, 2017).

While the study of the use of green sands in concrete, subbases, low-strength materials, and soils, has been promoted, core sands have had a more restrictive alternative management. Given its great availability, particle size, and its chemical composition, FS is also regarded as a suitable raw material for brick production. Its use can play a role in controlling the plasticity characteristics of the mixture of raw materials, as degreasing or as a porous material, in addition to providing carbon to the furnace.

Some researchers have studied the technological feasibility of using spent foundry sands in the ceramics industry on a laboratory scale (Raupp-Pereira et al., 2007; Mymrin et al., 2016; Lin D.F. et al., 2018). While Alonso-Santurde et al. (2012)

addressed a scaling-up study to produce ceramic bricks with two types of FS (green and core sand) at different firing cycles based on the technological properties of the final products only. On the other hand, a prerequisite for using residual material as secondary raw material should not only be technically suitable but also environmentally friendly. For this reason, the environmental evaluation of clay/green and core sands ceramic mixtures generated at an industrial scale, using different European compliance leaching tests has been carried out by our group in previous work (Alonso-Santurde et al., 2010). In the literature related to foundry sand, only Braçansa et al. (2006) and Pytel (2013) have considered the environmental evaluation of materials based on foundry sand through leaching tests and gaseous release analysis during the firing stage. The results show environmental impacts during the manufacturing similar to those registered when traditional materials are used, evidencing the absence of atmospheric emissions of hazardous substances and low level of heavy metal leaching compared to acceptable limits.

Although the benefits of incorporating residues into fired clay bricks are well known, most of these experiments have been prepared in the laboratory under controlled conditions using an electric furnace. Currently, they have not yet been scaled up to mass production in factories. However, the properties of clay bricks can vary greatly between laboratory and under actual field conditions in an industrial kiln (Muñoz et al., 2014; Abbas et al., 2017; Munir et al., 2018). Therefore, once the technical and environmental evaluation of fired products and estimation of the gas emissions generated in the firing process at a laboratory scale, using core sands have been demonstrated (previous section). And they have also been validated as the best alternative among the foundry by-products considered by the application of multi-criteria analysis (MCA) from a sustainability point of view. This chapter aims to carry out FS-fired clay bricks at an industrial scale', to be evaluated from an integral point of view. First, consider the technological and environmental properties of the new materials, as well as the emissions generated during the process. Second, incorporating the environmental information obtained into the LCA methodology to evaluate the sustainability of new products before they are available on the market,

Results of FS-fired clay bricks at industrial scale section include first an optimisation of the heating curve in the laboratory before performing the industrial scale mixtures. Then, the experimental procedure followed in the ceramic industry was described. Afterward technical and environmental evaluation of fired products at an industrial scale, estimation of the gas emissions generated in the process of manufacturing the facing bricks, and the LCA of the final bricks were done. Such tools determine environmental impacts and information necessary to decide on the feasibility of FS-fired clay bricks.

2.4.1. Raw Materials and Methodology

2.4.1.1. Optimisation of temperature ramps in the firing process

The optimisation of the process control/heating curve can be applied in all sectors of the ceramic industry, but it should be noted that, in practice, the heating curves in the clay processing industry are optimized considering the quality of the product and energy consumption. Therefore, the heating curves can only be changed if the technical properties of the final product allow it, and additional costs must be considered when altering the heating curves for emission reasons.

To optimize the heating curve, it was studied how the firing temperature affects the clay-foundry sand mixtures on the properties of loss of ignition (LOI), linear contraction, and water absorption. For this, mixtures were made from 0% residue to 50% sand. The properties were studied in triplicate.

2.4.1.2. Characterisation of Fired Products and Gas Emissions Estimation

Fired ceramic products were characterised in terms of compression strength (UNE-EN 772-1).

The leaching behaviour of potentially hazardous pollutants was determined by applying the equilibrium leaching test EN12457-2 proposed by European regulation as described in section 2.1.1.3.

The potential emissions (ψ) of pollutants (HCl, HF, SO_2, CO_2, and NO_x) were calculated using equation 1 displayed in section 2.1.1.4.

2.4.1.3. LCA Methodology

The Life Cycle Analysis (LCA) is a methodological tool that determines the potential environmental impacts associated with a product or a service, from the moment the raw materials are extracted until their final disposal (Güereca, 2006).

In this study, the LCA methodology has been applied to carry out a preliminary analysis of the environmental implications of incorporating foundry sand as a substitute for clay in brick production. The LCA model applied takes into consideration different phases of the brick life cycle: extraction of raw material and transportation to the plant, production of the brick, and different scenarios of the waste management system such as landfill and recycling of bricks as construction and demolition waste (RCD). The stages analogous to the two types of products, traditional and alternative, that produce the same type and amount of impacts, have not been taken into account in the study, such as the commissioning, the useful life of the brick, or the demolition stage.

The LCA methodology has been applied to the two types of ceramic bricks manufactured on a semi-industrial scale. Standard bricks are made with the addition of foundry sand with a clay-foundry sand ratio of 90-10 % (bricks B + S) and standard bricks without the addition of sand (100 % clay) (Brick B). The life cycle analysis (LCA) has been carried out based on the standard methodology ISO 14040 and ISO 14044 (ISO 2006a, 2006b). The experimental results are incorporated into the LCA model using SimaPro v.8 software with the Ecoinvent v.3 life cycle inventory database. The endpoint approach has been used with the Eco-Indicator 99 method to estimate the effects of different impact categories.

The key phases associated with a Life Cycle Analysis study are:

1. Definition and scope of objectives

2. Inventory analysis (LCI, life cycle inventory)

3. Impact assessment (LCIA, life cycle impact assessment)

4. Interpretation of the results

2.4.2. Results of FS-Clay Bricks at Industrial Scale

2.4.2.1. Production of FS-Fired Clay Bricks at Industrial Scale

The heating curve will be optimized, the process followed to develop the FS/clay mixtures at an industrial scale will be described and the results of the environmental properties and estimation of gaseous emissions obtained in these mixtures will be presented at this scale.

Scale-up from Laboratory Level to Pilot Plant. Heating Curve Optimisation

To evaluate the influence of the firing temperature on the weight loss suffered by the samples, the FS/clay samples are fired in a laboratory muffle at temperatures of 850, 950,1000, 1050, and 1100 ºC, as shown in the Figure 2.25. The results show that increasing the firing temperature causes increases in weight loss. Increasing the percentage of FS in the matrix reduces weight losses. This could be due to weight losses associated with raw materials. However, the variations of LOI with the percentage of residues are relatively small (4.2 - 4.6 %), so it is considered that the influence of the firing temperature in the analysed range does not have a significant influence on the weight loss. That is why temperatures of 850 ºC, characteristic of solid bricks, and 1050 ºC, characteristic of facing bricks, are selected. Additionally, an intermediate temperature of 950 ° C is selected to check the influence of the oven atmosphere, pieces are fired at 1050 ºC in an industrial oven.

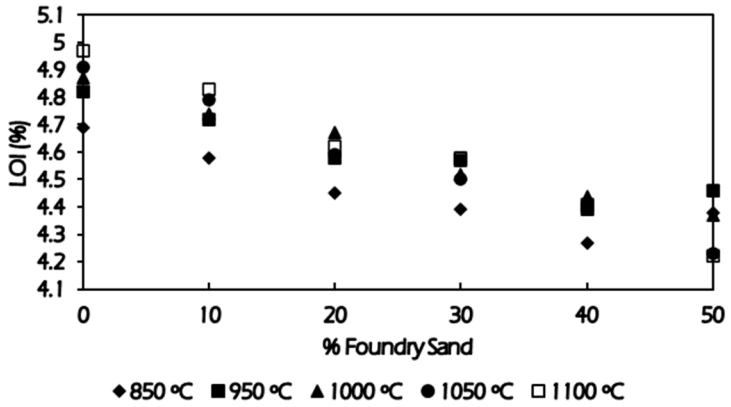

Figure 2.25. Influence of temperature on weight loss (LOI) of FS/clay mixtures.

The technological characterisation of the FS/clay pieces is carried out utilizing firing contraction and water absorption tests, as shown in Figure 2.26. In general terms, higher firing temperatures imply greater contractions of the pieces, indicating that the densification produced during ceramics is favoured by the temperature. Likewise, it is verified that the atmosphere of the industrial furnace is more efficient regarding the densification of the pieces. However, there are no clear trends regarding the influence of the percentage of FS on the shrinkage of the pieces, apart from pieces fired in an industrial kiln, in which the shrinkage decreases. This may be since the FS does not have a great sintering capacity, which means that high amounts of FS in the matrix make the sintering process difficult. The absorption tests show that higher firing temperatures imply lower water absorption values, which is because the higher the degree of sintering of the part, the lower the open porosity through which it can be introduced into the matrix (Alonso-Santurde et al., 2011).

Because of the results presented, it can be concluded that with the introduction of FS in the brick firing process at an industrial scale, no optimisation of the firing temperature would be produced, since better results are obtained at the firing temperature of the company Reciclados Cabezón.

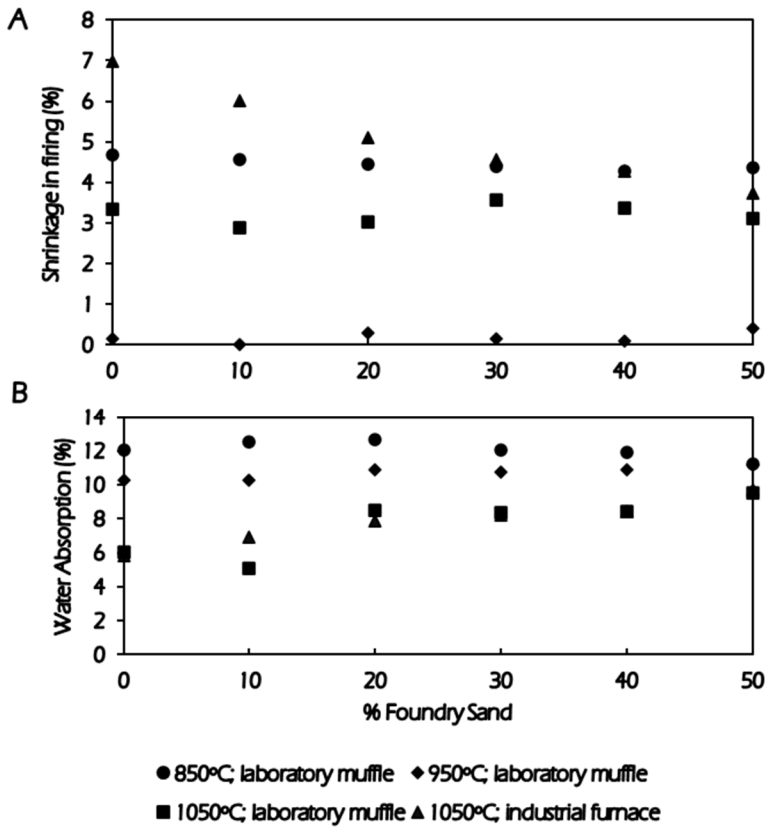

Figure 2.26. Technological characterisation of the clay-sand pieces: a) shrinkage firing and b) water absorption.

Production of Ceramic Products Incorporating Waste at Industrial Scale

From the results obtained on a laboratory scale, we proceeded to produce industrial-scale mixtures of clay with 10 % of FS. In addition, an agreement was reached with the company Reciclados de Cabezón to incorporate 1 % and 20 % of FS due to the good results obtained in the technological properties and the good visual appearance presented by the bricks made on a laboratory scale at the University of Cantabria.

The process carried out to produce these mixtures will be described. First, the clay was extracted from the quarry next to the company. This clay with very heterogeneous particle sizes is passed through a shredder where the size is reduced below 5 mm (Figure 2.27A) and at the exit, through a conveyor belt, the clay is taken to a feeder (Figure 2.27B).

Figure 2.27. Equipment of the Company Reciclados de Cabezon: A) Shredder; B) Feeder.

From the feeder, the clay is transported to a hammer mill (Figure 2.28A) to further reduce the particle size of the clay to below 2 mm. From the mill, the clay is taken to another feeder where the foundry sands are introduced for production at an industrial scale. The mixture leaves the feeder and reaches the mixer (Figure 2.28B). In the mixer, the addition of water occurs so that the mixture has the correct density for extrusion. To determine that the density of the mixture is adequate, operators use a pycnometer. Barium carbonate is also added to the mixer, which is a material that prevents efflorescence, and lignosulphonates improve the mechanical properties of the bricks.

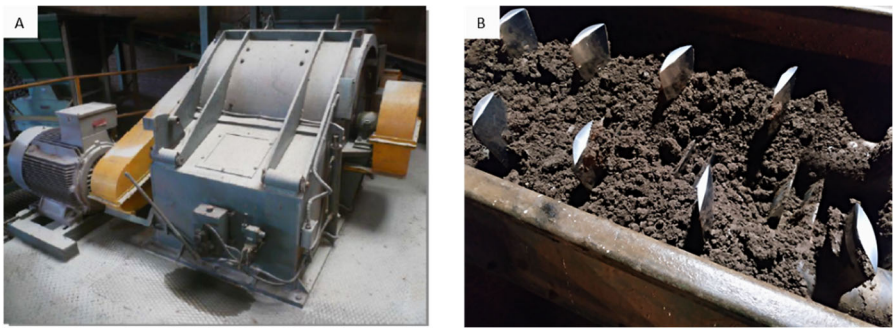

Figure 2.28. Equipment for the conditioning of clay-foundry sand mixtures: A) Hammer mill; B) Kneader.

The clay is transported from the kneader to the rolling mill (Figure 2.29A). In this conveyor belt, there is a magnet that attracts the metallic particles that the clay may have and that can interfere with the firing process of the bricks. In the rolling mill, the particle size of the clay is reduced again to below 0.7 mm, which is the working particle size of Reciclados de Cabezón. With the defined particle size and with the

correct density of the mixture, it is taken to the extruder (Figure 2.29B) where the bricks are produced.

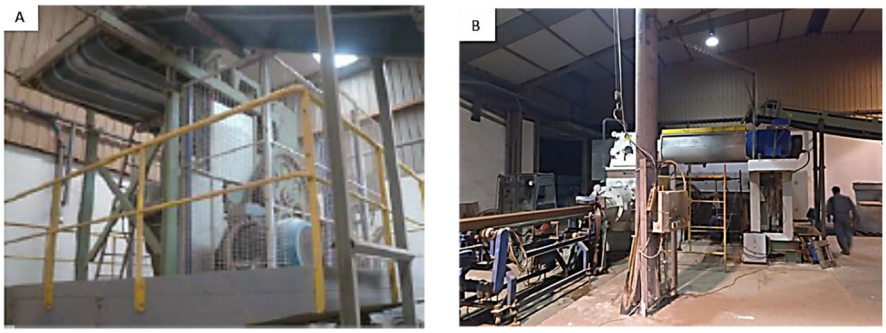

Figure 2.29. Company equipment: A) Laminator; B) Extruder.

The extruded mass is cut into bricks (Figure 2.30A) with the dimensions specified by the standard. The bricks are loaded into automatic racks and placed in the dryer. In the dryer, they will be at 105 ºC for 24 hours to eliminate the water introduced during the shaping process. After this time, the bricks are fired in the tunnel kiln (Figure 2.30B) following the industrial cycle of Reciclados Cabezón.

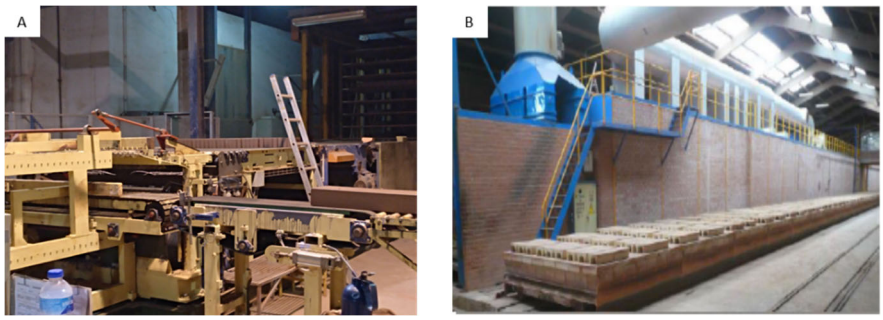

Figure 2.30. Cutting and firing of the pieces: A) Cutter; B) Tunnel kiln.

Once the clay-foundry sand pieces have been obtained, their technical and environmental properties are evaluated.

2.4.2.2. Technical and Environmental Assessment of Fired Products

In Figure 2.31 the bricks obtained with foundry sands-N are shown. At first glance, they are bricks that present the characteristic colour of facing bricks and also present a great consistency.

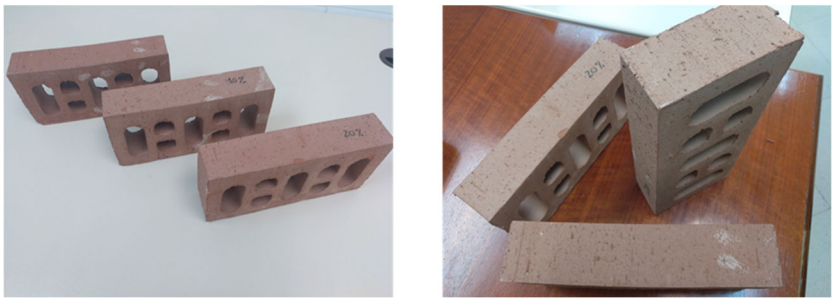

Figure 2.31. The visual appearance of the FS-Clay bricks.

Compression strength has been carried out in triplicate. The average value of compression strength and the standard deviation of FS/Clay bricks is presented in Table 2.13. As can be observed, the compression strength decreases when the percentage of FS increases. However, good results of compression strength are obtained and up to 20 % of FS can be incorporated on an industrial scale to produce facing bricks.

Table 2.13. The compression strength of FS/clay bricks is carried out at an industrial scale.

FS (%)	Compression Strength (MPa)	Standard deviation (MPa)
1	44.76	1.31
10	39.55	0.86
20	31.86	1.46

Environmental Assessment of the FS/clay Products

The equilibrium test has been carried out following the UNE-EN 12457-4 standard, with a liquid / solid ratio of 10. This leaching test involves the simulation of the management of this material at the end of its useful life when the material is converted into secondary aggregate or is managed as waste by depositing it in a landfill. The test has been carried out in duplicate. Table 2.14 shows the concentrations of the metals.

As shown in Table 2.14, Cr, Sb, Se, and Pb are below the detection limit of the equipment that is below the discharge limit for inert waste landfills. As and Mo have the same concentration regardless of the amount of residue introduced. As and Mo concentrations are also below the inert limit.

Table 2.14. Concentrations of pollutants (mg/kg) from compliance leaching test EN 12457-2 applied to clay-foundry sand pieces and the discharge limits established by Spanish Ministerial Order AAA / 661/2013.

By-product	% By-product	As	Cr	Mo	Pb	Sb	Se
FS	1	0.3	<0.05	0.1	<0.05	<0.02	<0.1
		0.4	<0.05	0.1	<0.05	<0.02	<0.1
	10	0.4	<0.05	0.1	<0.05	<0.02	<0.1
		0.3	<0.05	0.1	<0.05	<0.02	<0.1
	20	0.4	<0.05	0.1	<0.05	<0.02	<0.1
		0.4	<0.05	0.1	<0.05	<0.02	<0.1
		0.4	<0.05	0.1	<0.05	<0.02	<0.1
	Landfill Limit						
Inert	0.06	0.5	0.5	0.5	0.5	0,5	0,1
Non-hazardous	7	2	10	10	10	10	0,5

2.4.2.3. Estimation of Gaseous Emissions of Clay-Foundry Sands Mixtures at Industrial Scale

Finally, the gaseous emissions of the products developed at an industrial scale were re-estimated, as was done on a laboratory scale.

The S, Cl, F, C, and N content for the FS/clay mixtures before and after firing in the industrial kiln at 1050 ºC is in

Table 2.15. The content of the studied elements S, Cl, and F remains the same before and after the products are fired. The C is the only element that presents variations between its initial and final contents. N presents concentrations below the detection limit of the equipment.

Table 2.15. Initial and final concentrations of S, Cl, F, C, and N of the FS/clay products.

% FS	Concentration initial (mg/kg)					Concentration final (mg/kg)				
	S	Cl	F	C	N	S	Cl	F	C	N
1	900	100	200	6400	ND	900	100	200	500	ND
10	800	200	200	6400	ND	800	200	200	100	ND
20	900	100	200	6000	ND	920	100	200	200	ND

The emission of pollutants (HF, HCl, SO_x, CO_2, and NO_x) for the FS/clay mixtures fired at a temperature of 1050 ºC in the industrial furnace are summarized in Table 2.16. The emissions of SO_x, HCl, and HF are zero because the initial and final concentrations of S, Cl, and F remained constant. CO_2 emissions are the only ones that should be considered when introducing foundry sands-N in the ceramic process.

Table 2.16. Emission values of pollutants in clay-foundry sands products are calculated using the material balance of equation 1.

FS dosage (%)	Emissions (mg/kg)			
	SO_x	HCl	HF	CO_2
1	0	0	0	23035
10	0	0	0	24599
20	0	0	0	22649

2.4.2.4. Environmental Valorisation of the Process and New Ceramic Products

Life Cycle Analysis

The geographical area in which the study has been carried out is the Cantabria region, specifically in the Cabezón plant, and its objective has been to compare the environmental impacts associated with the life cycles of traditional clay-based brick (B) and the alternative brick based on clay with the addition of FS in 10% (B + S), knowing that both bricks fulfil similarly the functional requirements as construction materials. The functional unit selected for these analyses has been "one ton of finished product".

Two different end-of-life scenarios (S1 - S2) have been analysed for demolished bricks that are managed as construction and demolition waste (RCD). Scenario 1 (S1) is represented by the current state of the RCD management system in Cantabria and based on the estimates of the Ministry of the Environment that established that 53% of RCD is effectively recycled. Scenario 2 (S2) has been set according to the recycling and rejection target given for RCD by European legislation (Directive 2008/98 / CE) (EC 2008) which establishes a recycling target of 70 % for 2020.

FS is classified as non-hazardous waste according to the European Waste Catalog. The introduction of this residue in ceramic bodies as a substitute for clay avoids the generation of some impacts related to its management, normally through landfill disposal. Figure 2.32 shows the flow diagram of the life cycle of bricks (B and B + S) for the dumping and recycling of RCD as alternatives to the end-of-life phase.

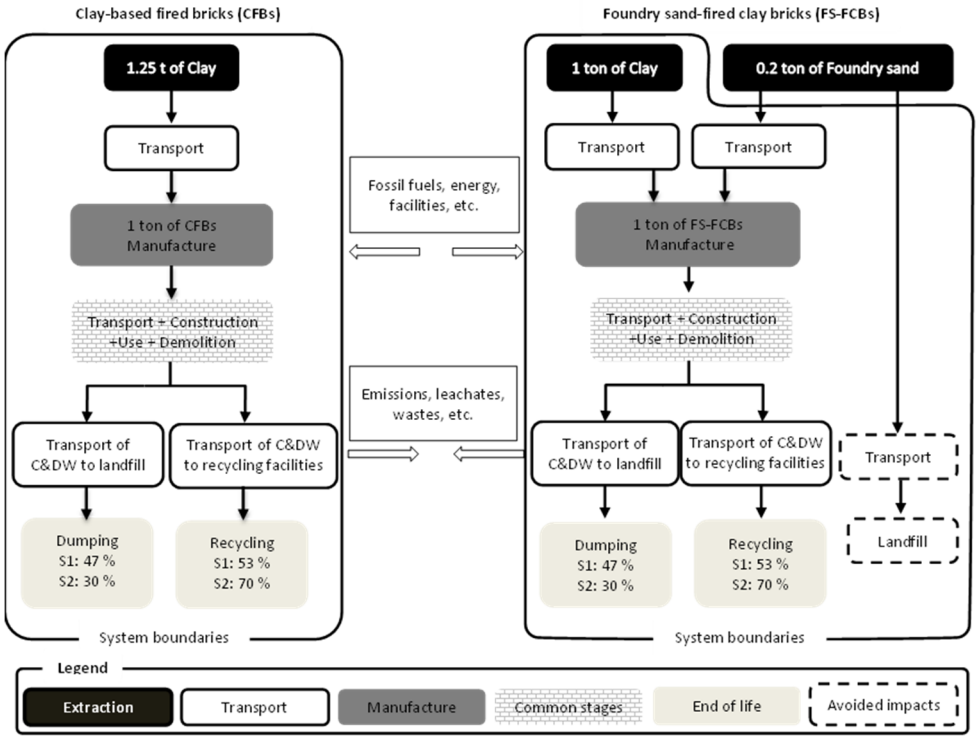

Figure 2.32. Life cycle flow diagram of the bricks produced (B and B + S) to apply the LCA tool.

Life cycle inventory:

i) Extraction and transportation of raw materials

The inputs of the system in this stage are limited to the consumption of diesel used by the machinery used to extract the clay from the quarry, as well as the trucks used to transport them to the plant, and the transport of the waste from the industrial plant to the brick production plant. The outputs, causing the impacts, correspond to those derived from atmospheric emissions resulting from the combustion of diesel, as well as from the depletion of resources produced by the extraction of clays. For the manufacture of 1 ton of finished product B an average clay consumption of 1.25 tonnes of clay is required, and for product B + P, 1.1 ton of clay and 0.15 tonnes of FS, as is observed in Table 2.17. There is a consumption of 0.49 liters of diesel per ton of finished product (Obis J. et al., 2006).

Table 2.17. Inventory data for the extraction and transportation stages of raw materials.

Concept	Unit	Amount B	Amount B+S	ACV Data Set
Clay	Ton	1,25	1,10	Clay/CH/pit operation/Conseq, U
FS	Ton	0	0,15	
Clay Transport	tKm	0	0	
FS Transport	tKm	0	3.45	Transport, freight, lorry 16-32 metric ton, EURO3/RER/Conseq, U

ii) Manufacture of ceramic products

In this stage, it is considered from when the clay is collected at the foot of the plant until the finished product is loaded for transport on site. The main environmental impacts that occur are those derived from different energy consumption: electricity, natural gas, and diesel. Table 2.18 shows the energy requirements for two ceramic products, one traditional and the other alternative (with 10 % FS) obtained through a study in an industrial plant (Quijorna, 2013). A decrease in the energy consumption of the alternative product is assumed due to the inclusion of FS in the mix, which acts as a degreaser and does not sinter. The emissions produced in the brick firing stage are also a potentially impactful stage to the environment. The emission data are those corresponding to the study of the laboratory stage, both for traditional brick (B) and for brick with 10 % FS (B + S). All these data are collected in Table 2.18.

Table 2.18. Inventory data for the brick production stage.

Concept	Unit	Amount B	Amount B+S	ACV Data Set
Electricity	MWh	50	47,5	Electricity, medium voltage / ES /market for/Conseq, U
Natural Gas	MJ	1664	1580	Electricity, high voltage/ES/ Electricity production, natural gas, at conventional power plant /Conseq, U
Diesel Oil	MJ	384,6	384,6	Diesel burned in building machine/GLO/market for/Conseq, U
Emissions during firing due to the transformation of raw materials (Clay and FS)				
CO_2	g	11323	21903	Emissions to air-CO_2
SO_2	g	958	926	Emissions to air-SO_2
NO_x	g	0	33	Emissions to air-NO_X
HCl	g	55	49	Emissions to air-HCl
HF	g	56	50	Emissions to air-HF

iii) Transportation, commissioning, useful life, and demolition of the building

This phase encompasses all the operations and processes that are intended to put the products into work, as well as the energy consumption and emissions that occur during the subsequent use of the building throughout its useful life. In the case of the demolition of the building, all those activities that have as their purpose the dismantling of the building or the constructive unit in which the ceramic products are included must be considered.

However, all these stages will not be included in the comparative analysis of both products, since it is assumed that the impacts caused are the same using brick B and brick B + S. The mortar used to build the wall and the water required for the mortar in the construction phase is the same for both products, so it is not included in the analysis (Calstar, 2014).

iv) End-of-use stage

A similar situation occurs with the recycled aggregates generated in the RCD treatment plant for both bricks. The number of aggregates obtained would be the same for B and B + S. As both would generate the same number of recycled aggregates, the positive impact that arises as a consequence of its transformation into a secondary product is equivalent, so it is not taken into account in this study.

In Spain, the GEAR project establishes a series of technical recommendations about the use of recycled aggregates according to geometric, physical-mechanical, chemical, and environmental requirements. To evaluate environmental performance, this study determines the need to apply the UNE EN-12457 leaching test to recycled aggregates and then compares the results with the limit value established by Order AAA / 661/2013 (BOE 2013) that updates the limit values of Directive 2003/33 / EC (EC 2003).

In the case of the alternative of dumping at the end of its useful life, the leachates from both bricks are taken into consideration, because this time, the different products give rise to leachates of different concentrations of metals.

The inputs of the system in this phase of the life cycle, for the two proposed scenarios, are the energy consumption due to the transport of the waste to the recycling plant or the landfill, the consumption of materials and energy for the daily operation in the landfill of non-hazardous waste and RCD's recycling plant. The outputs, causing the impacts, correspond to those derived from atmospheric emissions resulting from the combustion of diesel, and electricity consumption, as well as the leachate associated with the C&DW, managed in a landfill. The data corresponding to the inventory is shown in Table 2.19.

Table 2.19. Inventory data for the end-of-use stage of the product.

Concept		Ud	Amount B		Amount B+S		LCA Data set
			Esc. 1	Esc. 2	Esc. 1	Esc. 2	
Quantity managed in landfill		%	47	30	47	30	Not found
Transportation of RCD to landfill		tKm	103	66	103	66	Transport, freight, lorry 16-32 metric ton, EURO3/RER/Conseq, U
Clay for daily coating of the pour face		Kg	16,21	10,34	15,32	9,78	Clay/CH/pit operation/Conseq, U
Sand for intermediate cover in landfill		Kg	3,44	2,19	3,25	2,07	Gravel, round /CH/ gravel and sand quarry operation/Conseq, U
Electricity for landfill operation		kWh	0,08	0,05	0,08	0,05	Electricity, medium voltage/ES/market for/Conseq, U
Diesel for landfill operation		MJ	10,80	6,89	10,21	6,51	Diesel burned in building machine/GLO/market for/Conseq, U
Water for landfill operation		Kg	22,09	14,1	22,09	14,1	Water, fresh
Leaching of RCD in landfill	As	mg	164,5	105	164,5	105	Emissions to soil - As
	Mo	mg	47	30	47	30	Emissions to soil – Mo
Recycled RCD		%	53	70	53	70	Not found
RCD transport to treatment plant		tKm	122	162	122	162	Transport, freight, lorry 16-32 metric ton, EURO3/RER/Conseq, U
Electricity for separation (before plant)		kWh	1,96	2,59	1,96	2,59	Electricity, medium voltage/ES/market for/Conseq, U
Diesel oil for separation (before plant)		MJ	2,17	2,86	2,17	2,86	Diesel burned in building machine/GLO/market for/Conseq, U
Electricity treatment plant RCD		kWh	0,44	0,58	0,44	0,58	Electricity, medium voltage/ES/market for/Conseq, U
RCD gas oil treatment plant		MJ	7,09	9,40	7,09	9,40	Diesel burned in building machine/GLO/market for/Conseq, U

Finally, in Table 2.20, at this stage of the life cycle, it is necessary to consider the environmental impacts that are avoided by introducing a residue in a ceramic product. The management that is applied to the foundry sand is as already explained previously, it is the deposition in the landfill.

Table 2.20. Inventory data for the foundry sand management stage.

Concept	*Ud*	*Amount B+S*	*LCA Data Set*
Amount of FS	kg	1000	-
FS Transport to landfill	Km	27	Transport, freight, lorry 16-32 metric ton, EURO3/RER/Conseq, U
Clay for daily coating of the pour face	Kg	16,8	Clay/CH/pit operation/Conseq U
FS for intermediate cover in landfill	Kg	3.57	Gravel, round /CH/ gravel and sand quarry operation/Conseq, U
Electricity for landfill operation	kWh	0.175	Electricity, medium voltage/ES/market for/Conseq, U
Diesel for landfill operation	MJ	11,1	Diesel burned in building machine/GLO/market for/Conseq, U
Water for landfill operation	Kg	47,0	Water, fresh
There is no leaching of toxic species in landfills when depositing FS			

Impact evaluation

The life cycle impact assessment is oriented to the known situation and the evaluation of the quantity and significance of the potential environmental impacts of a defined system over a complete life cycle (ISO 2006a; 2006b).

The results obtained from the SimaPro8 software consist of associating each environmental load with its corresponding impact category, according to the characterisation factor specified by the methodology used. For the impact evaluation study, Eco-indicator 99 is applied, which includes global indicators of human health, quality of ecosystems, and resources, indicated as "Areas of Protection (AoP)" (Figure 2.33, Figure 2.34) and that can be divided into eleven categories of damage.

Figure 2.33 shows the comparison of the characterisation of bricks B and B + S according to the three AoP established by Eco-Indicator 99 for the two life cycles carried out (each life cycle analysis corresponds to one of the end-of-life scenarios for RCD, one that involves 53 % Recycling (R) and 47 % Landfill (L) and the second scenario that involves 70 % Recycling (R) and 30 % Landfill (L).

The results show that in general the life cycle of both bricks studied generates negative impacts for the three AoPs in the two analysed scenarios, being in all cases less harmful when FS is introduced into the brick as a raw material (lower impacts generated). The impact reductions obtained are the same in the two scenarios used, depending on the end-of-life stage of the products. This situation is related to the lower emissions generated during the manufacturing process for B + S. FS, composed mainly of silica, acts as a degreaser in the process. It has the effect of diluting some components of the clay that are degraded in the thermal process and

give rise to emissions, such as compounds with sulphur, chlorine, or fluorine. This difference in impact is fundamentally reflected in the "Human Health" indicator

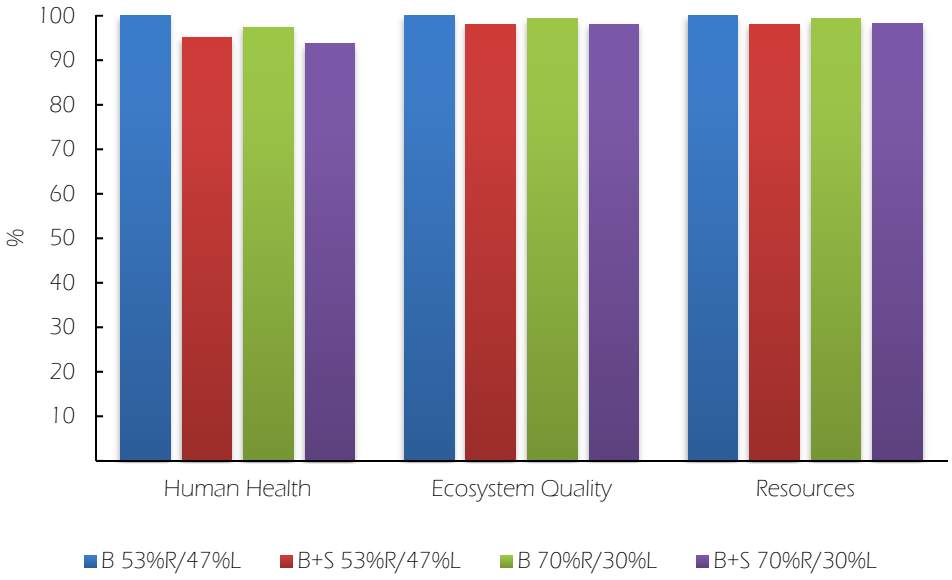

Figure 2.33. Results for each protection area (%), produced by the two types of products, in the two defined management scenarios. Method: Eco-indicator 99 (E) V2.09 / Europe EI 99 E / A / Damage assessment / Excluding infrastructure processes.

The introduction of FS in the production of bricks also avoids that this residue must be managed, with its corresponding impact on the environment. This fact is reflected in the difference in the "Resources" indicator since it avoids the use of land in landfills and the extraction of raw materials. In this case, the defined RCD management scenario also shows influence, being the scenario that poses the greatest recycling of RCD in which it causes the least impact.

In Figure 2.34 the same results are shown as in Figure 2.33, but this time in absolute terms, not in percentage, normalized to common units (Pt) to be able to be compared. In this Figure 2.34, the impacts associated with all the brick scenarios are similar, as previously shown, although the proportion of each of the impact categories can be seen globally. The greatest impacts are those related to Human Health, which is fundamentally related to emissions, followed by using resources (Resources). The impacts associated with the category ecosystem quality (Ecosystem quality) hardly weight the global calculation.

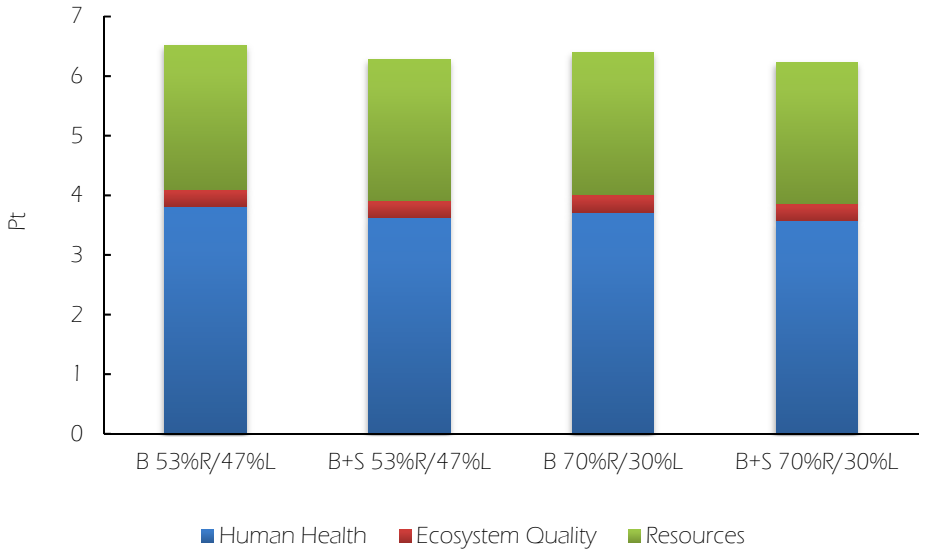

Figure 2.34. Results for the two types of products, in the two defined management scenarios, divided by each category of impact. Method: Eco-indicator 99 (E) V2.09 / Europe EI 99 E / A / single score / excluding infrastructure processes.

Figure 2.35 shows the characterisation of the impact categories for the two bricks with the eco-Indicator 99 method in the waste management scenarios S1 and S2.

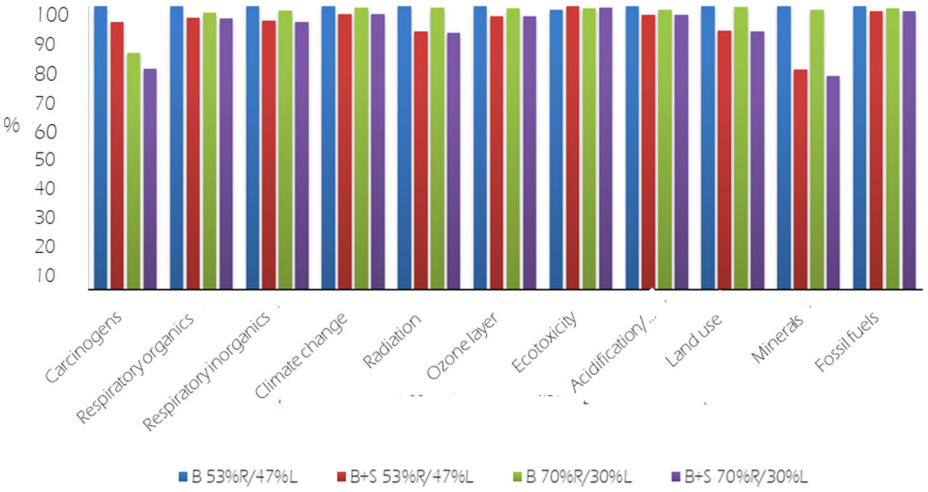

Figure 2.35. Results for each category of impact (%) of the two types of products, in the two defined management scenarios; Method: Eco-indicator 99 (E) V2.09 / Europe EI 99 E / A / characterisation / excluding infrastructure processes.

In Figure 2.35, in a more detailed way, it can be observed that bricks B and B + S produce negative impacts in all categories in the two evaluated scenarios, and that

also the incorporation of foundry sand in the bricks (B + S), implies a benefit in almost all categories of harm.

The only category that which the B + S brick shows a greater impact is *Ecotoxicity* because the B + S brick presents greater leaching in the end-of-life scenario when it is managed in a landfill.

The release of potentially toxic metals due to the elimination of RCDs at the end-of-life stage of the product represents a significant contribution to the potential impact on ecotoxicity. For this reason, the importance of the end-of-life scenario of the product being analysed is also very significant. In addition, it must be considered that when the FS is introduced into bricks, the metal leachate is avoided on the landfill floor, and therefore the incorporation of this residue increases the benefits in other categories. The greater contribution to *Carcinogens, Respiratory of Inorganics, Respiratory of organics, Climate Change, and Radiation* by brick B, is the result of, on the one hand, its higher energy consumption compared to B + S in the manufacturing phase, which translates into more particles, and more emissions of CO_2, CO, CH_4, C_2H_4, SO_2, N_2O. On the other hand, the CO_2 emissions avoided from the process of transporting the waste when it is introduced into the bricks makes the difference between the two bricks in these categories more pronounced. The lower NO_x emissions are also responsible for the higher incidence of brick B in depleting the ozone layer.

Acidification / Eutrophication is a category where NO_x and SO_2 emissions were evaluated. The B + S brick produces fewer amounts of SO_2 during the firing stage, although it increases in the transport of raw materials; in the case of NO_x compounds, they are somewhat higher for B + S during cooking, although the higher energy consumption of B for B + S in the production phase and the fact of avoiding transporting waste for B + S, is translated into an increase in global benefits (lower impacts) in the global analysis of the B + S brick (Figure 2.35).

In the case of *Minerals and Land Use*, the benefit obtained for B + S is related to the use of raw materials. In brick B + S, the clay for brick making is 1.1 tonnes while for brick B it is 1.25 tonnes. Also, clay and FS used in landfill operations when landfill sand is managed are avoided.

Considering the specific energy mix in Spain, the fact that B + S requires less energy during its life cycle translates into less coal combustion in power plants, which is attributed to a lower impact on the category of *Fossil Fuel*.

2.4.3. Conclusions

FS/clay bricks were fired at different temperatures to optimize the heating curve from the laboratory level to the pilot plant. It studied the weight losses through LOI variations, firing shrinkage, and water absorption of the FS/clay bricks. Considering the low LOI variations in the FS/clay bricks, it can be concluded that the influence of firing temperature does not have a significant influence on the weight loss of bricks. On the other hand, higher firing temperatures result in bricks with more contractions and lower water absorption values. It could be possible because the FS does not have a great sintering capacity, which means that a high amount of FS difficult for the sintering process. Therefore, it can be concluded that FS does not optimize the firing temperature of the ceramic process.

FB-FCBs with percentages of 1 %, 10 %, and 20 % of FS were produced at an industrial scale. The study of the optimisation of the firing temperature concluded that with the incorporation of this waste, the best working temperature was still the firing cycle used by the company. The compression strength, the environmental behaviour, and the gas emissions during the firing process were assessed to determine the feasibility of FS as a substitute for clay in ceramic processes. The visual appearance and the compressive strength results are like those obtained with 100% clay bricks. Considering the environmental behaviour of the FS-clay mixtures according to the order AAA/661/2013 regarding the discharge of waste, FB/clay bricks present concentrations of pollutants below the inert landfill limit. Finally, the estimation of gaseous emissions determined that no SOx, HCl, HF, or NOx are emitted, only CO2 emissions that present emissions similar to 100 % clay brick. The results obtained allow us to conclude that the FS can be incorporated into the ceramic process on an industrial scale.

Finally, an LCA was carried out to assess the environmental impact of FB/clay bricks compared with a conventional clay brick (without waste/by-products). The results suggest that the main impact associated with the life cycle of the construction materials analysed, despite the incorporation of FS, is related to energy consumption. The replacement of part of the clay used in the manufacture of the product with a residue such as foundry sand, generates a series of positive impacts on the environment, since on the one hand it reduces the amount of raw material used, decreases the energy requirement in the production stage and avoids the management of this waste, with its transport, processing, and dumping of the resulting waste. The applied management scenario (higher or lower percentage of Recycling) of construction and demolition waste (RCD) resulting in at the end of life of the bricks, does not have a great influence on the global indicator, although it is important in the category of Minerals impact for the recovery of materials from construction and demolition waste.

2.5. REFERENCES

- Abdulkareem OA, Mustafa Al Bakri AM, Kamarudin H, Khairul Nizar I, Saif AA. Effects of elevated temperatures on the thermal behaviour and mechanical performance of fly ash geopolymer paste, mortar and lightweight concrete. Constr Build Mater 2014;50:377–87. doi:10.1016/j.conbuildmat.2013.09.047.
- Ahmari S, Ren X, Toufigh V, Zhang L. Production of geopolymeric binder from blended waste concrete powder and fly ash. Constr Build Mater 2012;35:718–29. doi:10.1016/j.conbuildmat.2012.04.044.
- Ahmaruzzaman M. Industrial waste as low-cost potential adsorbents for the treatment of wastewater laden with heavy metals. Adv Colloid Interface Sci 2011;166:36–59. doi:10.1016/j.cis.2011.04.005.
- Aineto M, Acosta A, Iglesias I. The role of a coal gasification fly ash as clay additive in building ceramic. J Eur Ceram Soc 2006;26:3783–7. doi:10.1016/j.jeurceramsoc.2006.01.011.
- Aixiang Z, Weihao X, Jian X. Electroless Ni-P coating of cenospheres using silver nitrate activator. Surf Coatings Technol 2005;197:142–7. doi:10.1016/j.surfcoat.2005.01.009.
- Aksu Z, Yener J. A comparative adsorption/biosorption study of mono-chlorinated phenols onto various sorbents. Waste Manag 2001;21:695–702. doi:10.1016/S0956-053X(01)00006-X.
- Alexandri M, Papapostolou H, Komaitis M, Stragier L, Verstraete W, Danezis GP, et al. Evaluation of an integrated biorefinery based on fractionation of spent sulphite liquor for the production of an antioxidant-rich extract, lignosulphonates and succinic acid. Bioresour Technol 2016. doi:10.1016/j.biortech.2016.03.162.
- Al-Harahsheh MS, Al Zboon K, Al-Makhadmeh L, Hararah M, Mahasneh M. Fly ash based geopolymer for heavy metal removal: A case study on copper removal. J Environ Chem Eng 2015;3:1669–77. doi:10.1016/j.jece.2015.06.005.
- Alinnor IJ. Adsorption of heavy metal ions from aqueous solution by fly ash. Fuel 2007;86:853–7. doi:10.1016/j.fuel.2006.08.019.
- Almesfer N, Ingham J. Effect of Waste Glass on the Properties of Concrete. J Mater Civ Eng 2014;26:1–6. doi:10.1061/(ASCE)MT.1943-5533.
- Alonso-Santurde R., Coz A., Viguri J.R., Andrés A. Recycling of foundry by-products in the ceramic industry: Green and core sand in clay bricks. Constr. Build. Mater. 2012, 97-106.
- Alonso-Santurde, R.; Andrés, A.; Viguri, J.R.; Raimondo, M.; Guarini, G.; Zanelli, C.; Dondi, M. Technological Behaviour and Recycling Potential of Spent Foundry Sands in Clay Bricks. J. Environ. Manag. 2011, 92, 994–1002.
- Alonso-Santurde, R.; Coz, A.; Quijorna, N.; Viguri, J.R.; Andrés, A. Valorisation of Foundry Sand in Clay Bricks at Industrial Scale. J. Ind. Ecol. 2010, 14, 217–230.
- Álvarez-Ayuso E, Querol X, Plana F, Alastuey A, Moreno N, Izquierdo M, et al. Environmental, physical and structural characterisation of geopolymer matrixes synthesised from coal (co-)combustion fly ashes. J Hazard Mater 2008;154:175–83. doi:10.1016/j.jhazmat.2007.10.008.
- Al-Zboon K, Al-Harahsheh MS, Hani FB. Fly ash-based geopolymer for Pb removal from aqueous solution. J Hazard Mater 2011;188:414–21. doi:10.1016/j.jhazmat.2011.01.133.
- Amin, S.H.K.; Elmahgary, M.G.; Abadir, M.F. Preparation and characterisation of dry pressed ceramic tiles incorporating ceramic sludge waste. Ceram. Silik. 2019, 63, 11–20.
- Amorós, J.L.; Orts, M.J.; García-Ten, J.; Gozalbo, A.; Sánchez, E. Effect of the green porous texture on porcelain tile properties. J. Eur. Ceram. Soc. 2007, 27, 2295–2301.

- Anderson, M.; Elliott, M.; Hickson, C. Factory-scale proving trials using combined mixtures of three by-product waste (including incinerated sewage sludge ash) in clay building bricks. J. Chem. Technol. Biotechnol. 2002, 77, 345–351.
- Andini S, Cioffi R, Colangelo F, Grieco T, Montagnaro F, Santoro L. Coal fly ash as raw material for the manufacture of geopolymer-based products. Waste Manag 2008;28:416–23. doi:10.1016/j.wasman.2007.02.001.
- Andreola F, Barbieri L, Lancellotti I, Leonelli C, Manfredini T. Recycling of industrial waste in ceramic manufacturing: State of art and glass case studies. Ceram Int 2016;42:13333–8. doi:10.1016/j.ceramint.2016.05.205.
- Antiohos SK, Papageorgiou A, Papadakis VG, Tsimas S. Influence of quicklime addition on the mechanical properties and hydration degree of blended cements containing different fly ashes. Constr Build Mater 2008;22:1191–200. doi:10.1016/j.conbuildmat.2007.02.001.
- Antony Jeyasehar C, Saravanan G, Ramakrishnan AK, Kandasamy S. Strength and durability studies on fly ash based geopolymer bricks. Asian J Civ Eng 2013;14:797–808.
- Apiratikul R, Pavasant P. Sorption of Cu2+, Cd2+, and Pb2+ using modified zeolite from coal fly ash. Chem Eng J 2008;144:245–58. doi:10.1016/j.cej.2008.01.038.
- Arroyo F, Fernández-Pereira C, Olivares J, Coca P. Hydrometallurgical recovery of germanium from coal gasification fly ash: Pilot plant scale evaluation. Ind Eng Chem Res 2009;48:3573–9. doi:10.1021/ie800730h.
- Arroyo F, Font O, Fernández-Pereira C, Querol X, Juan R, Ruiz C, et al. Germanium recovery from gasification fly ash: Evaluation of end-products obtained by precipitation methods. J Hazard Mater 2009;167:582–8. doi:10.1016/j.jhazmat.2009.01.021.
- Assi LN, Deaver E, Elbatanouny MK, Ziehl P. Investigation of early compressive strength of fly ash-based geopolymer concrete. Constr Build Mater 2016;112:807–15. doi:10.1016/j.conbuildmat.2016.03.008.
- Astm. Standard Specification for Coal Fly Ash and Raw or Calcined Natural Pozzolan for Use. Annu B ASTM Stand 2010:3–6. doi:10.1520/C0618.
- Atiş CD, Görür EB, Karahan O, Bilim C, İlkentapar S, Luga E. Very high strength (120MPa) class F fly ash geopolymer mortar activated at different NaOH amount, heat curing temperature and heat curing duration. Constr Build Mater 2015;96:673–8. doi:10.1016/j.conbuildmat.2015.08.089.
- Babajide O, Musyoka N, Petrik L, Ameer F. Novel zeolite Na-X synthesized from fly ash as a heterogeneous catalyst in biodiesel production. Catal Today 2012;190:54–60. doi:10.1016/j.cattod.2012.04.044.
- Bai G, Teng W, Wang X, Zhang H, Xu P. Processing and kinetics studies on the alumina enrichment of coal fly ash by fractionating silicon dioxide as nano particles. Fuel Process Technol 2010;91:175–84. doi:10.1016/j.fuproc.2009.09.010.
- Bai GH, Teng W, Wang XG, Qin JG, Xu P, Li PC. Alkali desilicated coal fly ash as substitute of bauxite in lime-soda sintering process for aluminum production. Trans Nonferrous Met Soc China (English Ed 2010;20:s169–75. doi:10.1016/S1003-6326(10)60034-9.
- Bakharev T. Thermal behaviour of geopolymers prepared using class F fly ash and elevated temperature curing. Cem Concr Res 2006;36:1134–47. doi:10.1016/j.cemconres.2006.03.022.
- Barbare N, Shukla A, Bose A. Uptake and loss of water in a cenosphere-concrete composite material. Cem Concr Res 2003;33:1681–6. doi:10.1016/S0008-8846(03)00148-0.
- Başpinar, M.S., Kahraman, E., Gökhan, G., Demir I. Production of fired construction brick from high sulfate-containing fly ash with boric acid addition. Waste Manag Res 2010;28:4–10.

- Batchelor B. Overview of waste stabilisation with cement. Waste Manag 2006;26:689–98. doi:10.1016/j.wasman.2006.01.020.
- Beeghly J, Schrock M. Dredge material stabilisation using the pozzolanic or sulfo-pozzolanic reaction of lime by-products to make an engineered structural fill. Int J Soil, ... 2010;3:1–22.
- Belmonte, L.J.; Ottosen, L.M.; Kirkelund, G.M.; Jensen, P.E.; Vestbø, A.P. Screening of heavy metal containing waste types for use as raw material in Arctic clay-based bricks. Environ. Sci. Pollut. Res. 2018, 25, 32831–32843.
- Belyaeva ON, Haynes RJ. Comparison of the effects of conventional organic amendments and biochar on the chemical, physical and microbial properties of coal fly ash as a plant growth medium. Environ Earth Sci 2012;66:1987–97. doi:10.1007/s12665-011-1424-y.
- Bennetto E. 2007. Combining lifecycle and risk assessment of mineral waste reuse scenarios for decision making support. Environmental Impact Assessment Review, 27: 266-285.
- Berger E, Fitzgerald HB. 2009 World of Coal Ash (WOCA) Conference - May 4-7, 2009 in Lexington, KY, USA http://www.flyash.info/ 2009.
- Beshah, D.A.; Tiruye, G.A.; Mekonnen, Y.S. Characterisation and recycling of textile sludge for energy-efficient brick production in Ethiopia. Environ. Sci. Pollut. Res. 2021, 28, 16272–16281.
- Bhagat N, Batra V.S., Katyal D. 2011. Preparation and characterisation of ceramics from coal fly ash. Asian Journal of Chemistry, 23(1): 71-73.
- Bhattacharya AK, Naiya TK, Mandal SN, Das SK. Adsorption, kinetics and equilibrium studies on removal of Cr(VI) from aqueous solutions using different low-cost adsorbents. Chem Eng J 2008;137:529–41. doi:10.1016/j.cej.2007.05.021.
- Bhattacharya SS, Iftikar W, Sahariah B, Chattopadhyay GN. Vermicomposting converts fly ash to enrich soil fertility and sustain crop growth in red and lateritic soils. Resour Conserv Recycl 2012;65:100–6. doi:10.1016/j.resconrec.2012.05.008.
- Blanco F, García P, Mateos P, Ayala J. Characteristics and properties of lightweight concrete manufactured with cenospheres. Cem Concr Res 2000;30:1715–22. doi:10.1016/S0008-8846(00)00357-4.
- Blissett R.S. and Rowson N.A. 2012. A review of the multi-component utilisation of coal fly ash, Fuel 97:1-23.
- Bories C, Borredon ME, Vedrenne E, Vilarem G. Development of eco-friendly porous fired clay bricks using pore-forming agents: A review. J Environ Manage 2014;143:186–96. doi:10.1016/j.jenvman.2014.05.006.
- Brunner, P.H.; Rechberger, H. Waste to Energy—Key Element for Sustainable Waste Management. Waste Manag. 2015, 37, 3–12.
- Bukhari SS, Behin J, Kazemian H, Rohani S. Conversion of coal fly ash to zeolite utilizing microwave and ultrasound energies: A review. Fuel 2015;140. doi:10.1016/j.fuel.2014.09.077.
- Cabielles M, Montes-Morán MA, Garcia AB. Structural study of graphite materials prepared by HTT of unburned carbon concentrates from coal combustion fly ashes. Energy and Fuels 2008;22:1239–43. doi:10.1021/ef700603t.
- CAEF Report – The European Foundry Association Comission for economics & statistics. 2020. https://www.caef.eu/wp-content/uploads/2019/01/CAEF-Co7_2020-complete.pdf
- Calstar Products, 2014. SMaRT Environmental Product Declaration. Disponible en: http://cdn.calstarproducts.com/wp-content/uploads/2014/02/CalStar-EPD-Document-2014.pdf

- Cameán I, Garcia AB. Graphite materials prepared by HTT of unburned carbon from coal combustion fly ashes: Performance as anodes in lithium-ion batteries. J Power Sources 2011;196:4816–20. doi:10.1016/j.jpowsour.2011.01.041.
- CEDEX Catálogo de Residuos Utilizables en Construcción. Available online: http://www.cedexmateriales.es/catalogo-de- residuos/24/diciembre-2011/ (accessed on 16 January 2021).
- CEDEX. Ficha Técnica: Cenizas Volantes De Carbón Y Cenizas De Hogar O Escorias 2011:1–41.
- Chakraborty R, Bepari S, Banerjee A. Transesterification of soybean oil catalyzed by fly ash and egg shell derived solid catalysts. Chem Eng J 2010;165:798–805. doi:10.1016/j.cej.2010.10.019.
- Chand N, Sharma P, Fahim M. Correlation of mechanical and tribological properties of organosilane modified cenosphere filled high density polyethylene. Mater Sci Eng A 2010;527:5873–8. doi:10.1016/j.msea.2010.06.022.
- Chandra N, Sharma P, Pashkov GL, Voskresenskaya EN, Amritphale SS, Baghel NS. Coal fly ash utilisation: Low temperature sintering of wall tiles. Waste Manag 2008;28:1993–2002. doi:10.1016/j.wasman.2007.09.001.
- Chatterjee D, Ruj B, Mahata A. Adsorption and photocatalysis of colour removal from waste water using flyash and sunlight. Catal Commun 2001;2:113–7. doi:10.1016/S1566-7367(01)00017-6.
- Chávez-Valdez A, Arizmendi-Morquecho A, Vargas G, Almanza JM, Alvarez-Quintana J. Ultra-low thermal conductivity thermal barrier coatings from recycled fly-ash cenospheres. Acta Mater 2011;59:2556–62. doi:10.1016/j.actamat.2011.01.011.
- Chen-Tan NW, Van Riessen A, Ly C V., Southam DC. Determining the reactivity of a fly ash for production of geopolymer. J Am Ceram Soc 2009;92:881–7. doi:10.1111/j.1551-2916.2009.02948.x.
- Chimenos JM, Fernández AI, Del Valle-Zermeño R, Font O, Querol X, Coca P. Arsenic and antimony removal by oxidative aqueous leaching of IGCC fly ash during germanium extraction. Fuel 2013;112:450–8. doi:10.1016/j.fuel.2013.05.059.
- Chindaprasirt P, Chareerat T. High-strength geopolymer using fine high-calcium fly ash. J Mater ... 2010;23:264–71. doi:10.1061/(ASCE)MT.1943-5533.0000161.
- Cho H, Oh D, Kim K. A study on removal characteristics of heavy metals from aqueous solution by fly ash. J Hazard Mater 2005;127:187–95. doi:10.1016/j.jhazmat.2005.07.019.
- Cicek T, Tanriverdi M. Lime based steam autoclaved fly ash bricks. Constr Build Mater 2007;21:1295–300. doi:10.1016/j.conbuildmat.2006.01.005.
- Cokca E, Yilmaz Z. Use of rubber and bentonite added fly ash as a liner material. Waste Manag 2004;24:153–64. doi:10.1016/j.wasman.2003.10.004.
- Contreras, M.; Gázquez, M.J.; Romero, M.; Bolívar, J.P. Recycling of industrial waste for value-added applications in clay-based ceramic products: A global review (2015–19). In New Materials in Civil Engineering; Samui, P., Kim, D., Iyer, N.R., Chaudhary, S., Eds.; Butterworth-Heinemann: Oxford, UK, 2020; pp. 155–219. ISBN 9780128189610.
- Coronado M. 2014. Foundry waste as new resources in ceramic processes. Analysis and modeling of technological and environmental properties. Doctoral thesis. Universidad de Cantabria.
- Coronado M., Blanco T., Quijorna N., Alonso-Santurde, R., Andrés, A. 2015. Chapter 3: Types of waste, properties and durability of waste-based fired masonry bricks. F. Pacheco-Torgal, P.B. Lourenco, J.A. Labrincha, V.M. John, N.P. Rajamane, (Eds) Eco-efficient Masonry Bricks and Blocks: Design, Properties and Durability. WP Wood head Publishing, Oxford, UK.

- Coronado, M.; Andrés, A.; Cheeseman, C.R. Acid Gas Emissions from Structural Clay Products Containing Secondary Resources: Foundry Sand Dust and Waelz Slag. J. Clean. Prod. 2016, 115, 191–202.
- Cultrone G, Sebastián E, Elert K, de la Torre MJ, Cazalla O, Rodriguez-Navarro C. Influence of mineralogy and firing temperature on the porosity of bricks. J Eur Ceram Soc 2004;24:547–64. doi:10.1016/S0955-2219(03)00249-8.
- Cultrone, G.; Sebastián, E. Fly ash addition in clayey materials to improve the quality of solid bricks. Constr. Build. Mater. 2009, 23, 1178–1184.
- Davini P. Flue gas treatment by activated carbon obtained from oil-fired fly ash. Carbon N Y 2002;40:1973–9. doi:10.1016/S0008-6223(02)00049-0.
- De la Casa JA and Castro E. Fuel savings and carbon dioxide emission reduction in a fired clay bricks production plant using olive oil waste: A simulation study. J Clean Prod 2018; 185; 230-238. Doi: 10.1016/j.jclepro.2018.03.010.
- Deb PS, Sarker PK, Barbhuiya S. Effects of nano-silica on the strength development of geopolymer cured at room temperature. Constr Build Mater 2015;101:675–83. doi:10.1016/j.conbuildmat.2015.10.044.
- Deepthi M V., Sharma M, Sailaja RRN, Anantha P, Sampathkumaran P, Seetharamu S. Mechanical and thermal characteristics of high density polyethylene-fly ash Cenospheres composites. Mater Des 2010;31:2051–60. doi:10.1016/j.matdes.2009.10.014.
- Del Rio, D.D.F.; Sovacool, B.K.; Foley, A.M.; Griffiths, S.; Bazilian, M.; Kim, J.; Rooney, D. Decarbonizing the ceramics industry: A systematic and critical review of policy options, developments and sociotechnical systems. Renew. Sustain. Energy Rev. 2022, 157, 112081.
- Del Valle-Zermeño R, Formosa J, Chimenos JM, Martínez M, Fernández AI. Aggregate material formulated with MSWI bottom ash and APC fly ash for use as secondary building material. Waste Manag 2013;33:621–7. doi:10.1016/j.wasman.2012.09.015.
- Delgado C., Garitaonandia E., Unamunzaga L., Martínez A., García I., Ríos J., Rodríguez J.L. Integration of a novel mechanical sand reclamation technology in a Steel foundry to maximize SFS valorisation in foundry and construction applications. 58th International Foundry Conferce. 2018, Portorož, Slovenia.
- Demir, I.; Baspinar, M.S.; Orhan, M. Utilisation of kraft pulp production residues in clay brick production. Build. Environ. 2005, 40, 1533–1537.
- Dhir RK, Jones MR. Development of chloride-resisting concrete using fly ash. Fuel 1999;78:137–42. doi:10.1016/S0016-2361(98)00149-5.
- Diaz EI, Allouche EN, Eklund S. Factors affecting the suitability of fly ash as source material for geopolymers. Fuel 2010;89:992–6. doi:10.1016/j.fuel.2009.09.012.
- Ding J, Ma S, Shen S, Xie Z, Zheng S, Zhang Y. Research and industrialisation progress of recovering alumina from fly ash: A concise review. Waste Manag 2016;60:375–87. doi:10.1016/j.wasman.2016.06.009.
- Domínguez E a., Ullman R. "Ecological bricks" made with clays and steel dust pollutants. Appl Clay Sci 1996;11:237–49. doi:10.1016/S0169-1317(96)00020-8.
- Dondi, M.; Guarini, G.; Raimondo, M.; Ruffini, A. Orimulsion Fly Ash in Clay Bricks—Part 3: Chemical Stability of Ash-Bearing Products. J. Eur. Ceram. Soc. 2002, 22, 1749–1758.
- Duan P, Yan C, Luo W, Zhou W. Effects of adding nano-TiO2 on compressive strength, drying shrinkage, carbonation and microstructure of fluidized bed fly ash based geopolymer paste. Constr Build Mater 2016;106:115–25. doi:10.1016/j.conbuildmat.2015.12.095.

- Durán-Herrera A, Juárez CA, Valdez P, Bentz DP. Evaluation of sustainable high-volume fly ash concretes. Cem Concr Compos 2011;33:39–45. doi:10.1016/j.cemconcomp.2010.09.020.
- Duxson P, Fernández-Jiménez A, Provis JL, Lukey GC, Palomo A, Van Deventer JSJ. Geopolymer technology: The current state of the art. J Mater Sci 2007;42:2917–33. doi:10.1007/s10853-006-0637-z.
- ECOBA European Coal Combustion Products Association. Available online: https://www.gem.wiki/European_Coal_ Combustion_Products_Association (accessed on 16 January 2021).
- Elías, X. Reciclaje de Residuos Industriales: Residuos Solidos Urbanos y Fangos de Depuradora. Residuos Sólidos Urbanos y Fangos de Depurador; Ediciones Díaz de Santos: Madrid, Spain, 2009.
- Eliche-Quesada, D.; Corpas-Iglesias, F.A.; Pérez-Villarejo, L.; Iglesias-Godino, F.J. Recycling of sawdust, spent earth from oil filtration, compost and marble residues for brick manufacturing. Constr. Build. Mater. 2012, 34, 275–284.
- Eliche-Quesada, D.; Leite-Costa, J. Use of bottom ash from olive pomace combustion in the production of eco-friendly fired clay bricks. Waste Manag. 2016, 48, 323–333.
- Eliche-Quesada, D.; Sandalio-Pérez, J.A.; Martínez-Martínez, S.; Pérez-Villarejo, L.; Sánchez-Soto, P.J. Investigation of Use of Coal Fly Ash in Eco-Friendly Construction Materials: Fired Clay Bricks and Silica-Calcareous Non Fired Bricks. Ceram. Int. 2018, 44, 4400–4412.
- EPA, Environmental Protection Agency. Coal Combustion Residuals—Proposed Rule. 2008. Available online: http://www.epa. gov/osw/nonhaz/industrial/special/fossil/ccr-rule/ (accessed on 18 June 2021).
- Erol M, Küçükbayrak S, Ersoy-Meriçboyu A. Characterisation of sintered coal fly ashes. Fuel 2008;87:1334–40. doi:10.1016/j.fuel.2007.07.002.
- Estevinho BN, Martins I, Ratola N, Alves A, Santos L. Removal of 2,4-dichlorophenol and pentachlorophenol from waters by sorption using coal fly ash from a Portuguese thermal power plant. J Hazard Mater 2007;143:535–40. doi:10.1016/j.jhazmat.2006.09.072.
- European Comission. European Comission Reference Document on Best Available Techniques in the Ceramic Manufacturing Industry; European Comission: Brussels, Belgium, 2007.
- European Commission, Joint Research Centre; Borchardt, S.; Buscaglia, D.; Barbero Vignola, G.; Maroni, M.; Marelli, L. A Sustainable Recovery for the EU: A Text Mining Approach to Map the EU Recovery Plan to the Sustainable Development Goals; Publications Office of the European Union: Luxembourg, 2020; Available online: https://publications.jrc.ec.europa.eu/repository/handle/ JRC122301 (accessed on 19 March 2022).
- European Commission. No TitleCOM(2015) 614 Communication from the Commission to the European Parliament, the Council, the European Economic and Social Committee and the Committee of the Regions - Closing the Loop - an EU Action Plan for the Circular Economy. 2015.
- Feng J, Zhang R, Gong L, Li Y, Cao W, Cheng X. Development of porous fly ash-based geopolymer with low thermal conductivity. Mater Des 2015;65:529–33. doi:10.1016/j.matdes.2014.09.024.
- Fernández-Jiménez A, Palomo A, Pastor JY, Martín A. New cementitious materials based on alkali-activated fly ash: Performance at high temperatures. J Am Ceram Soc 2008;91:3308–14. doi:10.1111/j.1551-2916.2008.02625.x.

- Fernández-Pereira, C.; de La Casa, J.A.; Gómez-Barea, A.; Arroyo, F.; Leiva, C.; Luna, Y. Application of Biomass Gasification Fly Ash for Brick Manufacturing. Fuel 2011, 90, 220–232.
- Ferone C, Colangelo F, Messina F, Santoro L, Cioffi R. Recycling of pre-washed municipal solid waste incinerator fly ash in the manufacturing of low temperature setting geopolymer materials. Materials (Basel) 2013;6:3420–37. doi:10.3390/ma6083420.
- Flores Y, Flores R, Gallegos AA. Heterogeneous catalysis in the Fenton-type system reactive black 5/H2O2. J Mol Catal A Chem 2008;281:184–91. doi:10.1016/j.molcata.2007.10.019.
- Font O, Moreno N, Díez S, Querol X, López-Soler A, Coca P, et al. Differential behaviour of combustion and gasification fly ash from Puertollano Power Plants (Spain) for the synthesis of zeolites and silica extraction. J Hazard Mater 2009;166:94–102. doi:10.1016/j.jhazmat.2008.10.120.
- Font O, Querol X, Juan R, Casado R, Ruiz CR, López-Soler Á, et al. Recovery of gallium and vanadium from gasification fly ash. J Hazard Mater 2007;139:413–23. doi:10.1016/j.jhazmat.2006.02.041.
- Font O, Querol X, López-Soler A, Chimenos JM, Fernández AI, Burgos S, et al. Ge extraction from gasification fly ash. Fuel 2005;84:1384–92. doi:10.1016/j.fuel.2004.06.041.
- Freeman E, Gao Y-M, Hurt R, Suuberg E. Interactions of carbon-containing fly ash with commercial air-entraining admixtures for concrete. Fuel 1997;76:761–5. doi:10.1016/S0016-2361(96)00193-7.
- Freyburg S, Schwarz, A. 2007. Influence of the clay type on the pore structure of structural ceramics. J of the European Ceramic Society, 27: 1727-1733.
- Furnali E., Tonello G., Maschio S. 2010. Recycling of steel slag and glass cullet from energy saving lamps by fast firing production of ceramics. Waste Management, 30(8-9): 1714-1719.
- Galan E, González I, Fabbri B. Estimation of fluorine and chlorine emissions from Spanish structural ceramic industries. The case study of the Bailen area, Southern Spain. Atmos Environ 2002, 36, 5289-5298. Doi: 10.1016/S1352-2310(02)00645-3.
- Galán-Arboledas, R.J.; Álvarez de Diego, J.; Dondi, M.; Bueno, S. Energy, Environmental and Technical Assessment for the Incorporation of EAF Stainless Steel Slag in Ceramic Building Materials. J. Clean. Prod. 2017, 142, 1778–1788.
- Garcia-Ubaque, C.A.; Giraldo, L.; Moreno-Piraján, J.C. Quality Study of Ceramic Bricks Manufacture with Clay and Ashes from the Incineration of Municipal Solid Waste. Afinidad 2013, 561, 60–66.
- García-Ubaque, C.A.; Moreno-Piraján, J.C.; Giraldo-Gutierrez, L.; Sapag, K. Stabilisation/Solidification of Ashes in Clays Used in the Manufacturing of Ceramic Bricks. Waste Manag. Res. 2007, 25, 352–362.
- González A, Navia R, Moreno N. Fly ashes from coal and petroleum coke combustion: current and innovative potential applications. Waste Manag Res 2009;27:976–87. doi:10.1177/0734242X09103190.
- González, I.; Galán, E.; Miras, A.; Vázquez, M.A. CO_2 emissions derived from raw materials used in brick factories. Applications to Andalusia (Southern Spain). Appl. Clay Sci. 2011, 52, 193–198.
- González I, Barba-Brioso C, Campos P, Romero A, Galán E. Reduction of CO_2 reduction diffuse emissions from the traditional ceramic industry by the addition of Si-Al raw material. J Env Manag 2016; 180; 190-196. Doi: 10.1016/j.jenvman.2016.05.039.
- Gordon LE, Provis JL, Van Deventer JSJ. Non-traditional ("geopolymer") cements and concretes for construction of large CCS equipment. Energy Procedia 2011;4:2058–65. doi:10.1016/j.egypro.2011.02.088.

- Gunasekara C, Law DW, Setunge S, Sanjayan JG. Zeta potential, gel formation and compressive strength of low calcium fly ash geopolymers. Constr Build Mater 2015;95:592–9. doi:10.1016/j.conbuildmat.2015.07.175.
- Guo Y, Li Y, Cheng F, Wang M, Wang X. Role of additives in improved thermal activation of coal fly ash for alumina extraction. Fuel Process Technol 2012;110:114–21. doi:10.1016/j.fuproc.2012.12.003.
- Gupta, N.; Gedam, V.V.; Moghe, C.; Labhasetwar, P. Comparative Assessment of Batch and Column Leaching Studies for Heavy Metals Release from Coal Fly Ash Bricks and Clay Bricks. Environ. Technol. Innov. 2019, 16, 100461.
- Hamer, K.; Karius, V. Brick Production with Dredged Harbour Sediments. An Industrial-Scale Experiment. Waste Manag. 2002, 22, 521–530.
- Harris D. Coal Combustion By-Products Opportunities in fly ash trade and utilisation. Coaltrans Asia Conf., 2016.
- Heidemann M, Nierwinski HP, Hastenpflug D, Salgado Barra B. Geotechnical behaviour of a compacted waste foundry sand. Constr Build Mater 2021; 277; 122267. Doi: 10.1016/j.conbuildmat.2021.122267.
- Helmy AII. Intermittent curing of fly ash geopolymer mortar. Constr Build Mater 2016;110:54–64. doi:10.1016/j.conbuildmat.2016.02.007.
- Hemalatha T, Ramaswamy A. A review on fly ash characteristics- Towards promoting high volume utilisation in developing sustainable concrete. J Clean Prod 2017;147:546–59. doi:10.1016/j.jclepro.2017.01.114.
- Hernández-Expósito A, Chimenos JM, Fernández AI, Font O, Querol X, Coca P, et al. Ion flotation of germanium from fly ash aqueous leachates. Chem Eng J 2006;118:69–75. doi:10.1016/j.cej.2006.01.012.
- Hower, J.C.; Groppo, J.G.; Graham, U.M.; Ward, C.R.; Kostova, I.J.; Maroto-Valer, M.M.; Dai, S. Coal-Derived Unburned Carbons in Fly Ash: A Review. Int. J. Coal Geol. 2017, 179, 11–27.
- Hsu TC, Yu CC, Yeh CM. Adsorption of Cu2+ from water using raw and modified coal fly ashes. Fuel 2008;87:1355–9. doi:10.1016/j.fuel.2007.05.055.
- Hu YJ, Zhang HY, Li F, Cheng XL, Chen TL. Investigation into electrical conductivity and electromagnetic interference shielding effectiveness of silicone rubber filled with Ag-coated cenosphere particles. Polym Test 2010;29:609–12. doi:10.1016/j.polymertesting.2010.03.009.
- Huiskes DMA, Keulen A, Yu QL, Brouwers HJH. Design and performance evaluation of ultra-lightweight geopolymer concrete. Mater Des 2016;89:516–26. doi:10.1016/j.matdes.2015.09.167.
- Huo P, Yan Y, Li S, Li H, Huang W, Chen S, et al. H2O2 modified surface of TiO2/fly-ash cenospheres and enhanced photocatalytic activity on methylene blue. Desalination 2010;263:258–63. doi:10.1016/j.desal.2010.06.067.
- Huo P, Yan Y, Li S, Li H, Huang W. Preparation and characterisation of Cobalt Sulfophthalocyanine/TiO2/fly-ash cenospheres photocatalyst and study on degradation activity under visible light. Appl Surf Sci 2009;255:6914–7. doi:10.1016/j.apsusc.2009.03.014.
- Itskos G, Koukouzas N, Vasilatos C, Megremi I, Moutsatsou A. Comparative uptake study of toxic elements from aqueous media by the different particle-size-fractions of fly ash. J Hazard Mater 2010;183:787–92. doi:10.1016/j.jhazmat.2010.07.095.
- Izquierdo M, Querol X, Davidovits J, Antenucci D, Nugteren H, Fernández-Pereira C. Coal fly ash-slag-based geopolymers: Microstructure and metal leaching. J Hazard Mater 2009;166:561–6. doi:10.1016/j.jhazmat.2008.11.063.

- Izquierdo M, Querol X. Leaching behaviour of elements from coal combustion fly ash: An overview. Int J Coal Geol 2012;94:54–66. doi:10.1016/j.coal.2011.10.006.
- Izquierdo MT, Rubio B. Carbon-enriched coal fly ash as a precursor of activated carbons for SO2 removal. J Hazard Mater 2008;155:199–205. doi:10.1016/j.jhazmat.2007.11.047.
- Jain D, Khatri C, Rani A. Fly ash supported calcium oxide as recyclable solid base catalyst for Knoevenagel condensation reaction. Fuel Process Technol 2010;91:1015–21. doi:10.1016/j.fuproc.2010.02.021.
- Jain D, Khatri C, Rani A. Synthesis and characterisation of novel solid base catalyst from fly ash. Fuel 2011;90:2083–8. doi:10.1016/j.fuel.2010.09.025.
- Jayaranjan, M.L.D.; van Hullebusch, E.D.; Annachhatre, A.P. Reuse options for coal fired power plant bottom ash and fly ash. Rev. Environ. Sci. Biotechnol. 2014, 13, 467–486.
- Jha N, Badkul A, Mondal DP, Das S, Singh M. Sliding wear behaviour of aluminum syntactic foam: A comparison with Al10 wt% SiC composites. Tribol Int 2011;44:220–31. doi:10.1016/j.triboint.2010.10.004.
- Jha VK, Nagae M, Matsuda M, Miyake M. Zeolite formation from coal fly ash and heavy metal ion removal characteristics of??thus-obtained Zeolite X in multi-metal systems. J Environ Manage 2009;90:2507–14. doi:10.1016/j.jenvman.2009.01.009.
- Ji R, Zhang Z, Yan C, Zhu M, Li Z. Preparation of novel ceramic tiles with high Al2O3 content derived from coal fly ash. Constr Build Mater 2016;114:888–95. doi:10.1016/j.conbuildmat.2016.04.014.
- Jonker A., Potgieter J.H. 2005. An evaluation of selected waste resources for utilisation in ceramic materials applications. Journal of the European Ceramic Society, 25(13): 3145-3149.
- Kamble SP, Mangrulkar PA, Bansiwal AK, Rayalu SS. Adsorption of phenol and o-chlorophenol on surface altered fly ash based molecular sieves. Chem Eng J 2008;138:73–83. doi:10.1016/j.cej.2007.05.030.
- Kazemian A, Gholizadeh Vayghan A, Rajabipour F. Quantitative assessment of parameters that affect strength development in alkali activated fly ash binders. Constr Build Mater 2015;93:869–76. doi:10.1016/j.conbuildmat.2015.05.078.
- Kazemian H, Naghdali Z, Ghaffari Kashani T, Farhadi F. Conversion of high silicon fly ash to Na-P1 zeolite: Alkaline fusion followed by hydrothermal crystallisation. Adv Powder Technol 2010;21:279–83. doi:10.1016/j.apt.2009.12.005.
- Khatri C, Mishra MK, Rani A. Synthesis and characterisation of fly ash supported sulfated zirconia catalyst for benzylation reactions. Fuel Process Technol 2010;91:1288–95. doi:10.1016/j.fuproc.2010.04.011.
- Khatri C, Rani A. Synthesis of a nano-crystalline solid acid catalyst from fly ash and its catalytic performance. Fuel 2008;87:2886–92. doi:10.1016/j.fuel.2008.04.011.
- Kishor P, Ghosh AK, Kumar D. Use of Flyash in Agriculture: A Way to Improve Soil Fertility and its Productivity. Asian J Agric Res 2010;4:1–14. doi:10.3923/ajar.2010.1.14.
- Kockal, N.U. Utilisation of Different Types of Coal Fly Ash in the Production Of Ceramic Tiles; Sociedad Española de Cerámica y Vidrio: Madrid, Spain, 2012; Volume 51, pp. 297–304.
- Komljenovic M, Z. Bascarevic VB. Mechanical and microstructural properties of alkali-activated fly ash geopolymers. J Hazard Mater 2010;181:35–42. doi:10.1016/j.jhazmat.2010.04.064.
- Koshy N, Singh DN. Fly ash zeolites for water treatment applications. J Environ Chem Eng 2016;4:1460–72. doi:10.1016/j.jece.2016.02.002.
- Koukouzas N, Ketikidis C, Itskos G, Spiliotis X, Karayannis V, Papapolymerou G. Synthesis of CFB-coal fly ash clay bricks and their characterisation. Waste and Biomass Valorisation 2011;2:87–94. doi:10.1007/s12649-010-9055-1.

- Kru¯ min, š, J.; Kl, avin, š, M.; Ozola-Davida¯ ne, R.; Ansone-Be¯rtin, a, L. The Prospects of Clay Minerals from the Baltic States for Industrial-Scale Carbon Capture: A Review. Minerals 2022, 12, 349.
- Kumar A, Samadder SR, Elumalai SP. Recovery of Trace and Heavy Metals from Coal Combustion Residues for Reuse and Safe Disposal: A Review. Jom 2016;68:2413–7. doi:10.1007/s11837-016-1981-3.
- Kumar R, Kumar S, Mehrotra SP. Towards sustainable solutions for fly ash through mechanical activation. Resour Conserv Recycl 2007;52:157–79. doi:10.1016/j.resconrec.2007.06.007.
- Kumar S, Kumar R. Mechanical activation of fly ash: Effect on reaction, structure and properties of resulting geopolymer. Ceram Int 2011;37:533–41. doi:10.1016/j.ceramint.2010.09.038.
- Kumar S, Singh KK, Ramachandrarao P. Effects of fly ash additions on the mechanical and other properties of porcelainised stoneware tiles. J Mater Sci 2001;36:5917–22. doi:10.1023/A:1012936928769.
- Kumar Vadapalli VR, Klink MJ, Etchebers O, Petrik LF, Gitari W, White RA, et al. Neutralisation of acid mine drainage using fly ash, and strength development of the resulting solid residues. S Afr J Sci 2008;104:317–22.
- Kute S, Deodhar SV. Effect of Fly Ash and Temperature on Properties of Burnt Clay Bricks. J Inst Eng 2003;84:82–5.
- Labella M, Zeltmann SE, Shunmugasamy VC, Gupta N, Rohatgi PK. Mechanical and thermal properties of fly ash/vinyl ester syntactic foams. Fuel 2014;121:240–9. doi:10.1016/j.fuel.2013.12.038.
- Lee H, Ha HS, Lee CH, Lee YB, Kim PJ. Fly ash effect on improving soil properties and rice productivity in Korean paddy soils. Bioresour Technol 2006;97:1490–7. doi:10.1016/j.biortech.2005.06.020.
- Lee S, van Riessen A, Chon CM, Kang NH, Jou HT, Kim YJ. Impact of activator type on the immobilisation of lead in fly ash-based geopolymer. J Hazard Mater 2016;305:59–66. doi:10.1016/j.jhazmat.2015.11.023.
- Lee WKW, Van Deventer JSJ. Structural reorganisation of class F fly ash in alkaline silicate solutions. Colloids Surfaces A Physicochem Eng Asp 2002;211:49–66. doi:10.1016/S0927-7757(02)00237-6.
- Lee Y-R, Soe JT, Zhang S, Ahn J-W, Park MB, Ahn W-S. Synthesis of nanoporous materials via recycling coal fly ash and other solid waste: A mini review. Chem Eng J 2017;317. doi:10.1016/j.cej.2017.02.124.
- Leiva, C.; Arenas, C.; Alonso-Fariñas, B.; Vilches, L.F.; Peceño, B.; Rodriguez-Galán, M.; Baena, F. Characteristics of fired bricks with co-combustion fly ashes. J. Build. Eng. 2016, 5, 114–118.
- Leong HY, Ong DEL, Sanjayan JG, Nazari A. The effect of different Na2O and K2O ratios of alkali activator on compressive strength of fly ash based-geopolymer. Constr Build Mater 2016;106:500–11. doi:10.1016/j.conbuildmat.2015.12.141.
- Li J, Zhuang X, Font O, Moreno N, Vallejo VR, Querol X, et al. Synthesis of merlinoite from Chinese coal fly ashes and its potential utilisation as slow release K-fertilizer. J Hazard Mater 2014;265:242–52. doi:10.1016/j.jhazmat.2013.11.063.
- Li JJ, Cui J, Zhao NQ, Shi CS, Du XW. The properties of granular activated carbons prepared from fly ash using different methods. Carbon N Y 2006;44:1346–8. doi:10.1016/j.carbon.2005.11.031.

- Li L, Wang S, Zhu Z, Yao X, Yan Z. Catalytic decomposition of ammonia over fly ash supported Ru catalysts. Fuel Process Technol 2008;89:1106–12. doi:10.1016/j.fuproc.2008.05.002.
- Li Y, Zhang FS. Catalytic oxidation of Methyl Orange by an amorphous FeOOH catalyst developed from a high iron-containing fly ash. Chem Eng J 2010;158:148–53. doi:10.1016/j.cej.2009.12.021.
- Lin D-F, Luo H-L, Lin J-D, Zhuang M-L. Characterisations of temperature effects on sintered ceramics manufactured with waste foundry sand and clay. J Mater Cycles Waste Manag 2018; 20; 127-136. Doi: 10.1007/s10163-016-0553-5.
- Lin JX, Zhan SL, Fang MH, Qian XQ, Yang H. Adsorption of basic dye from aqueous solution onto fly ash. J Environ Manage 2008;87:193–200. doi:10.1016/j.jenvman.2007.01.001.
- Lin KL. Feasibility study of using brick made from municipal solid waste incinerator fly ash slag. J Hazard Mater 2006;137:1810–6. doi:10.1016/j.jhazmat.2006.05.027.
- Lingling X, Wei G, Tao W, Nanru Y. Study on fired bricks with replacing clay by fly ash in high volume ratio. Constr Build Mater 2005;19:243–7. doi:10.1016/j.conbuildmat.2004.05.017.
- Little, M.R.; Adell, V.; Boccaccini, A.R.; Cheeseman, C.R. Production of Novel Ceramic Materials from Coal Fly Ash and Metal Finishing Waste. Resour. Conserv. Recycl. 2008, 52, 1329–1335.
- Liu L, Singh R, Xiao P, Webley PA, Zhai Y. Zeolite synthesis from waste fly ash and its application in CO2 capture from flue gas streams. Adsorption 2011;17:795–800. doi:10.1007/s10450-011-9332-8.
- Liu W, Shen X qian, Li D hong. Fabrication of magnetic nanosized α-Fe- and Al2O3-Fe-coated cenospheres. Powder Technol 2008;186:273–7. doi:10.1016/j.powtec.2007.12.003.
- López-Antón MA, Díaz-Somoano M, Martínez-Tarazona MR. Mercury retention by fly ashes from coal combustion: Influence of the unburned carbon content. Ind Eng Chem Res 2007;46:927–31. doi:10.1021/ie060772p.
- Lu Z, Maroto-Valer MM, Schobert HH. Catalytic effects of inorganic compounds on the development of surface areas of fly ash carbon during steam activation. Fuel 2010;89:3436–41. doi:10.1016/j.fuel.2010.05.024.
- Luna Galiano Y, Fernández Pereira C, Vale J. Stabilisation/solidification of a municipal solid waste incineration residue using fly ash-based geopolymers. J Hazard Mater 2011;185:373–81. doi:10.1016/j.jhazmat.2010.08.127.
- Luo J, Zhang H, Yang J. Hydrothermal Synthesis of Sodalite on Alkali-Activated Coal Fly Ash for Removal of Lead Ions. Procedia Environ Sci 2016;31:605–14. doi:10.1016/j.proenv.2016.02.105.
- Ma X, Zhang Z, Wang A. The transition of fly ash-based geopolymer gels into ordered structures and the effect on the compressive strength. Constr Build Mater 2016;104:25–33. doi:10.1016/j.conbuildmat.2015.12.049.
- Ma Y, Hu J, Ye G. The pore structure and permeability of alkali activated fly ash. Fuel 2013;104:771–80. doi:10.1016/j.fuel.2012.05.034.
- Magalhaes J.M., Silva J.E., Castro F.P., Labrincha J.A., 2004. Effect of experimental variables on the inertisation of galvanic sludges in Clay-based ceramics. J of Hazardous Materials, 106B: 136-147.
- Manoharan V, Yunusa IAM, Loganathan P, Lawrie R, Skilbeck CG, Burchett MD, et al. Assessments of Class F fly ashes for amelioration of soil acidity and their influence on

growth and uptake of Mo and Se by canola. Fuel 2010;89:3498–504. doi:10.1016/j.fuel.2010.06.028.

- Maroto-Valer MM, Zhang Y, Granite EJ, Tang Z, Pennline HW. Effect of porous structure and surface functionality on the mercury capacity of a fly ash carbon and its activated sample. Fuel 2005;84:105–8. doi:10.1016/j.fuel.2004.07.005.
- Martin A, Pastor JY, Palomo A, Fern??ndez Jim??nez A. Mechanical behaviour at high temperature of alkali-activated aluminosilicates (geopolymers). Constr Build Mater 2015;93:1188–96. doi:10.1016/j.conbuildmat.2015.04.044.
- Matheswaran M, Karunanithi T. Adsorption of Chrysoidine R by using fly ash in batch process. J Hazard Mater 2007;145:154–61. doi:10.1016/j.jhazmat.2006.11.006.
- Matjie RH, Bunt JR, Van Heerden JHP. Extraction of alumina from coal fly ash generated from a selected low rank bituminous South African coal. Miner Eng 2005;18:299–310. doi:10.1016/j.mineng.2004.06.013.
- Mazzella A, Errico M, Spiga D. CO2 Uptake Capacity of Coal Fly Ash: Influence of Pressure and Temperature on Direct Gas-Solid Caronation. J Environ Chem Eng 2016;4:4120–8. doi:10.1016/j.jece.2016.09.020.
- McCarthy MJ, Dhir RK. Development of high volume fly ash cements for use in concrete construction. Fuel 2005;84:1423–32. doi:10.1016/j.fuel.2004.08.029.
- McKenzie, R.M. The Adsorption of Molybdenum on Oxide Surfaces. Aust. J. Soil Res. 1983, 21, 505–513.
- Meawad AS, Bojinova DY, Pelovski YG. An overview of metals recovery from thermal power plant solid waste. Waste Manag 2010;30:2548–59. doi:10.1016/j.wasman.2010.07.010.
- Mehta A, Siddique R. An overview of geopolymers derived from industrial by-products. Constr Build Mater 2016;127:183–98. doi:10.1016/j.conbuildmat.2016.09.136.
- Meng X feng, Li D hong, Shen X qian, Liu W. Preparation and magnetic properties of nano-Ni coated cenosphere composites. Appl Surf Sci 2010;256:3753–6. doi:10.1016/j.apsusc.2010.01.019.
- Mohammadinia A, Arulrajah A, Horpibulsuk S, Chinkulkijniwat A. Effect of fly ash on properties of crushed brick and reclaimed asphalt in pavement base/subbase applications. J Hazard Mater 2017;321:547–56. doi:10.1016/j.jhazmat.2016.09.039.
- Mohan S, Gandhimathi R. Removal of heavy metal ions from municipal solid waste leachate using coal fly ash as an adsorbent. J Hazard Mater 2009;169:351–9. doi:10.1016/j.jhazmat.2009.03.104.
- Monteiro RCC, Lima MMRA, Alves S. Mechanical characteristics of clay structural ceramics containing coal fly ash. Int J Mech Mater Des 2008;4:213–20. doi:10.1007/s10999-007-9049-8.
- Monteiro SN, Vieira CMF. On the production of fired clay bricks from waste materials: A critical update. Constr Build Mater 2014;68:599–610. doi:10.1016/j.conbuildmat.2014.07.006.
- Muñoz V. P, Morales O. MP, Letelier G. V, Mendívil G. MA. Fired clay bricks made by adding waste: Assessment of the impact on physical, mechanical and thermal properties. Constr Build Mater 2016;125:241–52. doi:10.1016/j.conbuildmat.2016.08.024.
- Muñoz Velasco, P.; Morales Ortíz, M.P.; Mendívil Giró, M.A.; Muñoz Velasco, L. Fired clay bricks manufactured by adding waste as sustainable construction material—A review. Constr. Build. Mater. 2014, 63, 97–107.
- Naganathan, S.; Mohamed, A.Y.O.; Mustapha, K.N. Performance of bricks made using fly ash and bottom ash. Constr. Build. Mater. 2015, 96, 576–580.
- Nath P, Sarker P. Effect of fly ash on the durability properties of high strength concrete. Procedia Eng 2011;14:1149–56. doi:10.1016/j.proeng.2011.07.144.

- Nayak N, Panda CR. Aluminium extraction and leaching characteristics of Talcher Thermal Power Station fly ash with sulphuric acid. Fuel 2010;89:53–8. doi:10.1016/j.fuel.2009.07.019.
- Nikolic I, Durovic D, Blecic D, Zejak R, Karanovic L, Mitsche S, et al. Geopolymerisation of coal fly ash in the presence of electric arc furnace dust. Miner Eng 2013;49:24–32. doi:10.1016/j.mineng.2013.04.007.
- Ogundiran MB, Nugteren HW, Witkamp GJ. Geopolymerisation of fly ashes with waste aluminium anodising etching solutions. J Environ Manage 2016;181:118–23. doi:10.1016/j.jenvman.2016.06.017.
- Ogundiran MB, Nugteren HW, Witkamp GJ. Immobilisation of lead smelting slag within spent aluminate-fly ash based geopolymers. J Hazard Mater 2013;248–249:29–36. doi:10.1016/j.jhazmat.2012.12.040.
- Olgun A, Erdogan Y, Ayhan Y, Zeybek B. Development of ceramic tiles from coal fly ash and tincal ore waste. Ceram Int 2005;31:153–8. doi:10.1016/j.ceramint.2004.04.007.
- Oner A, Akyuz S, Yildiz R. An experimental study on strength development of concrete containing fly ash and optimum usage of fly ash in concrete. Cem Concr Res 2005;35:1165–71. doi:10.1016/j.cemconres.2004.09.031.
- Ozcivici E, Singh RP. Fabrication and characterisation of ceramic foams based on silicon carbide matrix and hollow alumino-silicate spheres. J Am Ceram Soc 2005;88:3338–45. doi:10.1111/j.1551-2916.2005.00612.x.
- Ozola, R.; Krauklis, A.; Burlakovs, J.; Klavins, M.; Vincevica-Gaile, Z.; Hogland, W. Surfactant-Modified Clay Sorbents for the Removal of p-Nitrophenol. Clays Clay Miner. 2019, 67, 132–142.
- Pandey VC, Singh N. Impact of fly ash incorporation in soil systems. Agric Ecosyst Environ 2010;136:16–27. doi:10.1016/j.agee.2009.11.013.
- Pang J, Li Q, Wang W, Xu X, Zhai J. Preparation and characterisation of electroless Ni-Co-P ternary alloy on fly ash cenospheres. Surf Coatings Technol 2011;205:4237–42. doi:10.1016/j.surfcoat.2011.03.020.
- Panias D, Giannopoulou IP, Perraki T. Effect of synthesis parameters on the mechanical properties of fly ash-based geopolymers. Colloids Surfaces A Physicochem Eng Asp 2007;301:246–54. doi:10.1016/j.colsurfa.2006.12.064.
- Patrick N Lemougna, Wang Kai-tuo, Tang Qing, U Chinje Melo CX. Recent developments on inorganic polymers synthesis and applications Patrick. Ceram Int 2016;42:15142–59. doi:10.1016/j.ceramint.2016.07.027.
- Pedersen KH, Jensen AD, Skjøth-Rasmussen MS, Dam-Johansen K. A review of the interference of carbon containing fly ash with air entrainment in concrete. Prog Energy Combust Sci 2008;34:135–54. doi:10.1016/j.pecs.2007.03.002.
- Potgieter-Vermaak SS, Potgieter JH, Monama P, Van Grieken R. Comparison of limestone, dolomite and fly ash as pre-treatment agents for acid mine drainage. Miner Eng 2006;19:454–62. doi:10.1016/j.mineng.2005.07.009.
- Prakash K, Sridharan a. Beneficial Properties of Coal Ashes and Effective Solid Waste Management. Pract Period Hazardous, Toxic, Radioact Waste Manag 2009;13:239–48. doi:10.1061/(ASCE)HZ.1944-8376.0000014.
- Provis JL, Yong CZ, Duxson P, van Deventer JSJ. Correlating mechanical and thermal properties of sodium silicate-fly ash geopolymers. Colloids Surfaces A Physicochem Eng Asp 2009;336:57–63. doi:10.1016/j.colsurfa.2008.11.019.
- Pytal Z. Evaluation of potential applications of recycled moulding and core sands to production of ceramic building materials. Ceramics international 2014;40; 4351-8. doi 10.1016/j.ceramint.2013.08.104.

- Qiu W, Zheng Y. Arsenate removal from water by an alumina-modified zeolite recovered from fly ash. J Hazard Mater 2007;148:721–6. doi:10.1016/j.jhazmat.2007.03.038.
- Querol X, Moreno N, Umaa JC, Alastuey A, Hernández E, López-Soler A, et al. Synthesis of zeolites from coal fly ash: an overview. Int J Coal Geol 2002;50:413–23. doi:10.1016/S0166-5162(02)00124-6.
- Querol X, Umaña JC, Plana F, Alastuey A, Lopez-Soler A, Medinaceli A, et al. Synthesis of zeolites from fly ash at pilot plant scale. Examples of potential applications. Fuel 2001;80:857–65. doi:10.1016/S0016-2361(00)00156-3.
- Quijorna N., 2013. Incorporación de scoria Waeltz al sector cerámico: Ejemplo práctico de Ecología Industrial. Tesis Doctoral. Directora Ana Andrés. Universidad de Cantabria.
- Quijorna, N.; Coz, A.; Andres, A.; Cheeseman, C. Recycling of Waelz Slag and Waste Foundry Sand in Red Clay Bricks. Resour. Conserv. Recycl. 2012, 65, 1–10.
- Quijorna, N.; Miguel, G.S.S.; Andrés, A. Incorporation of Waelz Slag into Commercial Ceramic Bricks: A Practical Example of Industrial Ecology. Ind. Eng. Chem. Res. 2011, 50, 5806–5814.
- Ram LC, Masto RE. An appraisal of the potential use of fly ash for reclaiming coal mine spoil. J Environ Manage 2010;91:603–17. doi:10.1016/j.jenvman.2009.10.004.
- Ram LC, Masto RE. Fly ash for soil amelioration: A review on the influence of ash blending with inorganic and organic amendments. Earth-Science Rev 2014;128:52–74. doi:10.1016/j.earscirev.2013.10.003.
- Reiner M, Rens K. High-Volume Fly Ash Concrete: Analysis and Application. Pract Period Struct Des Constr 2006;11:58–64. doi:10.1061/(ASCE)1084-0680(2006)11:1(58).
- Rickard WDA, Williams R, Temuujin J, van Riessen A. Assessing the suitability of three Australian fly ashes as an aluminosilicate source for geopolymers in high temperature applications. Mater Sci Eng A 2011;528:3390–7. doi:10.1016/j.msea.2011.01.005.
- Ríos R. CA, Williams CD, Roberts CL. A comparative study of two methods for the synthesis of fly ash-based sodium and potassium type zeolites. Fuel 2009;88:1403–16. doi:10.1016/j.fuel.2009.02.012.
- Robert M. Dilmore RDN. AUTOCLAVED AERATED CONCRETE PRODUCED WITH LOW NOx BURNER/SELECTIVE CATALYTIC REDUCTION FLY ASH. J Energy Eng 2001;127:37–50.
- Rohatgi PK, Matsunaga T, Gupta N. Compressive and ultrasonic properties of polyester/fly ash composites. J Mater Sci 2009;44:1485–93. doi:10.1007/s10853-008-3165-1.
- Romero, M., Andrés, A., Alonso, R., Viguri, J., Rincón, J.M. Sintering behaviour of ceramic bodies from contaminated marine sediments. Ceramics International, 34(8): 1917-1924.
- Romero, M.; Pérez, J.M. Relation between the microstructure and technological properties of porcelain stoneware. A review. Mater. Constr. 2015, 65, e065.
- Rubel A, Andrews R, Gonzalez R, Groppo J, Robl T. Adsorption of Hg and NOX on coal by-products. Fuel 2005;84:911–6. doi:10.1016/j.fuel.2005.01.006.
- Rubio B, Izquierdo MT, Mayoral MC, Bona MT, Andres JM. Unburnt carbon from coal fly ashes as a precursor of activated carbon for nitric oxide removal. J Hazard Mater 2007;143:561–6. doi:10.1016/j.jhazmat.2006.09.074.
- Rubio B, Izquierdo MT. Coal fly ash based carbons for SO2 removal from flue gases. Waste Manag 2010;30:1341–7. doi:10.1016/j.wasman.2010.01.035.
- Sahoo PK, Kim K, Powell MA, Equeenuddin SM. Recovery of metals and other beneficial products from coal fly ash: a sustainable approach for fly ash management. Int J Coal Sci Technol 2016;3:267–83. doi:10.1007/s40789-016-0141-2.

- Saputra E, Muhammad S, Sun H, Ang HM, Tadé MO, Wang S. Red mud and fly ash supported Co catalysts for phenol oxidation. Catal Today 2012;190:68–72. doi:10.1016/j.cattod.2011.10.025.
- Saravanan G, Jeyasehar CA, Kandasamy S. Flyash Based Geopolymer Concrete – A State of the Art Review. J Eng Sci Technol Rev 2013;6:25–32.
- Sarker P, McKenzie L. Strength and Hydration Heat of Concrete using Fly Ash as a Partial Replacement of Cement Concrete Solutions 09 Paper 2c-3. Concr Solut 09, 24th Bienn Conf Concr Inst Aust 2009:1–9.
- Sena da Fonseca B, Galhano C, Seixas D. Technical feasibility of reusing coal combustion by-products from a thermoelectric power plant in the manufacture of fired clay bricks. Appl Clay Sci 2015;104:189–95. doi:10.1016/j.clay.2014.11.030.
- Sena Da Fonseca, B.; Vilão, A.; Galhano, C.; Simão, J.A.R. Reusing coffee waste in manufacture of ceramics for construction. Adv. Appl. Ceram. 2014, 113, 159–166.
- Shaheen SM, Hooda PS, Tsadilas CD. Opportunities and challenges in the use of coal fly ash for soil improvements - A review. J Environ Manage 2014;145:249–67. doi:10.1016/j.jenvman.2014.07.005.
- Sharif, N.M.; Lim, C.Y.; Teo, P.T.; Seman, A.A. Effects of body formulation and firing temperature to properties of ceramic tile incorporated with electric arc furnace (EAF) slag waste. AIP Conf. Proc. 2017, 1865, 1–7.
- Shemi A, Mpana RN, Ndlovu S, Van Dyk LD, Sibanda V, Seepe L. Alternative techniques for extracting alumina from coal fly ash. Miner Eng 2012;34:30–7. doi:10.1016/j.mineng.2012.04.007.
- Shi C, Jiménez AF, Palomo A. New cements for the 21st century: The pursuit of an alternative to Portland cement. Cem Concr Res 2011;41:750–63. doi:10.1016/j.cemconres.2011.03.016.
- Shi XS, Collins FG, Zhao XL, Wang QY. Mechanical properties and microstructure analysis of fly ash geopolymeric recycled concrete. J Hazard Mater 2012;237–238:20–9. doi:10.1016/j.jhazmat.2012.07.070.
- Simate GS, Maledi N, Ochieng A, Ndlovu S, Zhang J, Walubita LF. Coal-based adsorbents for water and wastewater treatment. J Environ Chem Eng 2016;4:2291–312. doi:10.1016/j.jece.2016.03.051.
- Singh, I.B.; Chaturvedi, K.; Morchhale, R.K.; Yegneswaran, A.H. Thermal Treatment of Toxic Metals of Industrial Hazardous Waste with Fly Ash and Clay. J. Hazard. Mater. 2007, 141, 215–222.
- Sokolar R, Smetanova L. Dry pressed ceramic tiles based on fly ash – clay body : Influence of fly ash granulometry and pentasodium triphosphate addition. Water 2010;36:215–21. doi:10.1016/j.ceramint.2009.07.009.
- Sokolar R, Vodova L. The effect of fluidized fly ash on the properties of dry pressed ceramic tiles based on fly ash-clay body. Ceram Int 2011;37:2879–85. doi:10.1016/j.ceramint.2011.05.005.
- Somerset V, Petrik L, Iwuoha E. Alkaline hydrothermal conversion of fly ash precipitates into zeolites 3: The removal of mercury and lead ions from wastewater. J Environ Manage 2008;87:125–31. doi:10.1016/j.jenvman.2007.01.033.
- Somna K, Jaturapitakkul C, Kajitvichyanukul P, Chindaprasirt P. NaOH-activated ground fly ash geopolymer cured at ambient temperature. Fuel 2011;90:2118–24. doi:10.1016/j.fuel.2011.01.018.
- Souza, V.P.; Toledo, R.; Holanda, J.N.F.; Vargas, H.; Faria, R.T. Pollutant Gas Analysis Evolved during Firing of Red Ceramic Incorporated with Water Treatment Plant Sludge. Ceramica 2008, 54, 351–355.

- Suárez-Ruiz I, Hower JC, Thomas GA. Hg and Se capture and fly ash carbons from combustion of complex pulverized feed blends mainly of anthracitic coal rank in Spanish power plants. Energy and Fuels 2007;21:59–70. doi:10.1021/ef0603481.
- Sukmak P, Horpibulsuk S, Shen SL, Chindaprasirt P, Suksiripattanapong C. Factors influencing strength development in clay-fly ash geopolymer. Constr Build Mater 2013;47:1125–36. doi:10.1016/j.conbuildmat.2013.05.104.
- Sukmak, P., S. Horpibulsuk and S-LS. Strength development in clay–fly ash geopolymer 2013;40:566–74. doi:10.1016/j.conbuildmat.2012.11.015.
- Surolia PK, Tayade RJ, Jasra R V. TiO2-coated cenospheres as catalysts for photocatalytic degradation of methylene blue, p-nitroaniline, n-decane, and n-tridecane under solar irradiation. Ind Eng Chem Res 2010;49:8908–19. doi:10.1021/ie100388m.
- Sutcu, M.; Erdogmus, E.; Gencel, O.; Gholampour, A.; Atan, E.; Ozbakkaloglu, T. Recycling of bottom ash and fly ash waste in eco-friendly clay brick production. J. Clean. Prod. 2019, 233, 753–764.
- Tanaka H, Fujii A, Fujimoto S, Tanaka Y. Microwave-Assisted Two-Step Process for the Synthesis of a Single-Phase Na-A Zeolite from Coal Fly Ash. Adv Powder Technol 2008;19:83–94. doi:http://dx.doi.org/10.1163/156855208X291783.
- Tanaka H, Fujii A. Effect of stirring on the dissolution of coal fly ash and synthesis of pure-form Na-A and -X zeolites by two-step process. Adv Powder Technol 2009;20:473–9. doi:10.1016/j.apt.2009.05.004.
- Tao H, Yao J, Zhang L, Xu N. Preparation of magnetic ZSM-5/Ni/fly-ash hollow microspheres using fly-ash cenospheres as the template. Mater Lett 2009;63:203–5. doi:10.1016/j.matlet.2008.09.034.
- Uaciquete, D.L.E.; Sakusabe, K.; Kato, T.; Okawa, H.; Sugawara, K.; Nonaka, R. Influence of unburned carbon on mercury chemical forms in fly ash produced from a coal-fired power plant. Fuel 2021, 300, 120802.
- Ukwatta A, Mohajerani A, Setunge S, Eshtiaghi N. A study of gas emissions during the firing process from bricks incorporating biosolids. Waste Manag 2018; 74; 413-426. Doi: 10.1016/j.wasman.2018.01.006.
- Vasic´, M.V.; Goel, G.; Vasic´, M.; Radojevic´, Z. Recycling of Waste Coal Dust for the Energy-Efficient Fabrication of Bricks: A Laboratory to Industrial-Scale Study. Environ. Technol. Innov. 2021, 21, 101350.
- Vassilev, S.V.; Baxter, D.; Andersen, L.K.; Vassileva, C.G. An Overview of the Composition and Application of Biomass Ash. Part 1. Phase–Mineral and Chemical Composition and Classification. Fuel 2013, 105, 40–76.
- Vecor Australia Pty Ltd. Company Profile/Rozelle, New South Wales, Australia/Competitors, Financials & Contacts—Dun & Bradstreet. Available online: https://www.dnb.com/business-directory/company-profiles.vecor_australia_pty_ltd.aefefd25a2d9 ed847d91b85bf5085cfc.html (accessed on 20 March 2021).
- Vincevica-gaile, Z.; Teppand, T.; Kriipsalu, M.; Krievans, M.; Jani, Y.; Klavins, M.; Hendroko Setyobudi, R.; Grinfelde, I.; Rudovica, V.; Tamm, T.; et al. Towards Sustainable Soil Stabilisation in Peatlands: Secondary Raw Materials as an Alternative. Sustainability 2021, 13, 6726.
- Visa M, Duta A. Methyl-orange and cadmium simultaneous removal using fly ash and photo-Fenton systems. J Hazard Mater 2013;244–245:773–9. doi:10.1016/j.jhazmat.2012.11.013.
- Vsévolod M, Alekseev K, Catai RE, Nagalli A, Aibuldinov YK, Bekturganov NS, Rose JL, Izzo RLS. Red ceramics from composites of hazardous sludge with foundry sand, glass waste

and acid neutralisation salts. J Env Chem Eng 2016; 4; 753-761. Doi: 10.1016/j.jece.2015.07.015.

- Wałek TT, Saito F, Zhang Q. The effect of low solid/liquid ratio on hydrothermal synthesis of zeolites from fly ash. Fuel 2008;87:3194–9. doi:10.1016/j.fuel.2008.06.006.
- Wang B, Li Q, Wang W, Li Y, Zhai J. Preparation and characterisation of Fe3+-doped TiO2 on fly ash cenospheres for photocatalytic application. Appl Surf Sci 2011;257:3473–9. doi:10.1016/j.apsusc.2010.11.050.
- Wang S, Terdkiatburana T, Tadé MO. Single and co-adsorption of heavy metals and humic acid on fly ash. Sep Purif Technol 2008;58:353–8. doi:10.1016/j.seppur.2007.05.009.
- Wang S, Zhang Y, Gu Y, Wang J, liu Z, Zhang Y, et al. Using modified fly ash for mercury emissions control for coal-fired power plant applications in China. Fuel 2016;181:1230–7. doi:10.1016/j.fuel.2016.02.043.
- Wang S. Application of Solid Ash Based Catalysts in Heterogeneous Catalysis. Environ Sci Technol 2008;42:7055–63. doi:10.1021/es801312m.
- Wang Y, Tsang DCW. Effects of solution chemistry on arsenic(V) removal by low-cost adsorbents. J Environ Sci (China) 2013;25:2291–8. doi:10.1016/S1001-0742(12)60296-4.
- Wang, L.; Sun, H.; Sun, Z.; Ma, E. New Technology and Application of Brick Making with Coal Fly Ash. J. Mater. Cycles Waste Manag. 2016, 18, 763–770.
- Wasekar PA, Kadam PG, Mhaske ST. Effect of Cenosphere Concentration on the Mechanical, Thermal, Rheological and Morphological Properties of Nylon 6. J Miner Mater Charact Eng 2012;11:807–12.
- Wei Y, Cheng S, Ko G. Effect of waste glass addition on lightweight aggregates prepared from F-class coal fly ash. Constr Build Mater 2016;112:773–82. doi:10.1016/j.conbuildmat.2016.02.147.
- Winnefeld F, Leemann A, Lucuk M, Svoboda P, Neuroth M. Assessment of phase formation in alkali activated low and high calcium fly ashes in building materials. Constr Build Mater 2010;24:1086–93. doi:10.1016/j.conbuildmat.2009.11.007.
- Wu CY, Yu HF, Zhang HF. Extraction of aluminum by pressure acid-leaching method from coal fly ash. Trans Nonferrous Met Soc China (English Ed 2012;22:2282–8. doi:10.1016/S1003-6326(11)61461-1.
- Xu H, Gong W, Syltebo L, Izzo K, Lutze W, Pegg IL. Effect of blast furnace slag grades on fly ash based geopolymer waste forms. Fuel 2014;133:332–40. doi:10.1016/j.fuel.2014.05.018.
- Xu X, Li Q, Cui H, Pang J, Sun L, An H, et al. Adsorption of fluoride from aqueous solution on magnesia-loaded fly ash cenospheres. Desalination 2011;272:233–9. doi:10.1016/j.desal.2011.01.028.
- Xu, G.; Shi, X. Characteristics and Applications of Fly Ash as a Sustainable Construction Material: A State-of-the-Art Review. Resour. Conserv. Recycl. 2018, 136, 95–109.
- Xuan X, Yue C, Li S, Yao Q. Selective catalytic reduction of NO by ammonia with fly ash catalyst. Fuel 2003;82:575–9. doi:10.1016/S0016-2361(02)00321-6.
- Yang F, Hlavacek V. Recycling of carbon-enriched coal fly ash. Powder Technol 1999;104:190–5. doi:10.1016/S0032-5910(99)00040-6.
- Yang J, Liu W, Zhang L, Xiao B. Preparation of load-bearing building materials from autoclaved phosphogypsum. Constr Build Mater 2009;23:687–93. doi:10.1016/j.conbuildmat.2008.02.011.
- Yao S.T., Ji X.S., Sarker P.K., Tang J.H., Ge L.Q., Xia M.S., Xi Y.Q. A comprehensive review on the applications of coal fly ash. Earth-Science Reviews. 141, 105-121.
- Yao ZT, Xia MS, Sarker PK, Chen T. A review of the alumina recovery from coal fly ash, with a focus in China. Fuel 2014;120:74–85. doi:10.1016/j.fuel.2013.12.003.

- Yao ZT, Xia MS, Ye Y, Zhang L. Synthesis of zeolite Li-ABW from fly ash by fusion method. J Hazard Mater 2009;170:639–44. doi:10.1016/j.jhazmat.2009.05.018.
- Yu X, Shen Z, Xu Z. Preparation and characterisation of Ag-coated cenospheres by magnetron sputtering method. Nucl Instruments Methods Phys Res Sect B Beam Interact with Mater Atoms 2007;265:637–40. doi:10.1016/j.nimb.2007.10.013.
- Yu Y. Preparation of nanocrystalline TiO2-coated coal fly ash and effect of iron oxides in coal fly ash on photocatalytic activity. Powder Technol 2004;146:154–9. doi:10.1016/j.powtec.2004.06.006.
- Yunusa IAM, Eamus D, DeSilva DL, Murray BR, Burchett MD, Skilbeck GC, et al. Fly-ash: An exploitable resource for management of Australian agricultural soils. Fuel 2006;85:2337–44. doi:10.1016/j.fuel.2006.01.033.
- Zaharia C, Suteu D. Coal fly ash as adsorptive material for treatment of a real textile effluent: Operating parameters and treatment efficiency. Environ Sci Pollut Res 2013;20:2226–35. doi:10.1007/s11356-012-1065-z.
- Zanelli, C.; Conte, S.; Molinari, C.; Soldati, R.; Dondi, M. Waste recycling in ceramic tiles: A technological outlook. Resour. Conserv. Recycl. 2021, 168, 105289.
- Zeng S, Wang J. Characterisation of mechanical and electric properties of geopolymers synthesized using four locally available fly ashes. Constr Build Mater 2016;121:386–99. doi:10.1016/j.conbuildmat.2016.06.011.
- Zhai M, Guo L, Sun L, Zhang Y, Dong P, Shi W. Desulphurisation performance of fly ash and CaCO3 compound absorbent. Powder Technol 2017;305:553–61. doi:10.1016/j.powtec.2016.10.021.
- Zhang A, Wang N, Zhou J, Jiang P, Liu G. Heterogeneous Fenton-like catalytic removal of p-nitrophenol in water using acid-activated fly ash. J Hazard Mater 2012;201–202:68–73. doi:10.1016/j.jhazmat.2011.11.033.
- Zhang J, Provis JL, Feng D, van Deventer JSJ. Geopolymers for immobilisation of Cr6+, Cd2+, and Pb2+. J Hazard Mater 2008;157:587–98. doi:10.1016/j.jhazmat.2008.01.053.
- Zhang T, Gao P, Gao P, Wei J, Yu Q. Effectiveness of novel and traditional methods to incorporate industrial waste in cementitious materials - An overview. Resour Conserv Recycl 2013;74:134–43. doi:10.1016/j.resconrec.2013.03.003.
- Zhang, Z.; Wong, Y.C.; Arulrajah, A.; Horpibulsuk, S. A Review of Studies on Bricks Using Alternative Materials and Approaches. Constr. Build. Mater. 2018, 188, 1101–1118.
- Zhou L, Chen YL, Zhang XH, Tian FM, Zu ZN. Zeolites developed from mixed alkali modified coal fly ash for adsorption of volatile organic compounds. Mater Lett 2014;119:140–2. doi:10.1016/j.matlet.2013.12.097.
- Zhu F, Takaoka M, Oshita K, Kitajima Y, Inada Y, Morisawa S, et al. Chlorides behaviour in raw fly ash washing experiments. J Hazard Mater 2010;178:547–52. doi:10.1016/j.jhazmat.2010.01.119.
- Zhuang XY, Chen L, Komarneni S, Zhou CH, Tong DS, Yang HM, et al. Fly ash-based geopolymer: Clean production, properties and applications. J Clean Prod 2016;125:253–67. doi:10.1016/j.jclepro.2016.03.019.
- Zimmer A, Bergmann CP. Fly ash of mineral coal as ceramic tiles raw material. Waste Manag 2007;27:59–68. doi:10.1016/j.wasman.2006.01.009.

Chapter 3.

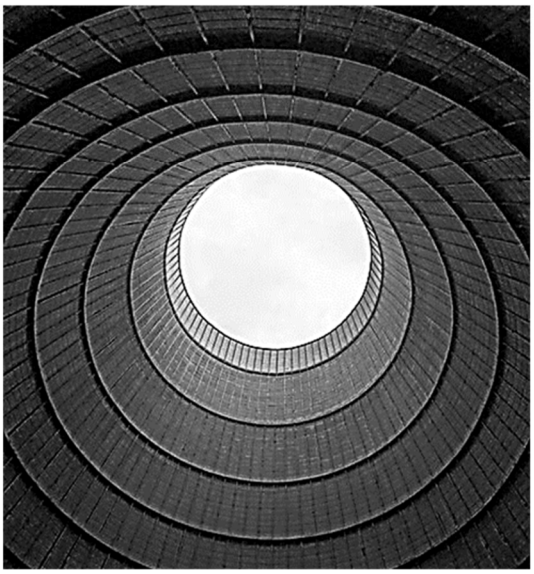

Coal combustion ashes in low energy clay ceramic process

3. Pulverized Coal Combustion Ashes in Low Energy Clay Ceramic Process

Nowadays, the great challenge in the construction industry focuses on the use of the new alkali-activated cement (AACs) or geopolymers. These "new alternative materials" can be manufactured totally without Portland cement. The AACs have based on a silico-aluminous precursor which in many cases are the same as those used as supplementary materials in mortars and concretes with cement substitution. Such is the case of metakaolin, fly ash, or granulated blast furnace slag (Pacheco Torgal 2008, Palomo 1999).

The European Commission has adopted an ambitious new Circular Economy Package with Horizon 2020. The focused development will contribute to "closing the loop" of production lifecycles through recycling and re-use. The proposed actions will extract the maximum value and use from raw materials, by-products and waste. In this context, the great goal in the AACs manufacture is the use of residual materials from various sources.

The waste valorisation makes to convert it into raw material, and the components of a product are planned so that they can be dismantled and reconverted into another cycle. This implies developing materials and products that serve in other systems, can be reused, and be not dangerous.

More than 4,500 articles were published about AACs during the period 2018-2020. In most of them, it is used residual materials. The literature identifies a broad spectrum of industrial, mining, and agroforestry by-products or waste and a series of aluminosilicate minerals as precursors such as volcanic ash, natural pozzolans, and similar (Robayo-Salazar et al., 2019). Among the waste found in the literature, the following have been used in the formulations of AACs: silicomanganese slag, residual sludge from obtaining alumina (red sludge) (Li et al., 2019; Nguyen et al., 2022), ashes from the combustion of rice husks (Fongang et al., 2015; Kamseu et al., 2015), tailings from the extraction of metals (Ahmari et al., 2014; Ren et al., 2015), palm oil ashes (Salami et al. 2016; Khankaje et al., 2016), waste from the ceramic industry (Keppert et al., 2018) and the glass industry (Manikandan et al., 2022), etc. However, the raw materials or by-products more extended studied are metakaolin, blast furnace slag (BFS), and coal fly ash (CFA). The metakaolin (MK) is studied in several papers (Favier et al., 2014; He et al., 2020; Liu et al., 2021). This precursor and the binary mixtures with other materials let to obtain geopolymers with high compressive strength and good durability properties (Ozer et al., 2015). BFS has been used as the only precursor and as a mixture with other materials (Bakharev et al., 2000). The

principal advantage of BFS is that it can be used with alkaline solutions with lesser alkalinity.

Finally, CFA is another of the most widely used materials in the production of AACs. The main reaction product formed in the alkali activation of CFA is an amorphous, three-dimensional alkaline inorganic polymer known as N-A-S-H (Fernández-Jiménez et al; 2019). Secondary reaction products may include zeolites such as Na-chabazite, zeolites A and P and faujasite (Fernández-Jiménez and Palomo 2005; Panias et al., 2007). Alkali activation of low calcium CFA is a complex process with multiple parameters being involved simultaneously. The kinetics of alkali activation depends on the chemical, mineral, and phase composition of fly ash, the fineness of CFA, the type and concentration of alkaline activator, and the curing temperature (Shekhovtsova et al., 2018). (Fernández-Jiménez and Palomo, 2003) reported that the percentage of unburned material, amount of reactive silica, particle size distribution, and content of vitreous phase in CFA are the most important factors influencing geopolymerisation, which is supported by (Soutsos et al., 2016) who noted as well the importance of average grain size of CFA.

3.1. Feasibility of Alkaline By-Products as Activator in CFA-Clay Bricks

The alkaline activator is an important part of the AACs. Usually, the caustic solution or alkaline salts have the function of accelerating the solubilisation of the precursor and allowing the formation of stable hydrates. The hydroxides and silicates of sodium and potassium are the most employed activators. In some cases, alkaline carbonates are also employed. The cation selected is a fundamental factor, since it affects all the steps of the alkaline activation process. Another important factor is the concentration of the activator. A greater concentration produces a major solubility and consequently greater mechanical behaviour. Nevertheless, Palomo et al. reported the existence of an optimal concentration (Palomo et al.,1999).

Activators have specific technological implications insofar as they may be used in liquid or solid form, a fact of significant environmental and economic consequence. Most studies, conducted with liquid hydroxide or alkaline salt activators mixed with a solid precursor, pursue aims relating to OH^- concentration, type of alkaline cation, or SiO_2/Na_2O (Palomo et al., 2021). Although the type most commonly used in laboratory, liquid activators may pose industrial-scale problems, as they are viscous, corrosive, hazardous, and expensive and therefore applicable to very specific construction scenarios.

Furthermore, sodium silicate has been extensively used as an alkaline activator in AAC and geopolymer concrete, since it generally results in the highest mechanical

strength development along with reduced permeability. This means, AACs with a more stable and dense structure (Tong et al., 2018). However, the use of sodium silicate markedly increases the embodied energy and CO_2 emissions associated with AACs, as a consequence of its manufacturing process. This typically involves the calcination of sodium carbonate (Na_2CO_3) and quartz sand (SiO_2) at temperatures between 1400 and 1500 °C (Tong et al., 2018; Palomo et al., 2021), generating CO_2 from the decomposition of Na_2CO_3 and from fuel used to reach these high temperatures (Fawer et al., 1999). The process is also expensive due to its energy consumption. The activating solution is the component that has a larger carbon footprint in AACs, mainly, when sodium or potassium silicates are used (Mellado 2014, Passuello 2017). The sodium silicate synthesis produces around 1.2 kg of CO_2 per kg of sodium silicate. This number represents 70-90 % of the total emission associated with the activating solution. Other authors rejected geopolymers as an environmentally friendly solution due to a significant negative influence of other impact categories, such as abiotic depletion, acidification, eutrophication, and human toxicity, which were increased particularly due to the amount of used alkaline activators (Habert et al., 2011; Turner and Collins, 2013; Fort et al., 2018).

In recent years, new alternative alkaline activators are produced. These new alkaline activators can be classified into two types: those in which a part of the synthetic products is replaced by a waste and those in which no synthetic products are employed. The carbon footprint of alkali hydroxides is lower than that for alkali silicates, by this reason many research groups are investigating the use of alternative silica sources to obtain a replacement for the silicate commercial one. These silica sources are rice husk ash, diatomaceous earth residues, glass waste, sugarcane straw ash, and silica fume among others (Passuello et al., 2017; Torres- Carrasco et al. 2015; Torres-Carrasco and Puertas, 2015). The development of alternative activators with reduced CO_2 footprint and thus better sustainability credentials, when used for geopolymer concrete, is therefore much desired and can lead to a significant reduction in the global warming potential of AACs.

The main objective of this study is to identify which alkaline by-products are suitable to replace sodium hydroxide or sodium silicate which form the activating solution of the source of aluminosilicate and prove how these substitutions influence flexural strength and water absorption in geopolymers. Flexural strength and water absorption were performed in quadruplicate and the equilibrium leaching test in triplicate.

3.1.1. Materials and Methodology

3.1.1.1. Activating Solutions from Alkaline By-products

Alkaline Activator, the most common activating compounds may be alkali or alkaline earth hydroxides such as (ROH, $R(OH)_2$), weak acid salts (R_2CO_3, R_2S, RF), strong acid salts (Na_2SO_4, $CaSO_4.2H_2O$) and silicic salts of the type $R_2O(n)SiO_2$ wherein R is an alkali ion of Na, K or Li type. In this regard, in this work hydroxide and sodium silicate were used. NaOH is pelleting with a purity of 99 %, while Na_2SiO_3 has a modulus SiO_2/Na_2O of 1.25.

The by-products from SOLVAY process, were classified into 2 types according to their state of aggregation, liquid and solid. In addition, the solid was divided into three classes according to their morphology: Powder with a diameter of less than 45 μm particle size, rocks with a much higher particle, and mud due to its high moisture.

- Liquid alkaline by-products:

Ca and Mg Slurry and CaO Slurry are whitish because they have solid white particles suspended, although the slurry of Ca and Mg is whiter than the slurry of CaO, as shown in Figure 3.1.

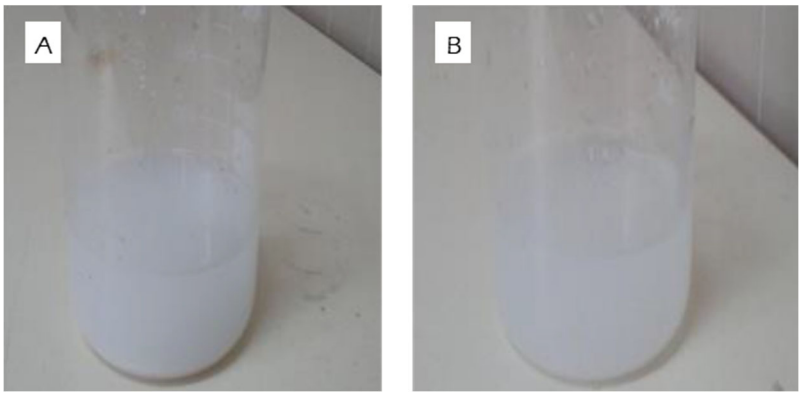

Figure 3.1. Ca and Mg Slurry (A), and CaO Slurry (B).

- Solid alkaline by-products:

a) Powder with a diameter of less than 45 μm particle size. In this group is sodium carbonate with a purity of 90 % and sodium bicarbonate also with a purity of 90 %. Both are white odourless Powders being very difficult to distinguish with the naked eye as seen in Figure 3.2.

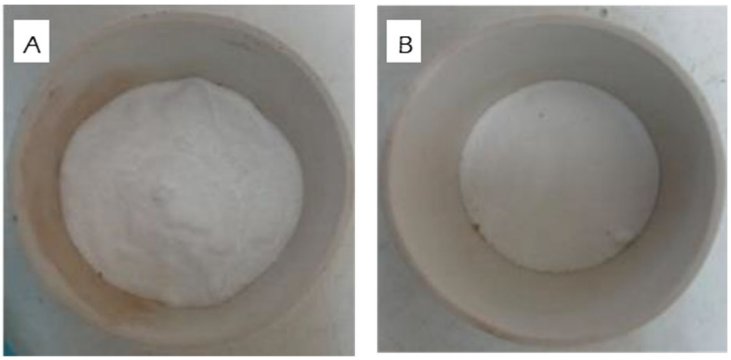

Figure 3.2. Na_2CO_3 Powder (A), and $HNaCO_3$ Powder (B).

b). Rocks. CaO rocks are crushed to obtain the required particle size for incorporation into the alkali-activation process. The required particle size is less than 1mm. In Figure 3.3, CaO rocks before and after crushing.

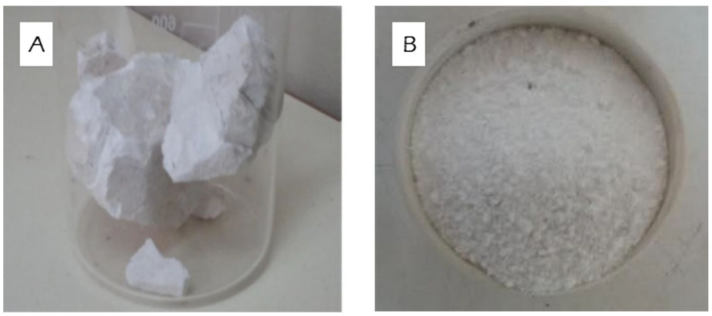

Figure 3.3. CaO rocks before (A), and after crushing (B).

c). Sludge: The Si-$CaCO_3$-$Ca(OH)_2$ is considered a Sludge due to its high moisture content which causes the particles join one with others forming larger particles, as seen in Figure 3.4. A drying process is necessary to reduce the moisture content and can mould the geopolymer in the hydraulic press.

Figure 3.4. Si-$CaCO_3$-$Ca(OH)_2$ Sludge.

3.1.1.2. Alkali-Activated Bricks processing

The design of experiments and the steps followed in the laboratory to obtain alkali-activated products by pressing are presented.

Design of Experiments

Considering other work done in the Department of Chemical and Process Engineering and Resources will consider the following formulation as the reference alkali-activated product. This reference alkali-activated product has the following relationships: fly ash/clay = 0.7, [NaOH] = 6M and Na_2SiO_3/NaOH = 0.4. It is working with a temperature and cure time of 75 °C and 48h. Four replications for every one of the properties measured have been done. Table 3.1 shows the formulations carried out in the laboratory of the Department of Chemical and Process Engineering and Resources at the University of Cantabria to study the feasibility of introducing alkaline by-products in the production of alkali-activated products.

Bricks by Pressing

The clay is subjected to a grinding process to achieve a particle size exceeding 0.5 mm. Then we proceed to the mixture of raw materials for 10 minutes, Fly Ash and Clay, with a laboratory mixer Raimondi, Iperbet model. The proportions of raw materials are calculated by weight. While the fly ash-clay mixture is carried out, the solution containing sodium hydroxide, sodium silicate, distilled water, and alkaline by-products is prepared. The proportions of raw materials are calculated by weight. Commercial alkaline activator (NaOH and/or Na2SiO3) was replaced by a 10 % -30 % -50 %-70 % and even 100 % of alkaline by-products.

At the time which the ten minutes of mixing (clay-fly ash) have passed and the solution was made, it is added with a pipette the solution onto the clay-ash mixture. The next step consists in mixing at least five minutes of the indicated components (clay, fly ash, and dissolution). Once the mixture of raw materials was done, we proceed to mould by pressing. To this end, a hydraulic press Nanetti Mignon model SS/EA, which reaches 200 bar pressure, was used. The mould used is prismatic 80x40x20 mm.

The samples are pre-cured for 24 hours at room temperature before the cooking cycle. A laboratory muffle furnace Hobersal, PR Model 12/300 capable of ramps temperature versus time of up to 16 points was used. The temperature of work is 75 ºC and the technological and environmental properties are measured after 7 days of curing.

Table 3.1. Design of formulations using alkaline by-products.

Fly Ash/Clay Bricks							
Substitution of NaOH commercial							
Sample	% NaOH Replaced	NaOH (g)	Na_2SiO_3 (g)	H_2O(g)	CFA (g)	Clay (g)	Alkaline by-products (g)
S1	-	17.45	35.3	64.14	205.9	294.1	0
S2	10	15.7	35.3	57.73	205.9	294.1	1.75
S3	30	12.22	35.3	45	205.9	294.1	5.24
S4	50	8.73	35.3	32.07	205.9	294.1	8.73
Substitution of Na_2SiO_3 commercial							
Sample	% Na_2SiO_3 Replaced	NaOH (g)	Na_2SiO_3 (g)	H_2O(g)	CFA (g)	Clay (g)	Alkaline by-products (g)
S5	10	17.45	31.77	64.14	205.9	294.1	3.53
S6	30	17.45	24.71	64.14	205.9	294.1	10.59
S7	50	17.45	17.65	64.14	205.9	294.1	17.65
Fly Ash Bricks							
Substitution of NaOH commercial							
Sample	% NaOH Replaced	NaOH (g)	Na_2SiO_3 (g)	H_2O(g)	CFA (g)	Clay (g)	Alkaline by-products (g)
S1	-	17.45	35.3	64.14	500	-	0
S2	10	15.7	35.3	57.73	500	-	1.75
S3	30	12.22	35.3	45	500	-	5.24
S4	50	8.73	35.3	32.07	500	-	8.73
Substitution of Na_2SiO_3 commercial							
Sample	% Na_2SiO_3 Replaced	NaOH (g)	Na_2SiO_3 (g)	H_2O(g)	CFA (g)	Clay (g)	Alkaline by-products (g)
S5	10	17.45	31.77	64.14	500	-	3.53
S6	30	17.45	24.71	64.14	500	-	10.59
S7	50	17.45	17.65	64.14	500	-	17.65

3.1.1.3. Characterisation of Alkali-Activated CFA-Clay based Bricks

The leaching behaviour of the materials was determined by the compliance leaching standard test UNE-EN 12457-2 using an L/S ratio=10, which simulates the conditions of an open landfill. The leachates were analysed to determine the leachate pH and the concentration of contaminants using inductively coupled plasma-collision cell mass (ICP-MS) in a Perkin Elmer Plasma, model Plasma 400. The contaminants under study are the following: As, Ba, Cd, Cr, Cu, Hg, Mo, Ni, Pb, Sb, Se, and Zn.

The technological properties measured in this work were water absorption and flexural strength. For alkali-activated bricks, the technological assessed were flexural strength and water absorption. Norms and the methods used in the study of technological properties are shown in Table 3.2.

Table 3.2. Norms and methods used to assess the technological properties of the alternative ceramics.

Technological Property	Norm	Method
Water absorption	(UNE EN 772-11, 2011)	Water immersion
Flexural strength	(UNE-EN 843-1, 1996)	Electronic Universal Tester

3.1.2. Results of Feasibility of using Alkaline By-Products in CFA-Clay based Bricks

The main objective of this study is to identify which alkaline by-products are suitable to replace sodium hydroxide or sodium silicate which form the activating solution of the source of aluminosilicate and prove how these substitutions influence flexural strength and water absorption in geopolymers. Flexural strength and water absorption were performed in quadruplicate and the equilibrium leaching test in triplicate.

3.1.2.1. Technological Properties

Physical Properties

Visual Appearance: Increasing the amount of alkaline by-products polymers become more whitish. Because these by-products were white Powder or liquids with suspended white particles as shown in Figure 3.5. Geopolymer bricks using Ca-Si-$CaCO_3(OH)_2$ Sludge and CaO rocks present cracks due to expansion in bricks.

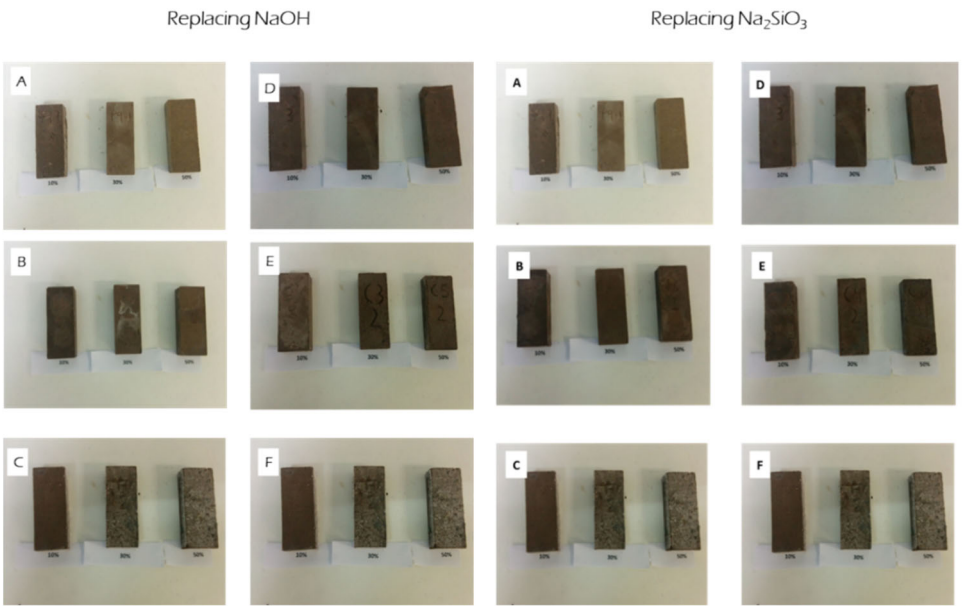

Figure 3.5. Geopolymers formation with $NaOH/Na_2SiO_3$ substitution of the following alkaline by-products: Ca and Mg Slurry (A), $HNaCO_3$ Powder (B), Ca-Si-$CaCO_3(OH)_2$ Sludge (C), CaO Slurry (D), Na_2CO_3 Powder (E), CaO Rocks (F).

Water Absorption: The specific absorption of bricks is the percentage of water absorbed in the assay expressed to the relative of dried brick. This rule was made for the determination of water absorption on the bricks used in construction, specified

in the UNE 67-019. The results of average water absorption and standard deviation are shown in Table A.6.1 and Table A.6.2 of Annex 6. The results of water absorption of geopolymers in which NaOH and Na_2SiO_3 have been replaced by the different alkaline by-products are shown in Figure 3.6(a)-(d). Four replications of water absorption have been done.

As shown in Figure 3.6(a)-(d), it can be seen how the water absorption decreases as increases the percentage of alkaline by-products is introduced for both types of geopolymers. Besides, the water absorption increases when the aluminosilicate source is only Fly Ash. There is a difference of 10 units in the results of water absorption between fly ash/clay geopolymers and fly ash geopolymers substituting NaOH and 8 units when Na_2SiO_3 is substituted. Therefore, it can say that the clay participates in the process of geopolymerisation providing aluminosilicate groups and decreasing the pore volume on the geopolymer. Alkaline by-products which have better water absorption are Na_2CO_3 Powder and $HNaCO_3$ Powder because lower values are obtained that the reference geopolymer for substitutions of 50% in the case of Fly Ash/Clay geopolymers. Ca and Mg and CaO Slurry present values of water absorption next to values of reference geopolymer. For fly ash geopolymers, alkaline by-products of Na_2CO_3 Powder, $HNaCO_3$ Powder, and Ca and Mg Slurry present values of water absorption below the values obtained for reference geopolymer. Alkaline by-products of CaO rocks and Ca-Si-$CaCO_3(OH)_2$ Sludge no water absorption values were obtained for the two types of geopolymer because these by-products cause an expansion in geopolymer bricks due to their high contents of calcium. Fly Ash/Clay geopolymers have values of water absorption close to the values obtained for fired clay bricks made by pressing. Therefore, the most appropriate method of moulding for these geopolymers would be pressing. On the other hand, fly ash geopolymers have values of water absorption equal to or higher than the values obtained for fired clay bricks by extrusion, so the most effective method for moulding these geopolymers is the extrusion.

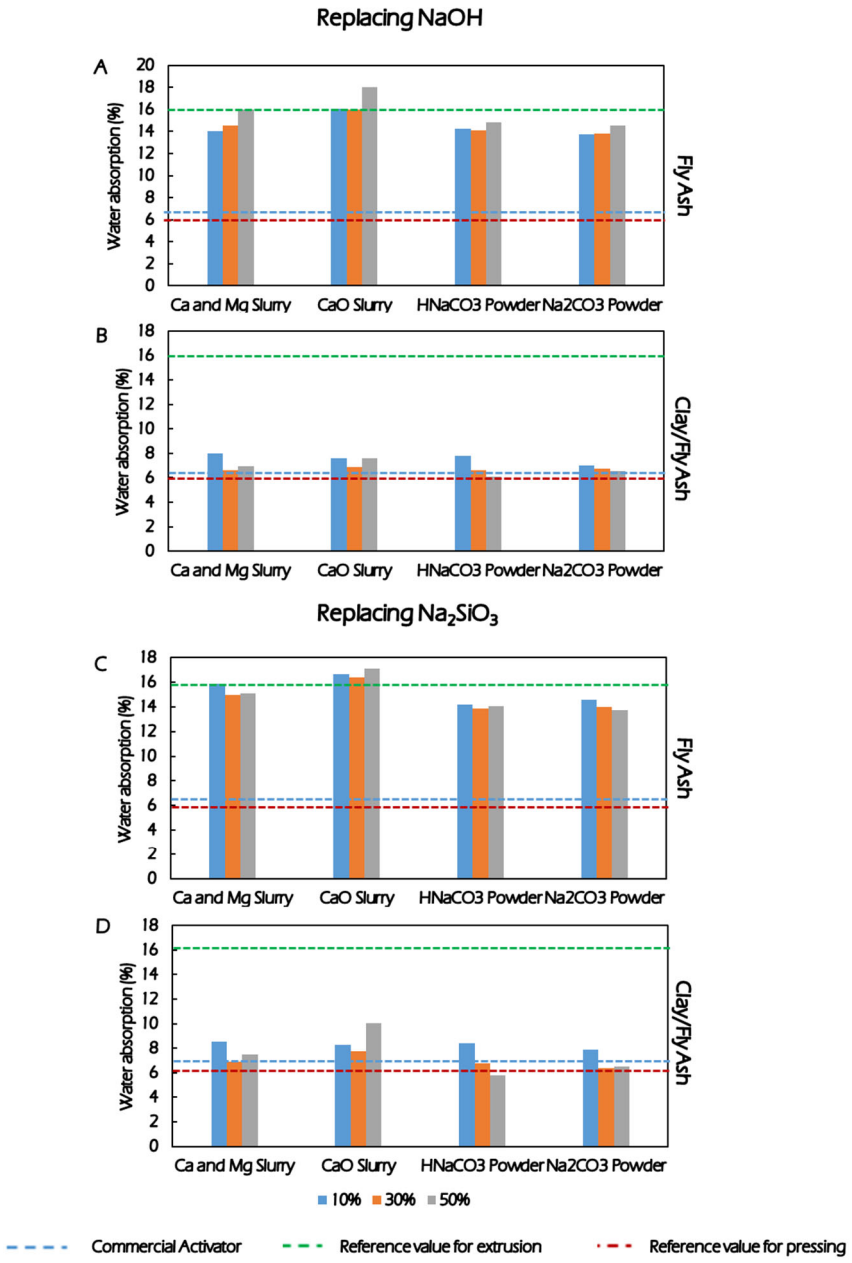

Figure 3.6. Influence of the utilisation of alkaline by-products on the water absorption by substituting NaOH using as aluminosilicate source: (a) Fly Ash; (b) Fly Ash/Clay, and by substituting Na_2SiO_3 using as aluminosilicate source: (c) Fly Ash; (d) Fly Ash/Clay.

Mechanical Properties

Flexural Strength: UNE-EN 843-1 standard is used to determine the flexural strength of the bricks. The results of the average flexural strength and standard deviation are shown in Table A.6.3 and Table A.6.4 of Annex 6. Four replications of flexural

strength have been done. The results of flexural strength of geopolymers in which NaOH has been replaced by the different alkaline by-products are shown in Figure 3.7 (a)-(d).

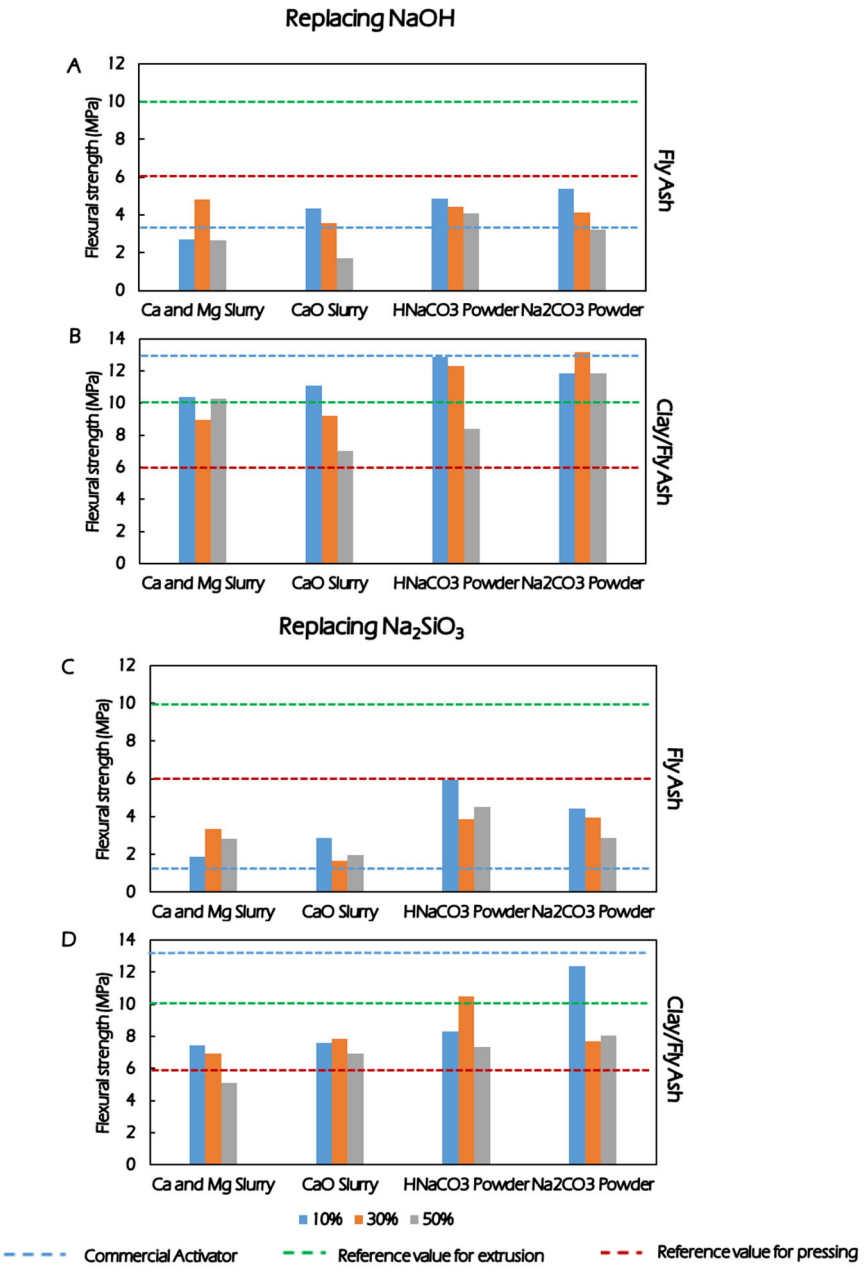

Figure 3.7. Influence of the utilisation of alkaline by-products on the flexural strength by substituting NaOH using as aluminosilicate source: (a) Fly Ash; (b) Fly Ash/Clay, and by substituting Na_2SiO_3 using as aluminosilicate source: (c) Fly Ash; (d) Fly Ash/Clay.

These properties show the consistency and mechanical resistance of the material. In Figure 3.7, the results obtained for geopolymers made with fly ash/clay geopolymers and made only with Fly Ash are shown. The reference sample is in which only commercial alkaline activators are used without being replaced for any alkaline by-product. As shown in Figure 3.7, flexural strength decreases with the increasing percentage of alkaline by-products introduced for the case of fly ash/clay geopolymers. For the case of fly ash geopolymers, flexural strength decreases with the increasing percentage of alkaline by-products, but less than fly ash/clay geopolymers. Fly ash geopolymers present a loss in flexural strength, between 10 and 50 % of substitution, of 2 units while for fly ash/clay geopolymers the loss between these percentages of substitution is 5 units. There is higher homogeneity in the results obtained with geopolymers of fly ash. Even so, there is a difference of 10 units in the results of water absorption between fly ash/clay geopolymers and fly ash geopolymers, so it can say that the clay participates in the process of geopolymerisation providing aluminosilicate groups and decreasing the pore volume on the geopolymers. Without clay, the more porous character of fly ash shows that water absorption is higher and flexural strength is lower due to the formation of internal pores in the geopolymers.

Alkaline by-products which have better flexural strength are Na_2CO_3 Powder and $HNaCO_3$ Powder because closer values are obtained that the reference geopolymer for substitutions of 30 % in the case of fly ash/clay geopolymers. For fly ash geopolymers, alkaline by-products of Na_2CO_3 Powder, $HNaCO_3$ Powder, and Ca and Mg Slurry present values of flexural strength above the values obtained for reference geopolymer. Therefore, in fly ash geopolymers the substitution of commercial NaOH with alkaline by-products enhances the flexural strength of bricks. Alkaline by-products of CaO rocks and Ca-Si-$CaCO_3(OH)_2$ Sludge no flexural strength values were obtained for the two types of geopolymer because these by-products cause an expansion in geopolymer bricks due to their high contents of calcium.

In the case of water absorption, fly ash/clay geopolymer have values of flexural strength like those obtained for fired clay bricks by pressing, while for fly ash geopolymers the most suitable moulding method would be the extrusion. In this case, a 50% incorporation of Ca and Mg Slurry in the fly ash/clay geopolymer moulding method could also be the extrusion.

3.1.2.2. Leachate pH using UNE EN 12457-4 test

Alkalinity is a measure of the ability of a compound to neutralize acids. The pH is strongly related to this property. In Figure 3.8 the pH measured in the leachate obtained in the compliance standard leaching test by replacing NaOH and Na_2SiO_3 with alkaline by-products is shown.

The ratio of ash/clay is 0.7. The results of the pH of the leachate of geopolymers formed exclusively from fly ash will not show, because for fulfilling the requirements as a structural component or to solidify/stabilize toxic waste, geopolymers must have a minimum strength that these not present. As the percentage of commercial activator substituted increases the pH decrease due to NaOH presenting more alkalinity than the alkaline by-products. In the case of Na_2SiO_3, pH values are higher than when commercial NaOH is replaced. The pH range between 11 and 12.5 independently of the waste alkali activator. Na_2CO_3 Powder and $NaHCO_3$ Powder have the highest pH values. Three replications of water absorption have been done.

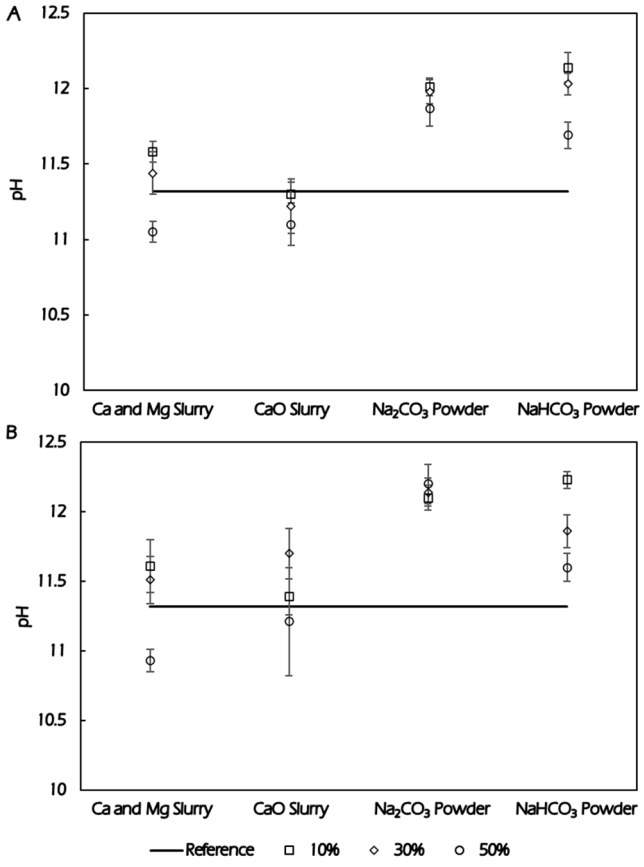

Figure 3.8. Leachate pH values of geopolymers: a) replacing NaOH and b) Na_2SiO_3 by alkaline by-products.

3.2. CHARACTERISATION OF SELECTED ALKALI ACTIVATED CFA-CLAY BASED BRICKS

To key to ensuring good mechanical performance and durability in alkaline, Portland or any other type of cement lies in strict control of the properties of the starting materials (Ruiz-Santaquiteria et al., 2013). AACs comprise a family of materials (chemically and mineralogy unrelated to OPC) generally consisting of two essential components: a cementitious precursor and a chemical additive or alkaline activator. Two main families of AACs can be defined: A) high and B) low Ca content materials. Hybrid cement comprises a third family, consisting of different combinations of A) and B) (Shi et al., 2011; Palomo et al., 2021). AACs obtained from alkaline activation of aluminosilicates are known to be conditioned by factors such as particle-size distribution, reactive amorphous/vitreous phase content, and the quantity of silica in the starting materials.

Fly ashes are not a "standard product" as their physical and chemical properties vary considerably not only from source to source but also over time from the same power station (Soutsos et al., 2016). (Ruiz-Santaquiteria et al., 2013) determined the reactive phase content under alkali activation conditions in CFA that dissolved in a 1% (v/v) HF solution and that the reactive SiO_2/Al_2O_3 ratio of these by-products could be quantified by ICP analysis of the resulting leachates. Many researchers have studied the effect of fineness on CFA reactivity, separating the material either by sieving under 45 μm (Duvallet et al., 2015; Kumar et al., 2015). Particle size separation produces an increase in the proportion of the vitreous phase since the largest particles consist essentially of reactive crystalline phases such as quartz, unburnt carbon, and hematite (Fernández-Jiménez et al., 2019).

The mechanisms governing the chemical reactions between precursor and alkaline activators differ with the family. As a rule, in model A), which includes the BFS (Bernal et al., 2014), the main reaction product is C-(A)-S-H gel, similar to C-S-H gel obtained during OPC hydration (Palomo et al., 2021). In model B), comprising MK or type F CFA precursors, the main reaction product is an M-A-S-H gel (M=alkaline cation) (Duxson et al., 2007), which is attributed to the same or higher mechanical performance than C-S-H.

Several techniques have been used characterise the alkali aluminosilicate reaction products of model B including, Nuclear Magnetic Resonance (NMR), Fourier Transform Infrared Spectroscopy (FT-IR), and X-Ray Diffratogram (XRD) (Bhagath Singh et al., 2016). The 29Si MAS NMR spectra exhibit a series of resonance separated by roughly 4-5 ppm and centred at -85.0, -89.0, -94.0, -98.5, and -102.5 ppm. These chemical shifts are characterised by tetrahedrally coordinated and fully polymerised (Q^4) silicon nuclei by 4, 3, 2, 1, and 0 AlO_4 tetrahedra, respectively, and associated

with the N-A-S-H (Ruiz-Santaquiteria et al., 2013). On the other hand, the FT-IR spectra of AACs present the following characteristics: 1) the band centred at about 1100 cm^{-1} in the silica trace, corresponding to the Si–O asymmetric stretching in tetrahedra (Lee and van Deventer, 2002; Phair and van Deventer, 2002), is shifted to lower wavenumbers (about 1000 cm^{-1}) as a consequence of polycondensation with alternating Si–O and Al–O bonds; 2) The formation of the geopolymer is also indicated by the band at about 870 cm^{-1} linked to Al–O symmetric stretching in tetrahedra (Lee and van Deventer, 2002); 3) Other bands related to the formation of the geopolymer are those at about 1420 and 1650 cm^{-1} related to O–H bending and H_2O stretching, respectively (Lee and van Deventer, 2002); and 4) the band at about 1460 cm^{-1} is related to the formation of carbonate by reaction of alkali metal hydroxide with atmospheric CO_2. At last, the XRD patterns for the AACs used as precursor CFA and commercial activators present the prominent features: 1) persistent of the crystalline phases of the initial CFA, confirming their low reactivity in alkaline media; 2) a shift hump of the pastes to slightly higher 2theta values (25-40º) attesting the formation of N-A-S-H gel; and 3) contain a series of reflections related to the presence of crystalline zeolites species such as faujasite, hydroxysodalite (Fernández-Jiménez et al., 2019).

Given the feasibility results obtained, a study of the microstructure of the geopolymers obtained with the alkaline by-products will be carried out. The best alkaline by-products for the synthesis of geopolymers are Na_2CO_3 Powder and $NaHCO_3$ Powder as demonstrated in the previous section. In this section, the objective is to study the reactivity of CFA as a precursor as well as the XRD patterns and functional groups of geopolymers obtained by using alkaline by-products as activators

3.2.1. Materials and Methodology

3.2.1.1. Selected Alkaline By-Products

In view of the feasibility results obtained, a study of the microstructure of the geopolymers obtained with the alkaline by-products will be carried out. The best alkaline by-products for the synthesis of geopolymers are Na_2CO_3 Powder and $NaHCO_3$ Powder as demonstrated in the previous section.

3.2.1.2. Alkali-Activated Bricks processing

Design of Experiments

This reference alkali-activated product has the following relationships: fly ash/clay = 0.7, [NaOH] = 6M and Na_2SiO_3/NaOH = 0.4. It is working with a temperature and

cure time of 75 °C and 48h. Four replications for each of the properties measured have been done. The geopolymer, carried out in this section, incorporates clay, higher percentages of alkaline by-products and the commercial activator substituted was Na_2SiO_3. Table 3.6 shows the formulations carried out in the laboratory of the Department of Chemical and Process Engineering and Resources at the University of Cantabria to study the feasibility of introducing alkaline by-products in the production of alkali-activated products.

Table 3.6. Design of formulations for alkaline by-products selected.

Alkaline by-product: Na_2SiO_3							
Sample	% Na_2SiO_3 Replaced	NaOH (g)	Na_2SiO_3 (g)	H_2O(g)	CFA (g)	Clay (g)	Alkaline by-products (g)
C1	10	17.45	31.77	64.14	205.9	294.1	3.53
C3	30		24.71	64.14	205.9	294.1	10.59
C5	50		17.65	64.14	205.9	294.1	17.65
C7	70		10.59	64.14	205.9	294.1	24.71
C9	100		-	64.14	205.9	294.1	35.3
Alkaline by-product: $HNaCO_3$							
Sample	% Na_2SiO_3 Replaced	NaOH (g)	Na_2SiO_3 (g)	H_2O(g)	CFA (g)	Clay (g)	Alkaline by-products (g)
B1	10	17.45	31.77	64.14	205.9	294.1	3.53
B3	30		24.71	64.14	205.9	294.1	10.59
B5	50		17.65	64.14	205.9	294.1	17.65
B7	70		35.3	64.14	205.9	294.1	24.71
B9	100		-	57.73	205.9	294.1	35.3

Bricks by Pressing

The methodology is described in section 3.1.1.3.

3.2.1.3. Characterisation of Alkali-Activated CFA-Clay based Bricks

In the selected Alkaline by-products in alkali-activated bricks the following properties and analytical methods were carried out:

The technological properties measured in this work were water absorption and flexural strength. The Norms and the methods used are described in section 3.1.1.3.

The analytical methods used in the characterisation of selected alkaline by-products were the following:

Reactivity: The fraction of the reactive phase and the reactive SiO_2/Al_2O_3 ratio of the starting materials were determined using selective chemical attack using a 1% (v/v) HF solution as illustrated in Figure 3.9. The acid attack was conducted by subjecting 1.0 g of each aluminosilicate to 100 ml of a 1.0 % by volume hydrofluoric acid solution for 5 h under stirring. After the chemical attack, the solid residue and the solution were separated by filtering using Albet®ash-less filter paper (% ash 0.01) for retention of particles under 2 μm. The resulting residue was washed with distilled

water until neutral pH from the funnel was achieved. Once the residue was completely dry, it was calcined together with the filter paper at 1000 °C in a platinum crucible for 1 h. The percentage of reactive phase content was quantified by subtracting the final mass of the residue from the initial mass of the aluminosilicate (see Figure 3.9). The percentage of silica and alumina released during the selective chemical attack was determined in the leachates through ICP. The ICP-AES analyses were conducted on a Varian 725-ES ICP atomic emission spectrometer with the following characteristics: plasma power, 1.40 kW; plasma gas flow, 15.00 l/min; nebuliser gas flow, 0.85 l/min; read time, 5 s. The concentrations of soluble silicon and aluminium determined by the ICP-AES technique correspond to the average of three measurements for a given liquid sample. Moreover, this procedure was conducted in duplicate to verify the precision of the measurements.

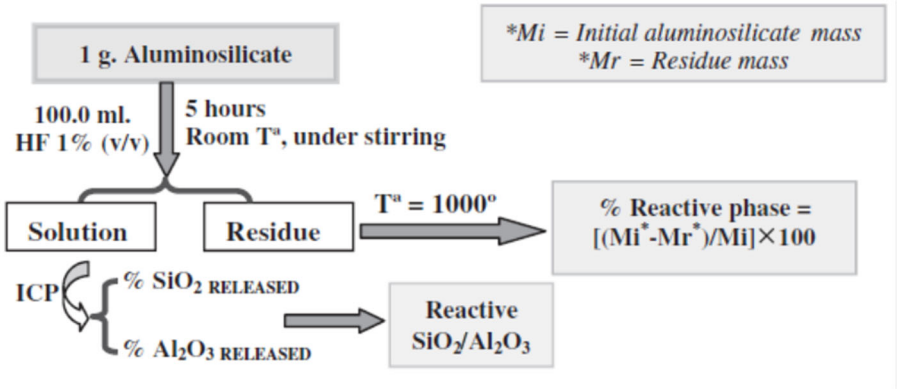

Figure 3.9. An experimental procedure was followed to quantify the percentage in weight of the potentially reactive phase and the reactive SiO_2/Al_2O_3 ratio in the starting aluminosilicates (Ruiz-Santaquiteria et al., 2013).

The percentage of reaction products generated during alkali activation (degree of reaction) was determined by selective chemical attack, using a 1:20 (v/v) HCl solution (Fernández-Jiménez et al., 2006b*) as depicted in Figure 3.10. The selective chemical attack was conducted by subjecting 1.0 g of each alkaline cement to 250.0 ml of a 1:20 (v/v) HCl solution for 3 h at room temperature under stirring. After the chemical attack, the solid residue and the solution were separated by filtering (the same type of filter paper as used for the acid attack measurements). The resulting residue was washed with distilled water until neutral pH from the funnel was achieved and once the residue was completely dry, it was calcined together with the filter paper at 1000 °C in a platinum crucible for 1 h. The percentage of reaction products generated in both cementitious systems was quantified by subtracting the final mass of the residue from the initial mass of alkaline cement (see Figure 3.10). The percentage of silicon and aluminium being a part of the reaction products was determined by analysis of the resulting leachates through ICP-AES, under the experimental conditions

described above. Given the precision in the measurements found for the silicon and aluminium concentrations using ICP, no duplicate experiments were conducted in this case.

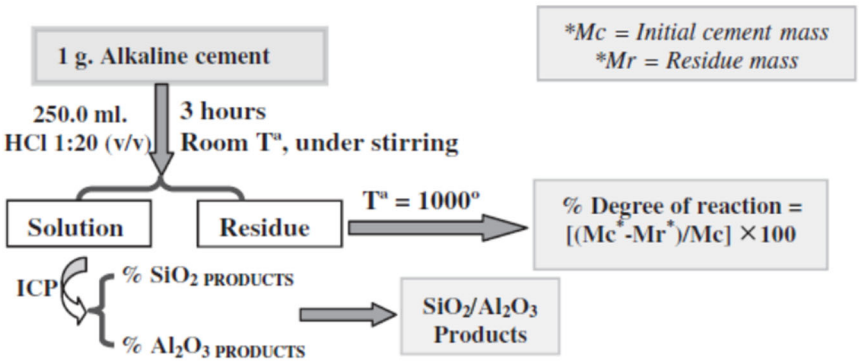

Figure 3.10. The experimental procedure was used to quantify the degree of reaction in the alkaline cement prepared and the SiO_2/Al_2O_3 ratio of the reaction products generated during alkaline activation (Ruiz-Santaquiteria et al., 2013).

Mineralogical characterisation of raw materials and geopolymers was carried out by Powder X-ray diffraction (XRD) using a D8 Advance Automatic Diffractometer in Bragg-Brentano geometry. Cu $K\alpha_1$ radiation (λ=1.5406) was employed with 0.03° 2θ steps and a constant 8 s acquisition time in the 10-70° 2θ range.

Functional groups characterisation of raw materials and selected geopolymers were carried out on an ATIMATTSON Genesis Series FTIR-TM spectrometer. The FTIR spectra were obtained by analysing compressed KBr pellets containing 1.0 mg of sample in 300 mg of KBr.

3.2.2. Selected Characterisation of Alkali Activated bricks

3.2.2.1. Technological Properties

Geopolymers should present the higher flexural strength and the lower water absorption excluding the alkaline by-products that have expanded in bricks. It has seen in section 3.1.2. that the geopolymers containing fly ash and clay, instead of just ash, have higher flexural strength and lower water absorption to reference geopolymer. Therefore, the use of geopolymers consisting only of fly ash is discarded.

Alkaline by-products that provide higher flexural strength and lower water absorption are Na_2CO_3 Powder and $HNaCO_3$ Powder. These two alkaline by-products are suitable for use as construction elements.

Solid alkaline by-products provide better physical properties to geopolymer, although these variations are not significant and any of these four materials could be used in the construction industry. The most influential factor in these properties would be moisture. A decrease in water content increases the silicate concentration in the aqueous phase, facilitating the polycondensation of the oligomers and the final hardening of the geopolymer structure decreasing the formation of cracks.

Torres et al., 2015*, Lodeiro et al., 2016*, Bobirica et al., 2015, and Sassoni et al., 2016 studied the substitution of soluble silicates and not the substitution of the alkaline ion. Such authors considered how it affected the incorporation of alkaline by-products to Na_2SiO_3. In this work, other alkaline by-products such as the Na_2CO_3 Powder and the $HNaCO_3$ Powder were incorporated. The flexural strength and water absorption using the alkaline by-products are represented in Figure 3.11. The results of the average water absorption and flexural strength and their standard deviation are shown in Table A.7.1 and Table A.7.2 of the Annex, respectively. Four replicates of water absorption and flexural strength have been carried out.

Flexural strength decreases as the dosage of alkaline by-products increases. With Na_2SiO_3 Powder substitutions of 10 %, flexure strength values are close to those of the reference geopolymer. From 30 % of substitution, a decrease in flexural strength occurs but remains constant regardless of the percentage of Na_2SiO_3 Powder introduced. For $HNaCO_3$ Powder lower flexural strength values are obtained in comparison with Na_2SiO_3 Powder geopolymers, so Na_2SiO_3 Powder favours the reaction of geopolymerisation when Na_2SiO_3 is replaced.

Water absorption decreases as the amount of alkali waste stream increases. From 30 % of substitution, water absorption values for both currents are below the value of the reference geopolymer. Therefore, it can be said that the geopolymerisation reaction has occurred with these alkaline by-products since there has been densification of bricks decreasing the pore volume.

Both alkaline by-products present values of water absorption and flexural strength closer to those obtained for fired clay bricks by pressing, although substitutions of 70 % $HNaCO_3$ Powder present values of flexural strength closer to fired bricks obtained by extrusion.

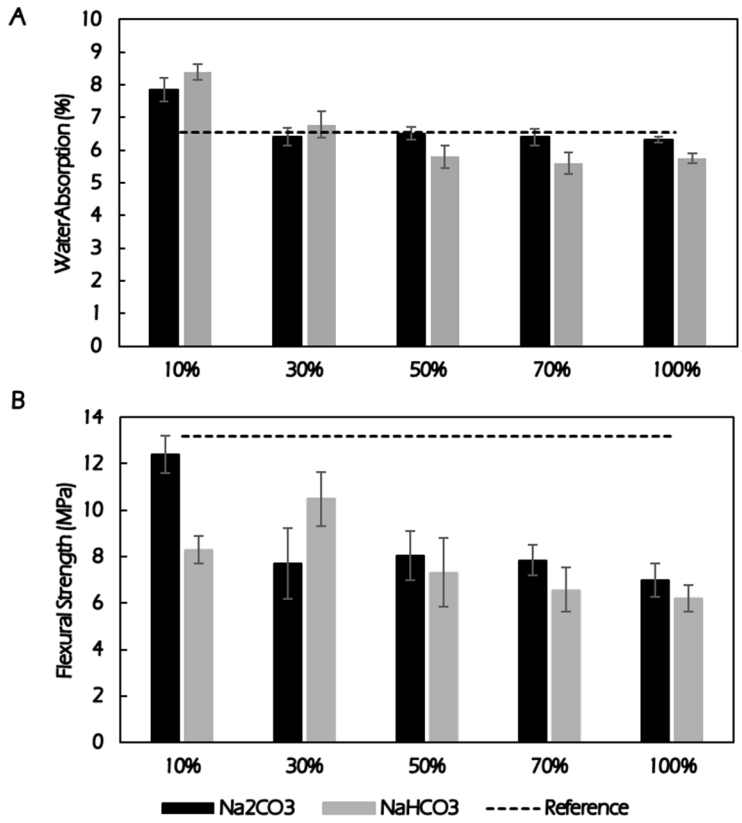

Figure 3.11. Influence of the use of Na_2CO_3 Powder and $HNaCO_3$ Powder on the technological properties: (a) Water absorption; (b) Flexural Strength.

3.2.2.2. Reactivity

Table 3.3 gives the percentages of potentially reactive phases in the aluminosilicates studied along with their reactive SiO_2/Al_2O_3 ratios. For comparison, bulk SiO_2/Al_2O_3 ratios calculated from the XRF results are also given.

According to the findings given in the table, all the materials have potentially reactive phase contents above 50 wt.%, which would initially translate into high reactivity in the alkaline activation process (Fernández-Jiménez and Palomo, 2003*).

Note that the bulk SiO_2/Al_2O_3 ratios found by XRF differ significantly from the reactive SiO_2/Al_2O_3 ratios determined using a selective chemical attack. The consequence of this observation, i.e., that neither all the silicon nor all the aluminium present in the materials is reactive, justifies the use of a specific methodology to determine this ratio.

It is generally expected that a higher reactivity of the starting material will generate a larger percentage of reaction products (N–A–S–H gel) and consequently, better properties of the final products, however, higher reactivity does not necessarily induce a better development of the final properties of geopolymers.

Table 3.3. Potentially reactive phase content and reactive SiO_2/Al_2O_3 ratio for the starting aluminosilicates.

	Initial Aluminosilicate	Selective chemical attack — HF 1% (v/v)			
	Bulk SiO_2/Al_2O_3 XRF	Reactive Phase (wt.%)	SiO_2 (wt.%)	Al_2O_3 (wt.%)	Reactive SiO_2/Al_2O_3
FA	2.36	63.68	34.41	18.35	1.88
Clay	3.70	57.60	24.02	11.34	2.12
P1*	3.06	60.10	28.30	14.22	1.99

** The results for P1 were calculated from the findings for fly ash (FA) and Clay separately.*

A certain minimum reactivity is required for the starting materials (reactive phase≥50 %) (Fernández-Jiménez and Palomo, 2003) to ensure satisfactory results, the final properties development of geopolymers is affected more by the composition (the reactive SiO_2/Al_2O_3 ratio) than on the amount of the reactive phase, i.e., a high potentially reactive phase content does not compensate for an unsuitably low reactive SiO_2/Al_2O_3 ratio.

From the chemical standpoint, the most important factor in geopolymer formation is the silica and reactive alumina content in the starting aluminosilicate, because silicon is the main component of the structural skeleton of the reaction products formed during alkaline activation of the material. Together with dissolved aluminium, in high alkalinity media, it forms polyhydroxysilicoaluminate type complexes (Fernandez-Jimenez and Palomo, 2003*; Fernandez-Jimenez et al., 2006*; Palomo et al., 2004*; Weng et al., 2005*). Figure 3.12 show the SiO_2/Al_2O_3 reactive ratio of the geopolymers obtained using the alkaline by-products.

According to the findings given in Figure 3.12, the SiO_2/Al_2O_3 reactive ratio decreased when the percentage of alkaline by-products increased. This is an expected result due to water glass plays an important role in the development of geopolymers. However, the results obtained show a SiO_2/Al_2O_3 reactive ratio above 1.30 which suppose a good development of the final properties of geopolymers. For the lowest percentage of alkaline by-products, close results to the reference were obtained, hence, alkaline by-products might be a potential product in the manufacturing of geopolymers.

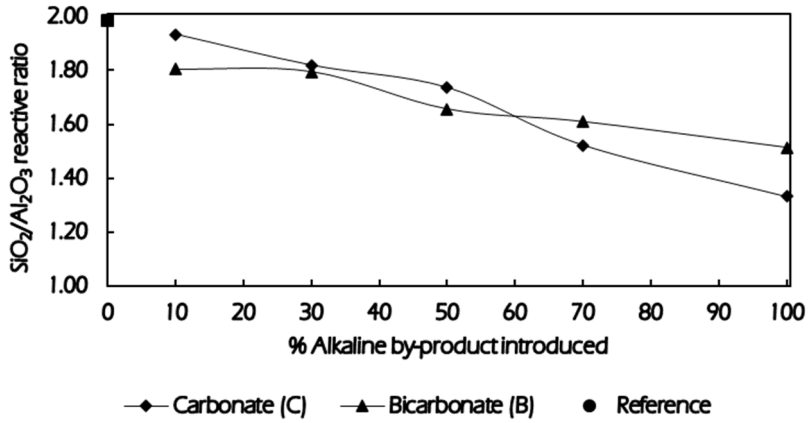

Figure 3.12. SiO_2/Al_2O_3 reactive ratio of the alkali-activated materials.

3.2.2.3. Microstructural Characterisation

Mineralogical characterisation of reaction products was done using XRD technique to identify the crystalline components in the system. Figure 3.13 (a) and (b) reproduce the X-ray diffractograms for the pastes using sodium carbonate and sodium bicarbonate, as well as the diffractogram for the reference geopolymer. In all cases, the diffraction pattern changed negligibly after the substitution of commercial activators with alkaline by-products. One characteristic of these materials was the shift in the position of the halo attributed to the vitreous phase in the initial ash to slightly higher 2q angles, an indication of the presence of an alkaline aluminosilicate (N-A-S-H) gel, the main reaction product. The minority crystalline phases (quartz, mullite, and nacrite) detected in the initial material remained apparently unaltered. Zeolite-like crystalline phases appeared in the post-activation spectra. The type of zeolite that crystallised depended on the activating solution used. Zeolite species such as sodalite hydrate ($Na_4Al_3Si_3O12OH$) and calcium aluminum oxide ($CaAl_2O_4$) with a Si/Al ratio of 2 (Breck, 1973) were detected on the diffractogram formed from fly ash activated with the alkaline by-products. Zeolite species such as sodalite hydrate and calcium aluminum oxide were also observed when the commercial activator was the activator. When the source of the silica was dissolved in alkaline by-products, the resulting diffractogram resembled the diffractogram for the paste prepared with a commercial activator very closely. Nonetheless, according to other studies (Criado et al., 2007), a considerable rise in the silica content in the medium retards the formation of zeolite species, inducing a decline in mechanical strength due to the absence of N-A-S-H gel.

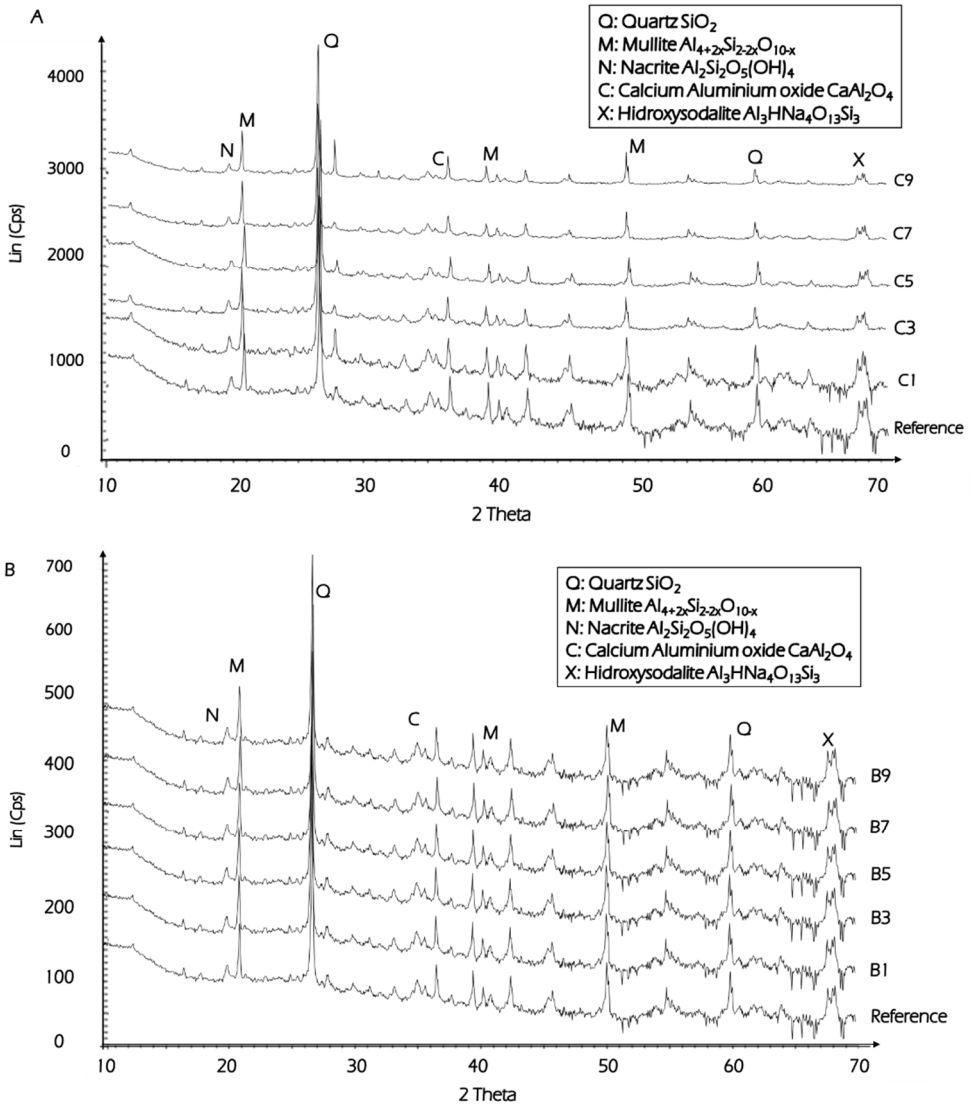

Figure 3.13. a) XRD of carbonate-based geopolymer; b) DRX of bicarbonate-based geopolymer.

Figure 3.14 (a) and (b) show the FTIR spectra obtained after activating the fly ash with the commercial activator and alkaline by-products. These materials contained both unreacted particles and reaction products (sodium aluminosilicate gel, the majority product, and minority crystalline zeolites). All these products consisted primarily of SiO_4 and AlO_4 tetrahedra. An analysis of the spectra showed that the most characteristic bands were a main band at around 1000 cm^{-1} associated with the asymmetric vibrations generated by T-O-T bonds (where T is Si or Al).

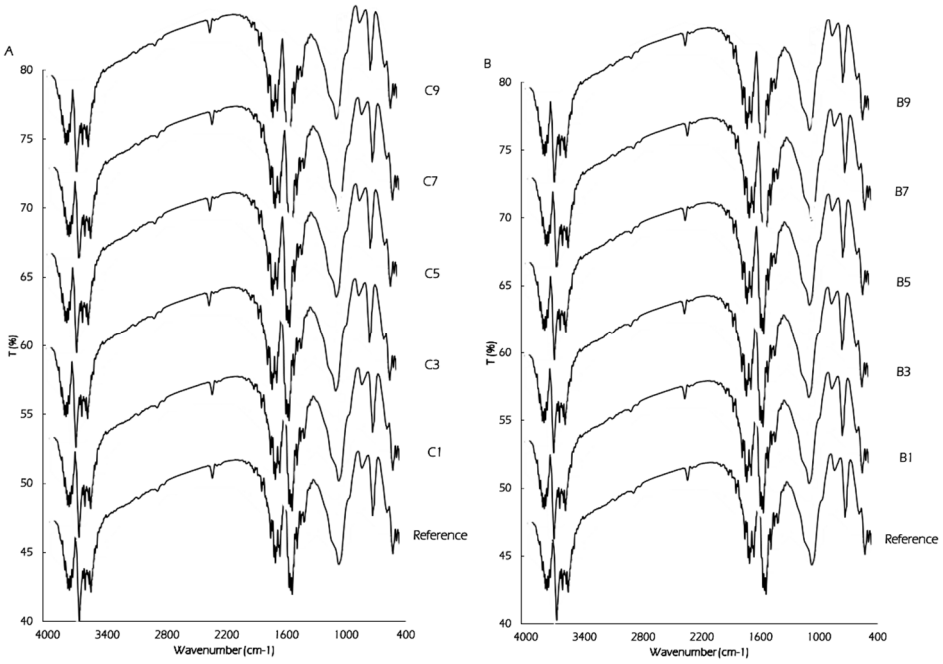

Figure 3.14. FTIR a) Carbonate-based geopolymer; b) Bicarbonate-based geopolymer.

In all the systems, regardless of the type of activator used, this band, located at around 1060 cm^{-1} in the original fly ash, narrowed and shifted to lower frequencies after the fly ash was activated: to around 1010-1004 cm^{-1}. These shifts indicate that the glass component in the fly ash reacted with the alkaline activator to form reaction products, primarily N-A-S-H, an aluminosilicate gel (Fernandez-Jimenez and Palomo, 2005b). The exact position of this band depended on the Si/Al ratio of the product formed. The shift was to lower frequencies due to the rise in the tetrahedral aluminium content (Fernandez-Jimenez and Palomo, 2005b). With the replacement of Si^{4+} by $Al^{3+,}$ the T-O-T angle became more acute, shifting the signal to lower frequencies due to the weaker bond and the fact that the Al-O bond is longer than the Si-O bond. The shift in these bands was observed to be more intense in the pastes activated with commercial activator than in the pastes activated with alkaline by-products. That means that the Si content was higher in the reaction products in the former two than in the latter (Fernandez-Jimenez and Palomo, 2005b; Mozgawa et al., 1999). The rest of the bands characteristic of N-A-S-H gel between 800 and 500 cm^{-1}, which were also present, were associated with the vibrations generated by the tetrahedral formed. A series of bands attributed to the presence of zeolites (detected with XRD) also appeared.

3.3. CFA-CLAY BINDERS FOR IMMOBILISATION OF TOXIC WASTE

The immobilisation of heavy metals in Ordinary-Portland-Cement (OPC)-based materials are widely investigated and implemented because of its low processing cost and ability to meet stringent technical requirements (Niu et al., 2018). However, it presents low effectiveness in several situations, such as in the case of various toxic waste, especially those containing salts of magnesium, tin, zinc, copper, and lead, and also for solidification of residues with high sulphide contents (Shi and Fernández-Jiménez, 2006; Paz-Gómez et al., 2021). On the other hand, from an environmental point of view, the production of OPC consumes large quantities of natural resources and energy in addition to contributing significant greenhouse gas emissions into the atmosphere: approximately 0.66 to 0.82 kg of CO_2 is produced per kg of OPC manufactured. With this emission level, the cement industry is responsible for 8 to 10 % of the anthropogenic emissions around the world (Vu and Gowripalan, 2018).

Nowadays, the great challenge in the solidification/stabilisation of hazardous waste focuses on the use of new ecological and sustainable binders for the immobilisation of heavy metals. In this context, alkali-activated binders (AABs) or geopolymers turn up as a feasibility binder's solution to the OPC. The production of geopolymers consists of the reaction of a powder precursor, with a high content of amorphous silico-aluminates, with high or low calcium content, and a strongly alkaline activating solution. The result after a curing time is a compact solid with good mechanical properties, which can be disposed of in a landfill or used in construction applications (Nguyen et al., 2021; Maldonado-Alameda et al., 2020). These binders have received much attention in the last decade as their production offers significant economic and environmental benefits, such as having a lower CO_2 footprint and reusing of industrial waste or by-products as precursors in the formulations of geopolymers. Another impor- tant advantage of the performance of these new binders in the immobilisation of certain chemical species is due to their three-dimensional microstructure, with an abundance of very small pores, very high alkalinity, and very good chemical stability (Vu and Gowripalan, 2018; Palomo et al., 2003). For these reasons, they are also proposed as adsorbents in waste treatment (Harja et al, 2015).

In this way, recent investigations on the use of geopolymer matrices to solidify/stabilize different hazardous waste-containing heavy metals have been reported: electric arc furnace dust (Cifrian et al. 2021; Pereira et al., 2009; Nikolic et al., 2020), municipal solid waste incineration fly ash (MSWI) (Maldonado-Alameda et al., 2020), lead–zinc smelting slag (Zhang et al., 2020; Ogundiran et al., 2013; Mao et al., 2019; Li et al., 2018), chromite ore processing residues (Huang et al., 2017; Yu et al., 2021), hexavalent chromium (Nikolic et al., 2017; Zhang et al. 2016), or galvanic solid waste (Barreto et al., 2020), among others. Immobilisation efficiency is measured mainly by the mechanical strength and the leaching reduction as indicators of

solidification and stabilisation, respectively. Thus, the selection of the leaching test method is key to assessing the degree of the heavy metal immobilisation of geopolymer matrices (Galiano et al., 2011; Bakhshi et al.; 2017). There are two leaching procedures commonly used in the literature: the Toxicity Characteristic Leaching Procedure (TCLP, 1992), which uses as a leaching reagent an acetic acid solution buffered to a pH of 3 to 5, and the Equilibrium Batch Leaching Test (EN-12457, 2002), which employs distilled water as a leaching solution. The results from these tests are compared, respectively, to the threshold limits established by the Environmental Protection Agency (EPA, Washington, WA, USA) and the 2003/33/EC Council Decision (EU, 2003), respectively, for accepting waste in landfills. In previous studies, the authors of this work have carried out the stabilisation of Electric Arc Furnace Dust (EAFD) into ceramic geopolymers based on coal fly ash and quarry clay as the precursor and aggregate (as an adsorbent), respectively, assessing the environmental behaviour in different scenarios, disposal, and utilisation using leaching tests (Cifrian et al. 2021).

Zinc production has steadily increased by 4% per annum in the last decade. In 2020, the global production of zinc was approximately 13 Mt (Zhang et al., 2021). The increase in zinc production also implies that the amount of generated waste (e.g., sludge, dust, and precipitated) and energy consumption rises (Martínez-Sánchez et al., 2019). Therefore, the management of heavy metal solid waste is a key factor to take into account in the environmental sustainability of the zinc industry (Zhang et al., 2021).

The Cadmium Sponge (CS) from the purification stage and the Anode Mud (AM) from the electrolysis stage represent significant zinc plant residues (ZPR) (Hoang et al., 2009). ZPR are hazardous waste because of their strong acidities, poor stabilities, and high heavy metal content (Wang et al., 2020). In the production of one ton of zinc refined by the RLE process, between 80 and 100 kg of Cadmium Sponge (Li et al., 2018) and 40 to 50 kg of Anode Mud are generated (Zhang et al., 2020). These residues contain considerable amounts of valuable metals, such as zinc, cadmium, copper, and nickel (Wang et al., 2020; Grudinsky et al., 2021). Several studies have investigated the recovery of cadmium and copper from Cadmium Sponge (Aparajith et al., 2010; Li et al., 2018; de Barros et al., 2021; Moradkhani et al.; 2012; Gharabaghi et al., 2012) and the recovery of noble metals from Anode Mud (Mahon and Alfantazi, 2014; Xing et al., 2020; Dreisinger et al., 2012). However, the global demand for Zn and the lack of development of recovery technologies on an industrial scale, due to technical problems or because they may give rise to secondary pollution, make it necessary for ZPR to be previously treated and disposed of in sanitary landfills (Zhang et al., 2020). Due to the high concentration of heavy metals and great acidity, these residues present potential environmental risks because of their significant heavy metals solubilisation. Therefore, ZPR is categorized as hazardous waste according to

the European Waste Catalogue (110207*) (Martínez-Sánchez et al., 2019), and they cannot be directly landfilled.

It is important to note that there are no published studies regarding the immobilisation of pollutants from ZPR through their introduction into ceramic geopolymers. Consequently, the aim of this work is the immobilisation of heavy metals from this type of acid waste as a treatment prior to disposal in a landfill using sustainable binders. First, the feasibility study of the S/S of Cadmium Sponge (CS) and Anode Mud (AM) in coal fly-ash/clay-based geopolymers using different processing techniques and activators were performed. The S/S products were evaluated by technical and environmental assessment according to EU Landfill regulation limits for the compressive strength and release of hazardous metals. Second, to optimize the geopolymer parameters, a factorial experimental design was performed using as response variables the release of critical pollutants for the stabilisation of zinc plant acid residues.

3.3.1. Materials and Methodology

Currently, approximately 80 % of zinc is produced from Sphalerite, a zinc sulfide mineral, by the roasting–leaching–electrowinning (RLE) process, which is a combination of pyrometallurgy and hydrometallurgy (Wang et al., 2020; Hu et al; 2017). The process of the roasting of zinc sulfide concentrates is a substantially cost-effective technology due to its self-sufficiency, a satisfactory removal of harmful impurities for the subsequent electrolysis, and the associated production of sulphuric acid (Grudinsky et al., 2021). In the leaching stage with strong hot sulphuric acid, other metals present in the calcine concentrate are also leached in addition to zinc (Ayala and Fernández, 2013). As metallic zinc electrolysis requires an electrolyte that is free from these pollutants, the sulphuric acid liquor needs a purification step to remove them (Ayala and Fernández, 2013). The purification of the leached liquor in these processes is carried out by adding zinc powder that removes the more noble impurities. As a result, the excess zinc powder, together with compounds of other metals (mainly cadmium and lead), form a residue known as Cadmium Sponge (CS) (Aparajith et al., 2010; Li et al., 2018). On the other hand, during electrolysis, to protect lead anodes from excessive corrosion, manganese compounds are added (Ayala and Fernández, 2013; Chandra et al., 2011; Mahon and Alfantazi, 2014). On the surface of the anodes, lead dioxide is formed by electro-oxidation, and manganese (present in the bath) deposits as manganese oxide. The deposited oxides are powdery and fall off to the bottom of the bath. At the end of the electrowinning cycle, the powder is removed from the bottom of the cell, an acid residue known as Anode Mud (AM) (Chandra et al., 2011; Jaimes et al., 2015; Huang et al., 2020; Zhang et al., 2020).

3.3.2.1. Acid Waste

Two different ZPRs were used, the Cadmium Sponge (CS) and the Anode Mud (AM) produced during the purification (Bakhsi et al., 2017) and the electrowinning stages (Chandra et al., 2011) respectively, of the RLE process. The CS has a greyish colour, a wide particle size distribution, and even forms large rocks.

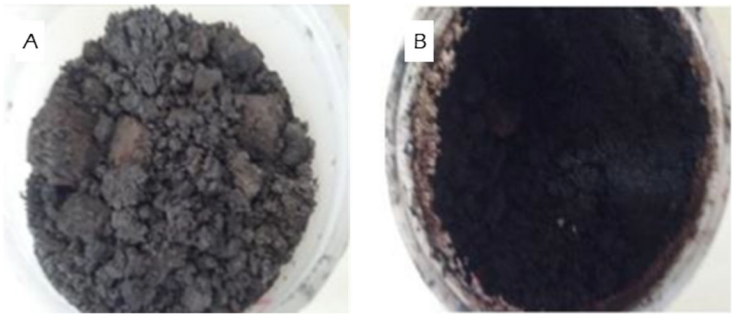

Figure 3.15. Acid waste used in this work: (a) Cadmium Sponges (CS); (b) Anode Mud (AM).

For a representative sample, the moisture content is 41%, the pH value is 4.2 and the conductivity is 2174 μS/cm; whereas the AM is black, which also presents particles of different sizes and has a bad smell that is difficult to work with. A representative sample of AM has a moisture content of 30% and a pH value of 2.0. The visual appearance of both acid waste is shown in Figure 3.15. The concentration of trace elements released after the application of EN 12457-2 leaching test is listed in Table 1. As acid waste are produced in an industrial process, high variability in the composition is expected.

To represent this fact, Table 3.4 collect the maximum and minimum trace elements leaching values of the acid waste produced for one year. Cd and Zn are the elements with the highest concentrations and present the major hazardousness in both acid waste. Pb and Ni are other elements to consider for immobilisation in Cadmium Sponges, while only Pb in the case of Anode Mud.

Table 3.4. Trace elements concentration in leachates obtained in EN 12457-2 leaching test of Cadmium Sponge (CS) and Anode Mud (AM).

Trace elements (mg/kg)	Range of Values- CS	CS	Range of Values-AM	AM	Landfill disposal limits*	
					HW	NHW
pH	3.92-7.70	4.2	< 2	< 2	—	—
As	0.01-0.42	0.41	0.05-0.16	0.16	25	2
Ba	0.05-6.48	0.025	0.05-0.35	0.06	300	100
Cd	**300-4800**	**2790**	**15-11700**	**461**	**5**	**1**
Cr	0.05-0.80	0.78	0.05-1.08	0.58	70	10
Cu	0.05-24.47	0.66	0.01-1440	8	100	50
Hg	< 0.01	0.01	< 0.01	< 0.01	2	0.2
Mo	0.05-0.85	0.1	0.05-0.42	0.1	30	10
Ni	0.05-14.72	4.5	0.05-18.45	0.88	40	10
Pb	0.05-6.75	6.7	0.05-6.50	6.3	50	10
Se	0.05-0.5	0.5	0.05-20.9	0.35	7	0.5
Sb	0.1-0.5	0.5	0.05-0.56	0.56	5	0.5
Zn	**33-6970**	**6690**	**1010-20900**	**5720**	**200**	**50**

* Decision 2003/33/EC: HW Hazardous Waste; NHW Non-Hazardous Waste

3.3.2.2. Geopolymer precursors and activators

For the immobilisation of the hazardous elements, in this work geopolymerisation has been proposed. For the synthesis of geopolymers, two precursors have been used together and two alternative alkaline activators have been applied.

Precursors used in this study were obtained from different sources in the same region (Cantabria, Spain). Low calcium fly ash (ASTM class F) (FA) was supplied by a coal combustion company located in Cantabria, Spain) and was used as the main silicoaluminate agent. Quarry clay was collected from a Spanish industrial ceramic and was used as a secondary silicoaluminate source, with an aggregate role mainly.

Two different activating solutions were used: a commercial solution based on sodium hydroxide and sodium silicate (SiO_2 25.5-28.5 %, Na_2O 7.5-8.5 %, density 1.345-1.382 g/mL), and an alternative solution, an industrial by-product based on sodium carbonate (Na_2CO_3), was supplied by Solvay Química S.L.) – (Barreda, Cantabria, Spain), substituting the commercial sodium silicate.

The composition of Fly Ash and clay was determined by inductively coupled plasma atomic emission spectrometry (ICP-AES) and X-ray fluorescence (XRF) in Activations Laboratories (Ancaster, ON, Canada). The elemental major and minor oxides and trace element concentrations in raw materials are given in Table 3.5. Both precursors, FA, and clay are mainly constituted by SiO_2 and Al_2O_3, key compounds in the manufacture of geopolymers.

Table 3.5. Major, minor oxides and traces elements in Flay Ash (FA) and Clay.

Raw Materials	FA	Clay
Composition (wt %)		
SiO_2	52.38	64.22
Al_2O_3	21.32	16.93
Fe_2O_3	6.88	5.94
K_2O	2.50	3.03
CaO	6.23	0.52
MgO	2.48	0.89
Na_2O	2.02	0.58
TiO_2	0.92	0.86
MnO	0.07	0.06
P_2O_5	0.82	0.08
LOI	5.39	5.78
Composition (mg/kg)		
As	44	30
Ba	2662.25	483
Cd	1.10	0.50
Cr	76.25	46
Cu	85.75	27
Hg	n.d.	n.d.
Mo	18	2
Ni	129	29
Pb	52.50	28
Sb	7.80	2.5
Se	0.55	0.02
Zn	291.25	139

n.d. not determined

3.3.2.3. Geopolimeric Matrices Preparation

Samples were developed at a laboratory scale, based on the results of the authors' previous studies (Cifrian et al., 2021) as shown in Figure 3.16.

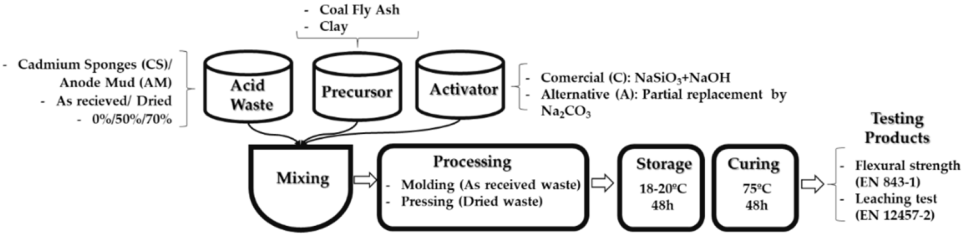

Figure 3.16. The methodology applied for the geopolymeric formulations development.

Table 3.6. Formulations for solidification/stabilisation of each acid waste, CS and AM.shows the formulations carried out in the laboratory for the solidification/stabilisation of the acid waste.

Table 3.6. Formulations for solidification/stabilisation of each acid waste, CS and AM.

Activator	Sample Name	Acid waste (g)	FA (g)	Clay (g)	NaOH (g)	Na_2SiO_3 (g)	Na_2CO_3 (g)	Acid waste / geopolymer ratio	L/S	[NaOH]
Com-mercial	C0	0	205.9	294.1	17.45	35.30	0	0		6M
	C50	500						0.5	0.21	
	C70	1167						0.7	0.22	
Alternati-ve	A0	0	205.9	294.1	17.45	24.71	10.59	0		6M
	A50	500						0.5	0.21	
	A70	1167						0.7	0.22	

FA, clay, and acid waste were mixed for 10 minutes to obtain a homogeneous mixture. The 6 M NaOH solution was prepared and cooled to room temperature. Then Na_2SiO_3 and/or Na_2CO_3 was added up to Na_2SiO_3/NaOH ratio fixed, depending on if commercial or alternative activator were used. In the end, the activator solution was added to the mixture of FA-clay-acid waste and mixed for 10 additional minutes. A sample without acid waste was developed as the reference sample. Furthermore, these formulations were studied with and without a drying pre-treatment for the two acid waste. The drying pre-treatment was carried out at 105 °C for 48 h.

To obtain the final specimens two different processes were applied, due to the behaviour of mixtures, when waste were or not were pre-treated. When acid waste were dried, specimens were obtained by uniaxial pressing under 50 bar with a Mignon SS/EA (Nanetti) laboratory a hydraulic press in a rectangular mould of 80 mm in length, 30 mm in width, and 16 mm in height. On the other hand, when acid waste was mixed without a drying pre-treatment, moulds were used to process the samples, due to the mixture being very fluid and cannot be pressed.

The samples were stored at ambient temperature (18-20°C) for 48 h. After this time, they were cured in an oven for 48 h at 75°C. Then, the samples were cooled and left for an additional 28 days at ambient temperature prior to performing any test.

3.3.2.4. Flexural strength and Leaching test

The EN 843-1 standard was used to determine the flexural strength of the cured pieces. This test was conducted by Servo-Hydraulic mechanical equipment of pressure cell Suzpecar MES-150, 15-ton capacity and an electronic control module MIC-101H.

The compliance leaching test EN 12457-2:2003 was used to determine the release of metals from the acid waste and S/S products in equilibrium conditions. According to this test, samples were milled to below 4 mm to promote contact between phases and consequent mobility of trace elements. The leaching agent used was deionized water. The leaching tests were performed at a liquid/solid ratio of 10 and 24 h of stirring.

Leachates were analysed for the critical elements included in the Landfill Decision 2003/33/CE. They were analysed using Inductive Coupled Plasma Atomic Emission Spectrometry (ICP-AES) in an accredited laboratory, Agrolab Ibérica SLU (Burgos, Spain).

The leaching of trace elements and the flexural strength of the geopolymers were analysed in triplicate and the results show the mean and its standard deviation.

3.3.2.5. Mathematical modeling and experimental design

A factorial experimental design was carried out to optimize the retention of critical pollutants of the two zinc plant acid residues. Two-level, three-factor experimental design was conducted, and five response variables were analysed.

The experimental design was mathematically adjusted according to second-order polynomial equations. In total eleven experiments had to be done as shown in equation 1.

$$n = 2^3 + 3 = 11 \qquad (1)$$

The mathematical adjustment and the response surface graphics were done by Stat graphics software using Box-Behnken design. Analysis of variance (ANOVA) was done, and the main individual and multiple effects were assessed through second-order polynomial equations as follows in equation 2.

$$y = a_0 + \sum_{i=1}^{k} b_i x_i + \sum_{i=1;j=1}^{k} d_{ij} x_i x_j \qquad (2)$$

3.3.2. CFA-Clay Binders for Immobilisation of Toxic Waste

3.3.2.1. Feasibility of the solidification/stabilisation (S/S) process

As a result of the alkali activation process, different monolithic samples of solidified/stabilized waste have been obtained. With the purpose that these products could fulfill the landfill policy framework, monolithic waste need to accomplish both technological and environmental requirements.

3.3.2.1.1. Technical behaviour of S/S products

The European Union through Decision 2003/33/EC establishes that the member states will determine the criteria for the deposition of monolithic waste. In this way, the Spanish law (RD 646/2020) establishes that to landfill a Hazardous waste previously S/S, as non-hazardous monolithic waste, it must support a minimum compressive strength of 3 MPa for 28 days. In Table 3.7 the results of compressive strength and density of the S/S products developed are presented.

Table 3.7. Compressive strength and density of Fly Ash/Clay geopolymer incorporating acid waste: Cadmium Sponge (CS) or Anode Mud (AM).

Sample	% Acid waste	Compressive strength[1] (MPa)	Density kg/m^3
C0	0	11.72±1.83	2021±19
CS-C50	50	6.61±0.70	1995±15
CS-C70	70	5.67±1.31	1922±32
AM-C50	50	4.57±0.58	1500±35
AM-C70	70	4.20±0.55	1465±21
A0	0	7.85±0.64	2021±19
CS-A50	50	4.48±0.80	1934±25
CS-A70	70	4.65±1.01	1901±12
AM-A50	50	3.83±0.48	1363±17
AM-A70	70	3.08±0.59	1337±14

[1] Landfill limit according to Spanish RD 646/2020 is 3 MPa

Results show that all the samples developed enough strength to fulfil the landfill requirement of 3MPa. The incorporation of acid waste does not favour the development of the compressive strength of geopolymers, and this effect is greater in the case of AM. Density is a key parameter in waste disposal too since it determines the landfill space to be used. In this case, the product density is much higher in the CS monoliths (around 1900kg/m^3) with both activators than in the AM monoliths (1337-1500kg/m^3). In both cases, with the commercial activator, a slightly higher density is obtained than with the alternative. Both properties, compressive strength, and density have a direct relationship. Also, indicate that the incorporation of the waste to the geopolymer matrix reduces the strength almost by half in relation to the reference geopolymers with both activators, while the density is slightly reduced.

3.3.2.1.2. Environmental behaviour of S/S products

The environmental behaviour of the samples has been evaluated through equilibrium leaching tests. The pH values of the leachates obtained from both types of monoliths from moulded and pressed products are represented in Figure 3.17.

The leachates from CS products have alkaline pH, due to the release of alkali from the geopolymers when immersed in deionized water (Cifrian et al., 2021). The pH values remain approximately constant regardless of the activator used, or the pre-treatment of the waste when the dosage of the waste is 50% with values between 11.46 and 11.77. However, at higher waste additions, the pH values with the commercial activator are slightly lower than with the alternative activator. On the other hand, leachates from AM products present moderate alkalinity due to the initial higher acidity of the waste. This initial acidity represents a significant problem for their disposal in a landfill, therefore, geopolymer binders can be a good alternative to traditional binders (Shi et al., 2011). In this case, there is a difference of one unit between the pH values of the products obtained with pre-treated or non-pre-treated waste. The pH value differs also with the dosage of waste, and the activator used, between 6.54 and 8.77.

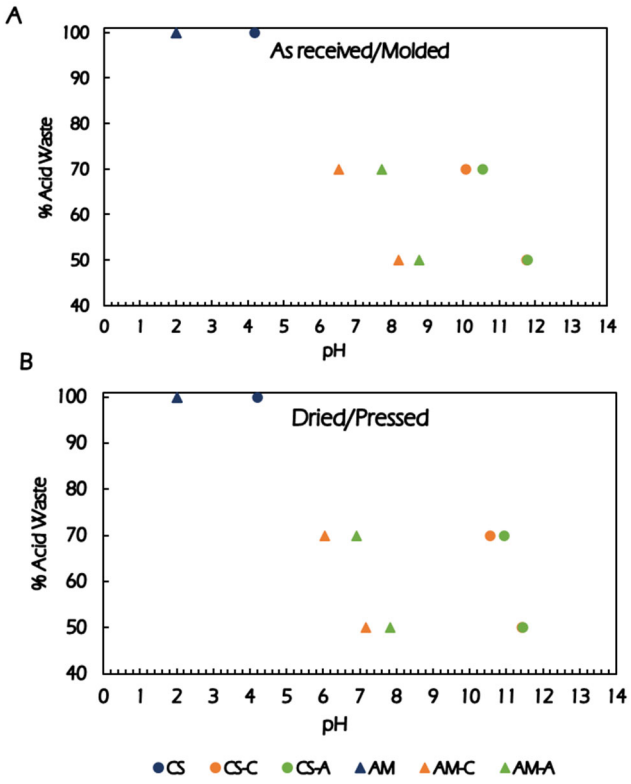

Figure 3.17. pH values of leachates of acid waste Cadmium Sponge (CS) and Anode Mud (AM) S/S: (A) as-received waste, processed by moulding; (B) pretreated waste, processed by pressing.

All the elements analysed in the leachates of the Compliance Leaching test: As, Ba, Cd, Cr, Cu, Mo, Ni, Pb, Sb, Se, Zn, and Cd except Hg, present a concentration higher

than the quantification limit. The concentration values (average of three replicates) are represented in Figure 3.18 (CS products) and Figure 3.19 (AM products).

The mobility of the elements analysed incorporating CS as-received waste and produced by moulding is represented in Figure 3.18 (a) and (b). In Table A.8.1 of Annex 8, the results compliance leaching test is collected. As can be observed, in general, the mobility of the elements increases as the amount of CS added increases. The elements with the highest mobility in the CS waste, Cd, Ni, Pb, and Zn (

Table 3.5), have different behaviours in the S/S products. While Ni, Pb, and Cd increase their leaching with a greater amount of waste added, in the case of Zn the behaviour is the opposite. The mobility of Ni, Pb, and Cd varies at 56 %, 67 %, and 85 % as the waste dosage increases (from 50 to 70 %), respectively. The mobility of Zn decreases as the amount of CS waste increases. The immobilisation of Zn in FA-clay-based geopolymers may be due to a physical microencapsulation mechanism (Izquierdo et al., 2010; Yilmaz et al., 2015; Komonweeraket et al., 2015; Loncnar et al., 2016; Wan et al., 2019). Another element to highlight is As, which has the highest concentration value, and hardly varies with the amount of waste added.

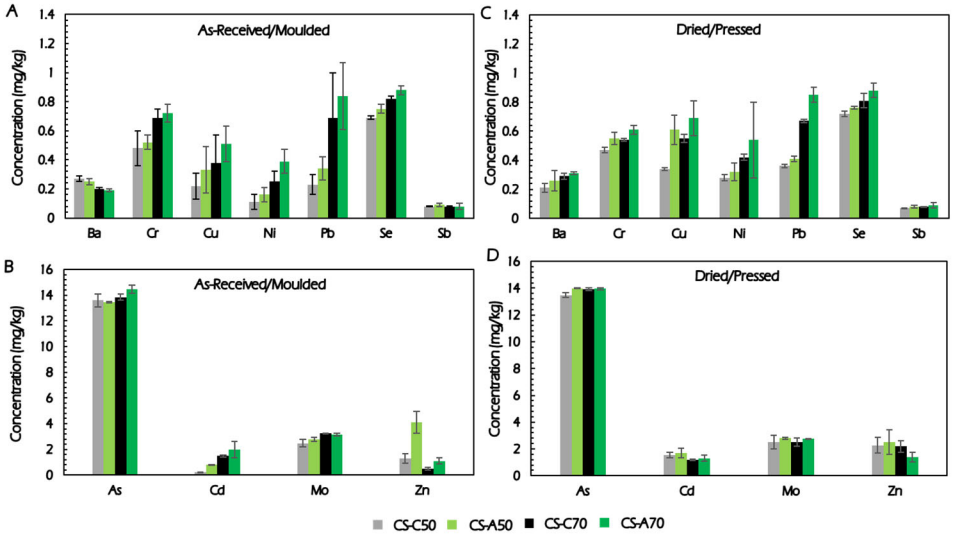

Figure 3.18. Mobility of contaminants of Cadmium Sponges (CS) S/S – commercial (C)/alternative (A) activator: (A) and (B) As-received waste and moulded; (C) and (D) Dried waste and pressed.

Considering the type of activator used, the majority of elements, As and Mo present values of mobility very similar. While, minority elements, Cu, Ni, and Pb present the most significant variations between the two activators. Commercial activators can immobilize Cu, Ni, and Pb in 34 %, 56 %, and 22 % more than the alternative ones, respectively.

Figure 3.18(c) and Figure 3.18(d) show the leaching results of the products obtained by pressing when the waste has been pre-treated. No significant decrease in mobility of contaminants obtained with pre-treated waste versus received waste is observed. Cd and Zn, the main contaminants from CS waste, have different behaviours. There is no influence on the leaching of the activator type in the S/S products with dried and pressed waste with major elements.

The mobility of the elements analysed incorporating Anode Mud (AM) as-received is represented in Figure 3.19(a) and (b). In Table A.8.2 of Annex 8, the results compliance leaching test is collected. As can be observed, the mobility of the elements tends to increase with the amount of AM waste added. Cu, Pb, Cd, and Zn, which are the elements with the highest mobility in the anode mud, present the most significant variation as the waste dosage increases in the S/S product. The mobility of these elements varies at 32 %, 42 %, 53 %, and 84 % as the amount of waste increases, respectively. The rest of the elements do not present significant mobility regardless of the waste added.

Considering the type of activator used, in relation to the elements associated with the waste, Cu, Pb, Cd, and Zn present slightly higher mobility using the alternative activator than the commercial one, except for the Cd. The rest of the elements present variations of mobility similar regardless of the type of activator used, less than 10 %.

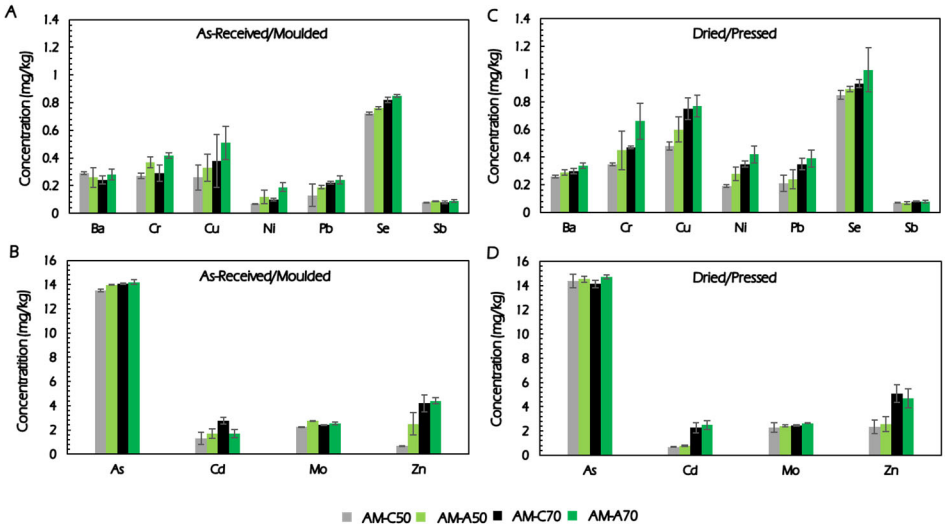

Figure 3.19. Mobility of contaminants of Anode Mud (AM) S/S – commercial (C)I/alternative (A) activator: (A) and (B) As-received waste and moulded; (C) and (D) Dried waste and pressed.

Figure 3.19(c) and (d) show the leaching results of the products obtained by dried and pressing. Cr, Cu, Cd, and Zn, with the highest mobility in the AM waste, present a similar behaviour; their mobility increases with the amount of dried waste added, at 25.5 %, 36 %, 70 %, and 53 % respectively. The rest of the elements show small variations of mobility regardless of the amount of dried waste added.

Regarding the activator used, the mobility of the elements presents a tendency like the products of dried waste added. The type of activator does not significantly affect

the mobility of the major elements, while the minor elements present variations in mobility between both activators.

Finally, comparing the results of mobility of both waste, CS and AM, introduced as-received/moulded or dried/pressed, the elements do not show significant variations. Concerning the main contaminants associated with acid waste, Cd and Zn, they present an irregular behaviour with the increase in the amount of waste. But for both elements, the immobilisation rate in the geopolymer matrices is very high. In the case of Cd, the leaching results of Cd^{2+} in deionized water can be attributed to the presence of Cd as a discrete hydroxide or similar alkali salt in the geopolymer matrix, and with little calcium presence, as in the case of matrices based on Fly Ash type F, the most stable phases host Cd^{2+}. At high pH values, the solubility of $Cd(OH)_2$ is very low, although it also appears to be sufficiently low at neutral pH values, which provides a reasonable degree of immobilisation, as observed in the results obtained (Provis and van Deventer, 2014). On the other hand, the immobilisation of Zn in alkali-activated fly ashes may occur by chemical retention in combination with physical encapsulation (Izquierdo et al., 2010; Yilmaz et al., 2015; Komonweeraket et al., 2015; Loncnar et al., 2016; Wan et al., 2019). The reaction of dissolved Zn with silica species present in the reaction medium of the geopolymer system leads to the formation of an insoluble Zn silicate phase (Nikolic et al., 2020). Other authors suggest that cationic species such as Zn^{2+} are adsorbed on geopolymer surfaces, and the more geopolymer gel formed, the more cations can be adsorbed, increasing physical microencapsulation (Wan et al., 2019). Few detailed studies of Zn immobilisation in alkali-activated fly ash matrices have yet been published. The results shown are relatively good, such as the immobilisation of a Zn-rich electric arc furnace dust using this type of binders obtained by Fernandez Pereira et al (Pereira et al., 2009; Provis and van Deventer, 2014).

On the other hand, the significant leaching of As and to a lesser extent the leaching of Mo in all the S/S products of both waste may be since it does not come from the residue but from the precursors, fly ash, and clay (

Table 3.5). Some authors reported that the incorporation of As from multicomponent mixed waste into geopolymers mobilized more arsenic than that available from untreated fly ash (Álvarez-Ayuso et al., 2008). It was observed that arsenic was associated with the iron-rich regions of fly ash particles, through the sorption of arsenic on iron hydroxide surfaces. It was also indicated that, when the pH values vary towards the alkaline range, the presence of excess alkali can lead to arsenic (III) solubility as arsenious acid or sodium arsenate (Maldonado-Alameda et al., 2020; Cifrian et al., 2021; Chen et al., 2022; Provis and van Deventer; 2009). In this way, Molybdenum, a trace element in coals and during the combustion process it becomes more concentrated in fly ash by-products, does not show any effect on the immobilisation, neither with the pre-treatment of the waste nor with the amount added. Molybdenum as a transition metal forms oxyanion species, so its immobilisation in this type of matrix tends to be problematic. Although most molybdenum compounds have low solubility in water, the presence of excess alkali can solubilize it as molybdate ion MoO_4^{-2}. Finally, Selenium is also found as a trace element in coal ashes and presents a leaching behaviour like As. As metalloids, the mobility of both increases when the pH values vary towards high alkalinity. In some geopolymerisation studies with coal fly ash, it has been shown that while there is a significant immobilisation of other trace elements, there is no notable effect on the leachable selenium concentration. Se mobility results showed higher leaching from geopolymer samples than from untreated ashes. It may be due to the availability of the inorganic phases of Se, mainly in the alkaline medium as selenate (SeO_4^{2-}) while in the acid medium as selenite (SeO_3^{2-}), being the selenate more soluble. As and Se, metalloids, together with Mo, transition metal, are considered as elements "bound with limited or mixed success" (Provis and van Deventer; 2014), that is, their availability to the environment has not been observed to be markedly reduced by geopolymerisation processes.

Immobilisation efficiency of Cd and Zn, major contaminants in both acid waste, was determined according to the percentage of the release of the contaminants of the S/S products with respect to the initial waste. The results for CS waste and AM waste were shown in Table 3.8 and Table 3.9 respectively.

As the amount of waste added to the FA-clay-based geopolymer increases, the efficiency decreases slightly. On the other hand, the commercial activator presents higher efficiency than the alternative activator. Even so, the immobilisation efficiency for Cd and Zn reaches values of efficiency above 99.40%. Similar high efficiencies, values higher than 90% immobilisation, are described for Zn-rich waste in Fly Ash-based geopolymers, in different studies (Pereira et al., 2009; Provis and van Deventer, 2014; Provis and van Deventer, 2009).

Table 3.8. Immobilisation efficiency of Cd and Zn from Cadmium Sponges (CS).

Type of processing	Immobilisation rate	CS	CS-C50	CS-A50	CS-C70	CS-A70
As received /Moulded	[Cd] (mg/kg)	2790	0.22±0.08	0.8±0.02	1.49±0.76	2.00±0.64
	[Zn] (mg/kg)	6690	1.3±0.36	4.1±0.84	0.5±0.21	1.1±0.56
	Cd (%)	-	99.99	99.97	99.94	99.92
	Zn (%)	-	99.98	99.94	99.99	99.98
Dried/ Pressed	[Cd] (mg/kg)	2790	1.54±0.05	1.7±0.22	1.18±0.18	1.3±0.35
	[Zn] (mg/kg)	6690	2.27±0.58	2.5±0.93	2.19±0.42	1.4±0.36
	Cd (%)	-	99.93	99.93	99.94	99.95
	Zn (%)	-	99.97	99.96	99.97	99.98

Table 3.9. Immobilisation efficiency of Cd and Zn from Anode Mud (AM).

Type of processing	Immobilisation rate	AM	AM-C50	AM -A50	AM -C70	AM -A70
As received /Moulded	[Cd] (mg/kg)	461	1.3±0.91	1.7±0.37	2.77±0.29	1.71±0.35
	[Zn] (mg/kg)	5720	0.7±0.01	2.5±0.93	4.3±0.54	4.7±0.26
	Cd (%)	-	99.72	99.63	99.40	99.62
	Zn (%)	-	99.98	99.95	99.60	99.57
Dried/ Pressed	[Cd] (mg/kg)	461	0.68±0.02	0.8±0.05	2.28±0.41	2.5±0.35
	[Zn] (mg/kg)	5720	2.34±0.54	2.5±0.62	4.98±0.74	4.17±0.39
	Cd (%)	-	99.85	99.82	99.50	99.46
	Zn (%)	-	99.95	99.95	99.57	99.57

3.3.2.1.3. *Accomplish landfill requirements*

Once the acid waste is S/S in the geopolymer matrix giving retention values greater than 99 %, the possibility of being disposed of in a controlled landfill based on the limits of non-hazardous waste established in the Decision 2003/33/EC is analysed in this section. The concentration of contaminants at 0, 50, and 70 % dosage of Cadmium Sponge (CS) and Anode Mud (AM) are represented in Figure 3.20 and Figure 3.21, respectively.

Ba, Cr, Cu, Mo, Ni, Pb, Sb, and Zn present concentrations below the non-hazardous limits for waste disposal regardless of the CS waste dosage, the treatment, or the type of activator used, as can be observed in Figure 3.20. Cd is below the non-hazardous limits when the Cadmium Sponge was immobilized as received by moulding using both types of activators. Nevertheless, Cd is above the non-hazardous limit when the

waste was dried and pressed. Therefore, the dried treatment of the waste favours the mobility of Cd. As can be observed in Figure 3.20, the amount of waste incorporated to increase the mobility of Cd increases, since Cd is one of the elements most representative of the cadmium sponge. Hence, Cd is above the non-hazardous limit for dosage of 70 % regardless of the treatment of waste or the type of activator used.

As and Se overcomes the non-hazardous limits even at 0 % of waste dosage demonstrating that these elements do not proceed from the Cadmium Sponge, but from precursors, the aluminosilicate sources used for the formation of geopolymer, coal fly ash, and clay. As and Se exceeds the non-hazardous limit regardless of the activator and the pre-treatment of waste.

In Figure 3.21, the concentration of contaminants in leachate after S/S of Anode Mud is represented concerning the non-hazardous waste disposal limits. The two geopolymer activators, with and without drying treatment at different Anode Mud (AM) dosages, 0, 50, and 70 % are plotted.

Ba, Cr, Cu, Mo, Ni, Pb, Sb, and Zn present concentrations below the non-hazardous limits for waste disposal regardless of the waste dosage, the treatment, or the type of activator used. In addition, Zn present less mobility when the 50 % Anode Mud was used as received for the two types of activators. In other elements, a similar tendency can be observed, although is most significant in the case of Zn.

Cd is below the non-hazardous limits when the Anode Mud waste was immobilized and dried for the two types of activators. Nevertheless, Cd is above the non-hazardous limit when the waste was used as received, although is close to the limit for the two activators.

As and Se overcomes the non-hazardous limits even at 0 % of waste dosage demonstrating that these elements do not proceed from the Anode Mud, same as for Cadmium Sponge. Finally, it can be concluded that the presence of As and Se is practically negligible in both residues, while their mobility is associated with the precursors used in the geopolymer matrix. In the case of As, in both, Fly ash and clay, and Se only with carbon by-products.

On the other hand, the mobility of Cd and Zn are associated with the addition of waste, obtaining a high immobilisation rate in the geopolymer matrix. In the case of Cd, in both CS and AM waste, with a dosage of 50 % of waste the landfill disposal limit is met, and with a dosage of 70 %, the values of concentrations are very close to the limits. Furthermore, the leaching of Zn is always below the limit.

Considering the activator used, the mobility of elements decreases using the commercial activator, although the concentrations of elements using the alternative activator $NaOH/Na_2CO_3$ are close to those obtained with the commercial activator

($NaOH/Na_2SiO_3$). Regarding the treatment of waste, the pre-treatment of the acid waste, far from improving the leaching results, for some elements, even worsens them. Therefore, in general, neither the type of activator nor the pre-treatment of the acid residues had a significant influence on the mobility of contaminants.

For these reasons, in the next step of this study, the optimisation and mathematical modeling, the geopolymeric matrices are going to be developed using only coal fly ash as the precursor, the alternative activator ($NaOH/Na_2CO_3$), and removing the pre-treatment step in the immobilisation of the acid waste.

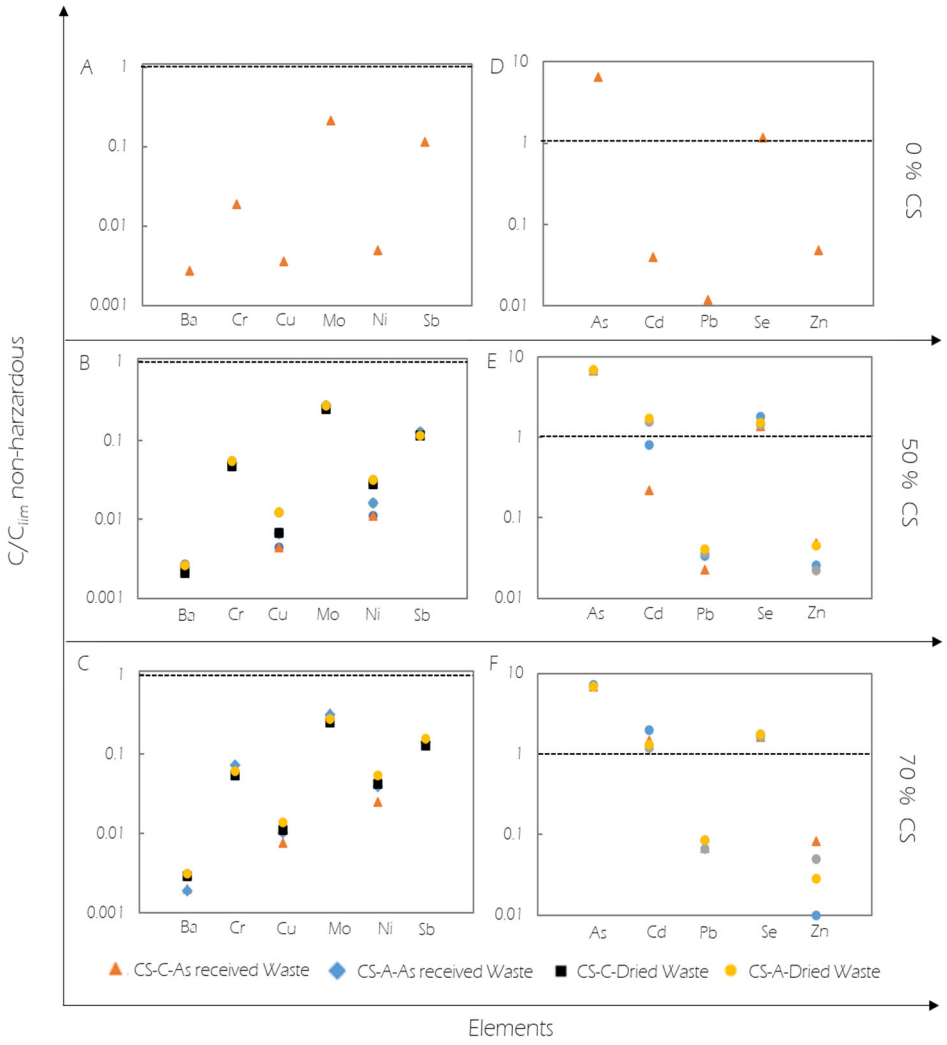

Figure 3.20. Contaminant concentration of geopolymers using commercial (C) or alternative (A) activator incorporating Cadmium Sponge (CS) with/without pretreatment regarding the non-hazardous waste landfill disposal limits: Ba, Cr, Cu, Mo, Ni, and Sb with 0 %, 50 % and 70 % (CS), (A), (B) and (C) respectively; As, Cd, Pb, Se, and Zn with 0 %, 50 %, and 70 % Cadmium Sponge (CS), (D), (E) and (F), respectively.

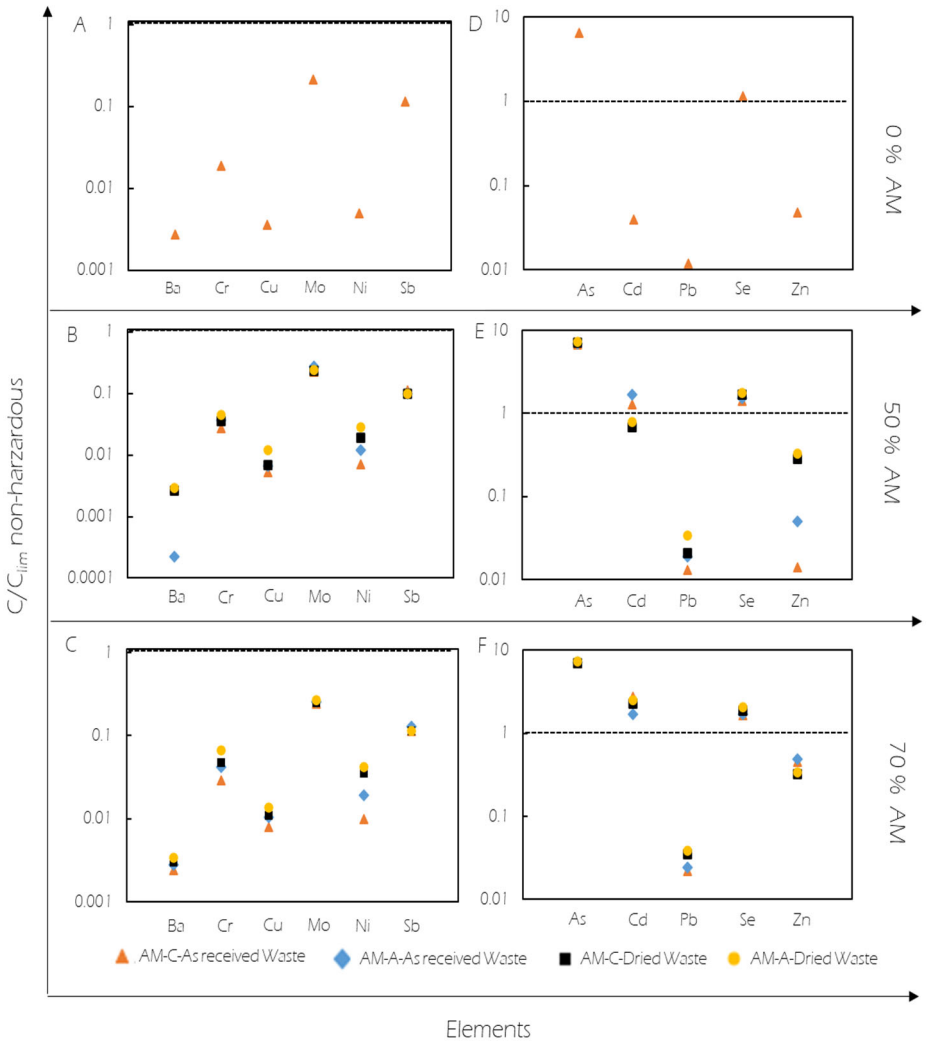

Figure 3.21. Contaminant concentration of geopolymers using commercial (C) or alternative (A) activator incorporating Anode Mud (AM) with/without pre-treatment regarding the non-hazardous waste landfill disposal limits: Ba, Cr, Cu, Mo, Ni, and Sb with 0%, 50%, and 70% Anode Mud (AM); (A); (B) and (C) respectively; As, Cd, Pb, Se, and Zn with 0%, 50% and 70%, Anode Mud (AM); (D); (E) and (F), respectively.

3.3.2.2. Optimisation and mathematical modelling of the S/S process

The immobilisation efficiency of both acid waste in geopolymer matrices has been demonstrated in the previous section. In all the cases studied, high retention of the major pollutants, Cd, and Zn, present in both acid waste has been observed. However, it is advisable to optimize the process through statistical analysis to determine the validity of the process variables in a greater range.

3.3.2.2.1. Optimisation of S/S formulations

A factorial experimental design to optimize the retention of critical pollutants of the two zinc plant acid residues, with three independent variables or factors, and five dependent variables or response variables were analysed.

The three independent variables or factors are acid waste-to-geopolymer ratio (X_1); liquid/solids ratio (X_2) where solids are the sum of the acid waste and the coal fly ash; and the molar concentration of NaOH (X_3). In X_1, the values studied in section 3.3.1 are maintained and an intermediate point is added. In addition, clay has been removed for the geopolymer formulations, therefore, only coal fly ash is used as a precursor. Due to the removal of clay, for processing the samples in this stage of the study only moulds were used. For this reason, the L/S ratio has been able to be increased (X_2). The objective of increasing the L/S ratio is to promote the increase of Si and Al concentrations in the aqueous phase, thus, improving the process of formation of the geopolymer system (Galiano et al., 2011; Panias et al., 2007; Rickard et al., 2011). Finally, in the variable X_3, different molar concentrations of the alkaline activator NaOH were studied. By increasing the concentration of NaOH in the aqueous phase of the geopolymer system, the dissolution rate of Si and Si-Al phases of the aluminosilicate sources increases, improving the efficiency of the geopolymer system. In Table 3.10 the three levels of the three selected independent variables or factors are shown.

Table 3.10. Experimental factorial design of the S/S process.

Variables	Levels		
	(-1)	(0)	(+1)
X_1: acid waste/geopolymer ratio	0.5	0.6	0.7
X_2: liquid/solid ratio	0.4	0.5	0.6
X_3: [NaOH] molar	6	8	10
Sample	X_1	X_2	X_3
P1	0.5	0.4	6
P2	0.5	0.4	10
P3	0.5	0.6	6
P4	0.5	0.6	10
P5	0.7	0.4	6
P6	0.7	0.4	10
P7	0.7	0.6	6
P8	0.7	0.6	10
P9	0.6	0.5	8
P10	0.6	0.5	8
P11	0.6	0.5	8

The five dependent variables or response variables studied were the density of S/S products and pH values and the concentration of As, Cd, and Zn in the leachate. As was chosen because forms oxyanion species that present the higher release from the geopolymer matrix (Izquierdo et al., 2009). Cd and Zn are the elements present at the highest concentrations in the acid waste. The acid waste was used as received and processed by moulding, so it can be removed in a pre-treatment step.

The results obtained for each of the experiments proposed in the factorial design of experiments for the S/S of CS and AM waste are shown in Table 3.11.

Table 3.11. Results of Cadmium Sponge (CS) and Anode Mud (AM) S/S in terms of pH values, geopolymer density, and concentrates of As, Cd, and Zn in the leachates (Leaching test EN 12457-2).

Sample	pH	Density (kg/m^3)	As (mg/kg)	Cd (mg/kg)	Zn (mg/kg)
P1 CS	11.30	1906.90	<0.1	<0.3	11.6
P2 CS	12.09	1535.20	<0.1	0.6	74.8
P3 CS	11.40	1924.90	0.2	0.3	2.40
P4 CS	12.06	1469.90	7.3	0.7	8.70
P5 CS	11.20	1465.10	<0.1	0.3	6.10
P6 CS	11.67	1607.30	1.8	<0.3	9.40
P7 CS	11.15	1991.60	<0.1	<0.3	17.8
P8 CS	11.94	1493.20	4.0	0.6	16.7
P9 CS	11.53	1997.00	4.5	<0.3	3.30
P10 CS	11.60	1713.50	4.7	<0.3	5.00
P11 CS	11.52	1733.40	1.7	<0.3	4.44
P1 AM	11.40	1389.48	<0.1	<0.3	4.48
P2 AM	11.56	1337.23	<0.1	<0.3	3.90
P3 AM	11.64	1348.82	<0.1	<0.3	14.3
P4 AM	11.70	1310.23	<0.1	<0.3	13.7
P5 AM	10.20	1343.84	<0.1	<0.3	4.90
P6 AM	10.51	1519.47	<0.1	<0.3	4.45
P7 AM	10.92	1384.54	<0.1	<0.3	0.60
P8 AM	11.12	1562.23	<0.1	<0.3	0.41
P9 AM	11.35	1351.28	<0.1	<0.3	5.20
P10 AM	11.38	1358.74	<0.1	<0.3	5.10
P11 AM	11.41	1350.19	<0.1	<0.3	5.30

Non-hazardous landfill limits: As < 2 mg/kg, Cd < 1mg/kg and Zn < 50 mg/kg (Decision 2003/33/EC).

The main difference with respect to the results obtained in the feasibility stage, using the mixture of Fly ash and Clay as precursors, is the drastic reduction in the leaching of Arsenic and Cadmium. All leaching results are below the landfill limits established for non-hazardous waste, < 2 mg/kg and < 1 mg/kg, respectively. In the case of CS products, for As, it is observed that samples that leach below the detection limit are associated with lower [NaOH] concentrations, which favour a lower solubility of sodium arsenate. In the case of S/S products with Anode Mud waste, the high reduction of As may be due to the increased presence of fly ash particles in the matrix

that provide regions rich in Fe, which favours the sorption of arsenic on iron hydroxide surfaces. While the immobilisation of Cd is associated with a significant increase in the range of pH values of the leachates of these materials in relation to the previous stage, at high pH values, the solubility of Cd $(OH)_2$ is very low. The concentration of Zn in the leachates in both acid waste does not exceed the limit, except in a single sample. On the other hand, the densities of these products are in the same order as the products developed using clay.

3.3.2.2.2. Mathematical modeling of the S/S process

Once the results obtained from the factorial design of experiments (Table 3.11) were analysed, the next step was to determine the mathematical model coefficients. Individual coefficients (a:X_1; b:X_2; c:X_3) and the combined ones (d: X_1X_2; e:X_1X_3; f:X_2X_3; g:X_1^2; h:X_2^2; i:X_3^2) were considered in the second-order polynomial equations. Nevertheless, only coefficients presenting statistically significant p-values below 0.05 were included in the equations meaning that the inlet variable significantly affects the response variable with a confidence level of 95 % (Table 3.12). As and Cd were not plotted nor mathematically adjusted since most of the experiments resulted in values below the detection limit of the ICP-AES.

According to the mathematical adjustment for Cadmium Sponge, the highest influence on pH values relies on NaOH molar concentration (X_3) and the combined effect of CS waste/geopolymer matrix ratio and NaOH concentration (X_1:X_3). The variable (X_3) has a positive effect on pH due to the alkalinity, while the combined effect of CS/geopolymer ratio and NaOH concentration has a negative effect due to the acidity of the Cadmium Sponge. Zn leachate concentration is affected by all the variables. The highest effect was observed in the NaOH concentration, and the combination of CS/geopolymer ratio and Liquid/Solid ratio (X_1:X_2) presented the highest coefficient. This combined effect favours the leaching of Zn due to the highest content of Zn that the CS has, while the other observed combined effect decreases the leaching of Zn.

In relation to Anode Mud waste, the pH values decrease mainly by the amount of acid residue added to the geopolymer matrix (X_1). The mathematical adjustment of the Zn concentration in the leachate shows quantitative effects of the variables X_1 and X_2 individually, which is neutralized with the combined effect of both. Therefore, the results do not allow trends, so it is necessary to perform response surfaces graphs.

Deviations between the predicted values, estimated using the statistical model, and the experimental values are below 2 % in the case of pH of the CS and AM leachates. Deviations below 5 % are in the case of AM geopolymer density and the Zn concentration of the AM leachate. The worst adjustment (<20 %) and consequently the highest difference between predicted and experimental values is the Zinc

concentration of the CS leachate. In general, all errors are very small, demonstrating adequate statistical data analysis.

Table 3.12. Mathematical adjustment of the response variables of the experimental design.

Cadmium Sponge (CS)	Regression Coefficient
$pH = 10.23+0.252 \cdot X_3-0.138 \cdot X_1 \cdot X_3$	$R^2 = 0.951$
$Zn = -206.14+58.92 \cdot X_3+616.19 \cdot X_1 \cdot X_2-45.71 \cdot X_1 \cdot X_3-54.0 \cdot X_2 \cdot X_3$	$R^2 = 0.735$
Anode Mud (AM)	**Regression Coefficient**
$pH = 13.86-6.33 \cdot X_1+3.79 \cdot X_1 \cdot X_2$	$R^2 = 0.880$
$Density = 2269-1690.43 \cdot X_1-150.16 \cdot X_3+277.60 \cdot X_1 \cdot X_3$	$R^2 = 0.880$
$Zn = -86.79+142.43 \cdot X_1+223.97 \cdot X_2-349.75 \cdot X_1 \cdot X_2$	$R^2 = 0.993$

In Figure 3.22 and Figure 3.23 the response surfaces are plotted for Cadmium Sponge and Anode Mud. The pH values in leachates, S/S product density, and mobility of Zn are represented as a function of the two inlet variables that affect them more.

From the results shown for both acid waste, when the amount of acid waste added increases, there is a decrease in the mobility of Zn in the leachate. While the concentration of NaOH slightly influences Zn mobility for CS products, no influence for the AM products is found.

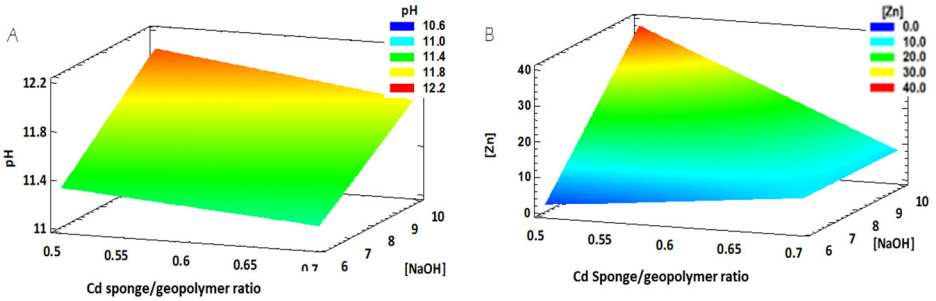

Figure 3.22. Response surface of Cadmium Sponge (CS): pH values and Zn concentration versus waste-geopolymer ratio and NaOH concentration, (A) and (B) respectively.

Considering the non-hazardous waste landfill disposal limit established by the Decision 2003/33/EC and Figure 3.22 (a) and (b) for Cadmium Sponge (CS), it can be concluded that the optimal operating range conditions for all the dependent variables are: acid waste/geopolymer ratio between 0.55-0.65, liquid/solid ratio above 0.55 and NaOH concentration of 6 M. In the case of the Anode Mud waste according to the response surfaces of Figure 3.23, optimal conditions are acid waste/geopolymer ratio of 0.7, liquid/solid ratio above 0.6 and NaOH concentration between 6-10 M.

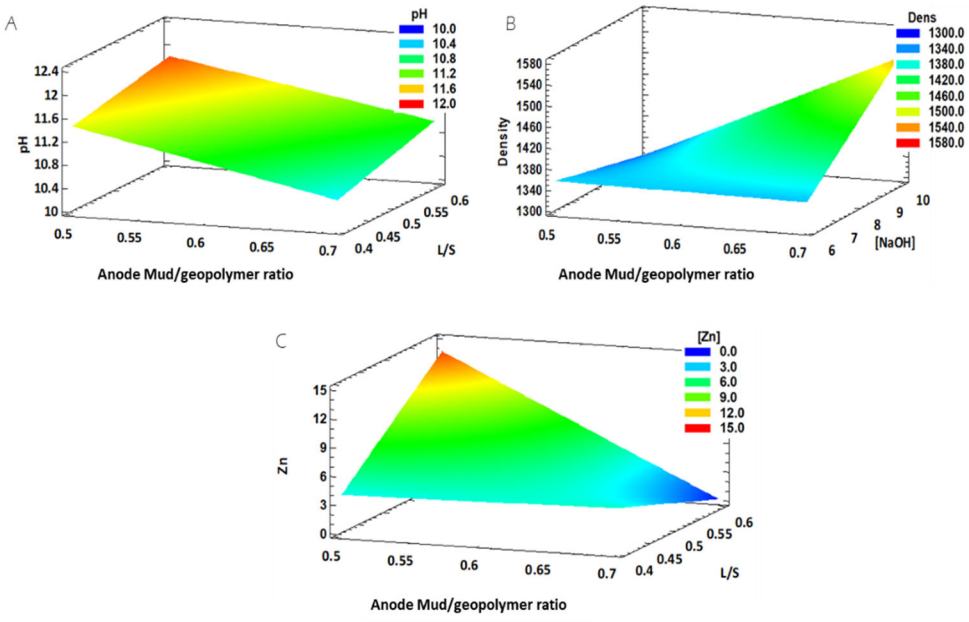

Figure 3.23. Response surface of Anode Mud (AM): pH values (A), geopolymer density (B), and Zn concentration (C) versus waste-geopolymer ratio, liquid-solid ratio, and NaOH concentration.

3.4. CONCLUSIONS

In this work it was studied the feasibility of alkaline activator of various alkaline by-products from SOLVAY process, two liquids (Ca and Mg Slurry and CaO Slurry), and 4 solids (Na_2CO_3 Powder, $HNaCO_3$ Powder, Si-$CaCO_3$- CaOH and CaO rocks). In addition, it also studied the influence of clay in the formation of geopolymers. In the feasibility of using alkaline by-products in geopolymerisation processes the Si-$CaCO_3$-CaOH and CaO rocks prevented activated alkali product formation due to the expansion in bricks, while the Ca and Mg Slurry, CaO Slurry, Na_2CO_3 Powder and $HNaCO_3$ Powder were suitable for activation of silicoaluminate matrix replacing commercial NaOH and Na_2SiO_3. For substitutions of 10, 30, and 50% of NaOH and Na_2SiO_3 by Ca and Mg Slurry, CaO Slurry, Na_2CO_3 Powder, and $HNaCO_3$ Powder water absorption results present similar values to the reference geopolymer and flexural strength have similar values at 10% substitution and close at the others substitutions. It can be concluded that these alkaline by-products can be used as substitutes for commercial activators. Clay plays an important role in the development of geopolymers. There is a difference of 9 units in the results of water absorption and 7 units of flexural strength results between fly ash/clay geopolymer and fly ash geopolymer, so it can say that the clay participates in the process of geopolymerisation providing aluminosilicate groups and improving the properties of geopolymers. Fly ash/Clay geopolymers present values of water absorption and flexural strength equal to or exceeding the reference values of these properties for fired clay bricks obtained by the pressing method, while for fly ash geopolymer the method most suitable is extrusion. More studies are needed to assess this conclusion.

Na_2CO_3 Powder and $HNaCO_3$ Powder present the best results of the alkaline by-products, so the influence of the alkaline by-products dosage on the properties of final products was studied. Both by-products have flexural strength and absorption water similar obtaining better results for the Na_2CO_3 Powder but it can be concluded that these streams can be used as substitutes for commercial activators because they participate in the geopolymerisation reaction and decrease the price of geopolymers. Na_2CO_3 Powder is the alkaline by-product that presents the best results of flexural strength and water absorption, hence it was studied the feasibility of using alkaline by-products from SOLVAY processes as geopolymer binder in the S/S process.

A more sustainable strategy for the solidification and stabilisation (S/S) of acid waste from the zinc production industry—Cadmium Sponge (CS) and Anode Mud (AM) as a treatment before disposal in a landfill—has been addressed.

For the development of geopolymers, they have been tested: (i) as precursors: coal fly ash and clay; (ii) as activators: a commercial one, based on sodium silicate and sodium hydroxide, and an alternative one, in which the silicates are partially replaced

by a sodium carbonate by-product; (iii) two dosages of acid waste (50 % and 70 %); and (iv) two processing methods: moulding (with as-received waste) and pressing (with dried waste).

The acid waste S/S values need to be evaluated both technically and environmentally to assess whether they meet the criteria for landfill disposal. All the samples meet the compressive strength limit required in landfills for monoliths (3 MPa). From the environmental point of view, in general, neither the type of activator nor the pre-treatment of the acid waste had a significant influence on the mobility of the contaminants.

The contents of As and Se are practically negligible in both waste, so their mobility in the S/S products is associated with the precursors used in the geopolymer matrix, in the case of As, in both fly ash and clay, and Se only with carbon by-products. On the other hand, the mobility of Cd and Zn is associated with the addition of waste, obtaining a high immobilisation rate greater than 99 %. In the case of Cd, in both waste, CS and AM, with a dosage of 50 %, the non-hazardous waste landfill disposal limit is met. Furthermore, the leaching of Zn is always below the limit.

Once the feasibility of the S/S process has been demonstrated, the optimisation has been carried out, removing clay from the geopolymer formulation, using only coal fly ash as a precursor, the alternative activator ($NaOH/Na_2CO_3$), and without pre-treatment of the acid waste. The geopolymer parameters, acid waste/geopolymer ratio, liquid/solid ratio, and NaOH molar concentration allow to obtain a significant reduction in the release of As and Cd, and Zn is kept at acceptable values for both acid waste. According to the mathematical adjustment and response surfaces, it can be concluded that the optimal operating range conditions for CS S/S products are a waste/geopolymer ratio between 0.55 and 0.65, liquid/solid ratio above 0.55, and NaOH molar concentration of 6, while, for the AM S/S products, these values are a waste/geopolymer ratio above 0.7, liquid/solid above 0.6, and NaOH concentration in the interval 6 to 10 M, which meet the non-hazardous waste landfill disposal limits for the S/S of zinc plant residues (ZPR).

3.5. REFERENCES

- Ahmari, S.; Parameswaran, K.; Zhang, L. Alkali Activation of Copper Mine Tailings and Low-Calcium Flash-Furnace Copper Smelter Slag. J. Mater. Civil Eng. 2015, 27(6), 04014193.
- Álvarez-Ayuso, E.; Querol, X.; Plana, F.; Alastuey, A.; Moreno, N.; Izquierdo, M.; Font, O.; Moreno, T.; Díez, S.; Vázquez, E.; et al. Environmental, physical and structural characterisation of geopolymer matrixes synthesised from coal (co-)combustion fly ashes. J. Hazard. Mater. 2008, 154, 175–183.
- Aparajith, B.; Kumar, A.; Hodder, D.; Gupta, M. Recovery of cadmium from hydrometallurgical zinc smelter by selective leaching. Hydrometallurgy 2010, 102, 31–36.
- Ayala, J.; Fernández, B. Reuse of Anode Slime Generated by the Zinc Industry to Obtain a Liquor for Manufacturing Electrolytic Manganese. JOM 2013, 65, 1007–1014.
- Bakharev, T.; Sanjayan, J.G.; Cheng, Y.-B. Effect of admixtures on properties of alkali-activated slag concrete. Cement Concrete Res. 2000, 30(9), 1367-1374.
- Bakhshi, M.; Mohammad, S.; Hosseini, R.; Rahimi, M. Cadmium Filter Cake of a Hydrometallurgical Zinc Smelter as a New Source for the Biological Synthesis of CdS Quantum Dots Using AASX (Air-assisted solvent extraction) for dilute solution View project. Int. J. Biotechnol. Bioeng. 2017, 11, 148–152.
- Barreto, L.S.S.; Ghisi, E.; Godoi, C.; Oliveira, F.J.S. Reuse of ornamental rock solid waste for stabilisation and solidification of galvanic solid waste: Optimisation for sustainable waste management strategy. J. Clean. Prod. 2020, 275, 122996.
- Bernal, S.A.; Provis, J.L.; Fernández-Jiménez, A.; Krivenko, P.V.; Kavalerova, E.; Palacios, M.; Shi, C. Binder Chemistry – High-Calcium Alkali- Activated Materials. Book Chapter of Alkali Activated Materials. 59-91.
- Bhagath Singh, G.V.P.; Subramaniam, K.V.L. Quantitative XRD study of amorphous phase in alkali activated low calcium siliceous fly ash. Const. Build. Mat. 2016, 124, 139-147.
- Bobirica, C., Shim, J-H., Pyeon, J-H., Park, J-Y. (2015). Influence of waste glass on the microstructure and strength of inorganic polymers. Ceramics International, 41(10), 13638-13649.
- Chandra, N.; Amritphale, S.; Pal, D. Manganese recovery from secondary resources: A green process for carbothermal reduction and leaching of manganese bearing hazardous waste. J. Hazard. Mater. 2011, 186, 293–299.
- Chen, Y.; Chen, F.; Zhou, F.; Lu, M.; Hou, H.; Li, J.; Liu, D.; Wang, T. Early solidification/stabilisation mechanism of heavy metals (Pb, Cr and Zn) in Shell coal gasification fly ash based geopolymer. Sci. Total Environ. 2022, 802, 149905.
- Cifrian, E.; Dacuba, J.; Llano, T.; Díaz-Fernández, M.D.C.; Andrés, A. Coal Fly Ash–Clay Based Geopolymer-Incorporating Electric Arc Furnace Dust (EAFD): Leaching Behaviour and Geochemical Modeling. Appl. Sci. 2021, 11, 810.
- De Barros, F.C.; Abreu, C.S.; de Lemos, L.R. Separation of Cd(II), Cu(II) and zinc sulfate from waste produced in zinc hydrometal- lurgy cementation. Sep. Sci. Technol. 2021, 56, 1360–1369.
- Dreisinger, D.; Glück, T.; Lu, J.; Xie, F.; Marte, K.; Parada, F. New Developments in the Recovery of Copper, Cobalt, Zinc and Manganese in the Boleo Process. In Proceedings of the 2012 SME Annual Meeting and Exhibit 2012, SME 2012, Meeting Preprints, Seattle, WA, USA, 19–22 February 2012; pp. 191–201.
- Duvallet, T.Y.; Frouin, L.; Robl, T.L. Effect of fly ash particles packing on performance of OPC-activated GGBS slag. 2015 World of Coal Ash (WOCA) Conference. Nashville, TN.

- Duxson, P.; Fernández-Jiménez, A.; Provis, J.L.; Lukey, G.C.; Palomo, A.; van Deventer, J.S.J. Geopolymer technology: the current state of the art. J. Mater. Sci. 2007, 42, 2917-2933.
- El-Eswed, B.I. Chemical evaluation of immobilisation of waste containing Pb, Cd, Cu and Zn in alkali-activated materials: A critical review. J. Environ. Chem. Eng. 2020, 8, 104194.
- Favier, A.; Hot, J.; Habert, G.; Roussel, N.; d'Espinose de Lacaillerie, J.-B. Flow properties of MK-based geopolymer pastes. A comparative study with standard Portland cement pastes. Soft Matter, 2014, 10, 1134-1141.
- Fawer, M.; Concannon, M.; Rieber, W. Life cycle inventories for the production of sodium silicates. Int. J. Life Cycle Ass. 1999, 4(4), 207-212.
- Fernández-Jiménez, A.; García-Lodeiro, I.; Maltseva, O.; Palomo, A. Mechanical-chemical activation of coal fly ashes: an effective way for recycling and make cementitious materials. Front. Mat. 2019, 6(51), 1-16.
- Fernández-Jiménez, A.; Palomo, A. Characterisation of fly ashes. Potential reactivity as alkaline cements. Fuel 2003, 82, 2259-2265.
- Fernández-Jiménez, A.; Palomo, A. Composition and microstructure of alkali activated fly ash binder: Effect of the activator. Cement Concrete Res. 2005, 35, 1984-1992.
- Fongang, R.T.T.; Pemndje, J.; Lemougna, P.N.; Melo, U.C.; Nanseu, C.P.; Nait-Ali, B.; Kamseu, E.; Leonelli, C. Cleaner production of the lightweight insulating composites: Microstructure, pore network and thermal conductivity. Energ. Buildings 2015, 107, 113-122.
- Fort, J.; Vejmelková E.; Konáková, D.; Alblová N.; Cáchová, M.; Keppert, M.; Rovnaníková, P., Cerný, R. Application of waste brick powder in alkali activated aluminosinosilicates: functional and environmental aspects. J. Clean. Prod. 2018, 194, 714-725.
- Galiano, Y.L.; Pereira, C.F.; Vale, J. Stabilisation/solidification of a municipal solid waste incineration residue using fly ash-based geopolymers. J. Hazard. Mater. 2011, 185, 373–381.
- Gharabaghi, M.; Irannajad, M.; Azadmehr, A.R. Leaching behaviour of cadmium from hazardous waste. Sep. Purif. Technol. 2012, 86, 9–18.
- Grudinsky, P.; Pankratov, D.; Kovalev, D.; Grigoreva, D.; Dyubanov, V. Comprehensive Study on the Mechanism of Sulfating Roasting of Zinc Plant Residue with Iron Sulfates. Materials 2021, 14, 5020.
- Habert, G.; d'Espinose de Lacaillerie, J.B.; Roussel, N. An environmental evaluation of geopolymer based concrete production: reviewing current research trends. J. Clean. Prod. 2011, 19, 1229-1238.
- Harja, M.; Buema, G.; Bulgariu, L.; Bulgariu, D.; Sutiman, D.M.; Ciobanu, G. Removal of cadmium(II) from aqueous solution by adsorption onto modified algae and ash. Korean J. Chem. Eng. 2015, 32, 1804–1811.
- He, R., Dai, N., Wang, Z. Thermal and Mechanical Properties of Geopolymers Exposed to High Temperature: A Literature Review. Adv. Civil Eng. 2020, 7532703.
- Hoang, J.; Reuter, M.; Matusewicz, R.; Hughes, S.; Piret, N. Top submerged lance direct zinc smelting. Miner. Eng. 2009, 22, 742–751.
- Hu, J.-L.; Yang, X.-S.; Liu, T.; Shao, L.-N.; Zhang, W. Adsorption characteristic of As(III) on goethite waste generated from hydrometallurgy of zinc. Water Sci. Technol. 2017, 75, 2747–2754.
- Huang, T.; Zhou, L.; Chen, L.; Liu, W.; Zhang, S.; Liu, L. Mechanism exploration on the aluminum supplementation coupling the electrokinetics-activating geopolymerisation that reinforces the solidification of the municipal solid waste incineration fly ashes. Waste Manag. 2020, 103, 361–369.

- Huang, X.; Zhuang, R.; Muhammad, F.; Yu, L.; Shiau, Y.; Li, D. Solidification/stabilisation of chromite ore processing residue using alkali-activated composite cementitious materials. Chemosphere 2017, 168, 300–308.
- Izquierdo, M.; Querol, X.; Davidovits, J.; Antenucci, D.; Nugteren, H.; Pereira, C.F. Coal fly ash-slag-based geopolymers: Microstructure and metal leaching. J. Hazard. Mater. 2009, 166, 561–566.
- Izquierdo, M.; Querol, X.; Phillipart, C.; Antenucci, D.; Towler, M. The role of open and closed curing conditions on the leaching properties of fly ash-slag-based geopolymers. J. Hazard. Mater. 2010, 176, 623–628.
- Jaimes, R.; Miranda-Hernández, M.; Lartundo-Rojas, L.; González, I. Characterisation of anodic deposits formed on Pb–Ag electrodes during electrolysis in mimic zinc electrowinning solutions with different concentrations of Mn(II). Hydrometallurgy 2015, 156, 53–62.
- Kamseu, E.; NGouloure, A.N.M.; Ali, B.N.; Zekeng, S.; Melo, U.C.; Rossignol, S.; Leonelli, C. Cumulative pore volume, pore size distribution and phasespercolation in porous inorganic polymer composites:Relation microstructure and effective thermal conductivity. Energ. Build. 2015, 88, 45-56.
- Keppert, M.; Vejmelková, E.; Bezdička, P.; Dolezelová, M.; Cáchová, M.; Schainherrová, L.; Pokorný, J.; Vysvaril, M.; Rovnaníková, P.; Černý, R. Red-clay ceramic powders as geopolymer precursors: Consideration of amorphous portion and CaO content. Appl. Clay Sci. 2018, 161, 82-89.
- Khankhaje, E.; Hussin, M.W.; Mirza, J.; Rafieizonooz, M.; Salim, M.R.; Siong h.c.; Warid, M.N.M. On blended cement and geopolymer concretes containing palm oil fluel ash. Mat. Design 2016, 89, 385-398.
- Komonweeraket, K.; Cetin, B.; Aydilek, A.H.; Benson, C.H.; Edil, T.B. Effects of pH on the leaching mechanisms of elements from fly ash mixed soils. Fuel 2015, 140, 788–802.
- Lee, W.K.W.; van Deventer, J.S.J. Structural reorganisation of class F fly ash in alkaline silicate solutions. Colloids and Surfaces A: Physicochem. Eng. Aspects. 2002, 211, 49-66.
- Li, B.; Wang, X.; Wei, Y.; Wang, H.; Barati, M. Extraction of copper from copper and cadmium residues of zinc hydrometallurgy by oxidation acid leaching and cyclone electrowinning. Miner. Eng. 2018, 128, 247–253.
- Li, S.; Huang, X.; Muhammad, F.; Yu, L.; Xia, M.; Zhao, J.; Jiao, B.; Shiau, Y.; Li, D. Waste solidification/stabilisation of lead–zinc slag by utilizing fly ash based geopolymers. RSC Adv. 2018, 8, 32956–32965.
- Li, Y.; Min, X.; Ke, Y.; Liu, D.; Tang, C. Preparation of red mud-based geopolymer materials from MSWI fly ash and red mud by mechanical activation. Waste Manage. 2019, 83, 202-208.
- Liu, L.C.; Zhang, Y.J.; Chen, H.; He, P.Y.; Hu, Z.S. Potential of Cost-Effective Phosphoric Acid-Based Geopolymer as Photocatalyst for Dye Wastewater Degradation. Integrated Ferroelectrics, 2021, 218(1). 208-214.
- Loncnar, M.; van der Sloot, H.A.; Mladenovicˇ, A.; Zupancˇicˇ, M.; Kobal, L.; Bukovec, P. Study of the leaching behaviour of ladle slags by means of leaching tests combined with geochemical modeling and mineralogical investigations. J. Hazard. Mater. 2016, 317, 147–157.
- Mahon, M.; Alfantazi, A. Manganese consumption during zinc electrowinning using a dynamic process simulation. Hydrometallurgy 2014, 150, 184–191.
- Maldonado-Alameda, À.; Giro-Paloma, J.; Alfocea-Roig, A.; Formosa, J.; Chimenos, J.M. Municipal Solid Waste Incineration Bottom Ash as Sole Precursor in the Alkali-Activated Binder Formulation. Appl. Sci. 2020, 10, 4129.

- Manikandan, P.; Natrayan, L.; Duraimurugan, S.; Vasugi, V. Influence of Waste Glass Powder as an Aluminosilicate Precursor in Synthesizing Ternary Blended Alkali-Activated Binder. Silicon, 2022, Article in Press.
- Mao, Y.; Muhammad, F.; Yu, L.; Xia, M.; Huang, X.; Jiao, B.; Shiau, Y.; Li, D. The Solidification of Lead-Zinc Smelting Slag through Bentonite Supported Alkali-Activated Slag Cementitious Material. Int. J. Environ. Res. Public Health 2019, 16, 1121.
- Martínez-Sánchez, M.; Solan-Marín, A.; Hidalgo, A.; Pérez-Sirvent, C. Characterisation and mobilisation of toxic metals from electrolytic zinc waste. Chemosphere 2019, 233, 414–421.
- Mellado, A.; Catalán, C.; Bouzón, N.; Borrachero, M.V.; Monzó, J.M.; Payá, J. Carbon footprint of geopolymeric mortar: Study of the contribution of the alkaline activating solution and assessment of an alternative route. RSC Advances, 2014, 4(45), 23846-23852.
- Mohr, S.; Giurco, D.; Retamal, M.; Mason, L.; Mudd, G. Global Projection of Lead-Zinc Supply from Known Resources. Resources 2018, 7, 17.
- Moradkhani, D.; Rasouli, M.; Behnian, D.; Arjmandfar, H.; Ashtari, P. Selective zinc alkaline leaching optimisation and cadmium sponge recovery by electrowinning from cold filter cake (CFC) residue. Hydrometallurgy 2012, 115–116, 84–92.
- Nguyen, T.A.; Guo, X.; You, F.; Saha, N.; Wu, S.; Scheuermann, A.; Ren, C.; Huang, L. Co-solidification of bauxite residue and coal ash into indurated monolith via ambient geopolymerisation for in situ environmental application. J. Hazard. Mater. 2021, 422, 126925.
- Nikolic´, I.; Đurovic´, D.; Markovic´, S.; Veselinovic´, L.; Jankovic´-Cˇ astvan, I.; Radmilovic´, V.V.; Radmilovic´, V.R. Alkali activated slag cement doped with Zn-rich electric arc furnace dust. J. Mater. Res. Technol. 2020, 9, 12783–12794.
- Nikolic´, V.; Komljenovic´, M.; Džunuzovic´, N.; Ivanovic´, T.; Miladinovic´, Z. Immobilisation of hexavalent chromium by fly ash-based geopolymers. Compos. Part B Eng. 2017, 112, 213–223.
- Niu, M.; Li, G.; Wang, Y.; Li, Q.; Han, L.; Song, Z. Comparative study of immobilisation and mechanical properties of sul- foaluminate cement and ordinary Portland cement with different heavy metals. Constr. Build. Mater. 2018, 193, 332–343.
- Ogundiran, M.B.; Nugteren, H.W.; Witkamp, G.J. Immobilisation of lead smelting slag within spent aluminate—Fly ash based geopolymers. J. Hazard. Mater. 2013, 248–249, 29–36.
- Ozer, I.; Soyer-Uzun, S. Relations between the structural characteristics and compressive strength in metakaolin based geopolymers with different molar Si/Al ratios. Ceramics Int. 2015, 41(8), 10532, 10192-10198.
- Pacheco-Torgal, F.; Castro-Gomes, J.; Jalali, S. Alkali-activated binders: A review Part 1. Historical background, terminology, reaction mechanisms and hydration products. Constr. Build. Mater. 2008, 22, 1305-1314.
- Palomo, A.; Fuente, J.L.D.; Palomo, A.; Fuente, J.L.D. Alkali-activated cementitous materials: Alternative matrices for the immobilisation of hazardous waste: Part I. Stabilisation of boron. Cem. Concr. Res. 2003, 33, 281–288.
- Palomo, A.; Maltseva, O.; García-Lodeiro, I.; Fernández-Jiménez, A. Portland Versus Alkaline Cement: Continuity or Clean Break: "A Key Decision for Global Sustainability". Frontiers Chem. 2021, 9, 705475.
- Panias, D.; Giannopoulou, I.P.; Perraki, T. Effect of synthesis parameters on the mechanical properties of fly ash-based geopolymers. Colloids Surf. A Physicochem. Eng. Asp. 2007, 301, 246–254.

- Panias, D.; Giannopoulou, I.P.; Perraki, T. Effect of synthesis parameters on the mechanical properties of fly ash-based geopolymers. Colloids and Surfaces A: Physicochem. Eng. Aspects, 2007, 301, 246-254.
- Panias, D.; Giannopoulou, I.P.; Perraki, T. Effect of synthesis parameters on the mechanical properties of fly ash-based geopolymers. Colloids and Surfaces A: Physicochem. Eng. Aspects 2007, 301, 246-254.
- Passuello, A.; Rodríguez, E.D.; Hirt, E.; Longhi, M.; Bernal, S.A.; Provis, J.L.; Kirchheim, A.P. Evaluation of the potential improvement in the environmental footprint of geopolymers using waste-derived activators. J. Clean. Prod. 2017, 166, 680-689.
- Paz-Gómez, D.C.; Vilarinho, I.S.; Pérez-Moreno, S.M.; Carvalheiras, J.; Guerrero, J.L.; Novais, R.M.; Seabra, M.P.; Ríos, G.; Bolívar, J.P.; Labrincha, J.A. Immobilisation of Hazardous Waste on One-Part Blast Furnace Slag-Based Geopolymers. Sustainability 2021, 13, 13455.
- Pereira, C.F.; Luna, Y.; Querol, X.; Antenucci, D.; Vale, J. Waste stabilisation/solidification of an electric arc furnace dust using fly ash-based geopolymers. Fuel 2009, 88, 1185–1193.
- Phair, J.W.; Van Deventer, J.S.J. Effect of the silicate activator pH on the microstructural characteristics of waste-based geopolymers. Int. J., Mineral Process. 2002, 66(1-4), 121-143.
- Praveen Kumar, T.R.; Sudheesh, C.; Sasi Kumar, S. The properties and performance of red mud-based geopolymeric masonry blocks. Int. J. chemTech Res. 2015, 8(2), 738-745.
- Provis, J.L.; van Deventer, J.S.J. Alkali Materials Activated RILEM-State-of-the-Art Report; Springer: Dordrecht, The Netherlands, 2014; Volume 13.
- Provis, J.L.; van Deventer, J.S.J. Geopolymers: Structures, Processing, Properties and Industrial Applications; Woodhead Publishing: Waltham, MA, USA, 2009.
- Ren, X.; Zhang, L.; Ramey, D.; Waterman, B.; Ormsby, S. Utilisation of aluminum sludge (AS) to enhance mine tailings-based geopolymer. J. Mater. Sci. 2015, 50, 1370-1381.
- Rickard, W.D.; Williams, R.; Temuujin, J.; van Riessen, A. Assessing the suitability of three Australian fly ashes as an aluminosilicate source for geopolymers in high temperature applications. Mater. Sci. Eng. A 2011, 528, 3390–3397.
- Robayo-Salazar, R.; Mejía-Arcila, J.; de Gutiérrez, R.M.; Martínez, E. Life cycle assessment (LCA) of an alkali-activated binary concrete based on natural volcanic pozzolan: A comparative analysis to OPC concrete. Constr. Build. Mater. 2018, 176, 103-111.
- Ruiz-Santaquiteria, C.; Fernández-Jiménez, A.; Skibsted, J.; Palomo, A. Clay reactivity: Production of alkali activated cements. App. Clay Sci. 2013, 73, 11-16.
- Salami, B.A.; Johari, M.A.M.; Ahmad, Z.A. Impact of added water and superplasticizer on early compressive strength of selected mixtures of palm oil fuel ash-based engineered geopolymer composites. Const. Build. Mat. 2016, 109, 198-206.
- Sassoni, E., Pahlavan, P., Franzoni, E., Bignozzi, M.C. (2016). Valorisation of brick waste by alkali-activation: A study on the posible use for mansory repointing. Ceramics International, 42(13), 14685-14694.
- Shekhovtsova, J.; Zhernovsky, I.; Kovtun, M.; Kozhukhova, N.; Zhernovskaya, I. Estimation of fly ash reactivity for use in alkali-activated cements – A step towards sustainable building material and waste utilisation. J. Clean. Prod. 2018, 178, 22-33.
- Shi, C.; Fernández-Jiménez, A.; Palomo, A. New Cements for the 21st century: The pursuit of an alternative to Portland cement. Cem. Concr. Res. 2011, 41, 750-763.
- Shi, C.; Fernández-Jiménez, A.M. Stabilisation/solidification of hazardous and radioactive waste with alkali-activated cements. J. Hazard. Mater. 2006, 137, 1656–1663.
- Shi, C.; Jimenez, A.F.; Palomo, A. New cements for the 21st century: The pursuit of an alternative to Portland cement. Cem. Concr. Res. 2011, 41, 750–763.

- Soutsos, M.; Boyle, A.P.; Vinai, R.; Hadjierakleous, A.; Barnett, S.J. Factors influencing the compressive strength of fly ash based geopolymers. Const. Build. Mat. 2016, 110, 355-368.
- Tong, K.T.; Vinai R.; Soutsos, M.N. Use of Vietnamese rice husk ash for the production of sodium silicate as the activator for alkali-activated binders. J Clean. Prod. 2018, 201, 272-286.
- Torres-Carrasco, M.; Puertas, F. Waste glass in the geopolymer prepartion. Mechanical and microstructural characterisation. J. Clean. Prod. 2015, 90, 397-408.
- Torres-Carrasco, M.; Puertas, F. Waste glass in the geopolymer preparation. Mechanical and microstructural characterisation. J. Clean. Prod. 2015, 90, 397-408.
- Turner, L.K.; Collins, F.G. Carbon dioxide equivalent (CO2-e) emissions: A comparison between geopolymer and OPC cement concrete. Constr. Build. Mater. 2013, 43, 125-130.
- Vu, T.H.; Gowripalan, N. Mechanisms of Heavy Metal Immobilisation using Geopolymerisation Techniques—A review. J. Adv. Concr. Technol. 2018, 16, 124–135.
- Wan, Q.; Rao, F.; Song, S.; Zhang, Y. Immobilisation forms of ZnO in the solidification/stabilisation (S/S) of a zinc mine tailing through geopolymerisation. J. Mater. Res. Technol. 2019, 8, 5728–5735.
- Wang, R.; Yan, Q.; Su, P.; Shu, J.; Chen, M.; Xiao, Z.; Han, Y.; Cheng, Z. Metal mobility and toxicity of zinc hydrometallurgical residues. Process Saf. Environ. Prot. 2020, 144, 366–371.
- Xing, W.D.; Sohn, S.H.; Lee, M.S. A Review on the Recovery of Noble Metals from Anode Slimes. Miner. Process. Extr. Met. Rev. 2020, 41, 130–143.
- Yang, K.-H.; Song, J.-K.; Song, K.I.I. Assessment of CO_2 reduction of alkali-activated concrete. J. Clean. Prod. 2013, 39, 265-272.
- Yılmaz, H. Characterisation and comparison of leaching behaviours of fly ash samples from three different power plants in Turkey. Fuel Process. Technol. 2015, 137, 240–249.
- Yu, L.; Fang, L.; Zhang, P.; Zhao, S.; Jiao, B.; Li, D. The Utilisation of Alkali-Activated Lead–Zinc Smelting Slag for Chromite Ore Processing Residue Solidification/Stabilisation. Int. J. Environ. Res. Public Health 2021, 18, 9960.
- Zhang, C.-M.; Shi, Y.; Jiang, L.-H.; Hu, Y.-Y.; Li, Q.; Li, H.-Q. Analysis of lead pollution control in anode slime micromorphology evolution induced by Mn2+ ions for cleaner production of zinc electrolysis. J. Clean. Prod. 2021, 297, 126700.
- Zhang, M.; Yang, C.; Zhao, M.; Yang, K.; Shen, R.; Zheng, Y. Immobilisation potential of Cr(VI) in sodium hydroxide activated slag pastes. J. Hazard. Mater. 2016, 321, 281–289.
- Zhang, P.; Muhammad, F.; Yu, L.; Xia, M.; Lin, H.; Huang, X.; Jiao, B.; Shiau, Y.; Li, D. Self-cementation solidification of heavy metals in lead-zinc smelting slag through alkali-activated materials. Constr. Build. Mater. 2020, 249, 118756.

Chapter 4.

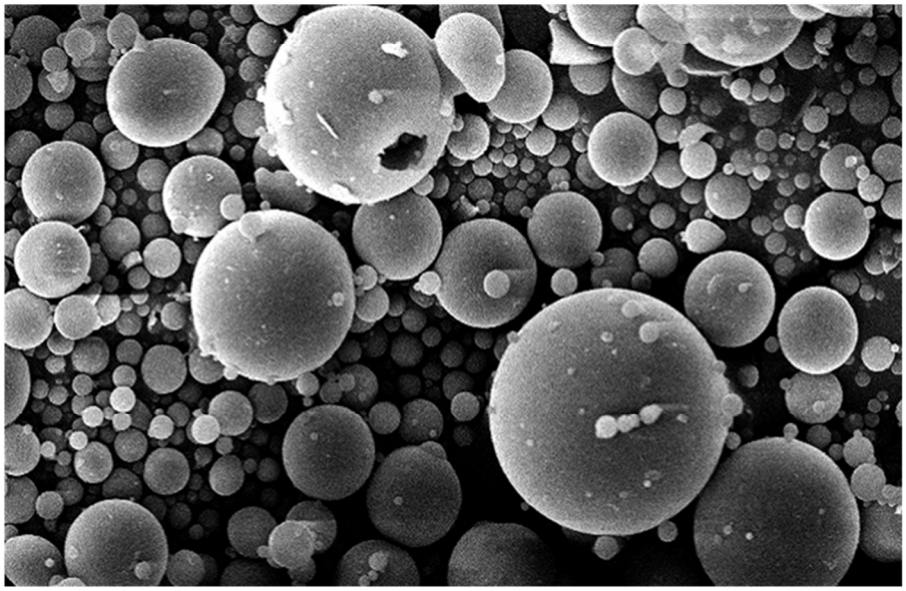

Coal fluidized bed combustion ashes in low energy clay ceramic process

4. Coal Fluidized Bed Combustion Ashes in Low-Energy Clay Ceramic Process

Circulating fluidized bed combustion (CFBC) is a coal combustion technology considered cleaner than conventional pulverized coal combustion, owing to its relatively lower firing temperature and reduced SO2 and NOx emissions. Therefore, CFBC has been considered more energy-efficient among available technologies, and it is the most used technology in the world. Coal-fired power plants using CFBC technology have been operating in the USA, Europe, and Japan since the 1980s, and can be found more recently in the emerging economies such as China, where more than 1000 CFBC boilers are currently operating (Zhou et al., 2020). Therefore, from a perspective of sustainability, protecting the environment and resource efficiency, it is necessary to make proper use of CFBC ash.

The chemical composition and characteristics of coal ash generated in CFBC boilers differ significantly from conventional boilers, since coal is fired at relatively lower temperatures, 850-900 ºC versus1200-1400 ºC, and a large amount of limestone or dolomite is often used as a adsorbent for desulphurisation. $CaCO_3$ decomposes to produce CaO, and then it reacts with SO_2 and O_2 to produce anhydrite ($CaSO_4$). Consequently, the CFBC bottom ash has a high unreacted CaO content and a large amount of desulphuration product $CaSO_4$ and shows hydraulic reactivity. Although on the one hand, its hydraulic reactivity can be considered as potential to be a cementing material, on the other hand it generates technical concerns, because they cause significant expansion (Cheng et al., 2013). Furthermore, the fact that the bottom ash has an irregular shape, with a wide range of particle size, implies that its use as an ingredient for concrete can cause difficulty in the quality control of the final product. In addition, its high SO_3 content does not meet the ASTM standards for additives of Portland cemen (ASTM C563 – 16). For all this, the use of CFBC ash as an additive or component in concrete is prohibited in Europe and North America.

On the other hand, potential applications of using high calcium CFBC ash have been collected in the literature, due to its hydraulic properties, which allows the ash itself to be used as an inorganic binder and/or applied as an secondary activator for other minerals such as supplementary cementitious materials in concrete, for example fine aggregate in high-volume slag cement mortar or in controlled low strength material mixture (Lee et al., 2020; Siddique et al., 2021; He et al., 2021; Alemu et al., 2022). Another application is its use as a precursor of alkaline activation processes (Xu et al., 2010; Topçu et al., 2011; Chindaprasirt and Cao, 2015). These types of processes are being widely studied to develop alternative cementitious binder system. Previous studies have shown that to obtain an alkali-activated product, three components are

important: raw material (source of alumina and silicates), filler and alkali-activators. In this sense, the alkaline activation of industrial waste such as coal fly, bottom ash or blast furnace slag used as raw material have been found to be effective, providing a beneficial use of this type of waste materials. While kaolinite, lateritic clay, stone dust and others are used as filler. Hydroxides and silicates of alkali, namely Na^+, K^+, Ca^{2+}, Li^+, are the most used alkaline activators. In recent studies, the choice of activator has been discussed (Davidovits, 2011; Provis and Deventer, 2009; Pacheco-Torgal, 2015). Na_2CO_3, CaO and $Ca(OH)_2$ are presented as alternatives to those typically used such as NaOH or Na_2SiO_3, and also significantly reduce the cost. But due to their lower alkalinity, they give lower mechanical strengths than with the classic activators. Although it has been observed that the combination of both types shows kinetic reactions and strength comparable with those activated only with the usual activators (Garcia-Lodeiro et al., 2014). Therefore, the application of alkali-activated bricks in building construction proves to be efficient, sustainable and competitive cost (Zhao et al., 2021).

Recent studies of alkaline activation of blends of CFBC fly and bottom ashes have been carried out to obtain controlled low strength material (CLSM), cementitious material that is in a flowable state at the time of placement. The engineering property of CLSM is far below that of conventional structural materials, 8.3 MPa, at most, at 28 days, according to American Concrete Institute. The manufacture of CLSM was carried out by means of an amount of a binder (CFBC fly ash and Blast furnace slag) an aggregate (CFBC bottom ash) and NaOH as activator (Park et al., 2017). And also using cement or sodium carbonate as activator and sand as filler (Jang et al., 2018). In these studies, engineering properties and hydration characteristics were evaluated.

To contextualize CFBC ashes, their way of valorisation and the possible products characteristics a bibliographic review is done. The review work encompasses 63 articles (the general information of this articles is gathered in Table A.9.1 of Annex 9. These 63 articles have been worked emphasising the different ashes characterisation methods and the different ways of valorisation of these ashes.

From the bibliographic review on the Fluidised Bed Coal Boiler (FBCB) process, it is concluded that there is a great variability in its conditions of operation, allowing the production of numerous types of ashes with different characteristics and therefore the resort of different industrial applications depending on the characteristics of these ashes (Zhang et al., 2022).

Among the different valorisation methods identified, three groups are found: i) the production of cement-based materials, in which properties associated with this type of materials are studied. The classical characterisations for this type of materials are those associated with the mechanical properties of the materials, giving less

importance to the molecular characterisation; ii) The production of alkaline activated materials by adding ground granulated blast furnace slag, GGBFS, giving greater importance to the mineralogical characterisation to see the effects of alkaline activation; ii) A final group that includes from mixed cements to self-hydration product in order to produce alkaline activated materials (Tendency of these recent years).

Considering most of the fly ash and bottom ash from CFBC power plants are land-filled because of their high-inherited sulphate and lime contents as previously noted, so it is necessary to look for effective applications to use mostly the bottom ash. The aim of this chapter is to analyse the possibilities of preparing sodium carbonate-activated binders firstly from CFBC bottom ash and secondly from blends of CFBC fly and bottom ashes including as additional binder sodium silicate in terms of engineering aspects, as compressive strength, water absorption and porosity. The reaction products were analysed by XRD, TG-DTA, SEM/EDS and FTIR.

4.1. CFBC Bottom Ash-Clay Binders

To reach a better understanding of the chances for the valorisation, Chemical, and Thermal characterisations were carried out for the Bottom ashes. Three different samples were analysed: A0: particle size < 0.3mm; A3: 0.3mm < size particle < 0.6 mm; A6: particle size < 0.6 mm.

4.1.1. CFBC Bottom Ash Characterisation

X-Ray Fluorescence of CFBC Bottom ashes.

Chemical compositions of the raw CFBC Bottom ashes are determined by X-ray fluorescence (XRF) analysis. ¡Error! La autoreferencia al marcador no es válida. shows the results for the different fractions (A0 particle size < 0.3 mm; A3 particle size < 0.6 mm; A6 particle size < 0.6 mm).

The XRF result shows the main component for the three fractions is CaO representing half of the composition, followed by S representing the 6-8 % of the composition, and SiO_2. It is possible to appreciate that the fraction with size particle > 0.6 mm contains more amount of SiO_2, around 18 %; this fraction is around the 2 % of the ashes mass. Even if SiO_2 is the third more present compound, both the SiO_2 and the Al_2O_3 are present in less amount than in common ashes.

Table 4.1. Bottom CFBC ash Chemical Characterisation. A0: particle size< 0.3mm; A3: 0.3mm<size particle<0.6 mm; A6: particle size<0.6 mm.

Analyte Symbol	SiO_2	Al_2O_3	Fe_2O_3(T)	MnO	MgO	CaO	Na_2O	S	TiO_2	P_2O_5	LOI	Total
Unit Symbol	%	%	%	%	%	%	%	%	%	%	%	%
Detection Limit	0.01	0.01	0.01	0.001	0.01	0.01	0.01	0.001	0.001	0.01	-	0.01
A0	3.83	0.95	0.38	0.013	0.35	48.15	0.05	8.02	0.074	0.03	1.96	55.81
A3	4.68	1.41	0.59	0.02	0.38	50.35	0.1	6.74	0.075	0.02	2.81	60.52
A6	18.44	5.73	1.99	0.068	0.52	44.63	0.28	7.83	0.25	0.04	7.9	80.29

Thermogravimetric analysis of CFBC Bottom Ashes

TG-DSC-MS curves were obtained on a SETARAM thermal analyser, model SETSYS-1700. The samples of approximately 20 mg were heated in platinum crucibles in a Nitrogen atmosphere, at a total flow rate of 50 ml min-1, with a heating rate of 10 ºC min^{-1} and a final temperature of 1350 ºC, maintained for one hour. All the TG measurements were blank curve corrected. Each experiment was repeated to check for consistency. The TG instrument was coupled to a Balzers Thermostar / OmniStar mass spectrometer (Pfeiffer vacuum) for evolved gas analysis. Quadrupole mass spectrometer model was QMS 200. The m/z signals selected were: 18 (H_2O^+), 44 (CO^{2+}), 64 (SO^{2+}), 80 (SO^{3+}). TG-MS analysis supplies in this work only qualitative information. Figure 4.1 shows the TG results for different Bottom CFBC ashes fractions. (A0: particle size< 0.3mm; A3: 0.3mm<size particle<0.6 mm; A6: particle size<0.6 mm. and A: raw ashes).

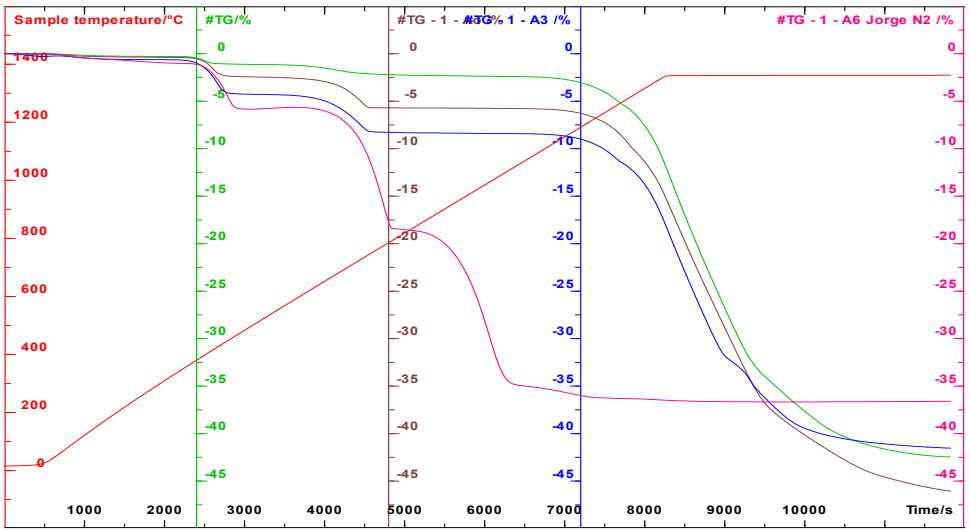

Figure 4.1. Bottom CFBC ashes.TG-DTG. A0: particle size<0.3mm; A3: 0.3mm<size particle<0.6 mm; A6: particle size<0.6 mm. and A: raw ashes.

From the thermal behaviour is possible to appreciate how the A6 fraction develops a significantly different behaviour, this fraction represents only 2 % of the mass; but its composition is different. When the A0 and A3 fractions together with the raw material (A) show more than 55 % of $CaSO_4$; the A6 fractions are composed of $CaSO_3$, $CaCO_3$, and $Ca(OH)_2$. Even if all the samples show the presence of all these components.

CFBC ashes comparative analysis

Once the Chemical Characterisation shows these results for the composition of the Bottom ashes it is compared with the typical composition from the literature. Figure 4.2 represent again inside the box the two normal quartiles for the amount for each component and the deviation of the rest of the data. In Figure 4.2A appear the four major components for most of the samples and in Figure 4.2B appear the rest of the components. The black cross in the figure represents the results of ashes considered in this work. These results are recently supported by other authors (Zhang et al., 2022).

It is obvious from this comparison that the ashes considered in this chapter differ from the typical composition for this kind of ashes. The low amount of SiO_2 and Al_2O_3 may be a problem for the development of solid matrix

From all articles reviewed there are four that share the characterisation with the bottom ash sample considered in this work (Anthony et al., 2000; Wang et al., 2008; Chi et al., 2014; Huynh et al., 2018) and shown in Table A.9.2 of Annex 9. In some cases, these articles, study the process of the combustion, and the development of deposits (agglomeration) in the oven or the operational issues over the CFBC process due to carbonation depending on the water rate and the temperature. In other cases, it is studied the effect of adding CFBC ashes to cement using the sand river as aggregate to develop roller compacted concrete (RCC) or the CFBC mixing with Ground granulated blast furnace slag (GGBFS) (S), rice husk ash (RHA) (R), to produce cement-free SRF binder.

The ashes in these studies were taken from different points in the process. They come from the bottom of the boilers (as bed material) or the baghouse of a CFB boiler. Some are called Fly CFBC ashes but don't specify any origin.

Apart from these four articles, they exist other nine articles that do have, not so the same characterisation but are still quite similar (Table A.9.3 of Annex 9). All these nine articles share the same characterisation for their ashes and are focused on different matters, but most of them tend to study the valorisation of the CFBC ashes by adding slag to produce alkali-activated materials.

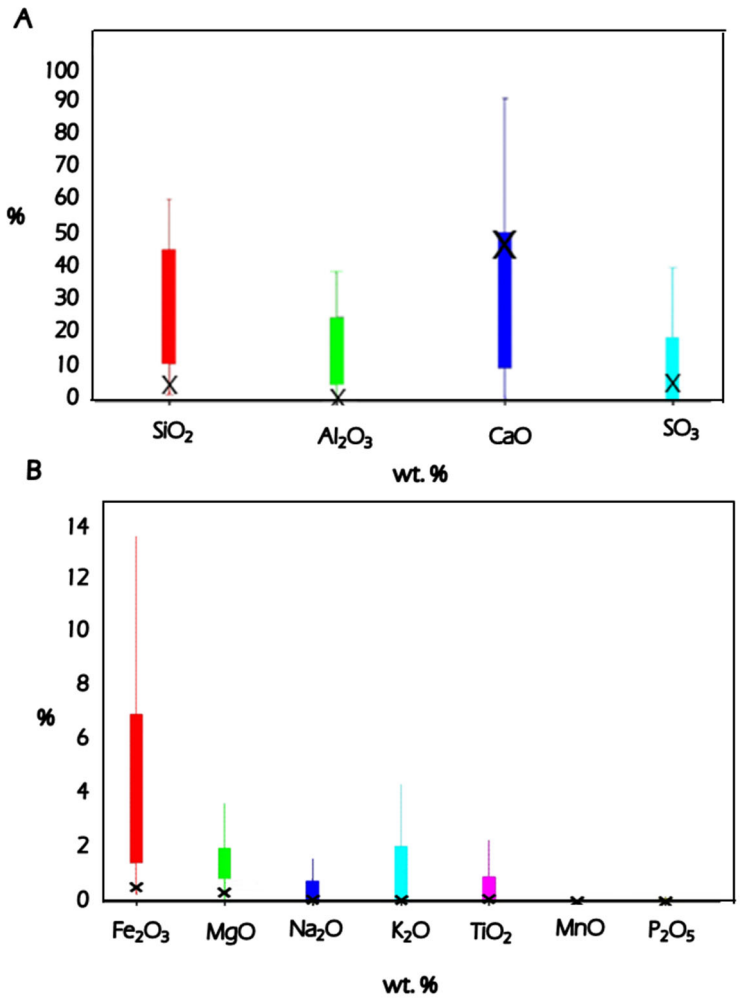

Figure 4.2. Chemical composition of CFBC ashes: (A) results of major compounds; (B) results of minor compounds.

4.1.2. Experimental studies. Alkali Activated Binders. First Approach

For the first approach, a series of experiments were carried out to analyse the viability of the valorisation of Circulated Fluidized Bed Combustion ashes. Figure 4.3 represent the pathway of these first studies over the CFBC ashes.

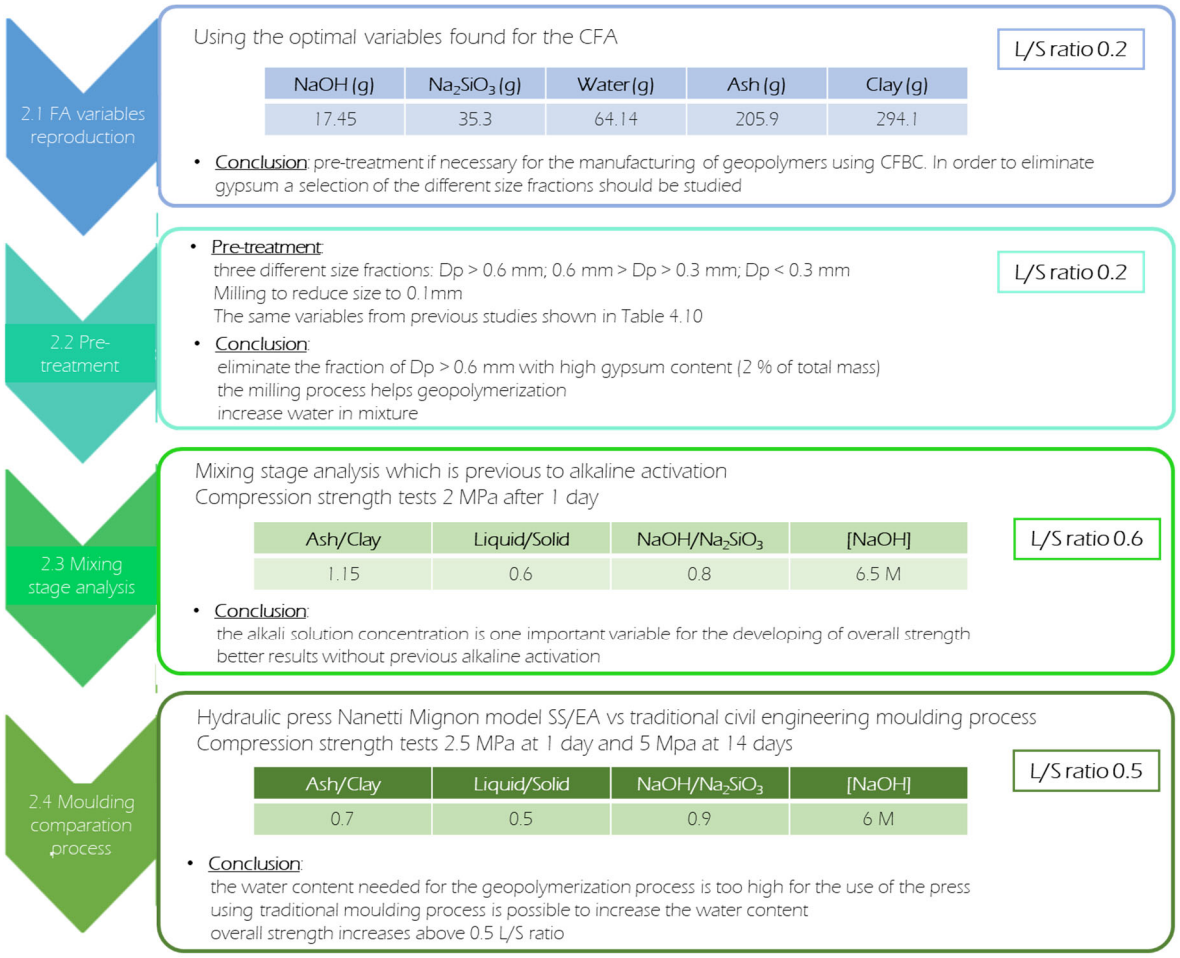

Figure 4.3. Pathway of the first studies over CFBC ashes.

The first attempt for the valorisation of the CFBC ashes was to reproduce the optimal process found for the coal fly ashes Main variables of the process are found in Table 4.2. The clay is subjected to a grinding process to achieve a particle size exceeding 0.5 mm. Then we proceed to the mixture of raw material for 10 minutes, Fly ash and clay, with a laboratory mixer Raimondi, Iperbet model. While the fly ash-clay mixture is carried out, the solution containing sodium hydroxide, sodium silicate, and distilled water is prepared.

Table 4.2. Design of experiment for Alkali Activated Binders from CFBC ashes.

NaOH (g)	Na_2SiO_3 (g)	Water (g)	Ashes (g)	Clay (g)
17.45	35.30	64.14	205.9	294.1

At the time in with the ten minutes of mixing have passed and the solution was made, the solution is added with a pipette onto the clay-ashes mixture. Once everything is mixed it is left for 10 more minutes.

Once the mixture is prepared it is mould by pressing. To this end, a hydraulic press Nanetti Mignon model SS/EA (Figure 4.4) was used. The mould is prismatic with 80x40x20 mm size. These samples are pre-cured for 48 hours at room temperature before the cooking cycle. A laboratory muffle furnace Hobersaql, PR model 12/300 capable of ramps temperature versus time of up to 16 points was used. The temperature of work is 75 ºC.

Figure 4.4. Hydraulic press Nanetti Mignon model SS/EA.

The bricks (Figure 4.5) developed very low overall resistance, with a crunchy structure. A study over pre-treatment is necessary for the manufacturing of building materials using CFBC bottom ashes.

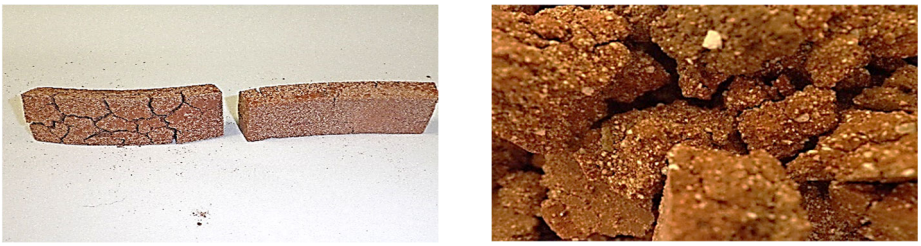

Figure 4.5. Alkali activation feasibility results: (A) Overall bricks view (left picture); .(B) Zoomed bricks view (right picture).

For the study over the pre-treatment, the ashes were divided into three different size fractions: D_p>0.6 mm; 0.6 mm>D_p>0.3 mm; 0.3 mm>D_p to see the effect of the size and the composition of the different fractions, in the other hand, all the ashes were milled to increase the surface area what should help any reaction process. The rest of the process was conducted as it was developed for the previous alkali activation attempt.

For the results of the bricks, Figure 4.6A, Figure 4.6B, and Figure 4.6C, it is determined that the milling pre-treatment is necessary; that eliminating the fraction D_p>0.6 mm. helps the process and that water content is not enough. For these reasons a change in the process of trying classical moulding methods is proposed.

Figure 4.6. Pre-treatment process products: (A) Using A6 fraction; (B) Using A3 fraction; and (C) Using A6 fraction.

For the alkali activation attempt, the ratio liquid/solid is pretended to increase until 0.5. For that to be possible the use of the classical moulding method is proposed since that amount of water was impossible to admit in the pressing procedure. The rest of the procedure is maintained as it was.

The bricks developed using classical moulding methods and more amount of water show interesting compressive resistance reaching 2 and 5 MPa on day 1 and day 14 respectively (Figure 4.7). For these results, it is concluded that it is possible to develop an alkali-activated building material with Bottom ashes.

Figure 4.7. Classic moulding products.

4.1.3. Feasibility Study. Process variables optimisation

From the previous work developed for the valorisation of these kinds of ashes, it is concluded that is possible to develop alkali-activated building materials using CFBC bottom ashes. To optimize the variables of the process some further work is developed.

Replacement of commercial activator by Solvay by-product.

One of the key variables in the process is the use of an activator, classical activators found in the literature for this kind of process are NaOH, Na_2CO_3, Na_2SO_4, and Na_2SiO_3 in this case, the NaOH that was being used it is compared with the sodium carbonate from Solvay process.

As the solubility is lower for the sodium carbonate it is proposed a try to see if previous homogenisation and activation help in the process. For this purpose, four samples are developed, two of them using NaOH and two of them using Na_2CO_3; for both cases, in one of the previous homogenisation is used and for the other test the process is followed as usual. The rest of the variables of the process are kept as it was developed before. Table 4.3 gather the component ratios.

Table 4.3. Process variables for Alkali Activation.

Ash/Clay	Liquid/Solid	NaOH/Na_2SiO_3
0.7	0.5	0.9

In the case of the NaOH, the results of the bricks using the previous activation showed good resistance (2 MPa) but seem to be able to develop more resistance with the time when it is used in the classical process.

In the previous homogenisation case for the sodium carbonate, the solids (ashes, clay, and sodium carbonate) are mixed before adding the liquid elements, in the other case the clay and the ashes are mixed, and the sodium carbonate is added in the liquid phase.

Figure 4.8. Alkali activated products using Na_2CO_3: (A) With previous homogenisation; and (B) without previous homogenisation.

The studies about the previous activation or homogenisation conclude that in the case of the use of NaOH, the previous activation doesn't help the process; but in the case of the sodium carbonate, samples including previous homogenisation show better resistances even if in both cases the overall resistance was better than for NaOH samples (Figure 4.8).

From this process, a study of the molarity of both activators is carried out to find the effect of the activator and its concentration in the bricks. Same ratios as used before are tried on being the variables to study, kind of activator and its concentration.

NaOH Set of experiments

From all the knowledge acquired and reproducing the same variables that were used in the last experiment, a battery of samples is prepared using different NaOH concentrations. Table 4.4 gather the different masses for each component used for the development of the samples.

Table 4.4. Amount of each component.

Sample	Clay (g)	Ash (g)	Na_2SiO_3 (sol.) (g)	NaOH(sol.) (g)	[NaOH]
A	300	426	193	177	2 M
B	300	426	193	177	4 M
C	300	426	193	177	6 M
D	300	426	193	177	8 M
E	300	426	193	177	10 M

The samples were set to cure for 7 and 28 days. After this time Compressive strength tests were carried out to study the products. Table 4.5 shows the result of these tests.

Table 4.5. Compressive strength test results.

Sample	[NaOH]	Compressive strength at 7 days (MPa)	Compressive strength at 28 days (MPa)
A	2 M	1.8	-
B	4 M	-	-
C	6 M	3.1	4.06
D	8 M	2.4	2.08
E	10 M	-	-

The results show evidence that better results of compressive strength for alkali-activated building materials with this kind of ashes are reached when the concentration of the NaOH is between 6M and 8M. These results showed that the resistance barely increase with time. Figure 4.9A and Figure 4.9B show the samples after the compressive strength test, As can be appreciated, the pyramid shape of the broken sample indicates good cohesion of the material.

Figure 4.9. Bricks after compressive resistance test: A) Sample C; and B) Sample D

Na_2CO_3 Set of Experiments

Once it is proven that a previous solid homogenisation is better for the geopolymer process, a set of experiments using Solvay by-product alkali activator is developed to find an optimum range of variables. The procedure is carried out following the previous set of experiment processes, replacing the NaOH for Na_2CO_3, applying previous homogenisation in the solid phase, and carrying out the compressive resistance test at 14 days. Table 4.6 gather the mass of the different components used in the mix and the compressive strength results.

Table 4.6. Experimental design and compressive strength test results.

	Clay (g)	Ash (g)	Na_2SiO_3 (sol.) (g)	Na_2CO_3(sol.) (g)	[Na_2CO_3]	Compressive strength at 14 days (MPa)
A2	300	426	193	177	2 M	*
B2	300	426	193	177	4 M	*
C2	300	426	193	177	6 M	7.16
D2	300	426	193	177	8 M	4.37
E2	300	426	193	177	10 M	*

(*): Result not available

From the experimental procedure, it is possible to appreciate that the mixture develops a faster setting than when using NaOH as an activator, reaching before and adequate hardening. Figure 4.10 show the bricks developed for this process. From the set of experiments, it is possible to conclude that it is possible to use sodium carbonate as activators for this kind of process (reaching higher hardness that the bricks where NaOH was used) and it is also concluded that the appropriate molarity range is around 6 or 8 (reaching 7 MPa in 14 days).

Figure 4.10. Alkali-activated products using Na_2CO_3.

After the compressive strength results, the best samples were reproduced to carry out a water absorption experiment, according to UNE 67-019. It was impossible to obtain any results due to the collapse of the bricks when immerse in water. This behaviour has been reported before in some studies (parkSM2018) when trying to produce alkali-activated building materials using CFBC ashes. This particularity could represent a problem valorising these kinds of products as a normal environment would affect them fast even if they develop proper compressive strengths.

4.1.3.1. Influence of Process Variables Experimental design

Once it is determined the viability of the development of alkali-activated materials using CFBC bottom ashes of Solvay, the study of some process variables is proposed. Some main concerns are the proper fraction to use, the temperature and the time of the curing process, and the role of the clay.

Temperature and curing time

The study of the temperature effect on the alkali activation of materials has been studied in several works, the main concerns of that are gathered in the list below.

- The heating temperature improved the polymerisation reaction process, which made a fast and alkali-activated solution constitute the matrix in the early stage.
- Follow ability is highly dependent on temperature.
- Higher temperatures reach better water absorption results.
- Compressive strength decreases on curing at a higher temperature for a longer period and breaks the granular structure of geopolymer mixture.

Anyway, it doesn't exist studies on the effect of the curing temperature on the alkali activation of CFBC ashes. Including temperature as one of the variables in the set of the experiment will allow analyse of its effect. For that, three different curing temperatures are included in the experimental design, 75 ºC, 30 ºC, and room temperature (20º C).

Particle diameter

On the other hand, as it was an asset before the fraction with a particle diameter >0.6 mm was being separated for the experiments due to the previous experiments and results. To check the effect of this fraction in the process two different fractions of the CFBC ashes are included in the experimental design. On one hand, the fraction that was used (A00: D_p<0.6 mm.), and on the other hand, the complete fraction of the raw material (A: whole fraction).

A set of experiments was designed based on the study of these process variables. It included the two different activators, NaOH and Na_2CO_3 with the intent of checking the reproducibility of the experiments. The rest of the variables were fixed according to optimum formulations, C and C2 (Table 4.8 and Table 4.10), and processes developed in previous studies. Table 4.11 represent the experimental design.

The compressive strength results of the bricks are gathered in Figure 4.11. The temperature is an interesting variable to study for this process, the bricks reached better resistance in shorter periods at high temperature (early-stage strength development) for the use of NaOH as an activator, but great results for environment temperature for the use of Na_2CO_3. On the other hand, the complete ashes fraction still gets weaker results not reaching enough strength for the compressive strength test.

The bricks were subdued to water immersion to check over their behaviour when immerse, even if all the samples collapsed in water, the bricks that had been cured at environment temperature showed more integrity.

Table 4.7. Variables optimisation experimental design of alkali activated binders.

Sample	Temperature (ºC)	Curing time (h)	Ash fraction	Activator	Sample reference
C11	75	24	A00	NaOH	C
C12	75	48	A00	NaOH	C
C13	Room	48	A00	NaOH	C
C21	75	24	A00	Na_2CO_3	C2
C22	75	48	A00	Na_2CO_3	C2
C23	Room	48	A00	Na_2CO_3	C2
C31	30	24	A	NaOH	C
C32	30	48	A	NaOH	C
C33	Room	48	A	NaOH	C
C41	30	24	A	Na_2CO_3	C2
C42	30	48	A	Na_2CO_3	C2
C43	Room	48	A	Na_2CO_3	C2

A00: D_p< 0.6mm; A: raw material.

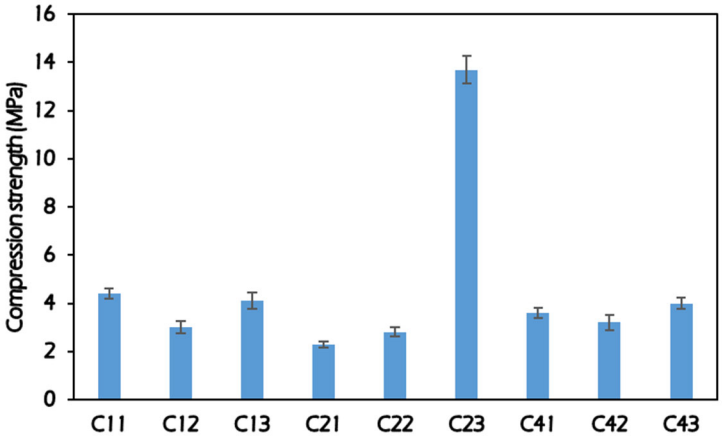

Figure 4.11. Compressive strength results (14 days) of alkali activated binders.

Clay's role in the geopolymer process

To check the effect of working with clay at low temperatures, an experiment reproducing optimum variables found in previous works for the C sample, but avoiding clay in the mixture was carried on (Table 4.8).

Table 4.8. Mixture formulation of CFBC bottom ash without clay.

Clay	Ash (g)	$NaSiO_3$ (g)	NaOH (g)	[NaOH]
-	213	96.5	88.5	6 M

The visual appearance of this sample improves by far the last not-using clay samples. The hardness is greater (Figure 4.12), reaching 16 MPa in the compressive strength test versus the 4 MPa of compressive strength that reached the clay sample. When immersed in water to taste the behaviour, the Alkali Activated Material that included clay in the mixture suffered from collapsing while the sample without clay lost part of its weight.

Figure 4.12. No clay alkali activate material.

To reach a better understanding of the chances for the valorisation, Chemical, and Thermal characterisations were carried out for the Bottom ashes. Three different samples were analysed: A0: particle size< 0.3mm; A3: 0.3mm<size particle<0.6 mm; A6: particle size<0.6 mm.

4.2. CFBC Fly and Bottom Ashes Based Alkali-Activated Binders

Previous studies carried out by the GER research group of the University of Cantabria to use the CFBC ashes as a construction material show the difference in behaviour of the fly ash versus the bottom ash. The preparation of alkali-activated ashes was carried out using an additional binder, soluble silicates, and NaOH or Na_2CO_3 as an activator with/without natural clay as a filler. While the CFBC bottom ash-based mixtures can exhibit characteristics of self-destruction when submerged in the water despite obtaining values of compressive strength greater than 10 MPa at 14 days in a dry condition. The characteristic of self-destruction can be attributed to the formation of ettringite and gypsum by the hydration of anhydrite, which induces excessive expansion. The CFBC fly ash-based mixtures showed values of compressive strength in the order of 37 MPa and 17MPa at 14 days, without and with clay respectively. No indication of self-destruction when submerged in water, keeping intact their physical integrity, the mixtures without clay. The best results were obtained using as activator sodium carbonate and not adding clay to the mixtures, so it is proposed as the aim of the present work, to analyse the possibilities of preparing sodium carbonate-activated bricks from blends of CFBC fly and bottom ashes including additional binder sodium silicate. An experimental study was systematically designed to assess the feasibility of utilizing the CFBC ash (both fly ash and bottom ash) in the fabrication of bricks in terms of engineering aspects, such as compressive strength, water absorption, and porosity. A study on the microstructure of the selected products was carried out following the next analytical techniques: X-ray diffraction- XRD, Thermogravimetric and Differential Thermal analysis-TG-DTA, Scanning electron microscopy-SEM, Fourier-transform infrared spectroscopy-FTIR. The results may give a way of recovery of CFBC bottom ash and also get a better understanding of the reaction mechanisms.

4.2.1. Materials and Methodology

4.2.1.1. Materials

The particle size distributions of the raw CFBC fly and bottom ashes are shown in Figure 4.13. As it can be appreciated the Fly ash presents smaller size distribution and a smaller range of sizes than Bottom Ashes. The Bottom gathers different size particles (from sizes below 0.1 mm to 0.6 mm).

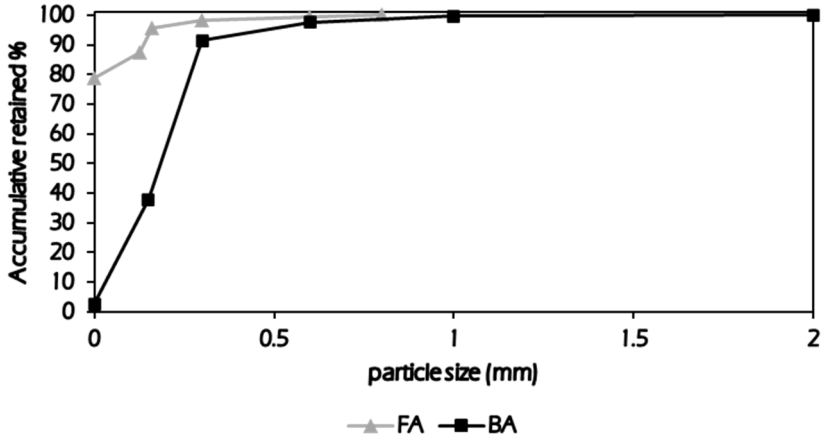

Figure 4.13. Particle size distributions of raw CFBC fly and bottom ashes.

Chemical compositions of the raw CFBC Fly and Bottom ashes are determined by X-ray fluorescent (XRF) analysis. The results are presented in The X-ray powder diffraction pattern of the CFCB fly ash and bottom ash (Figure 4.14. XRD patterns of CFCB ashes) have been fitted using the pattern matching routine in the Diffracplus EVA program. As can be seen, both FA and BA display similar mineralogy composition displaying anhydrite, lime, calcium sulphate, and quartz as major phases, in good agreement with the chemical analysis and a minor phase of calcium carbonate. A visual comparison between them shows that the quantity of lime is higher in FA and a small quantity of portlandite, $Ca(OH)_2$, is in BA which is attributed to the transformation of lime by water vapour (Nguyen et al., 2019). On the other hand, there was no halo peak found in the XRD pattern of asses which manifests the lack of glass phase contrary to some results found in the bibliography (Jang et al., 2017; Li et al., 2012).

. The chemical composition results show that these ashes present a lower amount of Al_2O_3 and SiO_2 than normal compositions from literature (Xun et al., 2018; Kang and Choi, 2018; Hlaváček et al., 2018), still, they exist some works that present CFBC with similar compositions (Anthony and Jia, 2000; Wang et al., 2008; Chi and Huang, 2014; Huynh et al., 2018). The main chemical difference is the presence of CaO as

the main FA component followed by SO_2 and the presence of SO_2 as the main BA component followed by CaO.

The X-ray powder diffraction pattern of the CFCB fly ash and bottom ash (Figure 4.14. XRD patterns of CFCB ashes) have been fitted using the pattern matching routine in the Diffracplus EVA program. As can be seen, both FA and BA display similar mineralogy composition displaying anhydrite, lime, calcium sulphate, and quartz as major phases, in good agreement with the chemical analysis and a minor phase of calcium carbonate. A visual comparison between them shows that the quantity of lime is higher in FA and a small quantity of portlandite, $Ca(OH)_2$, is in BA which is attributed to the transformation of lime by water vapour (Nguyen et al., 2019). On the other hand, there was no halo peak found in the XRD pattern of asses which manifests the lack of glass phase contrary to some results found in the bibliography (Jang et al., 2017; Li et al., 2012).

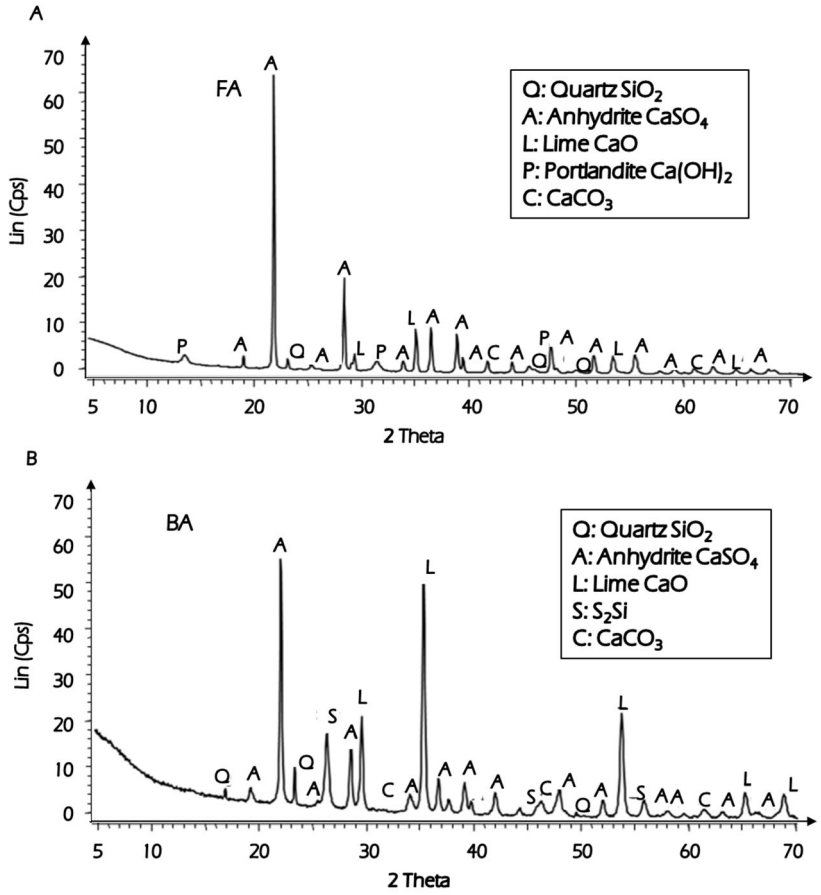

Figure 4.14. XRD patterns of CFCB ashes: (A) fly ash; (B) bottom ash.

Table 4.9. Chemical composition of CFBC fly and bottom ashes.

Mayor oxides (%)	Fly Ash	Bottom Ash
SiO_2	5.82	2.01
Al_2O_3	2.60	0.44
SO_2	38.9	61.6
Fe_2O_3	0.390	0.25
CaO	51.9	35.6
TiO_2	0.060	0.014
MgO	0.310	0.060
Trace elements (ppm)	**Fly Ash**	**Bottom Ash**
V	1001	2617
Cr	3.71	-
Ba	145	91.3
Ce	-	21.0
Mn	25.8	80.2
Ni	358	828
Cu	7.47	8.07
Zn	13.0	41.0
Ga	-	14.6
Ge	-	-
As	-	2.27
Se	1.60	-
Br	2.77	-
Rb	3.89	-
Sr	217	177
Y	9.16	5.96
Zr	57.6	42.4
Nb	7.64	5.25
Pb	9.50	-
Th	4.08	-
LOI (%)	5.50	2.50

Figure 4.15 provides SEM images of the particles of ashes. The BA are compounds of big particles, mostly anhydrite and lime, whereas the FA, smaller than BA, are compounds of different irregular particles showing anhydrite, in a smaller proportion than in the BA, and lime, in greater proportion than in the BA. Both materials show great heterogeneous morphology, far from the conventional carbon ash spherical

shape (Alengaram et al., 2018); this morphology may affect the reaction process (Nguyen et al., 2019) and may be due to the lower temperature in the combustion process (Li et al., 2012).

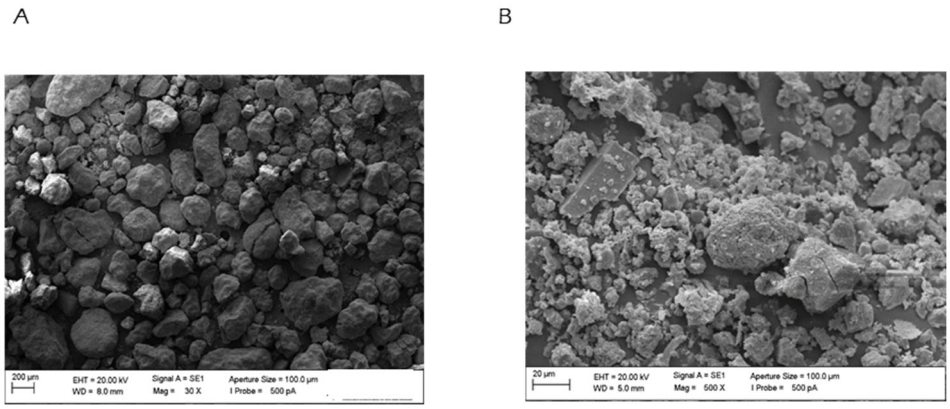

Figure 4.15. SEM micrographs of CFBC ashes: (A) Fly Ash; (B) Bottom Ash.

The alkali activator used in the mixing process, sodium carbonate, and Na_2CO_3, was provided by Solvay. Sodium silicate, Na_2SiO_3, a technical grade was used in the mix as an activator/precursor. The water used for all the experiments was ultrapure (type 1).

4.2.1.2. Alkali-activated binders preparation

The mix proportions of the samples are provided in Table 4.10. The units are expressed in mass ratios. The ratios L/S, Na_2SiO_3: water and the molarity of sodium carbonate were fixed according to previous studies. The variable in the experiment design was the ratio FA: BA. For each sample, the total mass added was 300 g.

The fabrication of the bricks was as follows: A designated amount of ashes and a solid alkali activator (sodium carbonate) were placed in a mixer and were stirred for 5 min to ensure the homogeneity of the solid mixture. While the solids mixture is carried out, the solution containing sodium silicate and distilled water is prepared. Then the solution is added with a pipette to the solids mixture. After all the liquid and solid were in the mixer, it was stirred for an additional 2 min. The fresh mixtures were then introduced into a prismatic mould with dimensions of 40x40x160 mm or 50x50x50 mm. The moulds were then sealed with polyethylene film and set to cure at 20 ± 2ºC. After the initial 48 hours of setting in moulds, the samples were unmoulded and subjected to further curing for 14 and 28 days.

Table 4.10. Mix design of alkali-activated binders (expressed in mass fraction).

Sample	Solid	Liquid	
	Ratio FA/BA	Na_2SiO_3 (solution)	Na_2CO_3 (6 M solution)
WG0	1/0	0.33	0.27
WG2	1/0.2	0.396	0.324
WG4	1/0.4	0.462	0.378
WG6	1/0.6	0.528	0.432
WG8	1/0.8	0.594	0.486
WG10	1/1	0.66	0.54
WG20	1/2	0.99	0.81
WG30	1/3	1.32	1.08
WG40	1/4	1.65	1.35

4.2.1.3. Sample Analysis

The bricks were investigated to determine the physical and mechanical properties of compressive strength, water absorption, and compressive strength after water immersion. A study on the microstructure of the selected products was carried out following the next analytical techniques: X-ray diffraction- XRD, Thermogravimetric and Differential Thermal analysis-TG-DTA, Scanning electron microscopy-SEM, Fourier-transform infrared spectroscopy-FTIR.

A compressive strength test was performed immediately after the 14-day curing had finished for the bricks (size: 40x40x160 mm) and after 28 days, according to (UNE-EN 1015-11:2000/A1:2007). Water absorption results were obtained according to UNE 67-019 (size: 50x50x50 mm).

For selected mixtures, thermal characterisation was studied by thermogravimetric (TG-DTA). Simultaneous TG-DSC-MS curves were obtained on a SETARAM thermal analyser, model SETSYS-1700. The samples of approximately 20 mg were heated in platinum crucibles in a Nitrogen atmosphere, at a total flow rate of 50 mL/min, with a heating rate of 10 ºC/min and a final temperature of 1350 ºC, maintained for one hour. All the TG measurements were blank curve corrected. Each experiment was repeated to check for consistency. The TG instrument was coupled to a Balzers Thermostar / OmniStar mass spectrometer (Pfeiffer vacuum) for evolved gas analysis. Quadrupole mass spectrometer model was QMS 200. The m/z signals selected were: 18 (H_2O^+), 44 (CO_2^+), 64 (SO_2^+), 80 (SO_3^+). TG-MS analysis supplies in this work only qualitative information.

Microstructural Characterisation is determined by SEM. The equipment used is a Carl Zeiss (model EVO MA15). Mineralogical characterisation of the selected samples and the ashes was carried out by XRD. Such analyses were performed in an air atmosphere on a Bruker D8 Advance diffractometer, using Cu Kα radiation and a LynxEye detector. Diffraction patterns were collected with an angular 2θ range

between 10° and 70° with a 0.03° step size and measurement time of 3 s per step, and a graphite monochromator. The instrumental resolution function of the diffractometer was obtained from the LaB6 standard.

FTIR spectra of samples were recorded on a Perkin-Elmer Frontier FTIR spectrometer using KBr disk technique in the wavenumber range of 400 cm^{-1} to 4500 cm^{-1} at room temperature.

4.2.2. CFBC Fly and Bottom Ashes Based Alkali-Activated Binders

The alkali activator used in the mixing process, sodium carbonate, and Na_2CO_3, was provided by Solvay. Sodium silicate, Na_2SiO_3, the technical grade was used in the mix as an activator/precursor. The water used for all the experiments was type 1.

4.2.2.1. Technological Properties

The compressive strength of the bricks at 14 and 28 days are shown in Figure 4.16. The results show reproducibility between the samples. There is a strong increase in the curing time. The sample with more amount of BA develops faster strength reducing the setting time; but it does not seem to have a direct effect on the resistance, all of them are close in a range from 15 to 30 MPa.

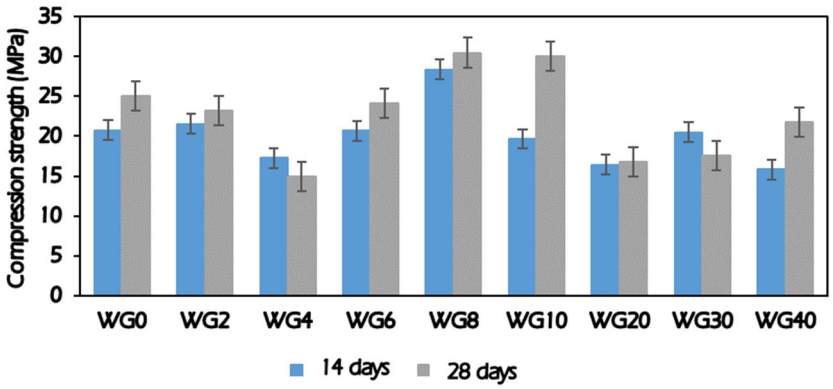

Figure 4.16. Compressive strength of WG binders (Table 4.10) after 14 and 28 days.

These compressive strength values are acceptable when compared to geopolymer mortars or bricks from literature using CFBC (Huynh et al., 2018; Chi and Huang, 2014; Song et al., 2015); although these resistance does not reach the results of some previous works where the ashes contain more amount of SiO_2 and Al_2O_3 (Nguyen et al., 2019); neither the results when the cement or other rich in SiO_2 and Al_2O_3 sources are used for the material matrix (Dung et al., 2016; Chi, 2016; Nguyen et al., 2015). Anyway, these materials show higher compressive strength than the usual for

the works using ashes with similar characteristics (Kang and Choi, 2018; Park et al., 2018; Park et al., 2017; Jang et al., 2018).

Water absorption is the ability of porous materials to retain a certain amount of water, in mortar is related to the internal structure, which limits/prevent the intrusion of water and affects the durability and mechanical properties of the mortar (Huynh et al., 2018). Samples were tested according to UNE 67-019 by water immersion. This procedure is relevant specifically in this case to test the behaviour of the products microstructures exposed to water, as in previous works (Report II Solvay; Park et al., 2018) the bricks manufactured with these kinds of ashes could show appropriate compressive resistance but collapse when tested.

In Figure 4.17 it is possible to appreciate the water absorption results for the samples after 28 days of curing. The water absorption values are higher than the typical values for fired clay bricks. The results range from 20.0 % to 32.0 %, except the brick that is only made from Fly ash develops a water absorbance of 7.15 %.

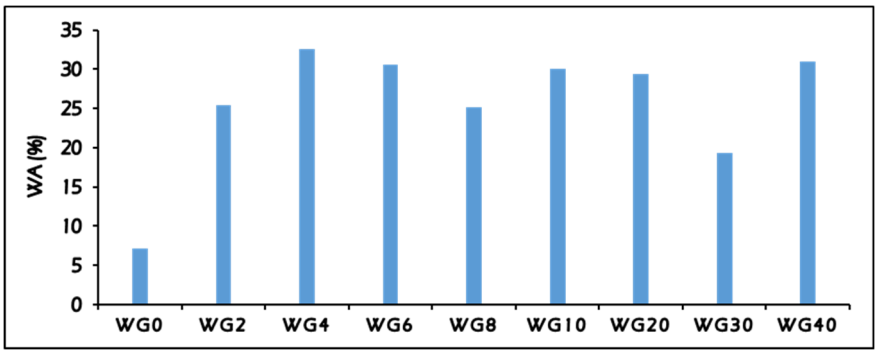

Figure 4.17. Water absorption of WG binders (Table 4.10 Mix Design).

On the other hand, Figure 4.18 shows the results of the compressive strength test after the water absorption test. Some studies have reported problems either in the integrity of some bricks after the water immersion (Jang et al., 2018; Report II Solvay) or in the compressive resistance drop after curing in water (Dung et al., 2014). The results in this study show that, even if the bricks' compressive strength is lower after the water immersion, the samples still show good compressive resistance.

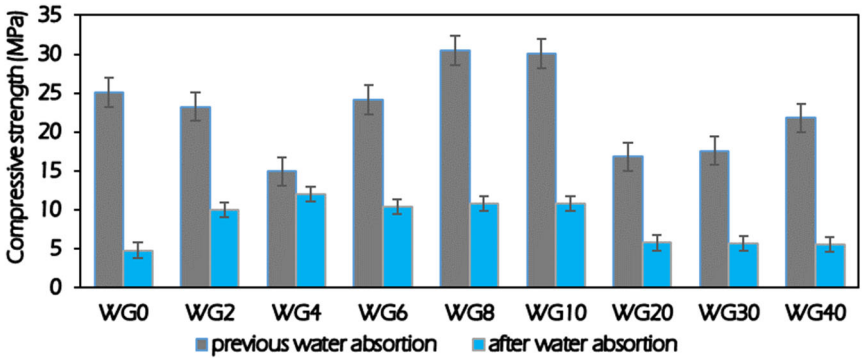

Figure 4.18. Compressive strength before and after the water absorption of WG binders (Table 4.10 Mix Design).

4.2.2.2. X-ray Diffraction results

The major crystalline phases present in three selected samples (WG0, WG10, and WG40) were also determined by XRPD. As shown in Figure 4.19 the mineral composition are similar to BA and FA (Figure 4.14) with the presence of a broad peak between 25 and 35° (2θ) that corresponds to the amorphous phase, probably due to hydrated calcium silicate, C-S-H gels (Nguyen et al., 2019). The presence of quartz in the three samples is indicative that the dissolution of the SiO_2 was not complete (Li et al., 2012) which came from the Na_2SiO_3 added to the mixture. Moreover, the presence of thernadite (Na_2SO_4) and calcium carbonate ($CaCO_3$), is due to sodium carbonate (Na_2CO_3) added to the mixture, and it is common for the three samples. Visual analysis shows that WG10 and WG40 have more presence of thernadite, which can be explained because of the mayor amount of anhydrite in the bottom ashes. In addition, the sample with more amount of bottom ashes (WG40) displays a mayor proportion of thernadite and anhydrite ($CaSO_4$) due to the higher amount of bottom ashes added.

Equations 1,2,3,4 and 5 show the possible reactions happening in the process.

$CaO + H_2O \rightarrow Ca(OH)_2$ (1)

$Ca(OH)_2 + Na_2CO_3 \rightarrow 2NaOH + CaCO_3$ (2)

$CaSO_4 + 2H_2O \rightarrow CaSO_4.2H_2O$ (3)

$CaSO_4 + Na_2CO_3 \rightarrow CaCO_3 + Na_2SO_4$ (4)

$xCa(OH)_2 + SiO_2 + (y-x)H_2O \rightarrow C_xSH_y$ (C-S-H) (5)

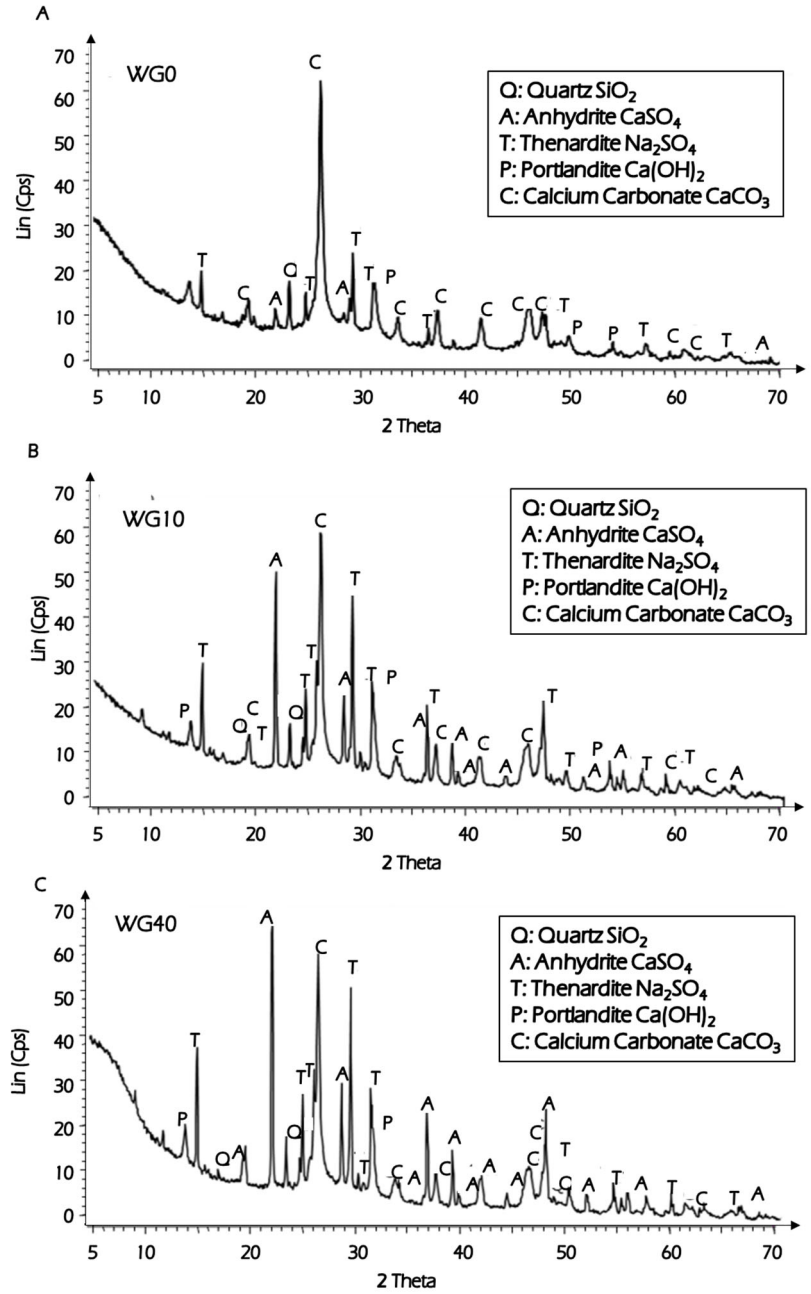

Figure 4.19. XRD patterns of reaction products after 28 days: (A) WG0 binder; (B) WG10 binder; (C) WG40 binder.

4.2.2.3. Thermogravimetric and Differential Thermal analysis-TG-DTA

Figure 4.20 shows the mass loss for the original CFBC FA and BA and also for some of the sodium carbonate activated CFBC ashes selected as representative (WG0, WG10 and WG40), cured for 28 days at room temperature and sealed before been analysed.

According to Figure 4.20, it can be observed that FA presents inappreciable moisture or dehydration products (20-260 ºC or up to 2000 s). This loss is low in the case of BA (1.44 %) but increases from WG0 to WG40 in the interval of 17.0-22.4 %, This loss could include the dehydration products of the gypsum formed from anhydrite and could contain dehydration products of amorphous C-S-H hydrates (Hlaváček et al., 2018; Sheng et al., 2012; Lee and Kim, 2017). Due to the lack of Al_2O_3 in the ashes composition and because ettringite was not identified by XRD, dehydration products of this compound are not considered.

The second loss observed in figure 10 corresponds to the dehydration of portlandite $Ca(OH)_2$ (mainly at temperatures about 400-550 ºC that correspond to 2400-3500 s (equation 6):

$$Ca(OH)_2 \rightarrow CaO + H_2O \qquad (6)$$

According to XRD and TG results, Ca (OH)2 is not present in FA and is present in a low amount in BA (1.02 %), being higher than the value in WG0 (5.01 %) and decreasing in WG10 and WG40 (2.42 and 2.65 % respectively). According to the TG initial composition of FA and BA, this compound seems to form in the process, by the hydration of lime present initially mainly in FA, but also BA.

The next interval, approximately from 3500 to 4750s (550 to 800 ºC) corresponds to a CO_2 loss, as a mass spectrum (MS) is identified in all the studied samples (equation 7) (Bae and Lee, 2015; Bernal et al., 2015).

$$CaCO_3 \rightarrow CaO + CO_2 \qquad (7)$$

The presence of $CaCO_3$ in FA and BA seems obvious, because of the reaction of the CaO or Ca $(OH)_2$ from the desulphurised sorbent with CO_2 obtained in the combustion process where the ashes are formed. In the conditions of the temperature of a CFBC, near 900ºC, the bottom ash must eliminate the CO_2 from $CaCO_3$.

In the case of FA, the loss continues up to more than 6000s (1000ºC), showing MS results in overlapping between CO_2 and SO_2 losses, and at the end, SO_3 loss. The presence of two peaks for CO_2 may differentiate the $CaCO_3$ initially formed or the $CaCO_3$ initially present in the desulphurised sorbent, which achieves a lower or higher decomposition temperature, respectively.

The loss of CFBC FA in the interval up to more than 6000s (1000 ºC) is higher (30.4 %), being only 6.35 % at higher temperatures. On the contrary is found in CFBC BA, whose main loss takes place at higher temperatures (1000 ºC to 1350 ºC), attributed to $CaSO_4$. In the case of FA, if the higher loss is attributed to $CaSO_3$ and the last to $CaSO_4$, the percentage of SO_2 would be in the same order found by XRF results (36.9 % in TG versus 38.9 % in XRF).

The reaction products after 28 days show a decreasing sequence of carbonate decomposition from WG0 to WG40. In the case of the 800-1000 ºC interval, no loss appears in the case of WG0, without SO_2 signal in the MS recorded, and low values for WG0 and WG40 of 4.59 % and 3.03 %, respectively. In the last interval (1000 ºC to 3500 ºC) the values oscillate between 10.58 % in WG10 to 13.52 % in WG40.

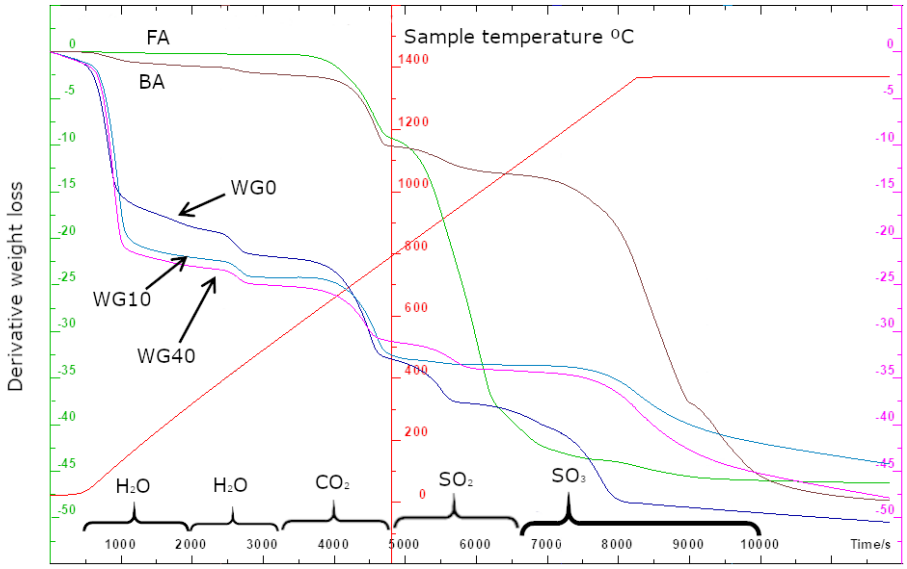

Figure 4.20. TG-DTG Fly Ash (FA), Bottom Ash (BA), WG0, WG10 and WG40 binders.

4.2.2.4. *Scanning electron microscopy-SEM*

Figure 4.21 show the microstructure of different samples and their surface composition examined by SEM/EDS.

For the three selected samples, it is possible to find structure and composition that may indicate the presence of gel C-S-H. It was easier to find this kind of structure in the samples without any BA added. This is explained by the fact that the FA are richer in SiO_2 and Al_2O_3.

On the other hand, there is thernadite (Na_2SO_4) appears in different shapes in the three samples, being easier to find in the samples with more amount of BA (WG40).

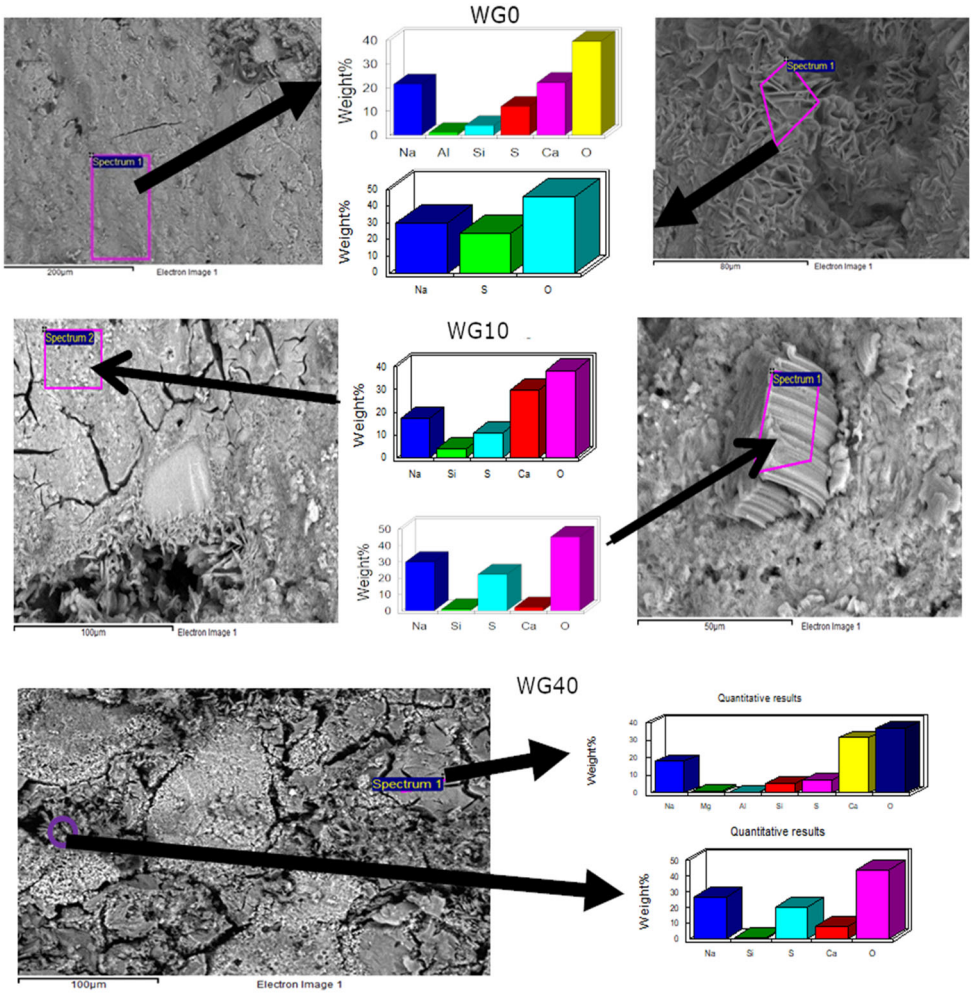

Figure 4.21. SEM-EDX WG0, WG10, and WG40 binders.

4.2.2.5. Fourier-transform infrared spectroscopy-FTIR

FTIR spectroscopy allows the identification of different types of chemical bonds in materials on a molecular level. Therefore, the differences between the absorption curve for the ashes and products may provide some evidence of the reactions happening.

In Figure 4.22 it is possible to appreciate the Fourier spectrum for the Fly Ash (FA) vs WG0 binder; Bottom Ash (BA) vs WG40 binder; and between the binders WG0, WG10, and WG40 (Table 4.10. Mix Design).

The band centered towards around 1120cm^{-1} represent the SO_4^{2-}, for both Ca and Na Band at around 594 cm^{-1} is assigned to S-O vibrations of SO_4^{2-} in gypsum ($CaSO_4{\cdot}2H_2O$). While the band at 2800 cm^{-1} shows the presence of Na_2SO_4 (Dung et al., 2014; Carmona-Quiroga and Blanco-Varela, 2013). The symmetrical deforming bands of water absorption (H_2O) appeared in the region 1600-1700 cm^{-1} and the bands located in regions above 3000 cm^{-1} were assigned for the symmetrical stretching vibration of absorbed water (H_2O) and stretching vibration of free OH (Nguyen et al., 2019; Carmona-Quiroga and Blanco-Varela, 2013). The isolated OH stretching at 3,638 cm^{-1} is attributed to the interaction of the water hydroxyl with the cations, associated with the $Ca(OH)_2$. The weak OH band in the case of the composites is related to the consumption of $Ca(OH)_2$ to produce other hydration products (Dung et al., 2014). The signals appearing at 1,442 cm^{-1} and around 876 cm^{-1} are attributed to C-O vending (CO_3^-) (García-Lodeiro et al., 2008). The presence of $CaCO_3$ issue the reaction between $Ca(OH)_2$ in specimens and CO_2 during the air curing. The vibrations in the region 964–980 cm^{-1} are assigned to the presence of Si-O stretching and the signals appearing at around 490 cm^{-1} correspond to the Si-O-Si (García-Lodeiro et al., 2008), which confirms the generation of calcium silicate hydrate (C-S-H). Other evidence related to the reaction process may include the band around 1645 cm^{-1} for H–O–H bending vibration, the increase of the vibration intensities indicates the formation of calcium silicate hydrates (Li et al., 2012), and the shift of the peak at 1045 cm^{-1} towards lower wavenumber, indicate the deformation of the lattice due to the pozzolanic reaction (Li et al., 2012). The FT-IR results indicate that the hydration products mainly include C–S–H, Na_2S0_4, $CaSO_4{\cdot}2H_2O$, $CaCO_3$ and $Ca(OH)_2$, which are in agreement with those of XRD, TG, and SEM.

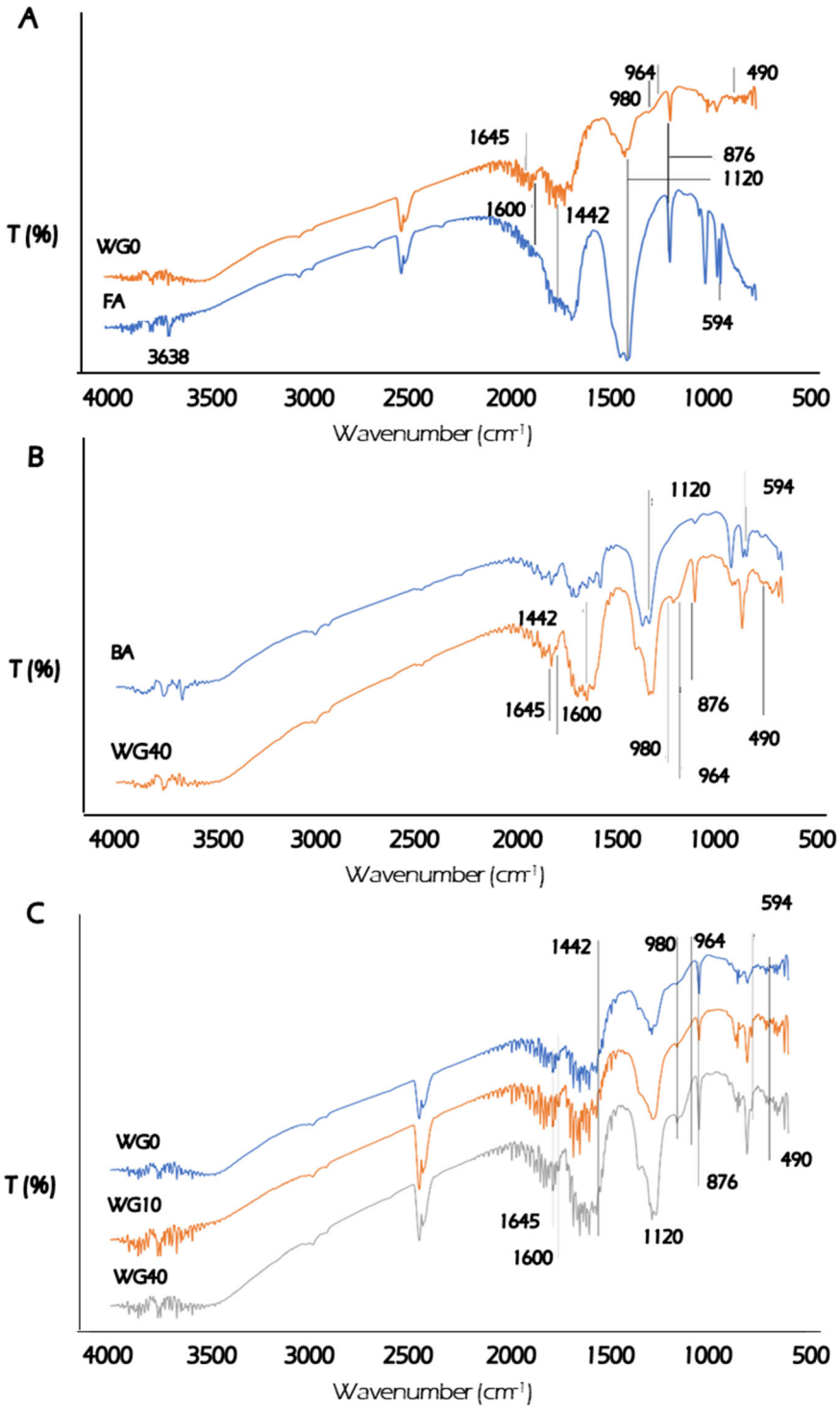

Figure 4.22. FTIR spectra of: (A) Fly Ash and WG0 binder; (B) Bottom Ash and WG40 binder; (C) WG0, WG10, and WG40 binders.

4.3. CONCLUSIONS

From the results of the experiment carried out only with the CFBC Bottom ashes (BA), it can be concluded that the chemical composition, high content of anhydrite and lime, some presence of portlandite, and low content of silica and alumina, disables the alkaline activation of these ashes. When these materials reach a decent hardness, they do not contain enough SiO_2 and Al_2O_3 to form three-dimensional networks. While the results obtained only with the CFBC Fly ashes (FA) contain the greater potential for geopolymerisation, due to difference from the previous ones shows small amounts of quartz and alumina, producing materials with high mechanical capacities that do not collapse when immersed in water.

The utilisation of CFBC Fly and Bottom ashes in different proportions mixed with Na_2SiO_3 and Na_2CO_3 to produce building material has been investigated along with the reactions appearing in the process. The compressive strength values of all of the sample mixtures ranged from 15 to 30 MPa after 14 and 28 days of curing, showing an increasing trend through the days. At a curing age of 28 days, the samples that incorporated a similar amount of FA and BA (WG8 and WG10) exhibited the maximum compressive strength value of all the investigated samples. The results show that, even if the compressive strength is lower after the water immersion, the samples still show good compressive resistance. The results from different analysis techniques indicate that the hydration products mainly include calcium silicate hydrate gel (C–S–H), thenardite (Na_2SO_4), gypsum ($CaSO_4$ $2H_2O$), calcium carbonate ($CaCO_3$), and portlandite ($Ca(OH)_2$).

The results obtained may give a way of recovery of CFBC bottom ash for its potential use as an eco-material, showing physical integrity by being cured in water and reaching compressive strength values greater than 10.0 MPa. And also fill a deficit in the understanding of the reaction mechanisms of blends of fly and bottom ashes activated with near-neutral salts, such as sodium carbonate.

4.4. REFERENCES

- Alemu A.S, Lee B.Y, Park S, Kim H-K. Self-healing of Portland and slag cement binder systems incorporating circulating fluidized bed combustion bottom ash. Con Build Mat 2022; 314; 125571. Doi: 10.1016/j.conbuildmat.2021.125571.
- Anthony, E J, and L Jia. 2000. "<Anthony EJ - Fuel 79 - 2000 - 1933-1942.Pdf>" 79: 1933–42.
- Anthony, E. J., L. Jia, A. P. Iribarne, G. Welford, J. Wang, and O. Trass. 2006. "Calcium Sulphide in FBC Boilers and Its Fate Using Liquid Water Reactivation." Fuel 85 (12–13): 1871–79. https://doi.org/10.1016/j.fuel.2006.01.014.
- Antonia López-Antón, M., D. Alan Spears, Mercedes Díaz-Somoano, Luis Diaz, and M. Rosa Martínez-Tarazona. 2015. "Enrichment of Thallium in Fly Ashes in a Spanish Circulating Fluidized-Bed Combustion Plant." Fuel 146 (January): 51–55. https://doi.org/10.1016/j.fuel.2015.01.007.
- ASTM C563. Approximation of optimum SO3 in hydraulic cement using compressive strength.
- Bae, Soon Jong, and Ki Gang Lee. 2015. "Carbonation Behavior of Fly Ash with Circulating Fluidized Bed Combustion (CFBC)." Journal of the Korean Ceramic Society 52 (2): 154–58. https://doi.org/10.4191/kcers.2015.52.2.154.
- Bonn, Bernhard, and Gudrun Pelz. 1995. "<Bonn B - Fuel 74-2- 1995 - 165-171.Pdf>" 74 (2): 165–71.
- C. Chen, Q. Li, L. Shen, J. Zhai. Feasibility of manufacturing geopolymer bricks using circulating fluidized bed combustion bottom ash. Environ. Technol. 33 (2012) 1313-1321.
- C. Ng, U. J. Alengaram, L. S. Wong, K. H. Mo, M. Z. Jumaat, S. Ramesh. Constr. Build. Mater. 186 (2018) 550-576.
- Cao, Yan, Chin Min Cheng, Chien Wei Chen, Mingchong Liu, Chiawei Wang, and Wei Ping Pan. 2008. "Abatement of Mercury Emissions in the Coal Combustion Process Equipped with a Fabric Filter Baghouse." Fuel 87 (15–16): 3322–30. https://doi.org/10.1016/j.fuel.2008.05.010.
- Chen, Chun Tao, Hoang Anh Nguyen, Ta Peng Chang, Tzong Ruey Yang, and Tien Dung Nguyen. 2015. "Performance and Microstructural Examination on Composition of Hardened Paste with No-Cement SFC Binder." Construction and Building Materials 76: 264–72. https://doi.org/10.1016/j.conbuildmat.2014.11.032.
- Chen, Xuemei, Yun Yan, Yuanzheng Liu, and Zhihua Hu. 2014. "Utilisation of Circulating Fluidized Bed Fly Ash for the Preparation of Foam Concrete." Construction and Building Materials 54: 137–46. https://doi.org/10.1016/j.conbuildmat.2013.12.020.
- Cheng C-Y, Yang Y-N, Huang A-N, Kuo H-P. Steam hydration of CFBC bottom ashes in a rotary kiln. Journal of the Taiwan Institute of Chemical Engineers. 2013; 44, 1060-1066. Doi: 10.1016/j.jtice.2013.05.025.
- Chi, Maochieh, and Ran Huang. 2014. "Effect of Circulating Fluidized Bed Combustion Ash on the Properties of Roller Compacted Concrete." Cement and Concrete Composites 45: 148–56. https://doi.org/10.1016/j.cemconcomp.2013.10.001.
- Chi, Maochieh. 2016. "Synthesis and Characterisation of Mortars with Circulating Fluidized Bed Combustion Fly Ash and Ground Granulated Blast-Furnace Slag." Construction and Building Materials 123: 565–73. https://doi.org/10.1016/j.conbuildmat.2016.07.071.
- Chunbo Wang, Lufei Jia, Yewen Tan, E.J. Anthony. Carbonation of fly ash in oxy-fuel CFB combustion. Fuel 87 (2008) 1108–1114.
- Davidovits J. Geopolymer: Chemistry & Applications; Institut Geopolymere: Saint Quentin, France, 2011.

- Dung, Nguyen Tien, Ta Peng Chang, and Chun Tao Chen. 2014. "Engineering and Sulfate Resistance Properties of Slag-CFBC Fly Ash Paste and Mortar." Construction and Building Materials 63: 40–48. https://doi.org/10.1016/j.conbuildmat.2014.04.009.
- Dung, Nguyen Tien, Ta Peng Chang, Chun Tao Chen, and Tzong Ruey Yang. 2016. "Cementitious Properties and Microstructure of an Innovative Slag Eco-Binder." Materials and Structures/Materiaux et Constructions 49 (5): 2009–24. https://doi.org/10.1617/s11527-015-0630-6.
- Dung, Nguyen Tien, Ta-Peng Chang, and Chun-Tao Chen. 2014. "Hydration Process and Compressive Strength of Slag-CFBC Fly Ash Materials without Portland Cement." Journal of Materials in Civil Engineering 27 (7): 04014213. https://doi.org/10.1061/(asce)mt.1943-5533.0001177.
- Dung, Nguyen Tien, Ta-Peng Chang, and Tzong-Ruey Yang. 2014. "Performance Evaluation of an Eco-Binder Made with Slag and CFBC Fly Ash." Journal of Materials in Civil Engineering 26 (12): 04014096. https://doi.org/10.1061/(asce)mt.1943-5533.0001019.
- E.J. Anthony, L. Jia. Agglomeration and strength development of deposits in CFBC boilers firing high-sulphur fuels. Fuel 79 (2000) 1933–1942
- Fu, Xiaoru, Qin Li, Jianping Zhai, Guanghong Sheng, and Feihu Li. 2008. "The Physical-Chemical Characterisation of Mechanically-Treated CFBC Fly Ash." Cement and Concrete Composites 30 (3): 220–26. https://doi.org/10.1016/j.cemconcomp.2007.08.006.
- G. Sheng, Q. Li, J. Zhai. Investigation on the hydration of CFBC fly ash. Fuel 98 (2012) 61-66.
- García-Lodeiro I, Fernández-Jiménez A, Pena P, Palomo A. Alkali activation of synthetic aluminosilicate glasses. Cer Int; 2014; 40; 5547-5558. Doi: 10.1016/j.ceramint.2013.10.146.
- Glinicki, Michal A., and Marek Zielinski. 2008. "Air Void System in Concrete Containing Circulating Fluidized Bed Combustion Fly Ash." Materials and Structures/Materiaux et Constructions 41 (4): 681–87. https://doi.org/10.1617/s11527-007-9273-6.
- Glinicki, Michal A., and Marek Zielinski. 2009. "Frost Salt Scaling Resistance of Concrete Containing CFBC Fly Ash." Materials and Structures/Materiaux et Constructions 42 (7): 993–1002. https://doi.org/10.1617/s11527-008-9438-y.
- H.R. Gavali, a. Bras, P. Faria, R.V. Ralegaonkar. Development of sustainable alkali-activated bricks using industrial waste. Constr. Build. Mater. 215 (2019) 180-191.
- He P, Zhang X, Chen H, Zhang Y. Waste-to-resource strategies for the use of circulating fluidized bed fly ash in construction materials: A mini review. Pow Tec; 2021; 393; 773-785. Doi: 10.1016/j.powtec.2021.08.035.
- Hlaváček, Petr, Rostislav Šulc, Vít Šmilauer, Christiane Rößler, and Roman Snop. 2018. "Ternary Binder Made of CFBC Fly Ash, Conventional Fly Ash, and Calcium Hydroxide: Phase and Strength Evolution." Cement and Concrete Composites 90: 100–107. https://doi.org/10.1016/j.cemconcomp.2017.09.020.
- Hoang-Anh Nguyen, Ta-Peng Chang, Jeng-Ywan Shih, Chun-Tao Chen, Tien-Dung Nguyen. Engineering properties and durability of high-strength self-compacting concrete with no-cement SFC binder. Construction and Building Materials 106 (2016) 670–677.
- Hoang-Anh Nguyen, Ta-Peng Chang, Jeng-Ywan Shih, Chun-Tao Chen, Tien-Dung Nguyen. Influence of circulating fluidized bed combustion (CFBC) fly ash on properties of modified high volume low calcium fly ash (HVFA) cement paste.2015
- Hoang-Anh Nguyen, Ta-Peng Chang, Jeng-Ywan Shih, Chun-Tao Chen. Influence of low calcium fly ash on compressive strength and hydration product of low energy super sulfated cement paste. Cement and Concrete Composites 99 (2019) 40–48
- Huynh, Trong Phuoc, Duy Hai Vo, and Chao Lung Hwang. 2018. "Engineering and Durability Properties of Eco-Friendly Mortar Using Cement-Free SRF Binder." Construction

and Building Materials 160 (x): 145–55. https://doi.org/10.1016/j.conbuildmat.2017.11.040.

- I.B. TopCu, M.U. Toprak, T. Uygunoglu. Durability and microstructure characteristics of alkali activated coal bottom ash geopolymer cement. J. Clean Prod. 81 (2014) 211-217.
- Ines García-Lodeiro, A. Fernández-Jimenez, M. Teresa Blanco, Angel Palomo. FTIR study of the sol–gel synthesis of cementitious gels: C–S–H and N–A–S–H. J Sol-Gel Sci Technol (2008) 45:63–72
- Iribarne, Agripanea P., Julio V. Iribarne, and Edward J. Anthony. 1997. "Reactivity of Calcium Sulfate from FBC Systems." Fuel 76 (4): 321–27. https://doi.org/10.1016/S0016-2361(96)00239-6.
- J.G. Jang, S.M. Park, S. Chung, JW. Ahn, HK Kim. Utilisation of circulating fluidized bed combustion ash in producing controlled low-strength materials with cement or sodium carbonate as activator. Constr. Build. Mater. Xxx (2017) xxx-xxx.
- Jang J.G, Park S-M, Chung S, Ahn J-W, Kim H-K. Utilisation of circulating fluidized bed combustion ash in producing controlled low-strength materials with cement or sodium carbonate as activator. Con Build Mat; 2018; 159; 642-651. Doi: 10.1016/j.conbuildmat.2017.08.158.
- Jang, Jeong Gook, Sol Moi Park, Sangho Chung, Ji Whan Ahn, and Hyeong Ki Kim. 2018. "Utilisation of Circulating Fluidized Bed Combustion Ash in Producing Controlled Low-Strength Materials with Cement or Sodium Carbonate as Activator." Construction and Building Materials 159: 642–51. https://doi.org/10.1016/j.conbuildmat.2017.08.158.
- Kang, Yong Hak, and Young Cheol Choi. 2018. "Development of Non-Sintered Zero-OPC Binders Using Circulating Fluidized Bed Combustion Ash." Construction and Building Materials 178: 562–73. https://doi.org/10.1016/j.conbuildmat.2018.05.184.
- Konist, A., A. Valtsev, L. Loo, T. Pihu, M. Liira, and K. Kirsimäe. 2015. "Influence of Oxy-Fuel Combustion of Ca-Rich Oil Shale Fuel on Carbonate Stability and Ash Composition." Fuel 139: 671–77. https://doi.org/10.1016/j.fuel.2014.09.050.
- Lawrence, A., V. Ilayaperumal, K. P. Dhandapani, S. V. Srinivasan, M. Muthukrishnan, and S. Sundararajan. 2013. "A Novel Technique for Characterizing Sintering Propensity of Low Rank Fuels for CFBC Boilers." Fuel 109: 211–16. https://doi.org/10.1016/j.fuel.2012.12.063.
- Lee H.K, Jeon S-M, Lee B.Y, Kim H-K, Use of circulating fluidized bed combustion bottom ash as a secondary activator in hgh-volume slag cement. Con Build Mat; 2020; 234; 117240. Doi: 10.1016/j.conbuildmat.2019.117240.
- Lee, Jae Hoon, and Ki Gang Lee. 2016. "Carbonation Behavior of Lightweight Foamed Concrete Using Coal Fly Ash." Journal of the Korean Ceramic Society 53 (3): 354–61. https://doi.org/10.4191/kcers.2016.53.3.354.
- Lee, Ki Gang, and Soon Jong Bae. 2018. "Carbonation of Circulating Fluidized Bed Combustion Fly Ash with Hybrid Reaction." Journal of the Korean Ceramic Society 55 (2): 160–65. https://doi.org/10.4191/kcers.2018.55.2.07.
- Lee, Seung Heun, and Guen Su Kim. 2017. "Self-Cementitious Hydration of Circulating Fluidized Bed Combustion Fly Ash." Journal of the Korean Ceramic Society 54 (2): 128–36. https://doi.org/10.4191/kcers.2017.54.2.07.
- Li, Xiang Guo, Quan Bin Chen, Bao Guo Ma, Jian Huang, Shou Wei Jian, and Bei Wu. 2012. "Utilisation of Modified CFBC Desulphurisation Ash as an Admixture in Blended Cements: Physico-Mechanical and Hydration Characteristics." Fuel 102: 674–80. https://doi.org/10.1016/j.fuel.2012.07.010.
- Li, Xiang Guo, Quan Bin Chen, Kuai Zhong Huang, Bao Guo Ma, and Bei Wu. 2012. "Cementitious Properties and Hydration Mechanism of Circulating Fluidized Bed

Combustion (CFBC) Desulphurisation Ashes." Construction and Building Materials 36: 182–87. https://doi.org/10.1016/j.conbuildmat.2012.05.017.

- Liu, Zhuo, Jianbo Li, Quanhai Wang, Xiaofeng Lu, Yuanyuan Zhang, Mingming Zhu, Zhezi Zhang, and Dongke Zhang. 2019. "An Experimental Investigation into Mineral Transformation, Particle Agglomeration and Ash Deposition during Combustion of Zhundong Lignite in a Laboratory-Scale Circulating Fluidized Bed." Fuel 243 (November 2018): 458–68. https://doi.org/10.1016/j.fuel.2019.01.134.
- Manzoori, A. R., and P. K. Agarwal. 1993. "The Role of Inorganic Matter in Coal in the Formation of Agglomerates in Circulating Fluid Bed Combustors." Fuel 72 (7): 1069–75. https://doi.org/10.1016/0016-2361(93)90310-X.
- Maochieh Chi, Ran Huang. Effect of circulating fluidized bed combustion ash on the properties of roller compacted concrete. Cement & Concrete Composites 45 (2014) 148–156.
- Maochieh Chi. Synthesis and characterisation of mortars with circulating fluidized bed combustion fly ash and ground granulated blast-furnace slag. Construction and Building Materials 123 (2016) 565–573
- Marks, Maria, Daria Jóźwiak-Niedźwiedzka, Michał A. Glinicki, Jan Olek, and Michał Marks. 2012. "Assessment of Scaling Durability of Concrete with CFBC Ash by Automatic Classification Rules." Journal of Materials in Civil Engineering 24 (7): 860–67. https://doi.org/10.1061/(asce)mt.1943-5533.0000464.
- Moon, Eun Jin, and Young Cheol Choi. 2019. "Carbon Dioxide Fixation via Accelerated Carbonation of Cement-Based Materials: Potential for Construction Materials Applications." Construction and Building Materials 199: 676–87. https://doi.org/10.1016/j.conbuildmat.2018.12.078.
- N. Toniolo, A. Rincón,J.A. Roether, P. Ercole, E. Bernardo, A.R. Boccaccini. Constr. Build. Mater. 188 (2018) 1077-1084.
- Nguyen Tien Dung, Ta-Peng Chang, Chun-Tao Chen, Tzong-Ruey Yang. Cementitious properties and microstructure of an innovative slag eco-binder. Materials and Structures (2016) 49:2009–2024
- Nguyen Tien Dung; Ta-Peng Chang; and Chun-Tao Chen. Hydration Process and Compressive Strength of Slag-CFBC Fly Ash Materials without Portland Cement. 2014 American Society of Civil Engineers.
- Nguyen Tien Dung; Ta-Peng Chang; and Chun-Tao Chen. Hydration Process and Compressive Strength of Slag-CFBC Fly Ash Materials without Portland Cement. 2014 American Society of Civil Engineers.
- Nguyen, Hoang Anh, Ta Peng Chang, Jeng Ywan Shih, and Chun Tao Chen. 2019. "Influence of Low Calcium Fly Ash on Compressive Strength and Hydration Product of Low Energy Super Sulfated Cement Paste." Cement and Concrete Composites 99: 40–48. https://doi.org/10.1016/j.cemconcomp.2019.02.019.
- Nguyen, Hoang Anh, Ta Peng Chang, Jeng Ywan Shih, Chun Tao Chen, and Tien Dung Nguyen. 2016. "Engineering Properties and Durability of High-Strength Self-Compacting Concrete with No-Cement SFC Binder." Construction and Building Materials 106: 670–77. https://doi.org/10.1016/j.conbuildmat.2015.12.163.
- Nguyen, Hoang Anh, Ta Peng Chang, Jeng Ywan Shih, Chun Tao Chen, and Tien Dung Nguyen. 2015. "Influence of Circulating Fluidized Bed Combustion (CFBC) Fly Ash on Properties of Modified High Volume Low Calcium Fly Ash (HVFA) Cement Paste." Construction and Building Materials 91: 208–15. https://doi.org/10.1016/j.conbuildmat.2015.05.075.

- Nguyen, Hoang-Anh, Ta-Peng Chang, and Jeng-Ywan Shih. 2017. "Engineering Properties and Bonding Behavior of Self-Compacting Concrete Made with No-Cement Binder." Journal of Materials in Civil Engineering 30 (3): 04017294. https://doi.org/10.1061/(asce)mt.1943-5533.0002136.
- P.M. Carmona-Quiroga, M.T. Blanco-Varela Ettringite decomposition in the presence of barium carbonate. Cement and Concrete Research 52 (2013) 140–148.
- Pacheco-Torgal F, Labrincha J.A, Leonelli C, Palomo A, Chindaprasirt P. Handbook of alkali-activated cements, mortars and concretes. Woodhead publishing: Waltham, MA, USA, 2015.
- Park S.M, Lee N.K, Lee H.K. Circulating fluidized bed combustion ash as controlled low-strength material (CLSM) by alkaline activation. Con Build Mat; 2017; 156; 728-738. Doi: 10.1016/j.conbuildmt.2017.09.001.
- Park, Jae Hyeok, Dong Ho Lee, Keun Hee Han, Jong Seon Shin, Dal Hee Bae, Tae Earn Shim, Jeong Hwan Lee, and Dowon Shun. 2019. "Effect of Chemical Additives on Hard Deposit Formation and Ash Composition in a Commercial Circulating Fluidized Bed Boiler Firing Korean Solid Recycled Fuel." Fuel 236 (September 2018): 792–802. https://doi.org/10.1016/j.fuel.2018.09.020.
- Park, Kyoungil, Jong Min Lee, Dong Won Kim, Gyu Hwa Lee, and Yong Kang. 2019. "Characteristics of Co-Combustion of Strongly Caking and Non-Caking Coals in a Pilot Circulating Fluidized Bed Combustor (CFBC)." Fuel 236 (September 2018): 1110–16. https://doi.org/10.1016/j.fuel.2018.09.052.
- Park, S. M., J. H. Seo, and H. K. Lee. 2018. "Binder Chemistry of Sodium Carbonate-Activated CFBC Fly Ash." Materials and Structures/Materiaux et Constructions 51 (3). https://doi.org/10.1617/s11527-018-1183-2.
- Park, S. M., N. K. Lee, and H. K. Lee. 2017. "Circulating Fluidized Bed Combustion Ash as Controlled Low-Strength Material (CLSM) by Alkaline Activation." Construction and Building Materials 156: 728–38. https://doi.org/10.1016/j.conbuildmat.2017.09.001.
- Petr Hlaváček, Rostislav Šulc, Vít Šmilauer, Christiane Rößler, Roman Snop. Ternary binder made of CFBC fly ash, conventional fly ash, and calcium hydroxide: Phase and strength evolution. Cement and Concrete Composites (2018).
- Pihu, T., H. Arro, A. Prikk, R. Rootamm, A. Konist, K. Kirsimäe, M. Liira, and R. Mõtlep. 2012. "Oil Shale CFBC Ash Cementation Properties in Ash Fields." Fuel 93: 172–80. https://doi.org/10.1016/j.fuel.2011.08.050.
- Pisupati, Sarma V, Ronald S Wasco, Joel L Morrison, and Alan W Scaroni. 1998. "<Pisupati SV - Fuel 75 - 1996 - 759-768.Pdf>" 75 (6): 759–68.
- Provis, J.L.; van Deventer, J.S.J. Geopolymers: Structures, Processing, Properties and Industrial Applications; Woodhead Publishing: Waltham, MA, USA, 2009.
- O. Li, H. Xu, F. Li, P. Li, L. Shen, J. Zhai. Synthesis of geopolymer composites ffrom blends of CFCB fly and bottom ashes. Fuel. 97 (2012) 366-372.
- R. Slavik, V. Bednarik, M. Vondruska, A. Nemec. Preparation of geopolymer from fluidized bed combustion bottom ash. J. Mat. Proc. Tech. 200 (2008) 265-270.
- Rao, A., E. J. Anthony, L. Jia, and A. Macchi. 2007. "Carbonation of FBC Ash by Sonochemical Treatment." Fuel 86 (16): 2603–15. https://doi.org/10.1016/j.fuel.2007.02.004.
- Rao, Arjun, Edward J. Anthony, and Vasilije Manovic. 2008. "Sonochemical Treatment of FBC Ash: A Study of the Reaction Mechanism and Performance of Synthetic Sorbents." Fuel 87 (10–11): 1927–33. https://doi.org/10.1016/j.fuel.2007.11.007.

- Rust, David, Robert Rathbone, Kamyar C. Mahboub, and Tom Robl. 2011. "Formulating Low-Energy Cement Products." Journal of Materials in Civil Engineering 24 (9): 1125–31. https://doi.org/10.1061/(asce)mt.1943-5533.0000456.
- S.A. Bernal, E.D. Rodríguez, R. Mejía de Gutiérrez, J.L. Provis. Performance at high temperature of alkali-activated slag pastes produced with silica fume and rice husk ash based activators. Materiales de Construcción Vol. 65, Issue 318, April–June 2015, e049
- S.M. Park, J.H. Seo, H.K. Lee. Binder chemistry of sodium carbonate activated CFBC fly ash. Mater. Struct. (2018) 51-59.
- S.M. Park, N.K. Lee, H.K. Lee. Citculating fluidized bed combustion ash as controlled low-strength material (CLSM) by alkaline activation. Constr. Build. Mater. 156 (2017) 728-738.
- Seung-Heun Lee and Guen-Su Kim. Self-Cementitious Hydration of Circulating Fluidized Bed Combustion Fly Ash. Journal of the Korean Ceramic Society Vol. 54, No. 2, pp. 128~136, 2017.
- Shen, Yan, Jueshi Qian, and Zhiwei Zhang. 2013. "Investigations of Anhydrite in CFBC Fly Ash as Cement Retarders." Construction and Building Materials 40: 672–78. https://doi.org/10.1016/j.conbuildmat.2012.11.056.
- Sheng, Guanghong, Jianping Zhai, Qin Li, and Feihu Li. 2007. "Utilisation of Fly Ash Coming from a CFBC Boiler Co-Firing Coal and Petroleum Coke in Portland Cement." Fuel 86 (16): 2625–31. https://doi.org/10.1016/j.fuel.2007.02.018.
- Sheng, Guanghong, Qin Li, and Jianping Zhai. 2012. "Investigation on the Hydration of CFBC Fly Ash." Fuel 98: 61–66. https://doi.org/10.1016/j.fuel.2012.02.008.
- Shimizu, Tadaaki, and Masanori Toyono. 2007. "Emissions of NOx and N2O during Co-Combustion of Dried Sewage Sludge with Coal in a Circulating Fluidized Bed Combustor." Fuel 86 (15): 2308–15. https://doi.org/10.1016/j.fuel.2007.01.033.
- Shon, Chang Seon, Anal K. Mukhopadhyay, Don Saylak, Dan G. Zollinger, and Gleb G. Mejeoumov. 2010. "Potential Use of Stockpiled Circulating Fluidized Bed Combustion Ashes in Controlled Low Strength Material (CLSM) Mixture." Construction and Building Materials 24 (5): 839–47. https://doi.org/10.1016/j.conbuildmat.2009.10.022.
- Siddique S, Kim H, Jang JG. Properties of high-volume slag cement mortar incorporating circulating fluidized bed combustion fly ash and bottom ash. Con Build Mat; 2021; 289; 123150. Doi: 10.1016/j.conbuildmat.2021.123150.
- Skodras, George, Panagiotis Grammelis, Maria Prokopidou, Emmanuel Kakaras, and George Sakellaropoulos. 2009. "Chemical, Leaching and Toxicity Characteristics of CFB Combustion Residues." Fuel 88 (7): 1201–9. https://doi.org/10.1016/j.fuel.2007.06.009.
- Song, Yuanming, Chuanchuan Guo, Jueshi Qian, and Tian Ding. 2015. "Effect of the Ca-to-Si Ratio on the Properties of Autoclaved Aerated Concrete Containing Coal Fly Ash from Circulating Fluidized Bed Combustion Boiler." Construction and Building Materials 83: 136–42. https://doi.org/10.1016/j.conbuildmat.2015.02.077.
- Soon Jong Bae and Ki Gang Lee. Carbonation Behavior of Fly Ash with Circulating Fluidized Bed Combustion (CFBC). Journal of the Korean Ceramic Society.
- Soundarrajan, Nari, Peter L. Rozelle, and Sarma V. Pisupati. 2012. "Development and Use of a Method for Prediction of the Ash Split in a CFBC Boiler to Improve the Energy Efficiency." Fuel 102: 9–15. https://doi.org/10.1016/j.fuel.2008.04.040.
- Talukdar, Jib, Prabir Basu, and Jay H. Greenblatt. 1996. "Reduction of Calcium Sulfate in a Coal-Fired Circulating Fluidized Bed Furnace." Fuel 75 (9): 1115–23. https://doi.org/10.1016/0016-2361(96)00054-3.
- TopÇu IB, Toprak MU. Properties of geopolymer from circulating fluidized bed combustion coal bottom ash. Mat Sci Eng A; 2011; 528; 1472-1477. Doi: 10.1016/j.msea.2010.10.062.

- Trong-Phuoc Huynh, Duy-Hai Vo, Chao-Lung Hwang. Engineering and durability properties of eco-friendly mortar using cement-free SRF binder. Construction and Building Materials 160 (2018) 145–155
- Wang, Chunbo, Lufei Jia, Yewen Tan, and E. J. Anthony. 2008. "Carbonation of Fly Ash in Oxy-Fuel CFB Combustion." Fuel 87 (7): 1108–14. https://doi.org/10.1016/j.fuel.2007.06.024.
- Wu, Tehsien, Maochieh Chi, and Ran Huang. 2014. "Characteristics of CFBC Fly Ash and Properties of Cement-Based Composites with CFBC Fly Ash and Coal-Fired Fly Ash." Construction and Building Materials 66: 172–80. https://doi.org/10.1016/j.conbuildmat.2014.05.057.
- Wu, Yinghai, Edward J. Anthony, and Lufei Jia. 2004. "Steam Hydration of CFBC Ash and the Effect of Hydration Conditions on Reactivation." Fuel 83 (10): 1357–70. https://doi.org/10.1016/j.fuel.2004.01.006.
- X Li, Q. Chen, K. Huang, B. Ma, B. Wu. Cementitious properties and hydration mechanism of circulating fluidized bed combustion (CFBC) desulphurisation ashes. Constr. Build. Mater. 36 (2012) 182-187.
- X. Li, Q Chen B. Ma, J. Huang, S. Jian, B. Wu. Utilisation of modified CFBC desulphurisation ash as an admixture in blended cements: Physico-mechanical and hydration characteristics. Fuel 102 (2012) 674-680.
- Xia, Yanqing, Yun Yan, and Zhihua Hu. 2013. "Utilisation of Circulating Fluidized Bed Fly Ash in Preparing Non-Autoclaved Aerated Concrete Production." Construction and Building Materials 47: 1461–67. https://doi.org/10.1016/j.conbuildmat.2013.06.033.
- Xu H, Li Q, Shen L, Wang W, Zhai J. Synthesis of thermostable geopolymer from circulating fluidized bed combustion (CFBC) bottom ashes. J Haz Mat; 2010; 175; 198-204. Doi: 10.1016/j.jhazmat.2009.09.149.
- Xu Xun, Xu Yuanyuan, Duan Liling. Effect of fineness and components of CFBC ash on performance of basic magnesium sulfate cement. Construction and Building Materials 170 (2018) 801–811
- Xu, Xun, Yuanyuan Xu, and Liling Duan. 2018. "Effect of Fineness and Components of CFBC Ash on Performance of Basic Magnesium Sulfate Cement." Construction and Building Materials 170: 801–11. https://doi.org/10.1016/j.conbuildmat.2018.03.054.
- Y. Shen, J. Qian, Z. Zhang. Investigations of anhydrite in CFBC fly ash as cement retarders. Constr. Build. Mater. 40 (2013) 672-678.
- Yoffe, O., A. Wohlfarth, Y. Nathan, S. Cohen, and T. Minster. 2007. "Oil Shale Fueled FBC Power Plant - Ash Deposits and Fouling Problems." Fuel 86 (17–18): 2714–27. https://doi.org/10.1016/j.fuel.2007.03.010.
- Yong Hak Kang, Young Cheol Choi. Development of non-sintered zero-OPC binders using circulating fluidized bed combustion ash. Construction and Building Materials 178 (2018) 562–573
- Yuanming Song, Chuanchuan Guo, Jueshi Qian, Tian Ding. Effect of the Ca-to-Si ratio on the properties of autoclaved aerated concrete containing coal fly ash from circulating fluidized bed combustion boiler. Construction and Building Materials 83 (2015) 136–142
- Zhai, Jianping, Feihu Li, Hui Xu, Lifeng Shen, Peiming Li, and Qin Li. 2012. "Synthesis of Geopolymer Composites from Blends of CFBC Fly and Bottom Ashes." Fuel 97: 366–72. https://doi.org/10.1016/j.fuel.2012.02.059.
- Zhang W, Wang S, Ran J, Lin H, Kang W, Zhu J. Research progress on the performance of circulating fluidized bed combustion ash and its utilisation in China. J Build Eng; 2022; 52; 104350. Doi: 10.1016/j.jobe.2022.104350.

- Zhang, Zhiwei, Jueshi Qian, Chao You, and Changhua Hu. 2012. "Use of Circulating Fluidized Bed Combustion Fly Ash and Slag in Autoclaved Brick." Construction and Building Materials 35: 109–16. https://doi.org/10.1016/j.conbuildmat.2012.03.006https://Doi:doi.org/10.1016/j.conbuildmat.2012.03.006.
- Zhao J, Tong L, Li B, Chen T, Wang C, Yang G, Zheng Y. Eco-friendly geopolymer materials: A review of performance improvement, potential application and sustainability assessment. J Clean Prod 2021; 307; 127085. Doi: 10.1016/j.jclepro.2021.127085.
- Zhou M, Chen P, Chen X, Ge X, Wang Y. Study on hydration characteristics of circulating fluidized bed combustion fly ash (CFBCA). Construction and Building Materials. 2020, 251, 118993. Doi: 10.1016/j.conbuildmat.2020.118993.

Final Remarks

5. FINAL REMARKS

Three hypotheses linked to specific research questions were formulated taking into account the premise drawn from the current state-of-art in this field. To test these hypotheses, specific objectives were established. These objectives were achieved using the design experimental procedure. Once the results were analysed, the final remarks of the research are presented.

Research question (i): What thermal waste can be incorporated into ceramic processes fulfilling technological, techniques, and environmental requirements?

Industrial thermal waste, from combustion and foundry, has been used in this work to check the feasibility within the incorporation of ceramic processes. Technological and environmental properties as well as the estimation of gas emissions during the firing process were evaluated at a laboratory scale. The results obtained have shown promising results being able to incorporate up to 20 % of the thermal waste following the firing cycle of two ceramic companies without compromising the requirements of the final products.

Once proven the feasibility of thermal waste, mathematical models have been established allowing us to predict the behaviour of final product properties with the incorporation of these residues into the range of waste fixed in this research. Regression coefficient values above 90 % were obtained.

From these mathematical models, an optimisation of the amount of thermal waste incorporated was carried out using MCA as a tool for decision-making. Technical, economic, and environmental criteria and different scenarios were fixed to define the waste and the suitable amount to carry out an industrial-scale proof. Foundry Sand was the waste that present the best results in the MCA.

An industrial test incorporating 1, 10, and 20 % of Foundry Sand was carried out to study the technological and environmental properties as well as the gas emissions during the firing process. Finally, an LCA has performed an environmental validation of conventional products and products incorporating 10 % of waste. Results obtained revealed that products incorporating waste present less impact than conventional ones.

The feasibility, optimisation, and validation of incorporating industrial thermal waste in the ceramic process were carried out. It can conclude that industrial thermal waste can substitute the clay in the ceramic process raising natural resource savings and increasing the end life of waste.

Research question (ii): Can thermal waste be incorporated into low-energy processes to achieve a carbon-neutral society?

Coal fly ash and six alkaline by-products, liquid and solid by-products were studied to assess their feasibility as a precursor and as an activator in geopolymer materials. The alkaline by-products were incorporated to substitute commercial activators. Formulations using a precursor blend of coal fly ash/clay and solely fly ash and different percentages of alkaline by-products as activators were carried out. Technological properties were evaluated to determine the suitability of these formulations. From the results obtained, it can be concluded that a blend of fly/ash and Na_2CO_3 and $HNaCO_3$ present the best performance in geopolymer materials.

Once demonstrated the feasibility of alkaline by-products, the reactivity of fly ash was determined to define the reactive SiO_2/Al_2O_3 ratio which is a key parameter in geopolymer formations. The precursor reactivity shows a ratio between 1.88-2.10. Therefore, it can be concluded that this low Ca fly ash can be used as a precursor in geopolymer materials.

Furthermore, the geopolymers obtained with the selected alkaline by-products were evaluated in a microstructural manner to determine if geopolymerisation was carried out. XRD patterns obtained reveal crystalline groups such as quartz and muscovite, typical of fly ash, as well as hydroxy sodalite and calcium aluminium oxide which is the minerals typically in N-A-S-H gel. On the other hand, FTIR spectra show shifts indicating that the glass component in the fly ash reacted with the alkaline activator to form reaction products, primarily N-A-S-H, an aluminosilicate gel. Looking at the results obtained in geopolymers, it can be concluded that selected alkaline by-products can be used as an alkaline activators in geopolymer materials substituting commercial activators.

Fly ash/clay-based geopolymer using different activators was used to S/S acid toxic waste. The S/S products were evaluated by technical and environmental assessment according to EU Landfill regulation limits for compressive strength and release of hazardous metals. From the result obtained, it can be concluded that geopolymers are presented as a promising way in S/S of hazardous waste due to their capacity to neutralised high acidic waste and their capacity to immobilise contaminants.

It was demonstrated that coal fly ash as a precursor and alkaline by-products as activators can be used in low-energy processes as was presented in this thesis. The incorporation of ashes in these materials allows energy efficiency in production processes as well as reduces the associated impacts on society.

Research question (iii): Can we use thermal waste, with low contents of Si and Al, in the development of low energy materials/binder?

Bottom ashes, from coal fluidized bed coal combustion (CFBC), were evaluated in a first approach in the production of alkali-activated binders as a source of aluminosilicates. The issue of these ashes is their high content of gypsum and their

heterogeneity of particle size. Different trials were carried out to determine the feasibility of bottom ashes in alkali-activated binders: pretreatment to remove the highest particle size, mixing of precursors and activators, and product obtention (pressing or moulding). From the results obtained, it was concluded that the removal of the particle with a size above 0.6 mm, a new mixing method that involves a previous homogenisation of solids and liquids and a traditional civil moulding process is needed to obtain binders with bottom ashes.

To optimise the variables of the process, a set of experiments was carried out to develop the alkali activation of bottom ashes in building materials. The main variables studied were the replacement of activators with alkaline by-products and the role of clay in binder products. In conclusion, Na_2CO_3 can be used as an activator replacing NaOH, and bottom ashes solely can be used as a precursor.

Considering the studies done, bottom ashes present high content of anhydrite and lime and low content of silica and alumina which limit the activation of this waste. On the other hand, fly ashes, from CFBC, present different characteristics than the bottom which make them suitable for geopolymerisation. It was studied a blend of CFBC fly and bottom ashes in different proportions as a precursor and a mixture of Na_2SiO_3 and Na_2CO_3 (by-product) as an activator. Technological properties and microstructural were carried out. From the results obtained, it can be concluded that the final products with a similar proportion of fly and bottom ashes exhibit the maximum compressive strength and present hydration products typically of a C-S-H gel.

CFBC fly and bottom ashes were presented as promising precursors in alkali-activated binders materials. However, more studies must be done to obtain a deeply knowledge of their behaviour in geopolymer products. The incorporation of these waste in these materials, without clay, enables energy and materials efficiency in production processes.

Results Dissemination

RESULTS DISSEMINATION

Some of the results exhibited in this thesis dissertation have been published in a high-impact scientific journal indexed in the Journal Citation Reports:

- Dacuba, J., Cifrian, E., Romero, M., Llano, T., Andrés, A. 2022. Influence of unburned carbon on environmental-technical behaviour of coal fly ash fired clay bricks. Applied Sciences 12(3765), 1-18. DOI: https://doi.org/10.3390/app12083765
- Dacuba, J., Llano, T., Cifrian, E., Andrés, A. 2022. Sustainable management strategy for Solidification/Stabilisation of zinc plant residues (ZPR) by fly ash/clay-based geopolymers. Sustainability 14(4438), 1-21. DOI: https://doi.org/10.3390/su14084438

In addition, other side work related to this thesis was published as co-author also in a scientific journal indexed in the JCR:

- Cifrian, E., Dacuba, J., Llano, T., Díaz-Fernández, M.C., Andrés, A. 2021. Coal fly ash-clay based geopolymer-incorporating EAFD: leaching behaviour and geochemical modeling. Applied Sciences 11(2), 1-17. DOI: https://doi.org/10.3390/app11020810

Next, oral communications and posters that were sent to relevant International Congresses during the execution of this thesis are shown below:

- Dacuba, J.; Díaz, C.; Thomas, C.; Andrés, A. 2015. Factors influencing illite clay-coal fly ash-based geopolymer formation. 9th International Conference on the Environmental and Technical Implications of Construction with Alternative Materials "WASCON 2015". Santander, Spain.
- Dacuba, J.; Díaz, C.; Thomas, C.; Andrés, A. 2015. Heat conditions and time curing influencing on alkaline-activated illite clay-coal fly ash bricks. 3th International Conference Waste: Solutions, Treatments, and Opportunities". Viana do Castelo, Portugal.
- Dacuba, J.; Díaz, C.; Valle-Zermeño, R.; Chimenos, J.M.; Andrés, A. 2016. Leaching behaviour of pollutants from alkaline-activated illite clay-coal fly ash formulations incorporating electric arc furnace dust. 6th International Conference on Engineering for Waste and Biomass Valorisation. Albi, France.
- Dacuba, J., Cifrian, E., del Valle-Zermeño, R., Chimemos, J.M., Andrés, A. 2016. Diffusion leaching test for assessing the resistance of EAFD-fly

ash/clay-based geopolymer to acid attack. ISWA World Congress. Novi Sad, Serbia.

- Dacuba, J., Cifiran, E., Andrés, A.. 2017. Effect of incorporating quarry clay on the production of alkali-activated Coal Fly Ash Brick. EuroCoalAsh 2017. Brno, Check Republic.
- Cifrian, E., Dacuba, J., Viguri, J.R., Andrés, A. 2017. Comparative life cycle assessment of the incorporation of electric arc furnace dust into ceramic products. 4th International Conference Waste: Solutions, Treatments, and Opportunities. Oporto, Portugal.
- Llano, T., Dacuba, J., Cifiran, E., Santos, J., Andrés, A. 2017. Sistemas Integrales de lixiviación como herramienta de Caracterización de Residuos aplicables a la Evaluación del Impacto de Deposición. REDISA VII Simposio Iberoamericano en Ingeniería de Residuos. Santander, Spain.
- Cifiran, E., Dacuba, J., Llano, T., Baquero, M., Andrés, A. 2017. Implicaciones en la aplicación de los criterios de admisión en vertederos en la UE. REDISA VII Simposio Iberoamericano en Ingeniería de Residuos. Santander, Spain.
- Romero-Rodriguez; A., Salamanca; M. J., Dacuba; J., Blasco; J., Viguri; J. R., Andrés, A. 2018. Ecotoxicological analysis of construction products on a marine ecosystem using sea urchin liquid phase bioassays. 10th International Conference on the Environmental and Technical Implications of Construction with Alternative Materials (WASCON). Tampere, Finland.
- Dacuba; J., Galloti, A., Parra, G., Romero-Rodriguez; Cifrian, E., Viguri; J. R., Andrés, A. 2018. Exploration of ecotoxicity tests for environmental assessment of coal fly ash-based geopolymers: Experience with the Daphnia Magna acute test. 10th International Conference on the Environmental and Technical Implications of Construction with Alternative Materials (WASCON). Tampere, Finland.
- Santos, J.; Cifrian, E.; Dacuba, J.; Fernández-Ferreras, J.; Pesquera, C.; de Pedro, I.; Andrés, A. 2021. Characterisation of CFBC fly and bottom ash-based sodium carbonate-activated binders. II Vitrogeowaste Vitrification, Geopolymerisation, Waste Management, Green Cements, and Circular Economy. Baeza, Spain.
- Dacuba, J.; Santos, J.; Cifrian, E.; Galán, B.; Andrés, A. Microstructural characterisation of geopolymers based on different alkaline byproducts. 8th International Conference on Engineering for Waste and Biomass Valorisation. Virtual congress.

Annexes

ANNEXES

A1. LITERATURE REVIEW OF CFA APPLICATIONS

Table A.1.1. Current/direct applications of CFA in aggregates manufacturing and agriculture.

	**Product:** Lightweight aggregates **Sector:** Cement, concrete, and ceramics		
Strengths	**Weaknesses**	**Main remarks**	**References**
☑ CFA with high unburnt carbon is suitable for the sintering process ☑ Lightweight aggregates have more pozzolanic properties than the CFA without the sintering process ☑ Low density suitable for light and insulation construction	☒ Decrease the compressive strength of the concrete for the same dosage of cement	❖ Lightweight aggregates' characteristics depend on the manufacturing process and the temperature at which the hardening is carried out	CEDEX (2011); Cicek and Tanriverdi (2007); Cultrone et al. (2004); Domínguez et al. (1996); Lingling et al. (2005); Yang et al. (2009); Wei et al.(2016); Lin (2006)
	**Product:** Additive for soil amelioration **Sector:** Agriculture		
Strengths	**Weaknesses**	**Main remarks**	**References**
☑ Chemical constituents of CFA can improve the agronomic and fertility properties of the soil ☑ Cost-effective and environmentally friendly to substituting for lime and dolomite ☑ The addition of CFA improves the microbiological activity and leads to higher plant biomass production ☑ CFA with a high level of unburned carbon enhances soil organic matter ☑ Increases the availability of nutrients in plants, improves the soil texture, aeration, percolation, and water retention in the treated zone ☑ Buffer the soil pH	☒ Lead to an increase in soil salinity for a higher concentration of total hardness, cations, and anions in CFA leachates ☒ Pose a contamination risk to soil, plants, and groundwater for comprising some toxic metals ☒ The application must be very specific depending on the properties of ash and soil ☒ Have potential phytotoxic effects when relatively high rates of CFA are applied	❖ Use weathered CFA collected from ash ponds than fresh ash ❖ Add locally available amendments (farm manure, sewage, or sludge) along with CFA to yield benefits from their synergistic interaction ❖ Long-term studies of the impact of CFA on soil health and crop quality	Kishor et al. (2010); Belyaeva and Haynes (2012); Bhattacharya et al. (2012); Lee et al. (2006); Manoharan et al. (2010); Pandey and Singh (2010); Prakash et al. (2009); Ram and Masto (2010); Ram and Masto (2014); Shaheen et al. (2014); Yunusa et al. (2006)

Table A.1.2 Current/direct applications of CFA in construction and civil engineering.

	**Product:** Concrete **Sector:** Construction		
Strengths	**Weaknesses**	**Main remarks**	**References**
☑ Partial replacement of cement with CFA reduces the water demand ☑ Enhance the workability of concrete ☑ Reduce the production costs of concrete and greenhouse gas emissions during the cement production process ☑ One of the best value-added uses and consumes a large quantity of ash ☑ Pre-treatment is not required ☑ Done at an industrial scale	☒ The construction industry and the thermal power plants are influenced by seasonal factors and subjected to operational peaks ☒ Reduce compressive strength of concrete at early ages, especially under cold weather conditions or having more than 40 % replacement of cement ☒ The cost involved in the transportation of ash from production to utilisation sites might limit the application ☒ Unburnt carbon in CFA inhibits air entraining performance and fluidity of fresh concrete	❖ Select the right quality CFA to enhance the cement rather than be detrimental to the final concrete mix ❖ Increase the additional amount of CFA at the premise of meeting the projects demand ❖ The unburned carbon in CFA should be < 6 %	Antiohos et al. (2008); ASTM (2010); CEDEX (2011)]; Cokca and Yilmaz (2004); Dhir and Jones (1999); Dilmore and Neufeld (2001); Duran-Herrera et al. (2011); Freeman et al. (1997); González et al. (2009); Hemalatha and Ramaswamy (2017); McCarthy and Dhir (2005); Nath and Sarker (2011); Oner et al. (2005); Reiner and Rens (2006); Sarker and McKenzie (2009); Zhang et al. (2013)
	**Product:** Grouting, asphalt filler, sub-grade stabilisation, pavement base course, general engineering fill, structural fill **Sector:** Civil engineering		
Strengths	**Weaknesses**	**Main remarks**	**References**
☑ The addition of CFA tends to decrease the propensity of the soil to absorb water and thus swelling of the soil results ☑ Pre-treatment is not required ☑ Done at an industrial scale ☑ Enhance the geotechnical properties of the soil ☑ Lower compressibility relative to other soils	☒ The addition of small amounts of CFA is required to avoid the leaching of heavy metals and sulphates. ☒ Unburnt carbon in CFA inhibits the use of CFA in these products.	❖ The distance between CFA sources and recycling sites needs to be considered ❖ The use of CFA is not intended for flood areas and windy areas ❖ Homogeneous mixtures of different types of CFA are required to get a good compaction paste ❖ The unburned carbon in CFA should be < 3 %	Beeghly and Schrock(2010); Berger and Fitzgerald (2009); CEDEX (2011); Kumar Vadapalli et al. (2008); Mohammadinia et al. (2017); Potgieter-Vermaak et al. (2006); Almesfer and Ingham (2014)

Table A.1.3. Future/indirect applications of CFA in ceramic, concrete, and cement industry.

Fired clay bricks/ Strengths	Weaknesses	Main remarks	References
☑ The chemical composition and proper size range make it suitable to be directly incorporated into ceramic pastes with almost no pre-treatment ☑ Partial substitution for kaolinite, feldspar, and quartz thus efficiently saves limited natural resources ☑ Unburned carbon produces ceramics with a high volume of pores which can be used as thermal and acoustic insulation ☑ High amounts of CFA can be used within this application	☒ The iron oxides in CFA have a negative effect on the thermal expansion coefficient of product ☒ CFA-clay body showed a high shrinkage after firing	❖ Encapsulation of CO_2 during the firing process to increase the pores of the products ❖ High concentrations of CaO, Na_2O, K_2O and MgO are more suitable for the development of these products ❖ The clay used plays an important role in the manufacture of these products	Aineto et al.(2006); Andreola et al. (2016); Başpinar et al.(2010); Bories et al.(2014); Chandra et al.(2008); Cultrone and Sebastián(2009); Erol et al.(2007); Ji et al.(2016); Kockal (2012); Koukouzas et al. (2011); Kumar et al.(2001); Kute and Deodhar (2003); Leiva et al.(2016); Lingling et al. (2005); Monteiro et al. (2008); Muñoz Velasco et al-a (2014); Muñoz Velasco et al-b (2016); Naganathan et al.(2015); Neves Monteiro et al. (2014); Olgun et al.(2005); Sena da Fonseca et al.(2015); Sokolar and Smetanova (2009); Sokolar and Vodova (2011); Zimmer and Begmann (2007)
Geopolymers/ Strengths	**Weaknesses**	**Main remarks**	**References**
☑ CFA can be used in high amounts and constitute the main ingredient of these products ☑ Geopolymers are a suitable alternative to Portland concrete and cement ☑ Geopolymers are synthesized at ambient temperature, reducing CO_2 emissions ☑ Geopolymers show better technological and durability properties than Portland concrete ☑ They can immobilize hazardous materials due to their three-dimensional structure	☒ Unburnt carbon in CFA inhibits air entraining performance and fluidity of geopolymer pastes ☒ Geopolymers require de use of chemicals such as NaOH that can be harmful to humans ☒ The chemicals used (i.e. NaOH or Na_2SiO_3) are expensive ☒ Geopolymer is sold as pre-cast or pre-mix materials due to the dangers associated with its preparation	❖ SiO_2/Al_2O_3 ratio, NaOH concentration and water content are the most important parameters ❖ The NaOH and Na_2SiO_3 should be substitute by waste to make and economically competitive product ❖ The use of different kind of slags with high amounts of CaO enhances the technological properties of geopolymers ❖ The unburned carbon in CFA should be less than 3 %	Abdulkareem et al. (2014); Ahmari et al.(2012); Al-Harahsheh et al. (2015); Álvarez-Ayuso et al. (2008); Al-Zboon et al.(2011); Andini et al. (2008); Assi et al. (2016); Atis et al. (2015); Bakharev (2006); Chen-Tan and van Riessen (2009); Chindaprasirt et al. (2010); Deb et al. (2015); Diaz et al.(2010); Duan et al.(2016); Duxson et al.(2007); Feng et al.

☑ They have rapid strength gain and cures quickly, making it an excellent option for quick builds ☑ They represent a good process to produce ceramic products at ambient temperature.			(2015); Fernández-Jiménez and Palomo (2008); Ferone et al. (2013); Gordon et al. (2011); Gunasekara et al. (2015); Helmy (2016); Huiskes et al. (2016); Izquierdo et al. (2009); Jeyasehar et al. (2013); Kazemian et al. (2015); Komljenovic et al. (2010); Kumar and Kumar (2011); Kumar et al. (2007); Lee and Deventer (2002); Lee et al. (2016); Lemougna et al. (2016); Leong et al. (2016); Luna et al. (2011); Ma et al. (2013); Ma et al. (2016); Martin et al. (2015); Nikolic et al. (2013); Ogundiran et al-a (2013); Ogundiran et al-b. (2016); Panias et al. (2006); Provis et al. (2008); Saravanan et al. (2013); Rickard et al. (2011); Shi et al. (2011); Shi et al.(2012); Somna et al. (2011); Sukmak et al-a (2013); Sukmak et al-b (2013); Winnefeld et al. (2009); Xu et al. (2014); Zeng et al. (2016); Zhang et al. (2008); Zhuang et al. (2016)

Table A.1.4. Future/indirect applications of CFA in catalysts, adsorbents, and zeolites manufacture.

Catalyst / Strengths	Weaknesses	Main remarks	References
☑ Employed as catalyst or catalyst support for various reactions, providing a cost-effective and environmentally friendly way of recycling CFA and significantly reduce its environmental effects ☑ One of the best CFA applications although consumes small quantity of waste.	☒ CFA catalysts have not been applied in industrial practice ☒ CFA contains some trace elements like Hg that can release, causing secondary pollution ☒ Pre-treatment is required	❖ More research is required to perform long-term stability of the catalysts ❖ SiO_2 and Al_2O_3 content above 70 %	Chakraborty et al. (2010); Chatterjee et al. (2001); Flores et al. (2008); Jain et al. (2010); Jain et al. (2011); Khatri and Rani (2008); Khatri et al. (2010); Li and Zhang (2010); Li et al. (2008); Saputra et al. (2012); Wang (2008); Xuan et al. (2003); Yu (2004); Zhang et al. (2012)
Adsorbent / Strengths	**Weaknesses**	**Main remarks**	**References**
☑ Low-cost potential adsorbents that can be directly used in both gaseous and aqueous applications ☑ CFA with high contents of unburned carbon increases the adsorption capacity ads the specific surface increase	☒ CFA have a limited adsorption capacity ☒ The properties of CFA are extremely variable, and the adsorption capacity varies greatly among ashes ☒ Difficulty of recovering the adsorption capacity of CFA after being used	❖ Select the right quality of CFA and pre-treatment to enhance the adsorption capacity ❖ The regeneration and disposal of adsorbents is needed to avoid second pollution	Ahmaruzzaman (2011); Aksu and Yener (2001); Alinnor (2007); Bhattacharya et al. (2008); Cho et al. (2005); Estevinho et al. (2007); Hsu et al. (2008); Itskos et al. (2010); Lee et al. (2017); Lin et al. (2008); López-Antón et al. (2007); Matheswaran and Karunanithi (2007); Mazzella et al. (2016); Mohan and Gandhimathi (2009); Rubel et al. (2005); Suárez-Ruiz et al. (2007); Visa and Duta (2013); Wang and Tsang (2013); Wang et al. (2008); Wang et al. (2016); Zaharia and Suteu (2013); Zhai et al. (2017)
Zeolites / Strengths	**Weaknesses**	**Main remarks**	**References**

☑ Potential adsorbents used in various engineering and agricultural applications for water purification, gas cleaning and soil amendment ☑ One of the best value-added uses, although consumes a relatively small quantity of ash	☒ Mullite and quartz in CFA are difficult to dissolved ☒ Efficiency and economic are the major limiting factors ☒ High unburned carbon inhibits zeolites formation ☒ Pre-treatment required	❖ Improvements in preparation process are required ❖ SiO_2 and Al_2O_3 content above 70 % ❖ CaO content below 15 %	Apiratikul and Pavasant (2008); Babajide et al. (2012); Font et al. (2009); Jha et al.(2009); Kamble et al. (2008); Kazemian et al. (2010); Lee et al. (2017); Li et al. (2014); Liu et al. (2011); Luo et al. (2016); Querol et al. (2001); Querol et al. (2002); Qiu and Zheng (2007); Ríos et al. (2009); Somerset et al. (2008); Tanaka and Fuji (2009); Tanaka et al. (2008); Walek et al. (2008); Yao et al (2009); Zhou et al. (2014)

Table A.1.5. Future/indirect applications of CFA compounds recovery: metals, cenospheres, and unburnt carbon.

Metals / Strengths	Weaknesses	Main remarks	References
☑ Increase industrial synergy opportunities ☑ Achieve significant economic and environmental benefits ☑ Metal recovery from CFA contributes to save natural resources	☒ CFA heterogeneity limits the recovery of valuable metals ☒ The efficiency and economic are major limiting factors	❖ The distance between CFA sources and recycling sites must be considered	Arroyo et al-a (2009); Arroyo et al-b (2009); Bai et al. (2010); Cheng-you et al. (2012); Chimenos et al. (2013); Font et al. (2005); Font et al. (2007); Guang-hui et al. (2010); Guo et al. (2012); Hernández-Expósito et al. (2006); Matjie et al. (2005); Meawad et al. (2010); Nayak and Panda (2010); Shemi et al. (2012); Yao et al. (2014)
Cenospheres / Strengths	**Weaknesses**	**Main remarks**	**References**
☑ Cenospheres are considered one of the most important value-added components of CFA ☑ Their sphericity and low density make them suitable to a variety of applications	☒ Separation processes are required ☒ Common wet separation processes require vast lands, large amounts of water and flotation	❖ The performance of depth separation should take into account of the ash discharge method, the properties of ash or the available land among others	Aixiang et al. (2005); Barbare et al. (2003); Blanco et al. (2000); Chand et al. (2010); Chávez-Valdez et al. (2011); Deepthi et al. (2010); Hu et al.

☑ Cenosphere properties have also been altered by coating with various metals	reagents and easily result in second pollution ☒ Costs and efficiency of the separation process are the major limiting factors		(2010); Huo et al. (2009); Huo et al. (2010); Jha et al. (2011); Labella et al. (2014); Liu et al. (2008); Meng et al. (2010); Ozcivici and Singh (2005); Pang et al. (2011); Rohatgi et al. (2009); Surolia et al. (2010); Tao et al. (2009); Wang et al. (2011); Wasekar et al. (2012); Xu et al. (2011); Yu et al. 2007
Unburnt Carbon / Strengths	Weaknesses	Main remarks	References
☑ The separation of the unburnt carbon allows to have CFA without unburnt carbon ☑ Main properties: high specific surface and adsorption capacity	☒ Separation processes are required ☒ Costs and efficiency of the separation process are the major limiting factors	❖ The performance of depth separation should take into account of the ash discharge method, the properties of ash or the available land among others	Cabielles et al. (2008); Cameán and Garcia (2011); Davini (2002); Izquierdo and Rubio (2008); Li et al. (2006); Lu et al. (2010); Maroto-Valer et al. (2005); Pedersen et al. (2008); Rubio and Izquierdo (2010); Rubio et al. (2007); Yang and Hlavacek (1999).

A2. TECHNOLOGICAL PROPERTIES OF CFA-CLAY BRICKS

Table A.2.1. Linear shrinkage of CFA-Clay bricks.

Sample	FAA (%)	Clay (%)	AV FAA/Clay A bricks	SD FAA/Clay A bricks	AV FAA/Clay B bricks	SD FAA/Clay B bricks
P1	100	0	6.05	0.975	6.05	0.975
P2	90	10	2.85	0.675	3.55	0.326
P3	80	20	2.45	0.411	2.6	0.335
P4	70	30	1.7	0.371	2.35	0.487
P5	60	40	2.15	0.379	1.4	0.518
P6	50	50	2.8	0.694	1.35	0.518
P7	40	60	2.9	1.282	1.35	0.224
P8	30	70	2.4	0.675	1.35	0.454
P9	20	80	1.4	0.762	1.3	0.447
P10	10	90	1.7	0.570	1.2	0.481
P11	0	100	1.35	0.454	1.35	0.518
Sample	FAB (%)	Clay (%)	AV FAB/Clay A bricks	SD FAB/Clay A bricks	AV FAB/Clay B bricks	SD FAB/Clay B bricks
P12	100	0	11.7	1.267	11.7	1.267
P13	90	10	5.95	1.866	7.85	0.822
P14	80	20	3.95	1.165	6.05	0.597
P15	70	30	4.650	0.454	5.8	0.481
P16	60	40	3.8	0.694	3.45	0.622
P17	50	50	1.9	0.675	3.1	0.576
P18	40	60	2.15	0.742	2.90	0.840
P19	30	70	1.85	0.720	2.8	0.019
P20	20	80	2	0.354	2.65	0.137
P21	10	90	2.45	0.694	1.65	0.742

Table A.2.2. Weight loss of CFA-Clay bricks.

Sample	FAA (%)	Clay (%)	AV FAA/Clay A bricks	SD FAA/Clay A bricks	AV FAA/Clay B bricks	SD FAA/Clay B bricks
P1	100	0	6.391	0.340	6.391	0.340
P2	90	10	6.266	0.252	6.421	0.049
P3	80	20	6.087	0.066	6.321	0.199
P4	70	30	6.078	0.087	6.022	0.047
P5	60	40	6.146	0.049	5.917	0.069
P6	50	50	6.926	0.137	5.898	0.048
P7	40	60	6.815	0.095	5.772	0.029
P8	30	70	6.846	0.085	5.721	0.048
P9	20	80	6.572	0.072	5.640	0.018
P10	10	90	6.636	0.040	5.503	0.033
P11	0	100	6.641	0.246	5.374	0.056
Sample	FAB (%)	Clay (%)	AV FAB/Clay A bricks	SD FAB/Clay A bricks	AV FAB/Clay B bricks	SD FAB/Clay B bricks
P12	100	0	28.84	0.150	28.84	0.150
P13	90	10	26.14	0.193	26.103	0.443
P14	80	20	24.136	0.072	23.288	0.052
P15	70	30	21.769	0.066	21.77	0.160
P16	60	40	19.477	0.070	19	0.107
P17	50	50	17.293	0.099	16.717	0.105
P18	40	60	15.012	0.062	14.672	0.176
P19	30	70	12.808	0.065	12.399	0.530
P20	20	80	10.773	0.048	10.190	0.085
P21	10	90	8.451	0.059	7.622	0.060

Table A.2.3. Bulk Density of CFA-Clay bricks.

Sample	FAA (%)	Clay (%)	AV FAA/Clay A bricks	SD FAA/Clay A bricks	AV FAA/Clay B bricks	SD FAA/Clay B bricks
P1	100	0	1569.300	0.517	1569.300	0.517
P2	90	10	1429.158	0.706	1474.626	0.761
P3	80	20	1534.547	0.905	1576.457	0.729
P4	70	30	1593.000	0.319	1673.204	0.943
P5	60	40	1672.332	0.071	1760.792	0.917
P6	50	50	1769.234	0.893	1882.399	0.980
P7	40	60	1857.827	0.800	1942.722	0.900
P8	30	70	1951.846	0.811	1981.256	0.470
P9	20	80	2018.041	0.632	2141.874	0.771
P10	10	90	2085.171	0.943	2241.362	0.862
P11	0	100	2182.415	0.221	2554.515	0.478
Sample	FAB (%)	Clay (%)	AV FAB/Clay A bricks	SD FAB/Clay A bricks	AV FAB/Clay B bricks	SD FAB/Clay B bricks
P12	100	0	1176.310	1.128	1176.310	1.128
P13	90	10	1131.133	0.165	1145.871	0.900
P14	80	20	1148.156	0.355	1194.886	0.893
P15	70	30	1240.450	0.928	1289.072	0.930
P16	60	40	1290.034	1.040	1391.627	0.964
P17	50	50	1351.209	0.715	1499.813	0.855
P18	40	60	1540.254	0.158	1619.771	0.944
P19	30	70	1674.644	0.631	1724.765	0.904
P20	20	80	1828.038	0.927	1928.012	0.882

P21	10	90	1965.245	0.890	2083.960	0.890

Table A.2.4. Water Absorption of CFA-Clay bricks.

Sample	FAA (%)	Clay (%)	AV FAA/Clay A bricks	SD FAA/Clay A bricks	AV FAA/Clay B bricks	SD FAA/Clay B bricks
P1	100	0	23.836	0.669	23.836	0.669
P2	90	10	21.698	0.532	19.692	0.986
P3	80	20	16.090	0.400	18.451	0.349
P4	70	30	15.696	0.830	15.443	0.292
P5	60	40	13.921	0.639	14.171	0.851
P6	50	50	12.069	1.373	11.173	0.305
P7	40	60	9.778	0.399	9.028	0.333
P8	30	70	7.560	0.314	8.088	0.485
P9	20	80	7.141	0.904	6.302	0.267
P10	10	90	6.716	0.631	5.375	0.474
P11	0	100	6.999	0.178	5.310	0.329
Sample	FAB (%)	Clay (%)	AV FAB/Clay A bricks	SD FAB/Clay A bricks	AV FAB/Clay B bricks	SD FAB/Clay B bricks
P12	100	0	30.461	1.909	30.461	1.909
P13	90	10	33.631	0.715	35.952	0.783
P14	80	20	31.941	0.577	32.676	0.662
P15	70	30	28.982	0.428	29.028	0.649
P16	60	40	25.352	0.497	27.534	0.493
P17	50	50	23.826	0.874	25.670	0.716
P18	40	60	17.589	0.413	20.661	0.92
P19	30	70	13.321	0.26	15.789	0.836
P20	20	80	10.898	0.327	9.065	0.421
P21	10	90	7.132	0.19	5.653	0.405

Table A.2.5. Flexural Strength of CFA-Clay bricks.

Sample	FAA (%)	Clay (%)	AV FAA/Clay A bricks	SD FAA/Clay A bricks	AV FAA/Clay B bricks	SD FAA/Clay B bricks
P1	100	0	3.986	0.995	3.986	0.995
P2	90	10	5.976	0.909	8.001	0.958
P3	80	20	8.709	0.961	9.006	0.854
P4	70	30	10.754	0.900	10.783	0.944
P5	60	40	12.118	0.945	13.030	0.895
P6	50	50	13.473	0.946	15.677	0.782
P7	40	60	13.591	0.592	16.269	0.810
P8	30	70	15.089	0.789	17.225	0.807
P9	20	80	18.514	0.992	21.856	0.681
P10	10	90	18.933	0.871	22.693	0.961
P11	0	100	16.213	0.867	19.009	0.696
Sample	FAB (%)	Clay (%)	AV FAB/Clay A bricks	SD FAB/Clay A bricks	AV FAB/Clay B bricks	SD FAB/Clay B bricks
P12	100	0	6.019	0.527	6.019	0.527
P13	90	10	5.592	0.400	2.692	0.868
P14	80	20	5.887	0.196	3.123	0.489
P15	70	30	5.915	0.473	4.788	0.615
P16	60	40	6.344	0.450	5.838	0.773
P17	50	50	6.638	0.680	4.377	0.778
P18	40	60	7.853	0.631	9.314	0.736

P19	30	70	10.051	0.998	10.750	0.925
P20	20	80	12.472	0.856	14.056	0.715
P21	10	90	16.160	0.826	17.674	0.726

A3. ESTIMATION OF GAS EMISSIONS DURING FIRING PROCESS

Table A.3.1. Content of raw materials before and after firing process.

Element	Initial content mg/kg			Final content mg/kg		
	Clay	FAA	FAB	Clay	FAA	FAB
S	200	1700	3100	180	1500	2980
Cl	200	200	200	180	200	200
F	200	200	100	100	150	100
C	300	4700	24400	200	3900	23200
N	< LOD	< LOD	< LOD	< LOD	< LOD	< LOD

LOD: Limit of detention

Table A.3.2. Emission values for ceramics factories proposals in Gonzalez et al., 2011.

	Acceptable Emission values (mg/kg)	Recommended values Intervention (mg/kg)	Compulsory values Intervention (mg/kg)
HF	<180	180-380	>380
HCl	<160	160-740	>740
SO_2	<450	450-2300	>2300

A4. TECHNOLOGICAL PROPERTIES OF FBS-CLAY BRICKS

Table A.4.1. Weight loss of FBs-Clay bricks.

By-Product	% By-Product	Average value	Standard deviation
FS	10	9.42	0.05
	20	6.13	0.12
	30	5.74	0.05
	40	5.92	0.23
FSL	10	7.53	0.52
	20	8.41	0.27
	30	9.82	0.33
	40	11.14	0.13
SD	10	6.71	0.29
	20	8.17	0.31
	30	9.75	0.29
	40	10.63	0.19
FS2	10	5.94	0.09
	20	5.3	0.10
	30	4.69	0.02
	40	4.17	0.12
CA	10	10.46	0.081
	20	13.09	0.77
	30	15.84	0.11
	40	18.09	0.03
WS	10	8.67	0.08
	20	11.12	0.09
	30	14.09	0.016
	40	16.78	0.16
F	10	6.13	0.40
	20	6	0.02
	30	5.65	0.05
	40	5.04	0.11
Reference	-	6.35	0.09

Table A.4.2. Linear shrinkage of FBs-Clay Bricks.

By-Product	% By-Product	Average value	Standard deviation
FS	10	0.92	0.38
	20	1.25	0.25
	30	1.75	0.90
	40	2.83	0.75
FSL	10	0.25	0.75
	20	1.17	0.72
	30	1.58	0.38
	40	1.67	0.52
SD	10	0.50	0.43
	20	1.16	0.29
	30	2.25	0.25
	40	2.75	0.75
FS2	10	1.33	0.63
	20	1.92	0.88
	30	2.17	1.01
	40	3.17	0.38
CA	10	-0.33	0.14
	20	-1.67	0.29
	30	-2.67	0.52
	40	-4.17	0.38
WS	10	0.75	0.25
	20	2.08	0.38
	30	3.25	0.25
	40	3.67	0.38
F	10	-0.50	0.25
	20	-1.75	0.66
	30	-1.83	0.38
	40	-2.67	0.88
Reference	-	2.17	0.63

Table A.4.3. Bulk density of FBs-Clay Bricks.

By-Product	% By-Product	Average value	Standard deviation
FS	10	2107.27	1.15
	20	2064.54	0.11
	30	1964.71	1.59
	40	1872.80	1.89
FSL	10	2045.92	1.62
	20	1995.04	1.56
	30	1925.64	1.14
	40	1854.37	1.89
SD	10	2038.42	1.54
	20	2107.45	2.83
	30	2088.60	1.22
	40	2063.36	2.57
FS2	10	2041.01	1.66
	20	2058.07	2.23
	30	2063.93	2.38
	40	2021.67	2.29
CA	10	1960.83	1.36
	20	1871.33	1.70
	30	1657.98	1.57
	40	1567.02	0.76
WS	10	1959.99	1.80
	20	1756.93	1.98
	30	1724.30	0.89
	40	1635.60	0.67
F	10	2081.28	1.36
	20	2029.81	0.82
	30	1916.76	1.47
	40	1915.29	0.73
Reference	-	2096.70	0.78

Table A.4.4. Water absorption of FBs-Clay Bricks.

By-Product	% By-Product	Average value	Standard deviation
FS	10	8.16	0.70
	20	9.5	0.52
	30	9.82	0.33
	40	10.01	0.11
FSL	10	10.49	0.36
	20	11.91	0.42
	30	15.15	1.07
	40	18.7	0.19
SD	10	8.51	0.55
	20	9.71	0.02
	30	11.33	0.30
	40	13	0.51
FS2	10	8.73	0.41
	20	9.06	0.22
	30	9.02	0.27
	40	9.73	0.23
CA	10	11.27	0.79
	20	11.74	0.49
	30	15.76	0.75
	40	18.02	0.14
WS	10	8.99	0.04
	20	11.59	0.24
	30	11.82	1.04
	40	14.16	0.52
F	10	8.2	0.21
	20	9.51	0.90
	30	9.76	0.11
	40	11.39	0.26
Reference	-	8.73	1.01

Table A.4.5. Flexural strength of FBs-Clay Bricks.

By-Product	% By-Product	Average value	Standard deviation
FS	10	10.50	0.62
	20	4.59	0.67
	30	3.21	0.89
	40	1.84	0.34
FSL	10	5.21	0.69
	20	4.43	0.67
	30	3.97	0.90
	40	2.49	0.72
SD	10	7.37	0.94
	20	5.22	1.13
	30	4.39	0.13
	40	7.79	0.69
FS2	10	5.29	0.44
	20	3.46	0.6
	30	2.90	0.14
	40	0.92	0.19
WS	10	9.29	0.5
	20	6.34	0.5
	30	6.58	0.84
	40	5.34	0.73
F	10	10.4	0.8
	20	7.63	0.46
	30	5.26	0.01
	40	3.93	0.94
Reference	-	31,59	1,70

Table A.4.6. Compression strength of FBs-Clay Bricks.

By-Product	% By-Product	Average value	Standard deviation
FS	10	26,37	0,65
	20	11,47	0,31
	30	8,02	0,29
	40	4,61	0,51
FSL	10	13,02	0,74
	20	11,08	0,63
	30	9,93	1,09
	40	6,24	0,36
SD	10	18,43	0,73
	20	13,05	0,15
	30	10,97	1,24
	40	19,48	1,11
FS2	10	13,23	0,45
	20	8,66	0,91
	30	7,26	0,59
	40	2,30	0,46
WS	10	11,72	0,80
	20	9,65	0,96
	30	8,78	1,45
	40	7,22	1,36
F	10	23,22	1,28
	20	15,85	0,87
	30	16,44	1,12
	40	13,34	1,03
Reference	10	26,04	1,25
	20	19,07	0,85
	30	13,15	0,79
	40	9,83	0,78
Referencia	-	31,59	1,70

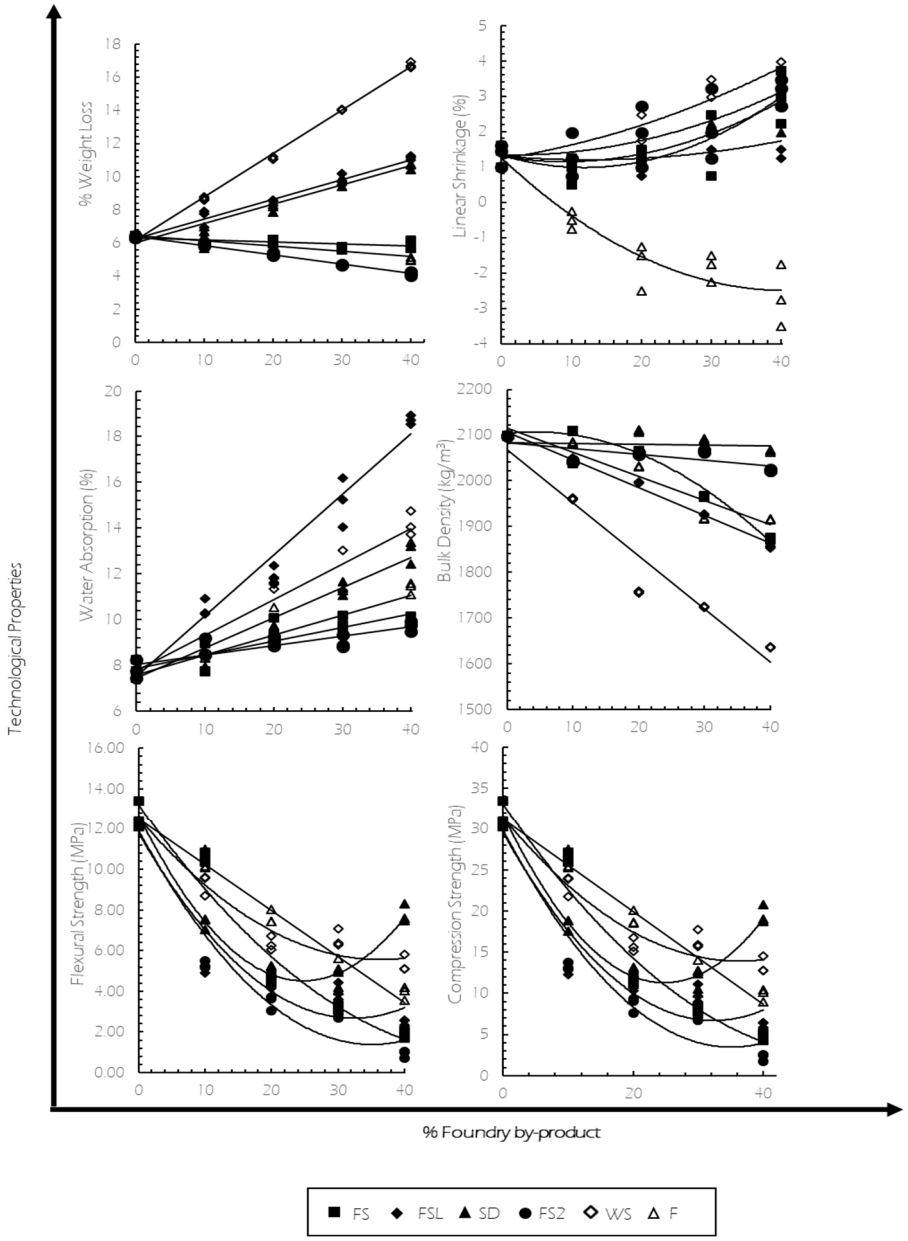

Figure A.4.7. Results obtained from the technological properties of the three replicas against the percentage of waste introduced.

A.5. GAS EMISSIONS DURING FIRING PROCESS

Table A.5.1 S, Cl, F, C and N content before and after the firing process.

	Initial Concentration (mg/kg)					Final Concentration (mg/kg)				
	S	Cl	F	C	N	S	Cl	F	C	N
Clay	650	250	100	3000	ND	200	200	50	100	ND
FS	500	100	ND	30100	1000	200	100	ND	100	900
FSL	7200	2100	800	10700	1000	820	800	100	500	1000
SD	8900	33000	3000	43500	ND	6400	1100	100	200	ND
FS2	ND	100	ND	100	ND	ND	100	ND	100	ND
WS	2700	500	700	206000	5000	2500	100	100	100	1000
F	2700	200	500	89500	2000	700	300	100	100	1000

ND: debajo del límite de detección.

A.6. TECHNOLOGICAL PROPERTIES OF THE FEASIBILITY OF ALKALINE BY-PRODUCTS IN CFA-CLAY ACTIVATED BRICKS

Table A.6.1. Water absorption of Fly Ash/Clay geopolymer and Fly Ash geopolymer replacing commercial NaOH.

Fly Ash/Clay Geopolymer			
Alkali Waste Stream	% NaOH replaced	Average Value	Deviation Standard
Reference	-	6.54	0.20
Ca and Mg Slurry	10	8.02	0.28
	30	6.62	0.34
	50	6.92	0.28
CaO Slurry	10	7.60	0.23
	30	6.86	0.04
	50	7.58	1.46
Ca-Si-$CaCO_3(OH)_2$ Sludge	Expansion in bricks		
Cao rocks	Expansion in bricks		
Na_2CO_3 Powder	10	7.02	0.15
	30	6.74	0.33
	50	6.58	0.26
$HNaCO_3$ Powder	10	7.81	0.08
	30	6.59	0.33
	50	6.08	0.25
Fly Ash Geopolymer			
Reference	-	15.81	0.58
Ca and Mg Slurry	10	14.06	2.44
	30	14.56	0.21
	50	15.95	1.83
CaO Slurry	10	16.07	0.82
	30	15.96	0.22
	50	18.03	0.63
Ca-Si-$CaCO_3(OH)_2$ Sludge	Expansion in bricks		
Cao rocks	Expansion in bricks		

Table A.6.1. (Cont.)

Fly Ash/Clay Geopolymer			
Alkali Waste Stream	% NaOH replaced	Average Value	Deviation Standard
Na_2CO_3 Powder	10	13.76	0.23
	30	13.82	0.34
	50	14.56	0.53
$HNaCO_3$ Powder	10	14.26	2.13
	30	14.12	0.68
	50	14.79	0.58

Table A.6.2. Water absorption of Fly Ash/Clay geopolymer and Fly Ash geopolymer replacing commercial Na2SiO3.

Fly Ash/Clay Geopolymer			
Alkali Waste Stream	% Na_2SiO_3 replaced	Average Value	Deviation Standard
Reference	-	6.54	0.20
Ca and Mg Slurry	10	8.53	0.24
	30	6.91	0.39
	50	7.51	1.14
CaO Slurry	10	8.28	0.28
	30	7.76	0.14
	50	10.07	0.61
Ca-Si-$CaCO_3(OH)_2$ Sludge	Expansion in bricks		
Cao rocks	Expansion in bricks		
Na_2CO_3 Powder	10	7.85	0.19
	30	6.41	0.76
	50	6.51	0.74
$HNaCO_3$ Powder	10	8.39	0.22
	30	6.78	0.12
	50	5.80	0.83
Fly Ash Geopolymer			
Reference	-	15.81	0.58
Ca and Mg Slurry	10	15.88	1.05
	30	14.95	0.57
	50	15.09	0.37
CaO Slurry	10	16.63	0.73
	30	16.40	0.57
	50	17.08	0.71
Ca-Si-$CaCO_3(OH)_2$ Sludge	Expansion in bricks		
Cao rocks	Expansion in bricks		
Na_2CO_3 Powder	10	14.57	0.22
	30	14.01	0.08
	50	13.71	0.37
$HNaCO_3$ Powder	10	14.16	0.39
	30	13.86	0.40
	50	14.04	0.70

Table A.6.3. Flexural Strength of Fly Ash/Clay geopolymer and Fly Ash geopolymer replacing commercial NaOH.

Fly Ash/Clay Geopolymer			
Alkali Waste Stream	% NaOH replaced	Average Value	Deviation Standard
Reference	-	13.18	1.46
Ca and Mg Slurry	10	10.39	0.93
	30	8.95	0.93
	50	10.26	1.08
CaO Slurry	10	11.10	0.94
	30	9.19	1.10
	50	7.03	0.89
Ca-Si-$CaCO_3(OH)_2$ Sludge	Expansion in bricks		
Cao rocks	Expansion in bricks		
Na_2CO_3 Powder	10	11.84	0.77
	30	13.16	3.23
	50	11.87	0.48
$HNaCO_3$ Powder	10	12.85	0.98
	30	12.29	1.38
	50	8.41	2.08
Fly Ash Geopolymer			
Reference	-	3.60	0.34
Ca and Mg Slurry	10	2.71	0.56
	30	4.81	0.76
	50	2.66	0.34
CaO Slurry	10	4.33	0.66
	30	3.56	0.62
	50	1.73	0.12
Ca-Si-$CaCO_3(OH)_2$ Sludge	Expansion in bricks		
Cao rocks	Expansion in bricks		
Na_2CO_3 Powder	10	5.38	0.26
	30	4.14	0.45
	50	3.21	1.66
$HNaCO_3$ Powder	10	4.85	0.45
	30	4.43	1.10
	50	4.10	0.57

Table A.6.4. Flexural strength of Fly Ash/Clay geopolymer and Fly Ash geopolymer replacing commercial Na_2SiO_3.

Fly Ash/Clay Geopolymer			
Alkali Waste Stream	% Na_2SiO_3 replaced	Average Value	Deviation Standard
Reference	-	13.18	1.46
Ca and Mg Slurry	10	7.44	0.89
	30	6.92	1.44
	50	5.13	0.90
CaO Slurry	10	7.61	0.73
	30	7.87	1.10
	50	6.93	1.05
Ca-Si-$CaCO_3(OH)_2$ Sludge	Expansion in bricks		
Cao rocks	Expansion in bricks		
Na_2CO_3 Powder	10	12.40	0.79
	30	7.72	1.52
	50	8.06	1.06
$HNaCO_3$ Powder	10	8.29	0.59
	30	10.48	1.18
	50	7.33	1.49
Fly Ash Geopolymer			
Reference	-	3.60	0.34
Ca and Mg Slurry	10	1.87	0.30
	30	3.34	0.27
	50	2.82	0.37
CaO Slurry	10	2.88	1.38
	30	1.67	0.36
	50	1.96	1.01
Ca-Si-$CaCO_3(OH)_2$ Sludge	Expansion in bricks		
Cao rocks	Expansion in bricks		
Na_2CO_3 Powder	10	4.42	0.55
	30	3.97	0.86
	50	2.89	0.83
$HNaCO_3$ Powder	10	5.94	0.96
	30	3.86	0.77
	50	4.52	0.79

A.7. TECHNOLOGICAL PROPERTIES OF SELECTION CHARACTERISATION PRODUCTS

Table A.7.1. Water Absorption of Fly Ash/Clay geopolymer replacing commercial Na_2SiO_3 with Na_2CO_3 Powder and $HNaCO_3$ Powder.

Alkali Waste Stream	% Na_2SiO_3 replaced	Average Value	Deviation Standard
Reference	-	6.54	0.20
Na_2CO_3 Powder	10	7.85	0.19
	30	6.41	0.76
	50	6.51	0.74
	70	6.40	0.25
	100	6.32	0.09
$HNaCO_3$ Powder	10	8.39	0.22
	30	6.78	0.12
	50	5.80	0.83
	70	5.6	0.34
	100	5.75	0.14

Table A.7.2. Flexural strength of Fly Ash/Clay geopolymer replacing commercial Na_2SiO_3 by Na_2CO_3 Powder and $HNaCO_3$ Powder.

Alkali Waste Stream	% Na_2SiO_3 replaced	Average Value	Deviation Standard
Reference	-	13.18	1.46
Na_2CO_3 Powder	10	12.40	0.79
	30	7.72	1.52
	50	8.06	1.06
	70	7.85	0.64
	100	6.99	0.72
$HNaCO_3$ Powder	10	8.29	0.59
	30	10.48	1.18
	50	7.33	1.49
	70	6.57	0.95
	100	6.21	0.58

A.8. ENVIRONMENTAL BEHAVIOUR OF S/S PRODUCTS

Table A.8.1. Measured values concentration of the contaminants of Fly Ash/Clay geopolymer incorporating CS according to Order AAA/661/2013.

Leaching Concentration (mg/kg)												
CS (%)	Binder	As	Ba	Cd	Cr	Cu	Mo	Ni	Pb	Se	Sb	Zn
100	CS	0.41	0.025	27900	0.78	0.66	0.1	4.5	6.7	0.5	0.5	66900
-	Commercial	13.25±0.61	0.27±0.02	0.04±0.001	0.19±0.01	0.18±0.09	2.16±0.06	0.05±0.001	0.12±0.09	0.58±0.01	0.08±0.001	2.44±0.91
50%	Commercial	13.6±0.5	0.27±0.02	0.22±0.02	0.48±0.12	0.26±0.09	2.48±0.28	0.11±0.05	0.23±0.07	0.69±0.01	0.08±0.001	1.3±0.36
50%	Alternative	13.46±0.05	0.25±0.02	0.8±0.02	0.52±0.05	0.33±0.16	2.78±0.14	0.16±0.25	0.34±0.08	0.75±0.03	0.08±0.01	4.1±0.84
70%	Commercial	13.84±0.24	0.20±0.01	1.49±0.76	0.69±0.06	0.38±0.19	3.26±0.01	0.25±0.27	0.69±0.31	0.82±0.02	0.08±0.001	0.5±0.21
70%	Alternative	14.48±0.32	0.19±0.01	2.00±0.64	0.72±0.06	0.51±0.12	3.14±0.09	0.39±0.68	0.84±0.23	0.88±0.03	0.08±0.02	1.1±0.56
Leaching Concentration (mg/kg) - Drying pre-treatment												
50%	Commercial	13.47±0.18	0.21±0.03	1.54±0.22	0.47±0.02	0.34±0.01	2.52±0.5	0.28±0.02	0.36±0.01	0.72±0.02	0.07±0.002	2.27±0.58
50%	Alternative	13.98±0.02	0.26±0.07	1.7±0.37	0.55±0.04	0.61±0.10	2.80±0.09	0.32±0.60	0.41±0.02	0.76±0.01	0.08±0.01	2.5±0.93
70%	Commercial	13.91±0.11	0.29±0.02	1.18±0.04	0.54±0.01	0.55±0.03	2.51±0.33	0.42±0.02	0.67±0.01	0.81±0.05	0.08±0.001	2.19±0.42
70%	Alternative	13.95±0.08	0.31±0.01	1.3±0.22	0.61±0.03	0.69±0.12	2.76±0.02	0.54±0.26	0.85±0.55	0.88±0.05	0.09±0.02	1.4±0.36

Table A.8.2. Measured values concentration of the contaminants of Fly Ash/Clay geopolymer incorporating AM according to Order AAA/661/2013.

Leaching Concentration (mg/kg)												
AM (%)	Binder	As	Ba	Cd	Cr	Cu	Mo	Ni	Pb	Se	Sb	Zn
100	AM	0.16	0.06	461	0.58	8	0.1	0.88	6.3	0.35	0.56	5720
-	Commercial	13.15±0.58	0.27±0.02	0.01±0.001	0.22±0.01	0.18±0.09	2.29±0.06	0.04±0.001	0.12±0.09	0.61±0.01	0.08±0.001	2.95±0.91
50%	Commercial	13.52±0.09	0.29±0.01	1.3±0.91	0.27±0.02	0.26±0.09	2.25±0.01	0.07±0.001	0.13±0.08	0.72±0.01	0.08±0.001	0.7±0.01
50%	Alternative	13.98±0.02	0.26±0.07	1.7±0.37	0.37±0.04	0.33±0.10	2.76±0.02	0.12±0.05	0.19±0.01	0.76±0.01	0.09±0.001	2.5±0.93
70%	Commercial	14.06±0.06	0.24±0.03	2.77±0.29	0.29±0.06	0.40±0.06	2.40±0.01	0.10±0.01	0.22±0.01	0.82±0.02	0.08±0.01	23.00±5.69
70%	Alternative	14.21±0.21	0.28±0.04	1.71±0.35	0.42±0.02	0.52±0.02	2.54±0.09	0.19±0.03	0.24±0.03	0.85±0.01	0.09±0.01	24.7±0.26
Leaching Concentration (mg/kg)- Drying pretreatment												
50%	Commercial	14.37±0.56	0.26±0.01	0.68±0.02	0.35±0.01	0.48±0.03	2.30±0.41	0.19±0.01	0.21±0.06	0.85±0.03	0.07±0.001	14.34±0.54
50%	Alternative	14.54±0.24	0.29±0.02	0.8±0.05	0.45±0.14	0.60±0.09	2.43±0.09	0.28±0.05	0.24±0.07	0.89±0.02	0.07±0.01	16.5±1.62
70%	Commercial	14.15±0.32	0.3±0.02	2.28±0.41	0.47±0.01	0.75±0.28	2.46±0.06	0.35±0.02	0.35±0.04	0.93±0.03	0.08±0.001	15.98±1.74
70%	Alternative	14.72±0.15	0.34±0.02	2.5±0.35	0.66±0.13	0.77±0.08	2.65±0.05	0.42±0.06	0.39±0.06	1.03±0.16	0.08±0.01	17.1±0.99

A9. LITERATURE REVIEW OF CFBC ASHES

Table A.9.1 State of the art of the CFBC ashes and (if applicable) its valorisation.

Reference	Title	Authors	Publication	Ashes used	valorisation	other purpose
Manzoori et al. 1993	The role of inorganic matter in coal in the formation of agglomerates in circulating fluid bed combustors	Manzoori, A.R., Agarwal, P.K.	Fuel, 72 (7), pp. 1069-1075.	Bottom anf fly ash CFBC	x	
Bonn et al. 1995	Formation and decomposition of N2O in fluidized bed boilers	Bonn, B., Pelz, G., Baumann, H.	Fuel, 74 (2), pp. 165-171.	bed ash, cyclone ash	x	
Talukdar et al. 1996	Reduction of calcium sulphate in a coal-fired circulating fluidized bed furnace	Talukdar, J., Basu, P., Greenblatt, J.H	Fuel, 75 (9), pp. 1115-1123	x	x	reaction study
Pisupati et al. 1996	Sorbent behaviour in circulating fluidized bed combustors: Relevance of thermally induced fractures to particle size dependence	Pisupati, S.V., Wasco, R.S., Morrison, J.L., Scaroni, A.W.	Fuel, 75 (6), pp. 759-768	x	x	fraction study
Iribiarne et al. 1997	Reactivity of calcium sulphate from FBC systems	Iribarne, A.P., Iribarne, J.V., Anthony, E.J	Fuel, 76 (4), pp. 321-327	x	x	reactivity study
Anthony and Jia 2000	Agglomeration and strength development of deposits in CFBC boilers firing high-sulphur fuels	Anthony, E.J., Jia, L.	Fuel, 79 (15), pp. 1933-1942	Bed ash CFBC A/B/C	x	
Wu et al. 2004	Steam hydration of CFBC ash and the effect of hydration conditions on reactivation	Wu, Y., Anthony, E.J., Jia, L.	Fuel, 83 (10), pp. 1357-1370	CFBC FA/BA	x	hydratation behaviour
Anthony et al. 2006	Calcium sulphide in FBC boilers and its fate using liquid water reactivation	Anthony, E.J., Jia, L., Iribarne, A.P., Welford, G., Wang, J., Trass, O.	Fuel, 85 (12-13), pp. 1871-1879	Bed/Cylone/baghouse comparation	x	Calcium sulphide study
Shimizu et al. 2007	Emissions of NOx and N2O during co-combustion of dried sewage sludge with coal in	Shimizu, T., Toyono, M	Fuel, 86 (15), pp. 2308-2315.	several samples	x	Emissions of NOx and N2O

	a circulating fluidized bed combustor					
Rao et al. 2007	Carbonation of FBC ash by sonochemical treatment	Rao, A., Anthony, E.J., Jia, L., Macchi, A.	Fuel, 86 (16), pp. 2603-2615	Bed ash CFBC	x	Sonochemical treatment of FBC ash
Sheng et al. 2007	Utilisation of fly ash coming from a CFBC boiler co-firing coal and petroleum coke in Portland cement	Sheng, G., Zhai, J., Li, Q., Li, F	Fuel, 86 (16), pp. 2625-2631	CFBC Fly Ash A/B	cement	
Yoffe et al. 2007	Oil shale fueled FBC power plant - Ash deposits and fouling problems	Yoffe, O., Wohlfarth, A., Nathan, Y., Cohen, S., Minster, T	Fuel, 86 (17-18), pp. 2714-2727	Several ashe deposit	x	circulation study
Fu et al. 2007	The physical-chemical characterisation of mechanically-treated CFBC fly ash	Fu, X., Li, Q., Zhai, J., Sheng, G., Li, F.	Cement and Concrete Composites, 30 (3), pp. 220-226.	CFBC fly ash	x	physical–chemical characterisation
Glinicki et al. 2007	Air void system in concrete containing circulating fluidized bed combustion fly ash	Glinicki, M.A., Zielinski, M	Materials and Structures/Materiaux et Constructions, 41 (4), pp. 681-687	CFBC FlyAsh	concrete	
Wang et al. 2008	Carbonation of fly ash in oxy-fuel CFB combustion	Wang, C., Jia, L., Tan, Y., Anthony, E.J.	Fuel, 87 (7), pp. 1108-1114	CFBC Fly ash	x	Caronation study
Rao et al. 2008	Sonochemical treatment of FBC ash: A study of the reaction mechanism and performance of synthetic sorbents	Rao, A., Anthony, E.J., Manovic, V.	Fuel, 87 (10-11), pp. 1927-1933.	Bed ash CFBC	x	Sono-chemical treatment of FBC ash
Cao et al. 2008	Abatement of mercury emissions in the coal combustion process equipped with a Fabric Filter Baghouse	Cao, Y., Cheng, C.-M., Chen, C.-W., Liu, M., Wang, C., Pan, W.-P.	Fuel, 87 (15-16)	x	x	mercury emission
Skodras et al. 2009	Chemical, leaching and toxicity characteristics of CFB combustion residues	Skodras, G., Grammelis, P., Prokopidou, M., Kakaras, E., Sakellaropoulos, G.	Fuel, 88 (7), pp. 1201-1209.	Fly ash (baghouse filter)/Under cooling exchanger ash/Bed ash	x	residues study
Glinicki and Zielinski 2009	Frost salt scaling resistance of concrete containing CFBC fly ash	Glinicki, M.A., Zielinski, M.	Materials and Structures, 42 (7), pp. 993-1002	CFBC FlyAsh	concrete	

Table A.9.1 (Cont.).

Reference	Title	Authors	Publication	Ashes used	valorisation	other purpose
Shon et al. 2010	Potential use of stockpiled circulating fluidized bed combustion ashes in controlled low strength material (CLSM) mixture	Shon, C.-S., Mukhopadhyay, A.K., Saylak, D., Zollinger, D.G., Mejeoumov, G.G.	Construction and Building Materials, 24 (5), pp. 839-847	stockpiled CFBC Ash	controlled low strength material (CLSM) mixture	
Pihu et al. 2012	Oil shale CFBC ash cementation properties in ash fields	Pihu, T., Arro, H., Prikk, A., Rootamm, R., Konist, A., Kirsimäe, K., Liira, M., Mõtlep, R	Fuel, 93, pp. 172-180	CFB Bottom ash/CFB Esp 1 field	Cementitious fields	
Li et al. 2012-a	Synthesis of geopolymer composites from blends of CFBC fly and bottom ashes	Li, Q., Xu, H., Li, F., Li, P., Shen, L., Zhai, J.	Fuel, 97, pp. 366-372	CBA/CFA	Geopolymer	
Sheng et al. 2012	Investigation on the hydration of CFBC fly ash	Sheng, G., Li, Q., Zhai, J.	Fuel, 98, pp. 61-66	CFBC Fly ash with/without limestone	x	self-cementitious study
Rust et al. 2012	Formulating low-energy cement products	Rust, D., Rathbone, R., Mahboub, K.C., Robl, T.	Journal of Materials in Civil Engineering, 24 (9), pp. 1125-1131	CFBC Ash	cement	
Zhang et al. 2012	Use of circulating fluidized bed combustion fly ash and slag in autoclaved brick	Zhang, Z., Qian, J., You, C., Hu, C.	Construction and Building Materials, 35, pp. 109-116	fly ash and slag	autoclaved brick	
Li et al. 2012-b	Cementitious properties and hydration mechanism of circulating fluidized bed combustion (CFBC) desulphurisation ashes	Li, X.-G., Chen, Q.-B., Huang, K.-Z., Ma, B.-G., Wu, B.	Construction and Building Materials, 36, pp. 182-187	CFBC ash	cementitious materials	hydration properties
Soundarrajan et al. 2012	Development and use of a method for prediction of the ash split in a CFBC boiler to improve the energy efficiency	Soundarrajan, N., Rozelle, P.L., Pisupati, S.V	Fuel, 102, pp. 9-15	Bottom ash1, FlyAsh1/Bottom ash2, FlyAsh2	x	prediction of the ash split
Marks et al. 2012	Assessment of Scaling Durability of Concrete with CFBC Ash by Automatic Classification Rules	Marks, M., Józwiak-Niedźwiedzka, D., Glinicki, M.A., Olek, J., Marks, M.	Journal of Materials in Civil Engineering, 24 (7), pp. 860-867.	CFBC ashes (K/T)	concrete CFBC	Rules study
Li et al. 2013	Utilisation of modified CFBC desulphurisation ash as an admixture in blended cements: Physico-mechanical and hydration characteristics	Li, X.-G., Chen, Q.-B., Ma, B.-G., Huang, J., Jian, S.-W., Wu, B.	Fuel, 102, pp. 674-680	CFBC ashes (collected ash-hoppers of the electrostatic precipitator) with/without limestone	blended cements	

Table A.9.1 (Cont.).

Reference	Title	Authors	Publication	Ashes used	valorisation	other purpose
Lawrance et al. 2013	A novel technique for characterizing sintering propensity of low rank fuels for CFBC boilers	Lawrence, A., Ilayaperumal, V., Dhandapani, K.P., Srinivasan, S.V., Muthukrishnan, M., Sundararajan, S.	Fuel, 109, pp. 211-216	CFBC agglomerate ashes	x	cyclone study
Shen et al. 2013	Investigations of anhydrite in CFBC fly ash as cement retarders	Shen, Y., Qian, J., Zhang, Z.	Construction and Building Materials, 40, pp. 672-678.	(CFBC) fly ash. HF: CFBC fly ash with high SO3 content./LF: CFBC fly ash with low SO3 content.	cement retarders	
Xia et al. 2013	Utilisation of circulating fluidized bed fly ash in preparing non-autoclaved aerated concrete production	Xia, Y., Yan, Y., Hu, Z	Construction and Building Materials, 47, pp. 1461-1467	(CFBC) fly ash (CFA)	non-autoclaved aerated concrete	
Chi et al. 2014	Effect of circulating fluidized bed combustion ash on the properties of roller compacted concrete	Chi, M., Huang, R.	Cement and Concrete Composites, 45, pp. 148-156	CFBC ash	fine aggregate in roller compacted concrete	
Dung et al. 2014-a	Performance evaluation of an eco-binder made with slag and CFBC fly ash	Dung, N.T., Chang, T.-P., Yang, T.-R.	Journal of Materials in Civil Engineering, 26 (12), art. no. 04014096	CFBC Fly Ash (CA)	eco-binder without cement, (SCA)	
Chen et al. 2014	Utilisation of circulating fluidized bed fly ash for the preparation of foam concrete	Chen, X., Yan, Y., Liu, Y., Hu, Z.	Construction and Building Materials, 54, pp. 137-146.	CFBC Fly Ash (CFA) flue outlet/ stacked ash (Gd)	foam concrete	
Dung et al. 2014-b	Engineering and sulphate resistance properties of slag-CFBC fly ash paste and mortar	Dung, N.T., Chang, T.-P., Chen, C.-T.	Construction and Building Materials, 63, pp. 40-48.	CFBC Fly Ash (CA)	SCA cement	
Wu et al. 2014	Characteristics of CFBC fly ash and properties of cement-based composites with CFBC fly ash and coal-fired fly ash	Wu, T., Chi, M., Huang, R.	Construction and Building Materials, 66, pp. 172-180	CFBC fly ash	cement-based composites	
Konist et al. 2015	Influence of oxy-fuel combustion of Ca-rich oil shale fuel on carbonate stability and ash composition	Konist, A., Valtsev, A., Loo, L., Pihu, T., Liira, M., Kirsimäe, K	Fuel, 139, pp. 671-677.		x	
Bae and Lee 2015	Carbonation Behaviour of fly ash with circulating	Bae, S.J., Lee, K.G.	Journal of the Korean Ceramic	fluidized bed fly ash	x	Reaction study

	fluidized bed combustion (CFBC)		Society, 52 (2), pp. 154-158			
Dung et al. 2015	Hydration process and compressive strength of slag-CFBC fly ash materials without portland cement	Dung, N.T., Chang, T.-P., Chen, C.-T	Journal of Materials in Civil Engineering, 27 (7), art. no. 04014213,	CFBC Fly Ash (CA)	SCA binder	
Chen et al. 2015	Performance and microstructural examination on composition of hardened paste with no-cement SFC binder	Chen, C.-T., Nguyen, H.-A., Chang, T.-P., Yang, T.-R., Nguyen, T.-D	Construction and Building Materials, 76, pp. 264-272	CFBC Fly Ash (C)	no-cement SFC binder	
López-Antón et al. 2015	Enrichment of thallium in fly ashes in a Spanish circulating fluidized-bed combustion plant	Antonia López-Antón, M., Alan Spears, D., Díaz-Somoano, M., Diaz, L.,	Fuel, 146, pp. 51-55.	CFBC Fly ash, CFBC Bottom ash (various samples)	x	
Song et al. 2015	Effect of the Ca-to-Si ratio on the properties of autoclaved aerated concrete containing coal fly ash from circulating fluidized bed combustion boiler	Song, Y., Guo, C., Qian, J., Ding, T.	Construction and Building Materials, 83, pp. 136-142	CFBC Fly Ash (CFBCFA1 /2)	autoclaved aerated concrete	

Table A.9.1 (Cont.).

Reference	Title	Authors	Publication	Ashes used	valorisation	other purpose
Nguyen et al. 2016	Influence of circulating fluidized bed combustion (CFBC) fly ash on properties of modified high volume low calcium fly ash (HVFA) cement paste	Nguyen, H.-A., Chang, T.-P., Shih, J.-Y., Chen, C.-T., Nguyen, T.-D.	Construction and Building Materials, 91, art. no. 6679, pp. 208-215.	CFBC Fly Ash (CFA)	high volume low calcium fly ash (HVFA) cement paste	
Nguyen et al. 2015	Engineering properties and durability of high-strength self-compacting concrete with no-cement SFC binder	Nguyen, H.-A., Chang, T.-P., Shih, J.-Y., Chen, C.-T., Nguyen, T.-D	Construction and Building Materials, 106, pp. 670-677	CFBC Fly Ash (CFA)	no-cement SFC binder	
Dung et al. 2016	Cementitious properties and microstructure of an innovative slag eco-binder	Dung, N.T., Chang, T.-P., Chen, C.-T., Yang, T.-R.	Materials and Structures/Materiaux et Constructions, 49 (5), pp. 2009-2024	CFBC Fly Ash (CA)	non-cement SCA eco-binder	
Lee and Lee 2016	Carbonation behaviour of lightweight foamed concrete using coal fly ash	Lee, J.H., Lee, K.G.	Journal of the Korean Ceramic Society, 53 (3), pp. 354-361.	CFBC Fly Ash	Lightweight Foamed Concrete	
Chi 2016	Synthesis and characterisation of mortars with circulating fluidized bed combustion fly ash and ground granulated blast-furnace slag	Chi, M.	Construction and Building Materials, 123, pp. 565-573.	CFBC Fly Ash	CFBC cement-based composites	
Lee and Kim 2017	Self-cementitious hydration of circulating fluidized bed combustion fly ash	Lee, S.-H., Kim, G.-S.	Journal of the Korean Ceramic Society, 54 (2), pp. 128-136	CFBC Fly Ash A (bituminous coal), CFBC Fly Ash B (petro coke)	x	Reaction study
Park et al. 2017	Circulating fluidized bed combustion ash as controlled low-strength material (CLSM) by alkaline activation	Park, S.M., Lee, N.K., Lee, H.K.	Construction and Building Materials, 156, pp. 728-738.	CFBC Fly ash, CFBC Bottom ash	controlled low-strength materials (CLSM)	
Jang et al. 2017	Utilisation of circulating fluidized bed combustion ash in producing controlled low-strength materials with cement or sodium carbonate as activator	Jang, J.G., Park, S.-M., Chung, S., Ahn, J.-W., Kim, H.-K.	Construction and Building Materials, 159, pp. 642-651	CFBC Fly ash, CFBC Bottom ash	controlled low-strength materials (CLSM)	
Lee and Bae 2018	Carbonation of circulating fluidized bed combustion fly ash with hybrid reaction	Lee, K.G., Bae, S.J	Journal of the Korean Ceramic Society, 55 (2), pp. 160-165	CFBC Fly Ash	x	Reaction study
Huynh et al. 2018	Engineering and durability properties of eco-friendly mortar using cement-free SRF binder	Huynh, T.-P., Vo, D.-H., Hwang, C.-L.	Construction and Building Materials, 160, pp. 145-155	CFBC (F) Fly Ash	cement-free SRF binder	
Nguyen et al. 2018	Engineering Properties and Bonding Behaviour of Self-Compacting Concrete Made with No-Cement Binder	Nguyen, H.-A., Chang, T.-P., Shih, J.-Y	Journal of Materials in Civil Engineering, 30 (3)	CFBC fly ash (CFA)	Self-Compacting Concrete	

Xu et al. 2018	Effect of fineness and components of CFBC ash on performance of basic magnesium sulphate cement	Xu Xun, Xu Yuanyuan, Duan Liling	Construction and Building Materials 170	CFBC ash	Basic magnesium sulphate cement	
Park et al. 2018	Binder chemistry of sodium carbonate-activated CFBC fly ash	S. M. Park . J. H. Seo . H. K. Lee	Materials and Structures (2018) 51:59	CFBC Fly Ash	x	Reaction study
Hlavacek et al. 2018	Ternary binder made of CFBC fly ash, conventional fly ash, and calcium hydroxide: Phase and strength evolution	Hlaváček, P., Šulc, R., Šmilauer, V., Rößler, C., Snop, R.	Cement and Concrete Composites, 90, pp. 100-107.	CFBC Fly ash	Ternary binder	
Kang and Choi 2018	Development of non-sintered zero-OPC binders using circulating fluidized bed combustion ash	Kang, Y.H., Choi, Y.C	Construction and Building Materials, 178, pp. 562-573	CFBC ashes	non-sintered zero-OPC binders	
Park et al. 2019	Effect of chemical additives on hard deposit formation and ash composition in a commercial circulating fluidized bed boiler firing Korean solid recycled fuel	Park, J.H., Lee, D.H., Hab, K.H., Shin, J.S., Bae, D.H., Shim, T.E., Lee, J.H., Shun, D.	Fuel, 236, pp. 792-802		x	
Nguyen et al. 2019	Influence of low calcium fly ash on compressive strength and hydration product of low energy super sulphated cement paste	Nguyen, H.-A., Chang, T.-P., Shih, J.-Y., Chen, C.-T.	Cement and Concrete Composites, 99, pp. 40-48.	CFA (CFBC Fly Ash)	ecological super-sulphated cement (SSC)	
Liu et al. 2019	An experimental investigation into mineral transformation, particle agglomeration and ash deposition during combustion of Zhundong lignite in a laboratory-scale circulating fluidized bed	Liu, Z., Li, J., Wang, Q., Lu, X., Zhang, Y., Zhu, M., Zhang, Z., Zhang, D	Fuel, pp. 458-468.	bottom ash, fly ash, ash agglomerate in bottom ash	x	Study the residues
Park et al. 2019	Characteristics of co-combustion of strongly caking and non-caking coals in a pilot circulating fluidized bed combustor (CFBC)	Park, K., Lee, J.-M., Kim, D.-W., Lee, G.-H., Kang, Y	Fuel, 236, pp. 1110-1116	Bottom and fly ash	x	
Park et al. 2019	Effect of chemical additives on hard deposit formation and ash composition in a commercial circulating fluidized bed boiler firing Korean solid recycled fuel	Park, J.H., Lee, D.H., Hab, K.H., Shin, J.S., Bae, D.H., Shim, T.E., Lee, J.H., Shun, D.	Fuel, 236, pp. 792-802		x	
Moon et al. 2019	Carbon dioxide fixation via accelerated carbonation of cement-based materials: Potential for construction materials applications	Moon, E.-J., Choi, Y.C	Construction and Building Materials, 199	CFBC ash	cement-based materials	

Table A.9.2 Most similar chemical composition ashes to CFBC ashes used in chapter 4.

Reference	Title	Authors	Publication
Anthony and Jia, 2000	Agglomeration and strength development of deposits in CFBC boilers firing high-sulphur fuels	Anthony, E.J., Jia, L.	Fuel, 79 (15), pp. 1933-1942
Wang et al. 2008	Carbonation of fly ash in oxy-fuel CFB combustion	Wang, C., Jia, L., Tan, Y., Anthony, E.J.	Fuel, 87 (7), pp. 1108-1114
Chi and Huang, 2014	Effect of circulating fluidized bed combustion ash on the properties of roller compacted concrete	Chi, M., Huang, R.	Cement and Concrete Composites, 45, pp. 148-156
Huynh et al. 2018	Engineering and durability properties of eco-friendly mortar using cement-free SRF binder	Huynh, T.-P., Vo, D.-H., Hwang, C.-L.	Construction and Building Materials, 160, pp. 145-155

Table A.9.3. Other ashes similar to CFBC ashes used in chapter 4.

Reference	Title	Authors	Publication
Dung et al. 2014	Performance evaluation of an eco-binder made with slag and CFBC fly ash	Dung, N.T., Chang, T.-P., Yang, T.-R.	Journal of Materials in Civil Engineering, 26 (12), art. no. 04014096
Dung et al. 2015	Hydration process and compressive strength of slag-CFBC fly ash materials without Portland cement	Dung, N.T., Chang, T.-P., Chen, C.-T	Journal of Materials in Civil Engineering, 27 (7), art. no. 04014213,
Chen et al. 2015	Performance and microstructural examination on composition of hardened paste with no-cement SFC binder	Chen, C.-T., Nguyen, H.-A., Chang, T.-P., Yang, T.-R., Nguyen, T.-D	Construction and Building Materials, 76, pp. 264-272
Nguyen et al. 2015	Influence of circulating fluidized bed combustion (CFBC) fly ash on properties of modified high volume low calcium fly ash (HVFA) cement paste	Nguyen, H.-A., Chang, T.-P., Shih, J.-Y., Chen, C.-T., Nguyen, T.-D.	Construction and Building Materials, 91, art. no. 6679, pp. 208-215.
Nguyen et al. 2016-a	Engineering properties and durability of high-strength self-compacting concrete with no-cement SFC binder	Nguyen, H.-A., Chang, T.-P., Shih, J.-Y., Chen, C.-T., Nguyen, T.-D	Construction and Building Materials, 106, pp. 670-677
Dung et al. 2016	Cementitious properties and microstructure of an innovative slag eco-binder	Dung, N.T., Chang, T.-P., Chen, C.-T., Yang, T.-R.	Materials and Structures/Materiaux et Constructions, 49 (5), pp. 2009-2024
Chi, 2016	Synthesis and characterisation of mortars with circulating fluidized bed combustion fly ash and ground granulated blast-furnace slag	Chi, M.	Construction and Building Materials, 123, pp. 565-573.
Nguyen et al. 2018	Engineering Properties and Bonding Behaviour of Self-Compacting Concrete Made with No-Cement Binder	Nguyen, H.-A., Chang, T.-P., Shih, J.-Y.	Journal of Materials in Civil Engineering, 30 (3)
Nguyen et al. 2016-b	Influence of low calcium fly ash on compressive strength and hydration product of low energy super sulfated cement paste	Nguyen, H.-A., Chang, T.-P., Shih, J.-Y., Chen, C.-T.	Cement and Concrete Composites, 99, pp. 40-48.

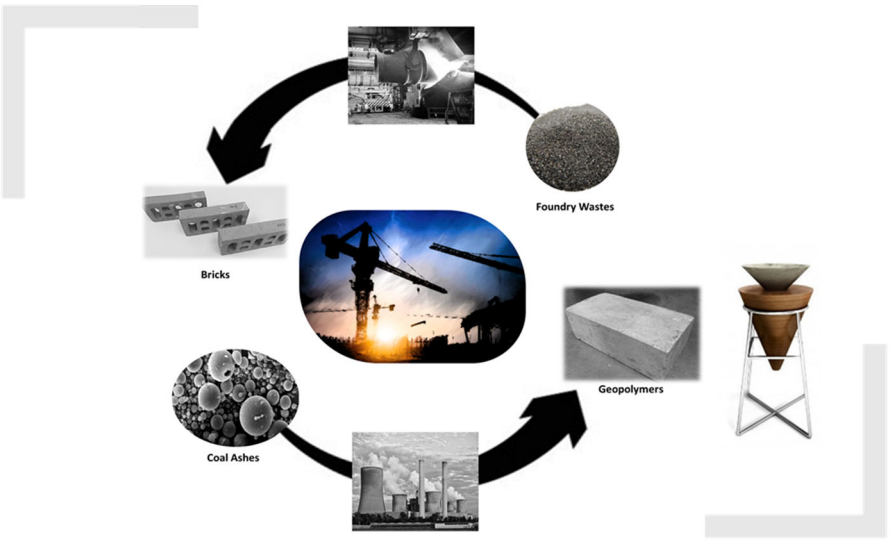

El sistema económico actual está basado en una producción lineal, donde cada uno de los procesos consume recursos naturales y genera residuos, que en su mayoría son depositados en vertederos. A lo largo de las últimas décadas, un nuevo pensamiento medioambiental está despertando y produciendo un cambio de mentalidad a todos los niveles. Las corrientes residuales procedentes de procesos industriales tienen potencial para su explotación en determinados ciclos productivos. El reto actual es delimitar qué procesos productivos son los más atractivos para absorber grandes cantidades de residuos, sin que esto conlleve un perjuicio en las propiedades de los productos finales, así como que causen daños al medioambiente.
El sector de la construcción lleva años introduciendo residuos industriales en sus productos. Desde el punto de vista productivo, el proceso cerámico presenta una gran variedad de materiales y composiciones para fabricar la amplia gama de productos cerámicos existentes. Por otro lado, el cemento Portland genera aproximadamente una tonelada de CO_2 por tonelada de cemento generado lo que hace a este sector responsable de emisiones globales de CO_2 significativas a la atmósfera. Por esta razón en la actualidad, la comunidad científica se está centrando en el desarrollo de nuevos cementos activados alcalinamente o geopolímeros.
De la necesidad de continuar rediseñando los procesos industriales tradicionales para lograr un sistema productivo interconectado, surge esta Tesis Doctoral, cuyo objetivo principal de esta tesis doctoral es incorporar y/o utilizar residuos industriales térmicos en procesos cerámicos y de baja energía (geopolímeros) para evaluar su viabilidad como materias primas secundarias en la producción de materiales de construcción impulsando prácticas de economía circular.
Con la realización de esta tesis, se ha demostrado y concluido la viabilidad de incorporar residuos industriales térmicos en procesos cerámicos y de baja energía. La incorporación de estos residuos permite una eficiencia de materiales en los procesos cerámicos, una eficiencia energética al poder ser utilizados en la obtención de geopolímeros y una eficiencia dual de materiales y energética al poder obtener geopolímeros exclusivamente con residuos sin emplear materias primas vírgenes. Se ha concluido que estos residuos se pueden convertir en los principales recursos en procesos productivos permitiendo crear producciones circulares en lugar de las producciones lineares actuales.

The current economic system is based on a linear production, where each of the processes consumes natural resources and generates waste, which is mostly buried in landfills. Throughout the last decades, a new environmental thought is awakening and producing a change of mentality at all levels. Residual flows from industrial processes have the potential to be exploited in certain production cycles. The current challenge is to define which production processes are the most attractive to absorb large amounts of waste, without this entailing a detriment in the properties of the final products, as well as causing damage to the environment.
The construction sector has been introducing industrial waste into its products for years. From a production point of view, the ceramic process presents a great variety of materials and compositions to manufacture the wide range of existing ceramic products. On the other hand, Portland cement generates approximately one ton of CO_2 per ton of cement generated, which means that this industry is responsible for significant global CO_2 emissions into the atmosphere. For this reason, the scientific community is currently focusing on the development of new alkali-activated cements or geopolymers.
From the need to keep redesigning traditional industrial processes to achieve an interconnected production system, this Doctoral Thesis was born. The main objective of this doctoral thesis is to incorporate and/or use thermal industrial waste in ceramic and low-energy processes (geopolymers) to evaluate its viability as secondary raw materials in the production of construction materials, promoting circular economy practices.
With the completion of this thesis, the feasibility of incorporating thermal industrial waste in ceramic and low-energy processes has been demonstrated and concluded. The incorporation of these residues allows material efficiency in ceramic processes, energy efficiency as they can be used to obtain geopolymers and dual material and energy efficiency as geopolymers can be obtained exclusively with waste without using virgin raw materials. It has been concluded that these residues can be converted into the main resources in production processes, allowing the creation of circular productions instead of the current linear productions.

UC UNIVERSIDAD DE CANTABRIA Escuela de Doctorado